IMPACT DES CHAMPS ÉLECTRIQUES PULSÉS À COURTE DURÉE D'IMPULSION/PAUSE SUR LE COLMATAGE DES MEMBRANES EN COURS DE PROCÉDÉS ÉLECTROMEMBRANAIRES : MÉCANISMES D'ACTION ET INFLUENCE SUR LES PERFORMANCES DES PROCÉDÉS

Thèse

SERGEY MIKHAYLIN

Doctorat en sciences et technologie des aliments

Philosophiae Doctor (Ph.D.)

Québec, Canada

Résumé

L'approvisionnement en eau potable fraîche, en aliments sains, en substances bioactives et en énergie peut être accompli par une technologie verte comme l'électrodialyse (ED). Actuellement, deux obstacles majeurs entravent l'utilisation d'une telle technologie par l'industrie, soit les phénomènes de colmatage membranaire et la polarisation de la concentration (CP). Les travaux récents ont démontré que l'application d'un champ électrique pulsé (CEP) pendant l'ED peut éliminer complètement le colmatage par les protéines et peut diminuer considérablement le colmatage par les minéraux. De plus, les impulsions de courant préviennent l'élargissement de la couche de CP. Malgré des résultats prometteurs d'application du CEP, la durée optimale des impulsions/pauses et l'influence du CEP sur le colmatage membranaire et la CP dans des solutions contenant les agents d'encrassement sont encore des questions ouvertes et discutables.

Les résultats de la thèse montrent que les champs électriques pulsés avec des durées d'impulsion/pause courtes peuvent être appliqués pour éliminer complètement le colmatage minéral sur les membranes échangeuses d'anions et pour contrôler le colmatage minéral sur le membranes échangeuses de cations au cours des procédés électromembranaires. De plus, l'application de courants surlimites provoquant la formation de vortex électroconvectifs a des avantages en matière de diminution du colmatage et d'amélioration de la performance des procédés. Il est démontré pour la première fois dans cette thèse qu'il est possible d'appliquer un champ électrique pulsé sur des cellule d'électrodialyse comprenant dans leur configuration membranaire une ou plusieurs membrane(s) bipolaire(s). Finalement, des traitements électromembranaires efficaces de solutions contenant des protéines peuvent être effectués par couplage avec des membranes d'ultrafiltration: ce couplage permet d'éviter la formation de colmatage protéique au sein de la cellule d'ED.

Abstract

Supply of fresh drinking water, healthy food, bio-active substances and power may be accomplished by ecofriendly electrodialysis (ED) technology. Nowadays, two main barriers such as membrane fouling and concentration polarization (CP) phenomena stand in the way of ED processes. Recent works demonstrated that application of pulsed electric field (PEF) during ED might completely eliminate protein fouling and drastically decrease fouling by minerals (scaling). Moreover, the current pulsations prevent widening of concentration polarization layer. In spite of the promising results of PEF application, the optimal duration of pulse/pause lapses and influence of PEF on membrane fouling and CP in the solutions containing fouling agents are still opened and disputable questions.

The thesis results demonstrate that PEF with short pulse/pause durations can be applied to electromembrane processes in order to avoid completely the scaling on anion-exchange membrane and to control the scaling on cation-exchange membrane. Moreover, "overlimiting" currents inducing the formation of electroconvective vortices are advantageous from the point of scaling decrease and improvement of process performance. The possible application of PEF to ED systems with bipolar membrane(s) was demonstrated for the first time. Furthermore, effective electromembrane treatments of solutions containing proteins could be performed with pretreatment by ultrafiltration membrane, which avoids the clogging of ED stack.

List of contents

CHAPTER V. HYBRID BIPOLAR MEMBRANE ELECTRODIALYSIS/ ULTRAFILTRATION TECHNOLOGY FOR CASEIN PRODUCTION: EFFECT

List of tables

List of figures

xviii

List of abbreviations

AEM   Anion exchange membrane

AFM   Atomic force microscopy

BM   Bipolar membrane

CEM   Cation exchange membrane

CP   Concentration polarization

CVC   Current-voltage curve

ChP   Chronopotentiogram

DBL   Diffusion boundary layer

DVB   Divinylbenzene

DR   Demineralization rate

EC   Energy consumption

ED   Electrodialysis

EDBM Bipolar membrane electrodialysis

EDBM-UF   Bipolar membrane electrodialysis with ultrafiltration module

EDBM-UF-PEF Bipolar membrane electrodialysis with ultrafiltration module and application of pulsed electric field

EDS   Energy dispersive x-ray spectroscopy

ICP   Inductively Coupled Plasma analysis

MF   Microfiltration

NF   Nanofiltration

PDMS Polydimethylsiloxane

PVC   Polyvinylchloride

RO   Reverse osmosis

SC   Scaling content

SCR   Space charge region

SEM   Scanning electron microscopy

CLSM Confocal laser scanning microscopy

IEM   Ion exchange membrane

LCD   Limiting current density

PEF   Pulsed electric field

UF   Ultrafiltration

UV   Ultraviolet

XRD   X-ray diffraction

…I don't care about snow,

Heat and pouring rain

When my friends are with me…

Russian song

A journey of a thousand miles

Begins with a single step

Lao Tzu

Acknowledgements

The three years of scientific journey have led to this thesis. The journey was full of positive moments, challenges, new friends and comrades, new cultures and, most of all, new insights leading to understanding how science is joyful and important in my life. Assuredly, there will be no journey at all without fellow-travelers. They were with me during the hard times sincerely supporting and inspiring me and during the successful times sharing the gladness and wishing new horizons. This section is a very good opportunity for me to tell how I love and appreciate all of you, my fellow-travelers!

First of all, I want to tell that whole my life I have a person with huge soul and warm heart who inspires and provides me an example of love, strength and passion. Mom, this person is you. I guess, there is no words to express my feelings to you. I understand how it was difficult to raise me without dad (my daddy died when I was 2 years old). However, you did it so well in spite of difficult times in Russia, my bad character and other obstacles. Looking how you struggle the challenges remaining always positive and finally attaining the goals, I just adopted this kind of behavior to myself and it helps me a lot! I really want you to be very happy and healthy, and I am trying to do my best to use every moment with you for making you happier. Additionally, I really want to thank my dear mother in God Natalia for being with our family whole my life, kindly supporting and giving the positive energy.

My dear supervisor, Laurent Bazinet, you are my guiding light. I will never forget the day I firstly met you in the airport. Actually, flight to Québec was my first travel abroad. I was really tired of flights and of course I worried about everything: my language, adaptation, studies etc. However, all worries were dissipated as soon as I saw you and talked to you receiving only positive emotions (though, a bit part of worries came back when I saw mountains of snow outside the airport). I do not remember even one moment when you were in a bad mood. This your quality is a great treasure and creates an impeccable and always positive atmosphere in the team. This kind of atmosphere is actually the best environment for doing the research. I want to thank you very much for the constructive discussions, very useful advices, professional opinion and kind support. You are excellent scientist and mentor. Moreover, I cannot forget to mention the parties organized by you at your home. It is there I firstly met your very friendly family. Dear Hélène, Soléne, Mathieu

and of course Laurianne, thank you very much for the cozy atmosphere of your house and light feelings I always acquired being with you. Laurianne, your handmade postcards and especially the picture of man, representing the friendship of Russia and Canada, warm my heart every day.

I would like to thank my co-directors Dr. Victor Nikonenko (Kuban State University, Russia) and Dr. Gérald Pourcelly (Institut Européen des Membranes, Université Montpellier, France) for the opportunity to continue my education in the Université Laval. I really appreciate useful and fruitful discussions with you as well as your wise advices and inspiring commentaries. Furthermore, I want to thank Dr. Victor Nikonenko and Dr. Natalia Pimenskaya for the supervision of the studies which have been carried out in the French-Russian International Associated Laboratory "Ion-exchange membranes and related processes" during collaboration in 2013. My dears Ekaterina Nevakshenova, Semyon Mareev, Nadezhda Melnik, Veronika Sarapulova, Ekaterina Knyaginicheva, Anton Kozmai and Mikhail Porozhny, I really appreciate your support and advices, thank you very much for the enjoyable time I had with you during collaboration 2013.

Dr. Jongyoon Han, Siwon Choi and Hyuckjin Jean Kwon, I really appreciate the opportunity to perform part of my experiments in Research Laboratory of Electronics (MIT, USA). Thank you for the support with experiments and discussions.

I would like to acknowledge Sophie Banville, Renée Michaud, André Lagacé, Hélène Fortier and all participants of INAF for the support and opportunities of international collaborations, for the organization of useful and interesting meetings and conferences as well as entertaining events.

I kindly appreciate the participation of Dr. Yves Pouliot in the pre-reading of this research work and I would also like to thank Drs. Gaétan Lantagne and Serge Kaliaguine for their kind participation in the thesis evaluation committee.

Special acknowledgements for Jacinthe Thibodeau, Élodie Rozoy and Monica Araya-Farias. You made my experimental work much comfortable by sharing your experience, helping with necessary equipment and reagents, and always being ready to support me. I would like as well to acknowledge Diane Gagnon, Mélanie Martineau, Pascal Lavoie and Pierre Côté from Faculté des sciences de l'agriculture et de l'alimentation (Université Laval) and André Ferland from Faculté des Sciences et de Génie (Université Laval), for your technical assistance during accomplishment of experimental work.

Foreword

This doctoral thesis is composed of 6 chapters. The first chapter is a literature review concerning the electrodialysis process itself and its related phenomena such as those associated to concentration polarization, to ion-exchange membrane fouling, its nature, the techniques used for fouling detection and for its nature identification, and the use of different techniques for fouling control. The second chapter proposes the problematic inherent to our subject of research, the hypothesis established and to be answered, and the main and specific objectives of this study. The following three chapters, written as three scientific papers, describe the works carried-out, the results obtained and the discussions and conclusions discerned. A general conclusion along with thereby given perspectives closes this thesis.

A first article was published in "Journal of Membrane Science (2014) Vol. 468, pp. 389-399" entitled "**Intensification of demineralization process and decrease in scaling by application of pulsed electric field with short pulse/pause conditions**". Authors: Sergey Mikhaylin, Victor Nikonenko, Gérald Pourcelly and Laurent Bazinet. This first article aims to evaluate the short pulse/pause conditions during ED of a model salt solution containing Ca^{2+} and Mg^{2+} ions in order to hamper membrane scaling and to intensify demineralization process.

Part of research for the second article was performed in collaboration with French-Russian International Associated Laboratory "Ion-exchange membranes and related processes" (Kuban State University, Krasnodar, Russia) and with "Research Laboratory of Electronics at MIT" (Massachusetts Institute of Technology, Cambridge, USA). This article submitted in "Journal of Membrane Science" is entitled "**How nanostructure and surface properties of cation-exchange membranes affect membrane scaling formation and electroconvective vortices: influence on performance of electrodialysis with pulsed electric field**". Authors: Sergey Mikhaylin, Victor Nikonenko, Natalia Pismenskaya, Gérald Pourcelly, Siwon Choi, Hyukjin Jean Kwon, Jongyoon Han and Laurent Bazinet. The second article aims to study the impact of CEM structure on development of water splitting and electroconvection to reveal the influence of these phenomena on scaling formation and ED performance during ED of model salt solution

with two PEF conditions (2s/0.5s and 2s/0.67s). These two PEF modes were chosen based on the results of previous article where they were the best modes in terms of scaling prevention and ED performance.

The third article to be submitted in "Green Chemistry" is entitled "**Hybrid bipolar membrane electrodialysis/ultrafiltration technology assisted by pulsed electric field for casein production**". Authors: Sergey Mikhaylin, Victor Nikonenko, Gérald Pourcelly and Laurent Bazinet. The third article describes the use of a new technique consisting of EDBM module coupling with UF module and application of PEF mode (EDBM-UF-PEF) to produce casein from skim milk. The goal of EDBM-UF-PEF technique is elimination of the EDBM stack clogging by caseins and prevention of CEM scaling.

In all cases, Mr. Sergey Mikhaylin is the lead author and was in charge of the conception, the planning and the execution of the practical works, as well as of the articles writing. Dr. Victor Nikonenko and Dr. Gérald Pourcelly, thesis co-directors and co-authors of the three articles, have contributed to the planning of the experiences, to the discussion of the results obtained, and to the revision of the articles. Dr. Laurent Bazinet, thesis director and co-author of the three articles written, was responsible for the conception of the practical works, for the discussion of the results obtained and for the revision of the written articles. Dr. Natalia Pismenskaya, co-author of the second article, supervised the experimental part performed in French-Russian International Associated Laboratory "Ion-exchange membranes and related processes" (Kuban State University, Krasnodar, Russia) and was responsible for the discussion of the results obtained. Ms. Siwon Choi and Mr. Hyukjin Jean Kwon, co-authors of the second article, fabricated the microfluidic devices and built-up the measurement system in "Research Laboratory of Electronics at MIT" (Massachusetts Institute of Technology, Cambridge, USA). Dr. Jongyoon Han, co-author of the second article, supervised the microfluidic visualization experiments in "Research Laboratory of Electronics at MIT" (Massachusetts Institute of Technology, Cambridge, USA).

Introduction

Electrodialysis (ED) is one of the highly developed modern membrane technologies, which have intensive applications in the food industry. It is used to concentrate, purify, or modify food. There are many favorable advantages of using ED, such as low energy consumption, modular design, high efficiency, and suitability for the heat sensitive food products. This method differs from other approaches such as ultrafiltration, reverse osmosis, nanofiltration etc. because it does not separate according to the size of the particles. ED is an electrochemical separation process in which ion-exchange membranes (IEM) in combination with an electrical potential difference (electric field) are used to remove ionic species from an aqueous solution (Strathmann 2004). Bipolar membrane electrodialysis (EDBM), a variety of ED with special membranes allowing H^+ and OH^- generation, can be used for the regeneration of acids and bases, changing product pH, protein precipitation etc. (Bazinet, Lamarche et al. 1998). In spite of the wide application range of ED, the major problems interfering to its scale-up are concentration polarization (CP) and membrane fouling. CP phenomenon is the emergence of concentration gradient at a membrane/solution interface, which arises due to the ability of a membrane to transport more readily certain type of species under the effect of current (Hoek, Guiver et al. 2013). At a certain current value, CP provokes the development of coupled phenomena such as water splitting and current-induced convection. Water splitting (generation of H^+ and OH^-) leads to the decrease in current efficiency and the increase in energy consumption of the ED. However, current-induced convection (usually electroconvection) enhances the ion transfer towards the membrane surface contributing, ipso facto, to the increase in current efficiency. Additionally, during the ED treatment, certain species can attach to the IEM surface with formation of film or crystalline deposit or can poison membrane pores and channels. Fouling phenomenon leads to the decrease in membrane selectivity and membrane alteration what affect the process economics: cleaning procedures and membrane replacement may cost up to 40 percent of the overall process costs. The main strategies for CP and fouling control are modification of the membrane structure, improving the membrane module construction and pretreatment procedures. In spite of the effectiveness of these approaches, they usually demand substantial investments.

Pulsed electric field (PEF) technique has been proven as a solution against fouling and CP phenomena (Mishchuk, Koopal et al. 2001; Ruiz, Sistat et al. 2007; Cifuentes-Araya, Pourcelly et al. 2011; Malek, Ortiz et al. 2013). A pulsed mode of current consists of applying hashed current: during a definite duration, the system is under the influence of a constant current density (Pulse lapse - T_{on}) and then the current is turned off during a fixed time (Pause lapse - T_{off}). The inhibition of CP at PEF mode is performed during the pause lapse when ions do not migrate through the IEM allowing the decrease of concentration gradient near the IEM interfaces, i.e. shrinkage of CP layer. Additionally, PEF modes allow successful control of membrane fouling. Indeed, Ruiz et al. (Ruiz, Sistat et al. 2007) demonstrated the complete elimination of protein fouling on anion-exchange membrane (AEM), Lee at al. (Lee, Moon et al. 2002) and Park et al. (Park, Lee et al. 2003) reported the prevention of humate fouling on AEM, while Casademont et al. (Casademont, Sistat et al. 2009) and Cifuentes-Araya et al. (Cifuentes-Araya, Pourcelly et al. 2011) reported the decrease of mineral fouling called scaling. Among all membrane fouling types, scaling seems to be the most widespread and troublesome due to the strong affinity of scaling agents to the membrane ion-exchange groups. Hence, scaling control and prevention are difficult issues. Cifuentes-Araya et al. (Cifuentes-Araya, Pourcelly et al. 2012; Cifuentes-Araya, Pourcelly et al. 2013; Cifuentes-Araya, Astudillo-Castro et al. 2014) studied profoundly the mechanisms of scaling formation and found that pH and pulse/pause duration play the most important role in scaling control. Firstly, pH control at the interfaces of IEM is of importance since scaling is very sensitive to pH: alkaline pH favors the scaling formation while acid pH inhibits scaling. Two phenomena may affect the pH during ED treatment such as water splitting and OH- leakage (Cifuentes-Araya, Pourcelly et al. 2012; Cifuentes-Araya, Pourcelly et al. 2013). Secondly, pulse/pause duration is important as well since it affects the water splitting phenomenon as well as scaling composition and quantity. Wide range of pulse/pause durations (from 33.3s to 5s) was tested by Cifuentes-Araya et al. (Cifuentes-Araya, Pourcelly et al. 2013) and a model 3D curve was plotted suggesting the use of shorter pulse/pause durations as the following step in control of scaling and improvement of demineralization. In spite of the thorough studies of mechanisms of scaling control and the importance of water splitting arising during development of CP and OH⁻ leakage, there is a lack of knowledge concerning the influence of current-induced convection (particularly electroconvection) and intrinsic membrane properties on scaling formation at PEF.

2

In this context, the main goal of the present project was to test the short pulse/pause modes and to find the optimal PEF conditions allowing better scaling control as well as to understand the influence of electroconvection and intrinsic membrane properties on scaling formation and ED performance.

To attain this goal, three specific objectives were studied:

1) to study the feasibility of using short pulse/pause lapses in control of IEM scaling and to find the optimal pulse/pause duration;

2) to understand the influence of electroconvection and intrinsic membrane properties on scaling formation and ED performance under the optimal PEF modes;

3) to explore the scaling formation and process performance during electroacidification of skim milk by electrodialysis with bipolar membranes at optimal PEF modes.

CHAPTER 1. LITERATURE REVIEW

I.1 Electrodialysis (ED)

I.1.1   Principle of ED

Electrodialysis (ED) is a modern fast-paced method, which has multiple applications in water-treatment, chemical, pharmaceutical and agri-food industries (Shaposhnik and Kesore 1997; Strathmann 2010; Kotsanopoulos and Arvanitoyannis 2013; Ramchandran and Vasiljevic 2013; Strathmann, Grabowski et al. 2013). This method is a combination of two components. The first component is dialysis, proposed by Nollet (Nollet 1752) for the separation of water and alcohol. In dialysis, the driving force used is a concentration gradient. Separation of substances occurs when certain particles move through a semipermeable membrane from the solution with the higher concentration of these particles to the solution with the lower concentration. The second component is electrolysis, proposed by Nicholson et al. (Nicholson, Carliebe et al. 1800) for water decomposition. Electrolysis is the passage of direct electric current through the system containing two electrodes and ionic solutions (or molten salts), resulting in a chemical reaction at the electrodes and separation of substances. Thus, conventional electrodialysis is the method for separation of ionic species by application of direct electric current on the system consisting of two electrodes and ionic solutions separated by permselective ion-exchange membranes (IEMs).

Figure I.1 represents the typical electrodialysis module with a consecutive distribution of IEMs. There are two types of IEMs used such as cation- and anion-exchange membranes. Their purpose is comprised in separation according to the charge of ions, which would like to move to the different electrodes when current is applied: anions to the anode, cations to the cathode. Anion-exchange membranes (AEMs) let anions moving trough and block the migration of cations, while cation-exchange membranes (CEMs) let cations moving trough and block the migration of anions. IEMs will be discussed in more details in the following sections. Ionic species have different transport numbers in solutions

and in membranes what allows to demineralize and to concentrate solutions as well as to separate ionic mixtures.
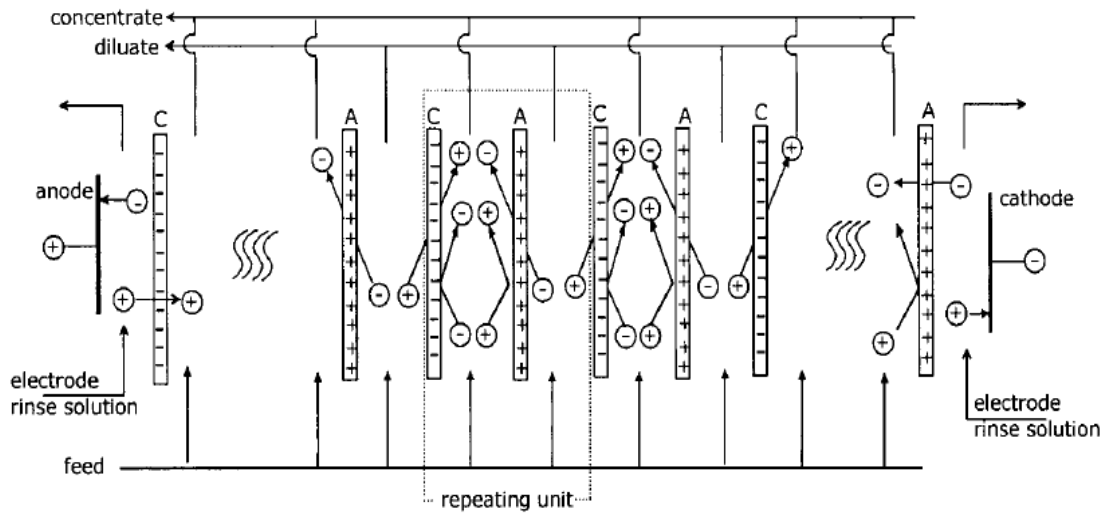
Fig.I.1: Schematic diagram illustrating the principle of desalination by electrodialysis in a stack with cation- and anion-exchange membranes in alternating series between two electrodes (Strathmann 2004).

I.1.2   Mass transfer through the IEMs

The transfer of ions between the membrane and solution is a complex phenomenon, which consists of diffusion, migration and convection components (Yaroslavtsev, Nikonenko et al. 2003; Sata 2004; Strathmann 2004; Nikonenko, Pismenskaya et al. 2010; Bazinet and Castaigne 2011). The contribution of diffusion flux ($J_{i(d)}$) can be expressed as the local gradient of the chemical potential which arises from gradients of concentration or pressure (Eq.I.1).

$$J_{i(d)} = \frac{D_i}{RT} C_i \left(-\frac{d\mu_i}{dx}\right)$$

<div align="right">eq. I.1</div>

where D_i is the diffusion coefficient of the ion i, R the gas constant, T the absolute temperature, μ_i the chemical potential. If the pressure difference between the solution and the membrane is neglected, the chemical potential is given by

6

$$\mu_{i(d)} = \mu_i^0 + RTlna_i \qquad \text{eq. I.2}$$

where μ_i^0 is the chemical potential in the reference state, a_i the activity of ion i. Assuming a dilute solution, ionic activities (a_i) can be replaced by ionic concentrations (C_i). Differentiation of Eq.I.2 in transport direction x, i.e. in direction perpendicular to the membrane surface leads to:

$$\frac{d\mu_{i(d)}}{dx} = RT\frac{dlnC_i}{dx} \qquad \text{eq. I.3}$$

Thus $J_{i(d)}$ is:

$$J_{i(d)} = -D_i\frac{dC_i}{dx} \qquad \text{eq. I.4}$$

The contribution of migration flux ($J_{i(e)}$) can be expressed as the local gradient of the electrical potential $\left(\frac{d\varphi}{dx}\right)$:

$$J_{i(e)} = -u_i z_i C_i \frac{d\varphi}{dx} \qquad \text{eq. I.5}$$

Here z_i is the ionic valence, u_i the ionic electrochemical mobility, which can be expressed according to the Nerst-Einstein equation:

$$u_i = D_i\frac{F}{RT} \qquad \text{eq. I.6}$$

Thus $J_{i(e)}$ is:

$$J_{i(e)} = -D_i\frac{F}{RT}z_i C_i\frac{d\varphi}{dx} \qquad \text{eq. I.7}$$

The third contribution to the mass transfer is related to the convective flux $J_{i(c)}$ arising due to hydrostatic and osmotic pressure gradients:

$$J_{i(c)} = C_i v \qquad \text{eq. I.8}$$

where v is the velocity of convective transport. Thus, the total ionic flux can be expressed as a sum of diffusion, migration and convection fluxes:

$$J_i = J_{i(d)} + J_{i(e)} + J_{i(c)} \qquad \text{eq. I.9}$$

$$J_i = -D_i \left(\frac{dC_i}{dx} + z_i C_i \frac{F}{RT} \frac{d\varphi}{dx} \right) + C_i v \qquad \text{eq. I.10}$$

In electrodialysis the pressure difference across the membrane is kept as low as possible to minimize viscous flow (Strathmann 2004). Since the convection term is considered negligible in relation to the others terms, equation (1.10) becomes:

$$J_i = -D_i \left(\frac{dC_i}{dx} + z_i C_i \frac{F}{RT} \frac{d\varphi}{dx} \right) \qquad \text{eq. I.11}$$

Current (I) in the electrodialytic system arises during the movement of ions in the presence of an electric potential gradient and may be expressed as

$$i = \frac{I}{A} = F \sum_{i=1}^{n} z_i J_i \qquad \text{eq. I.12}$$

where i is the current density, A the membrane surface, F the Faraday constant, z_i the ionic valence and J_i the ionic flux.

I.1.3 Transport numbers and membrane permselectivity

In electrodialysis the transfer of current is related to the ion transfer in solutions and in ion-exchange membranes (Strathmann 2004; Nikonenko, Pismenskaya et al. 2010). In solution, current is carried by both sorts of ions, however cations and anions usually carry different portions of the overall current. The current passing through the IEM is mostly carried by counterions. The part of the current transferred by a certain type of ion is characterized by their transport numbers (Damaskin 2001). In the solution, ionic transport numbers can be calculated as

$$t_+ = \frac{u_+}{u_+ + u_-} \text{ and } t_- = \frac{u_-}{u_+ + u_-} \qquad \text{I.13}$$

where t_+, u_+ and t_-, u_- are the transport numbers and electrochemical mobilities of cations and anions in the solution. In the solution of binary electrolyte $t_+ + t_- = 1$ (Damaskin 2001). In the membrane phase ionic transport numbers depend on the solution concentration (C) and concentration of the membrane ion-exchange groups ($\bar{C}_R$) and can be approximately estimated by the following equations (Sata 2004)

$$\bar{t}_+ = \frac{\bar{u}_+\left(\sqrt{\bar{C}_R^2 + 4C^2} + \bar{C}_R\right)}{\bar{u}_+\left(\sqrt{\bar{C}_R^2 + 4C^2} + \bar{C}_R\right) + \bar{u}_-\left(\sqrt{\bar{C}_R^2 + 4C^2} - \bar{C}_R\right)} \qquad \text{I.14}$$

$$\bar{t}_- = \frac{\bar{u}_-\left(\sqrt{\bar{C}_R^2 + 4C^2} - \bar{C}_R\right)}{\bar{u}_+\left(\sqrt{\bar{C}_R^2 + 4C^2} + \bar{C}_R\right) + \bar{u}_-\left(\sqrt{\bar{C}_R^2 + 4C^2} - \bar{C}_R\right)} \qquad \text{I.15}$$

where $\bar{t}_+$, $\bar{u}_+$ and $\bar{t}_-$, $\bar{u}_-$ are the transport numbers and electrochemical mobilities of cations and anions in the membrane phase. Transport numbers play crucial role in the estimation of membrane permselectivity, which is one of the most important parameters in terms of the efficiency of electrodialysis. It is possible to distinguish two types of ion-exchange membrane permselectivity such as permselectivity to the ions with certain charge (counter-

ion and co-ion transfer) and permselectivity to the ions of the same charge (Zabolotsky and Nikonenko 1996; Sata, Sata et al. 2002; Sata 2004). The first type of permselectivity is explained by the Donnan membrane equilibrium (Strathmann 2004) and may be calculated as

$$P(CEM) = \frac{\bar{t}_+ - t_+}{t_-} \qquad \text{I.16}$$

$$P(AEM) = \frac{\bar{t}_- - t_-}{t_+} \qquad \text{I.17}$$

where P(CEM) and P(AEM) are the permselectivities of CEM and AEM respectively. The ideal permselective IEM has a P value equal to 1. It means that through the ideal permselective membrane, current is transfered only due to counter-ions. The second type of ion-exchange membrane permselectivity is related to the ability of IEM to transfer counter-ions, which have a certain charge (Sata, Sata et al. 2002; Strathmann 2004; Gärtner, Wilhelm et al. 2005; Van Geluwe, Braeken et al. 2011). For example, for two different cations (A and B) permselectivity of CEM (P_B^A) may be calculated as

$$P_B^A = \frac{\bar{t}_A / \bar{t}_B}{C_A / C_B} \qquad \text{I.18}$$

Where $\bar{t}_A$ and $\bar{t}_B$ are transport numbers of cation A and B in the membrane phase, and C_A and C_B are the concentrations (equivalent) of cations A and B at the membrane surface of the desalting side of solution respectively.

I.1.4 <u>Concentration polarization phenomena and limiting current density</u>

As was discussed above, ionic transport numbers are different in solution (t_i) and in membranes ($\bar{t}_i$). For example, for the NaCl in solution t_{Cl}=0.61 and t_{Na}=0.39, however in the CEM $\bar{t}_{Na} \approx 1$ and $\bar{t}_{Cl}$ is close to zero (Vasil'eva, Shaposhnik et al. 2006; Nikonenko, Pismenskaya et al. 2010). This difference in transport numbers allows demineralization and

concentration of solution. However, the same difference in transport numbers causes the emergence of concentration gradients in the thin layers of solution near the membrane surfaces. These thin layers of solution are called diffusion boundary layers (DBL) and phenomena of concentration gradients are called the concentration polarization (CP) phenomena. It was believed that the maximal value of ionic flux is related to the maximal concentration gradient, when the solution concentration near the membrane surface from the diluate side becomes very small in comparison to the concentration of bulk solution. Further increase of the current density carrying by ions with increasing the potential difference is impossible (Peers 1956; Peers 1958). This state of the electrodialytical system was called limiting state and current density corresponding to this state was called limiting current density (LCD). In works devoted to the study of CP phenomena in electromembrane systems it was found that near the LCD there is an increase of the system resistance and generation of H^+ and OH^- ions. (Kressman and Tye 1956; Cowan and Brown 1959; Kressman 1969). The first effect leads to the increase in energy consumption and cost of ED and the second effect leads to the decrease in current efficiency and sedimentation when the solution contains components which are sensitive to pH changes (Bobreshova 1980; Casademont, Pourcelly et al. 2007; Cifuentes-Araya, Pourcelly et al. 2011). Figure I.2 represents the simple model of the concentration profile in the desalting and concentrating channels, where δ is the thickness of the DBL, C_i the concentration in the bulk solution and $C_{1(2)s}$ the solution concentration near the membrane surface.
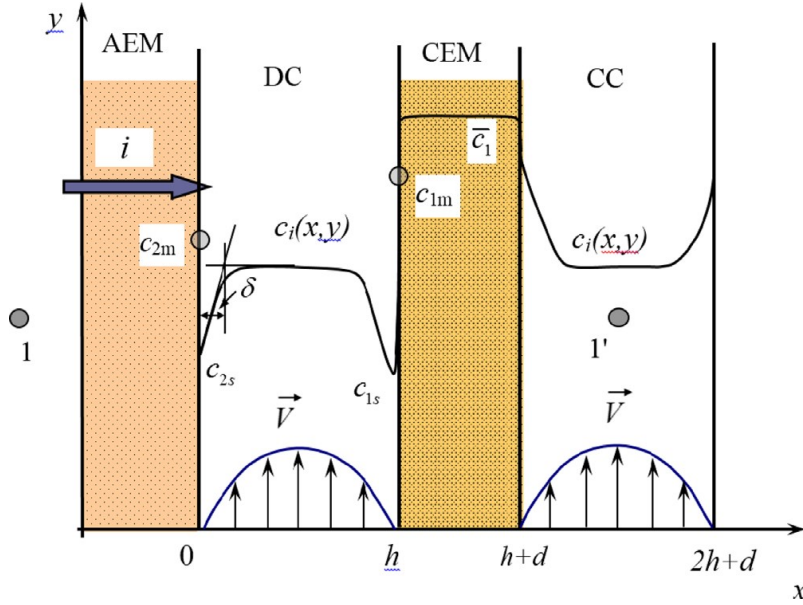
Fig.I.2: Schematic representation of an elementary ED cell with an anion-exchange (AEM) and a cation-exchange (CEM) membranes; DC and CC are desalting and concentrating channels, respectively (Urtenov, Uzdenova et al. 2013).

To describe ion transfer in electromembrane systems the concentration gradient in the interface is normally used (Nikonenko, Pismenskaya et al. 2010; Urtenov, Uzdenova et al. 2013)

$$\left(\frac{\partial c}{\partial x}\right)_{x=\delta} = \frac{C_s - C_0}{\delta} = -\frac{i}{FD}(t_i - \bar{t}_i) \qquad \text{I.19}$$

where δ is the thickness of the DBL, C_s and C_0 are the solution concentrations near the membrane surface and in the bulk solution, i the current density, F the Faraday constant, D the electrolyte diffusion coefficient, t_i and $\bar{t}_i$ are ionic transport numbers in solution and membrane respectively. Equation I.19 shows that concentration gradient increases with increasing current density. In the limiting state, the solution concentration near the membrane surface is close to zero ($C_0 \approx 0$). Thus, the limiting current density value may be calculated as

$$i_{lim} = \frac{C_0 DF}{\delta(t_i - \bar{t}_i)} \qquad \text{I.20}$$

or the limiting current density of each counter-ion (Zabolotsky and Nikonenko 1996) can be calculated as

12

$$i_{\lim i}^{0} = \frac{D_i C_i F}{\delta}\left(1 - \frac{z_i}{z_A} - \frac{z_i}{z_A}\frac{i_{\lim A}\delta}{D_A C_A F}\right)$$

I.21

where indexes i and A relate to counter-ion and co-ion respectively. The visualization of CP and consequently formation and development of diffusion layers during ED in a wide range of current densities was demonstrated by Vasil'eva et al. (Vasil'eva, Shaposhnik et al. 2006) (Fig.I.3).
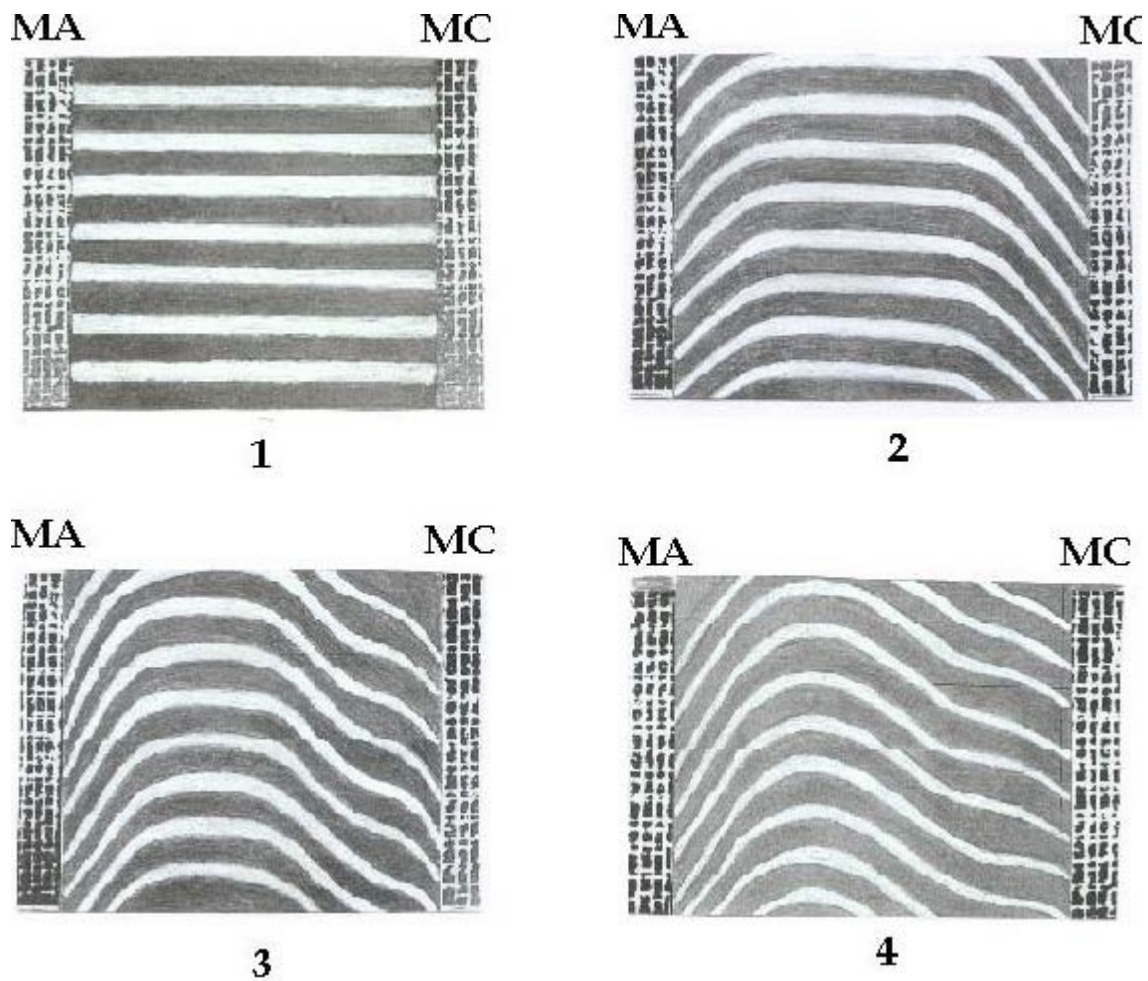
Fig.I.3: Interferograms of the solution in the desalination compartment for electrodialysis of 1.0×10^{-2} mol/l of sodium chloride solution under the flow rate of 1.26×10^{-3} m/s, intermembrane distance of 1.5×10^{-3} m, coordinate in the direction of solution feed 1.1×10^{-2} m. Current densities, A/m^2: $1 - 0$; $2 - 18.5$ (1.1 i_{lim}) ; $3 - 59.7$ (3.6 i_{lim}) ; $4 - 126.0$ (7.5 i_{lim}).

Kim et al. (Kim, Wang et al. 2007) visualized CP phenomena using the permselective nanochannel and in further investigations (Kim, Ko et al. 2010) it was proposed original method for the sea water desalination using CP phenomena with decrease in salinity from 500 mM to 10 mM. The analysis of CP phenomena as well as investigations of the DBL structure was carried out in some works (Sata 1969; Taky, Pourcelly et al. 1992; Taky, Pourcelly et al. 1992; Krol, Wessling et al. 1999; Kozmai, Nikonenko et al. 2010; Mishchuk 2010) by means of electrochemical methods, in other works (Makai 1978; Blavadze 1988; Bobreshova, Kulintsov et al. 1990; Manzanares 1991; Zabolotskii, Shel'deshov et al. 2006; Zabolotskii, Sharafan et al. 2008) with application of rotating-disk technique and by Kwak et al. (Kwak, Guan et al. 2013) with application of the microfluidic ED platform. Furthermore, modeling of the DBL conditions and description of the ED system when current density reaches the limiting value was performed by (Spiegler 1971; Tanaka, Iwahashi et al. 1994; Nikonenko, Zabolotsky et al. 2002; Zabolotskii, Manzanares et al. 2002; Tanaka 2004; Rubinstein and Zaltzman 2010). Nowadays, due to the deep investigations of the CP phenomena, it is possible to see (Fig.I.4) differences between the conventional and contemporary representations of the structure of DBL arising during CP.
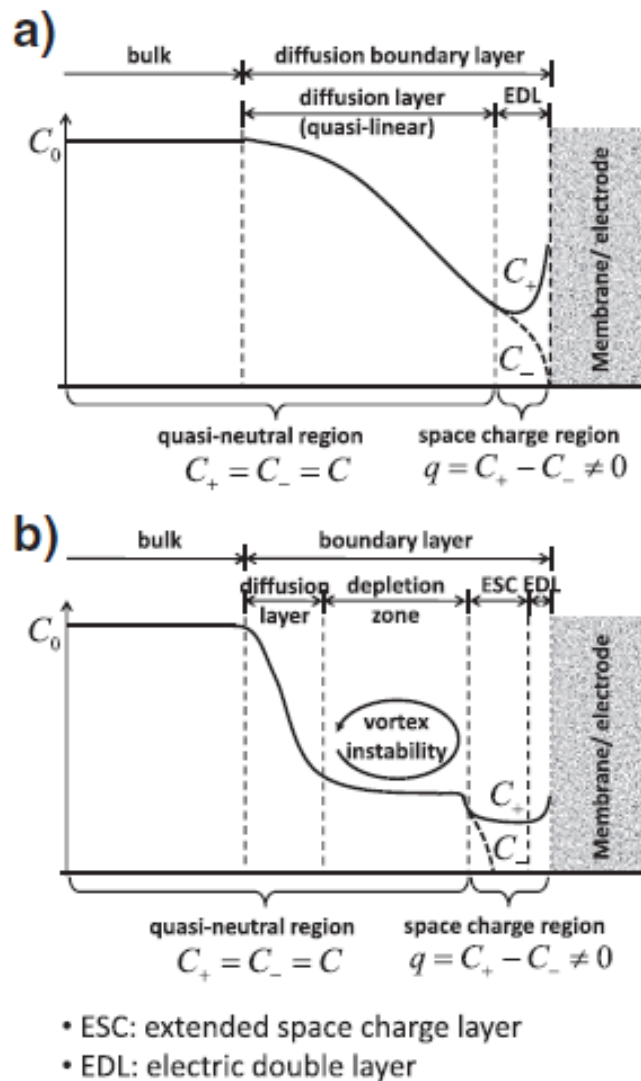
Fig.I.4: Structure of boundary layers represented in a) conventional model and b) contemporary model. C_0, C_+, and C_- indicate the concentration of bulk, counterion (solid line), and coion (dotted line), respectively (adapted from (Kwak, Guan et al. 2013)).

The main differences between conventional (Fig. I.4 a)) and contemporary (Fig. I.4 b)) models are in the representation of DBL and space charge region (SCR). Firstly, in the contemporary model, the thickness of diffusion layer is lower and that is due to the occurrence of a depletion zone forming by current-induced convection, which will be discussed further (Nikonenko, Pismenskaya et al. 2010; Kwak, Guan et al. 2013; Urtenov, Uzdenova et al. 2013). Secondly, in the conventional model SCR consists only of an electrical double layer, however the contemporary model divides SCR into electrical double layer and extended charge region. These investigations of CP phenomena and particularly structure of membrane boundary layers are of great importance in terms of

15

understanding the mechanisms of ionic transfer and increasing the efficiency of ED process (Nikonenko, Kovalenko et al. 2014).

I.1.5 <u>Overlimiting current density</u>

From the above description of the CP phenomena, it is possible to speculate that when the ED system reaches its limiting state (LCD) and electrical resistance increases drastically there is no point in further increasing the potential difference. However, it was found experimentally that further increase in potential difference leads to the significant increase in current (Rubinstein, Staude et al. 1988; Maletzki, Rösler et al. 1992) This state of ED system is called "overlimiting" and is now considered as a perspective direction for the improvement of ED processes (Nikonenko, Kovalenko et al. 2014).

I.1.5.1 <u>Water splitting phenomenon</u>

One of the processes occurring during development of CP and causing the current increment is the water splitting phenomenon. Generation of H^+ and OH^- ions at the surface of IEMs was first noted by Kressman and Tye (Kressman and Tye 1956) and at the surface of bipolar membranes by Frilette (Frilette 1956) in 1956. Furthermore, this fact was proved in a wide range of works (Cooke 1961; Kressman 1969; Simons 1979; Kuroda, Takahashi et al. 1983; Rubinstein, Warshawsky et al. 1984). One can anticipate that the generation of H^+ and OH^- ions occurs when the concentration of electrolyte near the membrane surface reaches zero value. However, the chronopotentiometric measurements (Cooke 1961) and investigations by means of interferometry (Forgacs, Leibovitz et al. 1975; Gavish and Lifson 1979) revealed that water splitting takes place when the concentration attains values of 10^{-3} - 10^{-4} mM. It is worth to emphasize that the transfer of H^+ through the CEM is much weaker than transfer of OH^- ions through the AEM when the current density exceeds LCD (Simons 1979; Krol, Wessling et al. 1999). This fact was explained by differences in transport numbers. It was found that the transport numbers of H^+ have values ranging from $4 \cdot 10^{-5}$ to $11 \cdot 10^{-2}$ (Cooke 1961; Kononov 1971; Gnusin 1972; Rubinstein, Warshawsky et al. 1984) while transfer of OH^- ions occurred at higher velocity and transport numbers attain values of $3 \cdot 10^{-2}$ to $6 \cdot 10^{-1}$ (Cooke 1961; Kononov 1971; Gnusin 1972; Simons 1979; Rubinstein, Warshawsky et al. 1984). The studies of such differences in water splitting

16

phenomenon between different IEMs were carried out by (Kharkats 1988; Taky, Pourcelly et al. 1992; Taky, Pourcelly et al. 1992; Elattar, Elmidaoui et al. 1998; Ottosen, Hansen et al. 2000; Shaposhnik, Vasil'eva et al. 2002; Belova, Lopatkova et al. 2006). The results showed that at the current values near to the LCD the concentration of electrolyte in the vicinity of the CEM is higher than in the vicinity of the AEM where concentrations of H^+ and OH^- ions are commensurable with concentration of these ions in water. This fact was explained by the presence of convection near the surface of the CEM, which can improve the ion transfer and hamper water dissociation (Zabolotsky, Nikonenko et al. 1998; Krol, Wessling et al. 1999; Krol, Wessling et al. 1999; Vasil'eva, Shaposhnik et al. 2006; Nikonenko, Pismenskaya et al. 2010; Pis'menskaya, Nikonenko et al. 2012). The higher water splitting rate on AEM was also observed by means of noise spectra analysis (Fang, Li et al. 1982; Fang, Li et al. 1982). The white noise indicating the water dissociation was registered in the vicinity of the AEM, however near the CEM surface the flicker-noise indicating the development of convection was observed. Another explanation of the preferable water splitting near the AEM can be understood from mechanism of this phenomenon. In fact, water dissociation at the IEM interface occurs via interactions with membrane ion-exchange groups. It was found experimentally that the nature of the membrane ion-exchange groups play the crucial role in generation of H^+ and OH^- ions (Oda and Yawataya 1968; Kressman and Tye 1969; Makai 1978; Simons 1979; Simons 1984; Krol, Wessling et al. 1999). Simons (Simons 1985) proposed the following mechanism of interactions of water molecules with ion-exchange groups

$$AH + H_2O \underset{k_{-1}}{\overset{k_1}{\rightleftharpoons}} A^- + H_3O^+ \qquad\qquad I.22$$

$$A^- + H_2O \underset{k_{-2}}{\overset{k_2}{\rightleftharpoons}} AH + OH^- \qquad\qquad I.23$$

$$B + H_2O \underset{k_{-3}}{\overset{k_3}{\rightleftharpoons}} BH^+ + OH^- \qquad\qquad I.24$$

$$BH^+ + H_2O \underset{k_{-4}}{\overset{k_4}{\rightleftharpoons}} B + H_3O^+ \qquad\qquad I.25$$
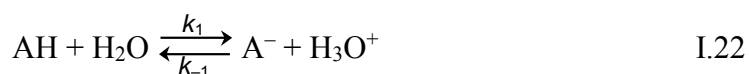
Comparing the rate constants of water splitting from eq. I.22 − I.25 and from the common water dissociation

$$H_2O \xrightarrow[\substack{k_r = 1,4 \cdot 10^{11} L/(mol \cdot s)}]{\substack{k_d = 2,5 \cdot 10^{-5} s^{-1}}} H^+ + OH^-$$

I.26
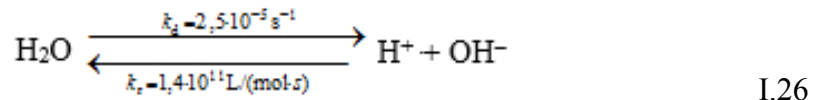
Simons showed that acceleration of this reaction by catalysis with ion-exchange groups might be significant. For example, for the reaction with tertiary amino groups the limiting stage is reaction (I.25) with rate constant $k_4 > 2.5$ s^{-1} (Simons 1979). This value is five orders higher than the dissociation constant (k_d) without ion-exchange groups. It is possible to range the membrane ion-exchange groups in order of increase in rate constants (Nikonenko, Pismenskaya et al. 2010)

$$-N^+(CH_3)_3 < -SO_3^- < -PO_3H^- < = NH, -NH_2^+ < \equiv NH \equiv < -COO^- < -PO_3^{2-}$$
$$k_{lim}, s^{-1} \quad 0 \qquad 3 \times 10^{-3} \quad 3 \times 10^{-2} \quad 10^{-1} \qquad 1 \qquad 10 \qquad 10^2$$

I.27
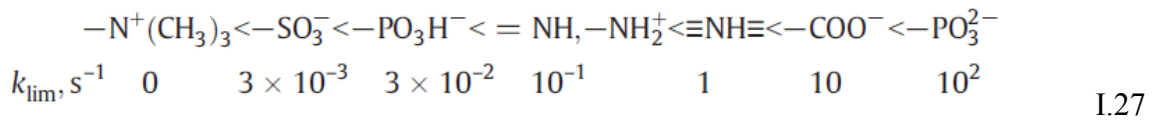
Thus, one can see using CEM with sulfo groups and AEM with tertiary amino groups that the water splitting rate will be 3 orders higher on AEM. Furthermore, acceleration of H$^+$ and OH$^-$ generation was observed in ED systems containing inorganic ions and hydroxides or organic substances, which are able to precipitate on ion-exchange groups (Oda and Yawataya 1968; Kressman and Tye 1969; Kressman 1969; Sakashita, Fujita et al. 1983; Strathmann, Krol et al. 1997; Lee, Moon et al. 2002; Tanaka 2007; Berezina, Kononenko et al. 2008). It is worth to note that the total increment of the water splitting in the "overlimiting" current is really small (around 5 %) and this mechanism cannot be considered as main mechanism (Nikonenko, Kovalenko et al. 2014).

I.1.5.2 Exaltation effect

Another possible mechanism of ion transfer when CP is developed is current exaltation. In membrane systems this effect was firstly described by Kharkats (Kharkats 1985). Exaltation effect arises due to the attraction of counter-ions by-products of water splitting. For example, in desalting channel of ED system with desalination of NaCl solution the increase of current in the "overlimiting" region may be due to attraction of Na^+ by OH^- produced on the CEM surface and due to attraction of Cl^- by H^+ produced on AEM surface. The exalted current is described by the above mechanism called the Kharkats current. For the above example it can be calculated as

$$i_{Na^+}^C = i_{\lim Na^+}^C + i_{OH^-} \frac{D_{Na^+}}{D_{OH^-}}$$

I.28

$$i_{Cl^-}^A = i_{\lim Cl^-}^A + i_{H^+} \frac{D_{Cl^-}}{D_{H^+}}$$

I.29

where $i_{Na^+}^C$ and $i_{Cl^-}^A$ are the Kharkats currents related to CEM and AEM respectively, i_{OH^-} and i_{H^+} the currents generated by water splitting products, D_{Na^+}, D_{Cl^-} and D_{OH^-}, D_{H^+} the diffusion coefficients of counter-ions and water splitting products. It was found that the ratio of diffusion coefficients of counter-ions to diffusion coefficients of water splitting products is of the order of 10^{-1}. This fact leads to the conclusion that the increment in salt counter-ion flux due to the exaltation effect is rather low (around 20 %) (Nikonenko, Pismenskaya et al. 2010).

I.1.5.3 Current-induced convection

The most powerful mechanism leading to the essential exceeding of the current above its limiting value is current-induced convection (Zabolotsky, Nikonenko et al. 1998; Krol, Wessling et al. 1999; Rubinstein and Zaltzman 2000; Pismenskaya, Nikonenko et al.

2007; Nikonenko, Pismenskaya et al. 2010; Pis'menskaya, Nikonenko et al. 2012; Nikonenko, Kovalenko et al. 2014). It is possible to distinguish two types of current-induced convection such as gravitational convection and electroconvection (Nikonenko, Pismenskaya et al. 2010).

I.1.5.3.1   Gravitational convection

This type of current-induced convection arises due to the volume force $\vec{F}_g$ as

$$\vec{F}_g = \vec{g}\Delta\rho \qquad \text{I.30}$$

where $\vec{g}$ is the free-fall acceleration and $\Delta\rho$ the density gradient caused by the gradients of concentration and/or temperature (Zabolotsky, Nikonenko et al. 1996; Nikonenko, Pismenskaya et al. 2010). It is well known that when membranes are placed vertically and there is horizontal density gradient, the volume force $\vec{F}_g \neq 0$ and convection arises without threshold. If the membranes are placed horizontally and there is a vertical density gradient, two cases are possible. First, if the lighter solution layer is under the more dense solution the volume force $\vec{F}_g = 0$ and there is no gravitational convection. Second, in the case of inverse order of solutions disposition the volume force $\vec{F}_g \neq 0$ which leads to the solution mixing. The threshold in development of gravitational convection may be determined by the Rayleigh number (Ra) as

$$Ra = GrSc = \frac{gX_0{}^3\Delta\rho}{\nu D\rho} \qquad \text{I.31}$$

where Ra is the product of the Grashof (Gr) and the Schmidt (Sc) numbers, ν the viscosity, D the electrolyte diffusion coefficient, X_0 the characteristic distance where the variation in the solution density (ρ) takes place. It was found that gravitational convection occurs when Ra is around 1700 (Vessler 1986). In addition, the experimental data and calculations show that gravitational convection can lead to an essential contribution to mass transfer only at

20

relatively high (>0.05M) concentrations, if the intermembrane spacing is rather large (>6 mm) and the flow velocity small (<0.4 cm s^{-1}) (Nikonenko, Pismenskaya et al. 2010).

I.1.5.3.2   Electroconvection

Solution mixing caused by application of potential difference to electromembrane system when there is no density gradients is called electroconvection. Electroconvection can occur in the volume (volumetric electroconvection) and near the membrane surface (electro-osmotic motion). Volumetric electroconvection usually does not play noticeable role in the mass transfer due to the close values of diffusion coefficients of cations and anions (Grigin 1986; Bruinsma and Alexander 1990). The role of the volumetric electroconvection may be essential when diffusion coefficients of cations and anions differ by more than two orders, which could be possible during ED of some high-molecular weak electrolytes. The second type of electroconvection is conventionally considered as the main, which accelerates the mass transfer. The electroconvection near the membrane surface is considered as an electro-osmotic motion and may be distinguished into two principal kinds (Dukhin and Mishchuk 1989; Nikonenko, Pismenskaya et al. 2010; Pis'menskaya, Nikonenko et al. 2012). The electro-osmosis of the first kind arises under the limiting current region due to the action of tangential electric field upon the quasi-equilibrium diffusion part of DBL, which has almost the same structure to that for zero current. This phenomenon has insignificant increment in the mass transfer (Nikonenko, Pismenskaya et al. 2010). Electro-osmosis of the second kind occurs in the overlimiting current region due to the action of an electric force upon the non-equilibrium space charge region. This phenomenon gives birth to the development of electroconvective vortices, which play crucial role in the increment of the overlimiting current. Nowadays, when one speaks about electroconvection in electromembrane systems it usually means electro-osmosis of the second kind. Thus, in the frameworks of the present work during further considerations of electroconvection this term will be understood as electro-osmosis of the second kind. There are two main conventional mechanisms explaining the formation of electro-osmotic instability such as Dukhin-Mishchuk and Rubinstein-Zaltzman electroconvection modes (no forced flow). Dukhin and Mishchuk firstly explained electroosmosis of the second kind considering an ion-exchange resin particle. They

proposed that an electric field should have two components. First component (normal) creates an extended space charge region (SCR) and the second (tangential) brings in motion the charged fluid, resulting in electroconvective mixing (Mishchuk, Gonzalez et al. 2001). Tangential component appears when there is some kind of membrane surface heterogeneity, which leads to the non-uniform distribution of SCR and consecutively to the deflection of current lines from the normality. Rubinstein and Zalzman found that electro-osmosis of the second kind also takes place on the homogeneous membrane surfaces where there is no tangential component (Rubinstein and Zaltzman 2000). These authors proposed that in case of homogeneous surface electro-osmotic vortices appear due to the hydrodynamic instability of the ED system at sufficiently high voltages. Recent works of Kwak et al. (Kwak, Pham et al. 2013) and Urtenov et al. (Urtenov, Uzdenova et al. 2013) considered formation of electroconvective vortices under the forced flow. In this case, concentration distribution is not uniform in the longitudinal direction: the electrolyte concentration decreases with the distance from the channel inlet. The electroconvection mode is induced by tangential electric force as was described above for Dukhin-Mishuk mode. However, membrane surface nonflatness or electric heterogeneity are not necessary when forced flow occurred. For the forced flow, it is possible to distinguish stable relatively small electroconvective vortices (at relatively low voltages) and unstable electroconvective vortices (at a certain voltage threshold about 1 V per cell pair). Contemporary methods of investigations of the electro-osmotic instability such as using of interferometry and microfluidic ED platforms coupled with electrochemical methods and modeling allow deeper understanding of this phenomenon. Nikonenko et al. (Nikonenko, Pismenskaya et al. 2010; Nikonenko, Kovalenko et al. 2014) emphasized perspectives of ED processes at overlimiting currents where electroconvection plays crucial role. The present work also emphasizes the importance of electroconvection that is why this phenomenon will be widely discussed in the following sections on IEMs.

I.2   <u>Ion-exchange membranes (IEMs)</u>

During the above discussion it was revealed that ion-exchange membranes (IEMs) are key components of each ED system. Hence, the present section will aim the description of different types of IEMs, their structure, properties and behavior during ED. Now these

materials evolve rapidly to be suited to high-leveled demands of the modern industrial market. In general, the development of IEMs aims the attainment of following properties (Mizutani 1990; Xu 2005; Nagarale, Gohil et al. 2006; Strathmann, Grabowski et al. 2013):

- High permselectivity (IEM should be highly permeable to the counter-ions or specific counter-ions);

- Low electrical resistance (IEM should provide high permeability under the driving force as a potential gradient);

- Good chemical stability (IEM should be stable in a wide range of pH and in the presence of oxidizing agents);

- Good mechanical stability (IEM should be stable to the mechanical action and should have a low degree of swelling or shrinking in transition from dilute to concentrate ionic solutions);

- Flatness and uniformity of properties over a large membrane area;

- Good durability in practical use;

- Reasonable cost.

I.2.1 Classification of IEMs

All ion-exchange materials can be divided into three large classes (Yaroslavtsev, Nikonenko et al. 2003; Nagarale, Gohil et al. 2006; Volkov, McHedlishvili et al. 2008; Yaroslavtsev and Nikonenko 2009) as

- *Organic* ion-exchange materials
- *Inorganic* ion-exchange materials
- *Hybrid* (organic/inorganic) ion-exchange materials

Since the present work will focus on organic ion-exchange materials, then consideration of this special type of ion-exchange materials will further takes place. Conventional classification of organic ion-exchange materials may be based on their structure and preparation procedure or on their function as a separation medium (Xu 2005; Kariduraganavar, Nagarale et al. 2006; Nagarale, Gohil et al. 2006; Yaroslavtsev and

Nikonenko 2009; Strathmann, Grabowski et al. 2013). A first classification divides membrane by preparation procedure on two large classes such as

- **Homogeneous** IEMs which are obtained by the copolycondensation or copolymerization of monomers, which provides the uniformity of the polymer material;
- **Heterogeneous** IEMs are chemical composites of ion-exchange resins, binder polymer and reinforced material.

Second classification considers the function of IEMs:

- **Monopolar ion-exchange membranes**
  - **Cation-exchange membranes** (CEM) which have negatively charged fixed groups and are permeable to cations;
  - **Anion-exchange membranes** (AEM) which have positively charged fixed groups and are permeable to anions;
- **Bipolar membranes** (BM) which consist of cation-exchange and anion-exchange layers laminated together.

A more detailed classification of IEMs is given by (Xu 2005; Kariduraganavar, Nagarale et al. 2006; Nagarale, Gohil et al. 2006; Yaroslavtsev and Nikonenko 2009).

I.2.1.1 Homogeneous IEMs

Homogeneous IEMs are present in the form of thin films in which ion-exchange component forms a continuous phase. The procedure of making the homogeneous IEMs can be divided in three categories (Kariduraganavar, Nagarale et al. 2006; Nagarale, Gohil et al. 2006; Yaroslavtsev and Nikonenko 2009; Strathmann, Grabowski et al. 2013):

1. Polymerization or polycondensation of monomers; at least one of them should contain moieties which could be further converted into ion-exchange groups;
2. Introduction of ion-exchange moieties into a preformed solid film;
3. Introduction of ion-exchange moieties into a polymer such as polysulfon, followed by dissolving the polymer and casting it onto a film.

The nature of fragments forming homogeneous IEMs is very diverse (Strathmann, Grabowski et al. 2013). The conventional polycondensation usually deals with

phenolsulfonic acid for CEMs and m-phenylene diamine or aliphatic diamine compounds for AEMs with using formaldehyde as a crosslinking agent (Fig.I.5).
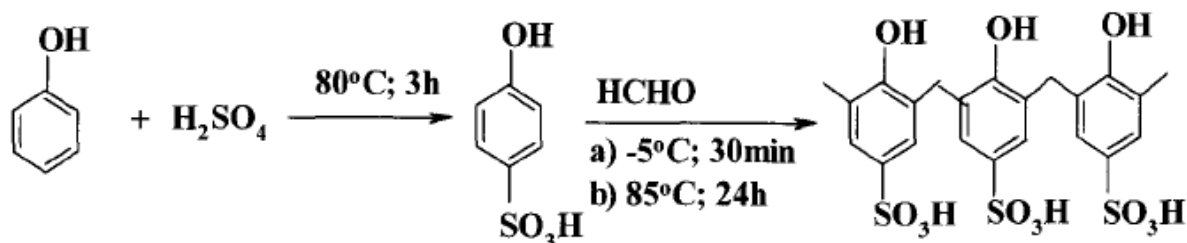
Fig.I.5: Polycondensation process (Kariduraganavar, Nagarale et al. 2006).

One of the most studied types among all IEMs is the fluorinated type developed by DuPont company and called Nafion (Fig.I.6). Synthesis of the Nafion membranes is a four-step procedure: a) the reaction of tetrafluoroethylene with SO_3 to form the sulphone cycle, b) the condensation of these products with sodium carbonate followed by co-polymerization with the tetrafluoroethylene to form the insoluble resin, c) hydrolysis of this resin to form a perfluorosulphonic polymer and d) chemical exchange of the counter ion Na^+ with the proton in an appropriate electrolyte (Nagarale, Gohil et al. 2006).
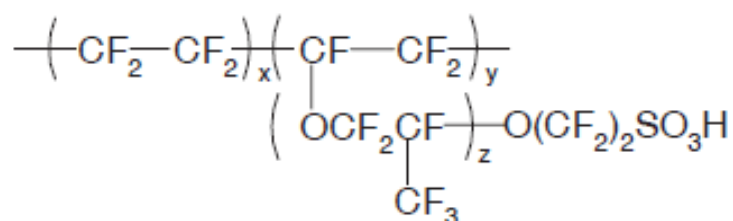
Fig.I.6: Nafion structure (Nagarale, Gohil et al. 2006).

Polymerization of vinyl based monomers followed by sulfonation or amination in solution was commercialized by Tokuyama Soda Co. (Neosepta) and Asahi Glass Co. Another widely used method for homogeneous IEMs preparation is the paste method (Mizutani and Nishimura 1980; Nishimura and Mizutani 1981; Mizutani 1990). The paste, consisting mainly of a monomer with a functional group appropriate to introduce an ion exchange group (F-monomer), divinylbenzene (DVB), a radical polymerization initiator, and a finely powdered polyvinylchloride (PVC), is coated onto PVC cloth as reinforcing material, which is wound, together with separating film, onto a roll. The monomers are then

copolymerized by heating to prepare the base membrane, onto which the ion-exchange groups are introduced. The scheme of paste method is presented on Figure I.7.
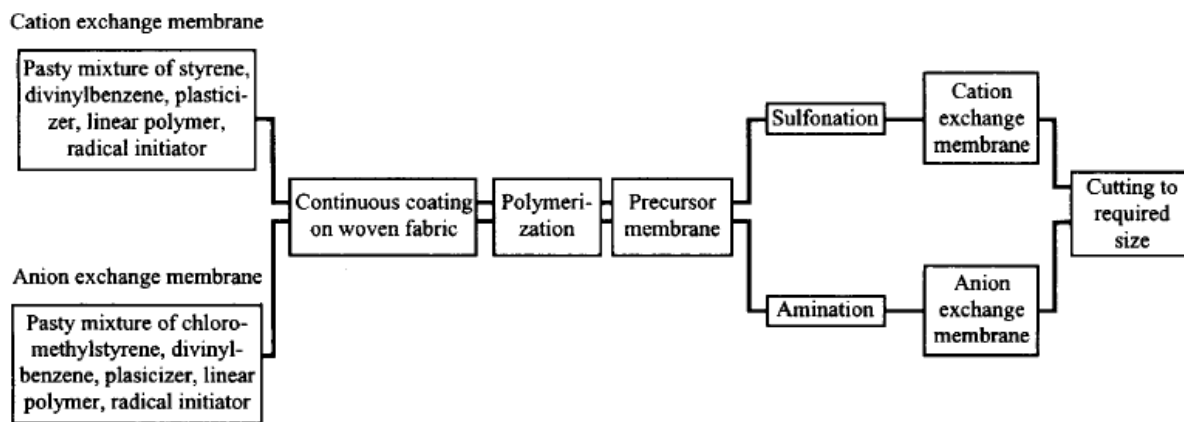
Fig.I.7: Example of a continuous production process for an IEM (Sata 2004).

Complete description of methods of preparing IEMs are widely described in other works (Xu 2005; Kariduraganavar, Nagarale et al. 2006; Nagarale, Gohil et al. 2006). Nowadays due to deep investigations of the membrane structure, it is possible to discuss the structure models and ion transfer mechanisms occurring in ED system. There are several models proposing the structure of homogeneous membranes (Hsu and Gierke 1982; Kreuer, Rabenau et al. 1982; Hsu and Gierke 1983; Eikerling, Kornyshev et al. 1997; Haubold, Vad et al. 2001; Kreuer 2010). Apparently, the most investigated is the structure of Nafion membrane. Figure I.8 represents the Kreuer model of Nafion membrane and sulfonated polyetherketone membrane (Kreuer 2010). This good example demonstrates that different materials and procedures of membrane preparation play important role in formation of the membrane micro- and nanostructure. Nafion membrane has good-connective wide channels without dead-end channels and small $-SO_3^-/-SO_3^-$ separation. These advantages of Nafion play crucial role in a wide usage of this homogeneous membrane in modern industrial processes (Heitner-Wirguin 1996; Mauritz and Moore 2004; Xu 2005; Nagarale, Gohil et al. 2006; Kreuer 2010; Kreuer 2012; Yaroslavtsev 2013). Assuredly, the structure organization affects the membrane behavior during ED treatment and predetermine the efficiency of the process. Wider discussion of connection between membrane structure, properties and behavior during ED processes will be provide in the following sections.

26
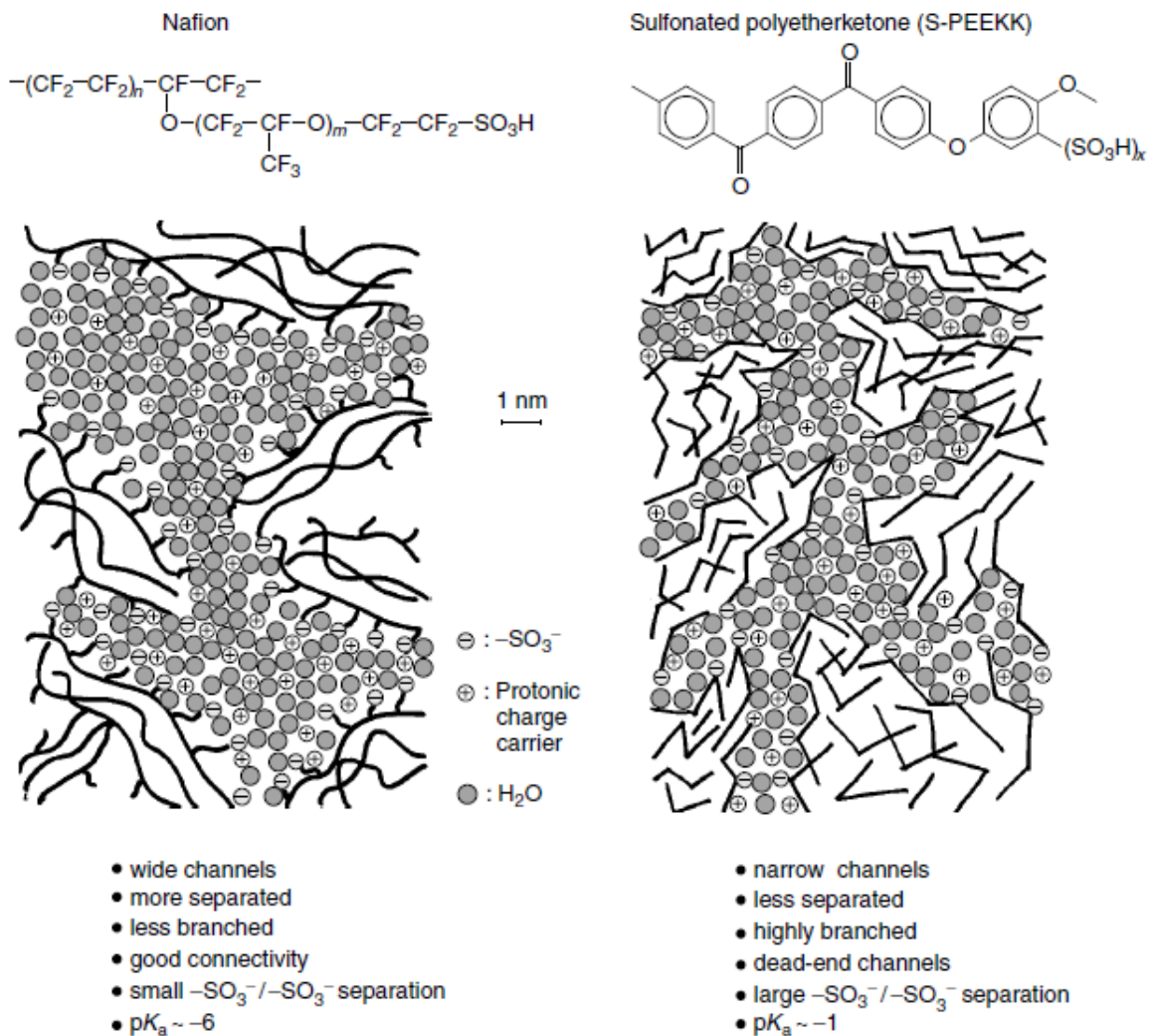
Fig.I.8: Stylized view of Kreuer of the nanoscopic hydrated structures of Nafion and sulfonated polyetherketone (Kreuer 2010).

I.2.1.2 Heterogeneous IEMs

In comparison with homogeneous membranes where the membrane nanostructure is represented as a continuous phase, the heterogeneous membrane is represented as a mixture from ion-exchange resin powder, binder polymer and reinforcing network (Vyas, Shah et al. 2000; Vyas, Shah et al. 2001; Nagarale, Gohil et al. 2006; Yaroslavtsev and Nikonenko 2009)(Fig.I.9). There are several possible procedures of preparing heterogeneous membranes such as (Kariduraganavar, Nagarale et al. 2006; Nagarale, Gohil et al. 2006):

1. Calendaring ion-exchange resin particles into an inert plastic film such as polyvinylchloride, polyethylene or polypropylene;

2. Dry moulding of inert film forming polymers and ion-exchange particles and then milling the mould stock;

3. Resin particles can be dispersed in a solution containing a film forming binder and then the solvent is evaporated to give ion-exchange membrane.
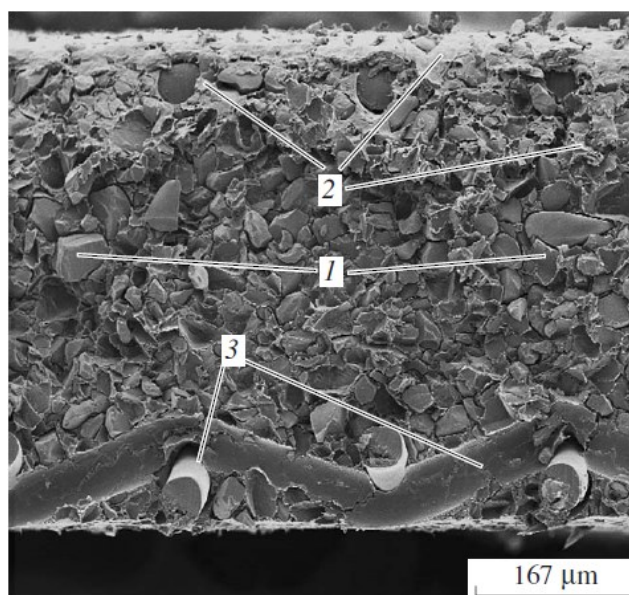
Fig.I.9: Microphotograph of the cut of the MA-40 membrane. (1) Particles of the anion-exchange resin, (2) polyethylene, (3) and threads of a reinforcing network (Yaroslavtsev and Nikonenko 2009).

As for the homogeneous membranes, the structure of the heterogeneous membranes plays key role in the membrane properties and behavior during ED process (Vyas, Shah et al. 2000; Vyas, Shah et al. 2001; Gohil, Shahi et al. 2004; Sata 2004; Volodina, Pismenskaya et al. 2005; Belova, Lopatkova et al. 2006; Kariduraganavar, Nagarale et al. 2006; Berezina, Kononenko et al. 2008). The heterogeneous ion-exchange membranes show the good dimensional stability in comparison to the homogeneous membranes. This may be due to the absence of micro-voids in the homogeneous ion-exchange membranes, since during the polymerization it forms the continuous phase. In the case of heterogeneous membranes, the loss of solvent due to evaporation introduces micro-voids between the resin particles and

binder regions. These microvoids are sufficient to accommodate solvent molecules solvating the ionic species in the resin, so solvation does not manifest the dimensional changes of the membranes (Nagarale, Gohil et al. 2006). The decrease in size of the ion-exchange resin particles seems to be advantageous in terms of improving the burst strength and in terms of increasing the particle surface area what leads to the increase in ion-exchange capacity and the decrease in resistance (Vyas, Shah et al. 2000; Vyas, Shah et al. 2001; Kariduraganavar, Nagarale et al. 2006). Moreover, the mechanical strength can be improved by using suitable reinforcing material (Vyas, Shah et al. 2000).

I.2.1.3 <u>Monopolar IEMs</u>

Monopolar IEMs are divided into two large classes such as cation-exchange membranes (CEMs) and anion-exchange membranes (AEMs). The main difference between them is the different charge of the fixed ion-exchange groups. For CEMs these groups are charged negatively which allows the migration of cations, but rejects the migration of anions. The negatively charged moieties may be presented in form of $-SO_3^-$, $-COO^-$, $-PO_3^{2-}$, $-PO_3H^-$, $-C_6H_4O^-$, etc. (Xu 2005; Yaroslavtsev and Nikonenko 2009; Bazinet and Castaigne 2011). For AEMs fixed groups are charged positively and that allows migration of anions, but blocks migration of cations. The conventional fixed charged groups for AEMs are $-NH_3^+$, $-NRH_2^+$, $-NR_2H^+$, $-NR_3^+$, $-PR_3^+$, $-SR_2$ (Xu 2005; Bazinet and Castaigne 2011). Figure I.10 represents the major applications of monopolar IEMs in modern industrial processes.
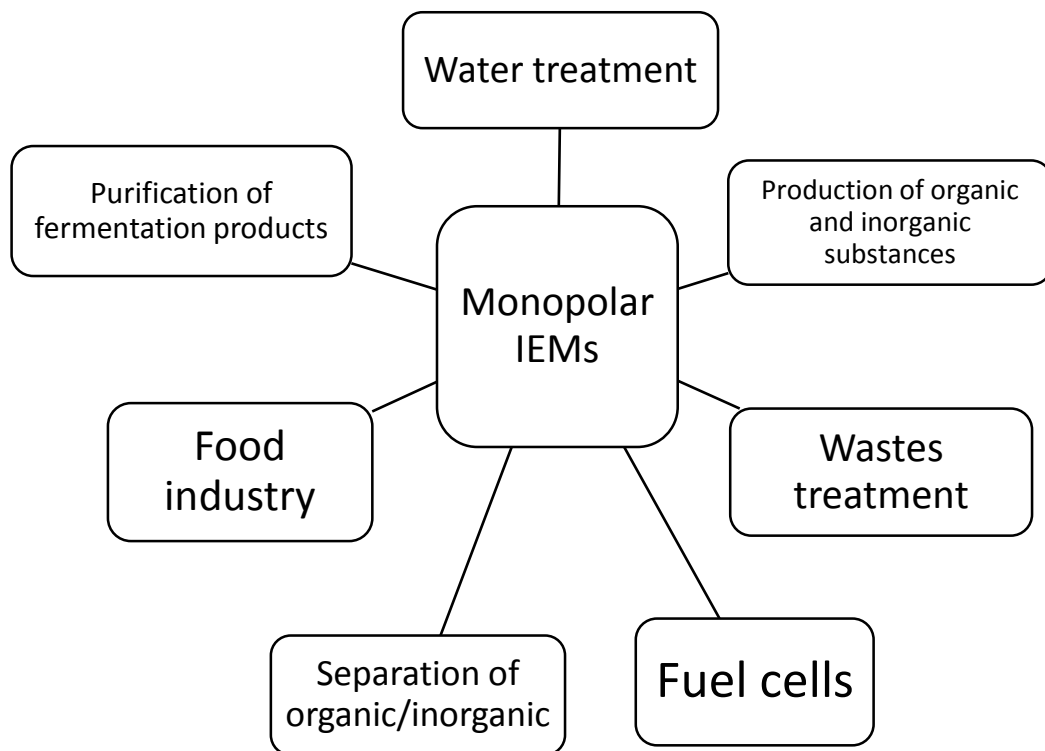
Fig.I.10: Schematic representation of the diversified industrial applications of monopolar IEMs (Girard, Fukumoto et al. 2000; Bazinet 2005; Xu 2005; Nagarale, Gohil et al. 2006; Huang, Xu et al. 2007; Strathmann 2010; Bazinet and Castaigne 2011; Fidaleo 2011; Kotsanopoulos and Arvanitoyannis 2013; Strathmann, Grabowski et al. 2013; Yaroslavtsev 2013).

I.2.1.4 Bipolar IEMs

Bipolar membranes (BM) consist of two layers such as a cation-exchange layer and an anion exchange layer. The production of this membrane type is performed by lamination of two different ion-exchange layers. The main feature of BMs, which determines their application in a wide range of industries, is a water-splitting process with production of protons and hydroxyl ions (Fig.I.11). For the facilitation of water splitting reaction, the most part of BM have hydrophilic junction between two layers of IEMs. Furthermore, it is worth to note that according to the catalytic mechanism of water splitting (section 1.1.5.1) better generation of H^+ and OH^- occurs when the ion-exchange groups are weak acids (bases). For acceleration of water splitting BMs can be modified by heavy metal ion

complexes such as ruthenium trichloride, chromic nitrate, indium sulfate, hydrated zirconium oxide etc. (Oda and Yawataya 1968; Xu 2005; Tanaka 2007).
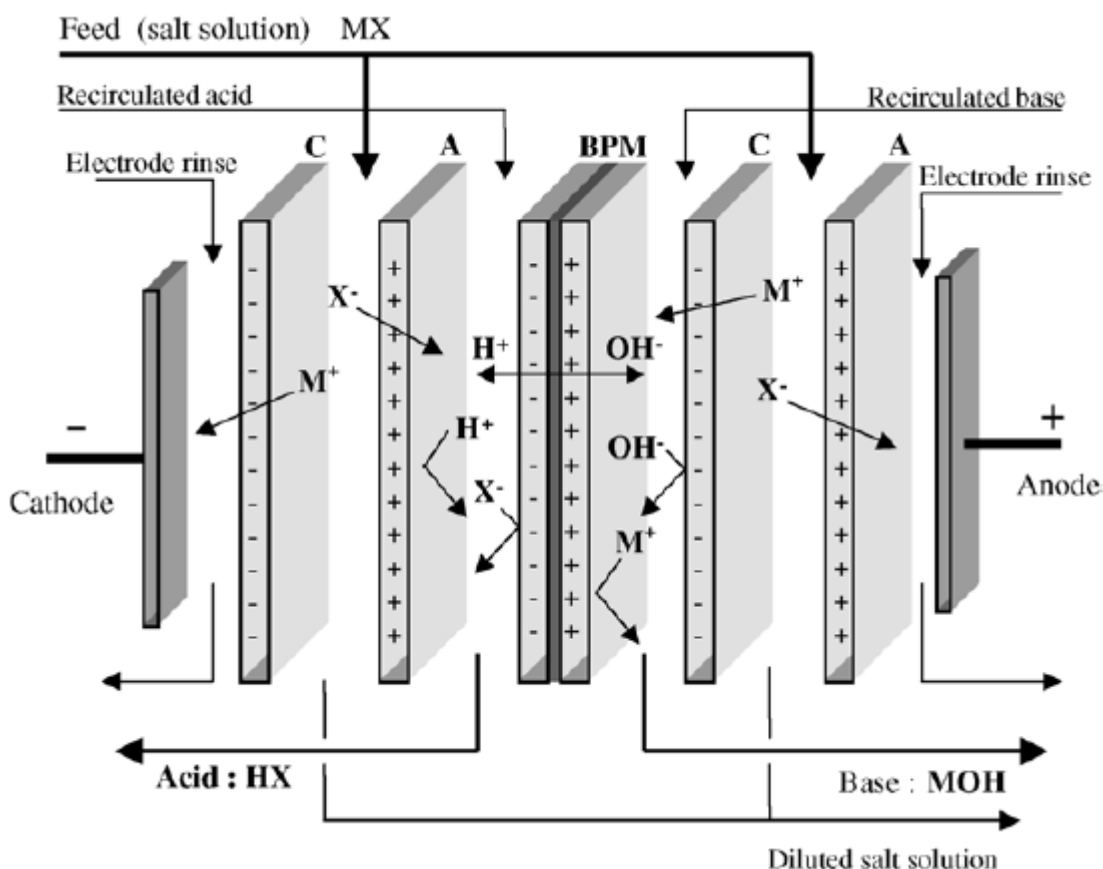
Fig.I.11: Electrodialysis with bipolar membranes for the conversion of a salt MX into its respective acid HX and base MOH (Xu 2005).

There are several methods allowing production of BMs (Frilette 1956; Simons 1986; Bauer, Gerner et al. 1988; Simons 1993; Strathmann, Rapp et al. 1993; Wilhelm, Pünt et al. 2001; Xu 2005) and the major methods are:

- direct preparation from AEMs and CEMs with heat and pressure or with adhesive paste;
- casting a cation-exchange (or anion-exchange) polyelectrolyte on a commercial anion exchange membrane (or on a cation exchange membrane) respectively;
- preparing from the same base membrane by simultaneous functionalizing at the two membrane sides;

The main limitations of BMs are the unsatisfactory chemical stability at high pH values, the membrane instability and poor water splitting at high current densities. Casting method seems to be the most appropriate among all methods because it allows to obtain BM with good mechanical properties, low potential drop, possibilities to operate at high current densities etc. (Bauer, Gerner et al. 1988; Strathmann, Rapp et al. 1993; Xu 2005). The main fields of application of BMs are presented on Figure I.12.
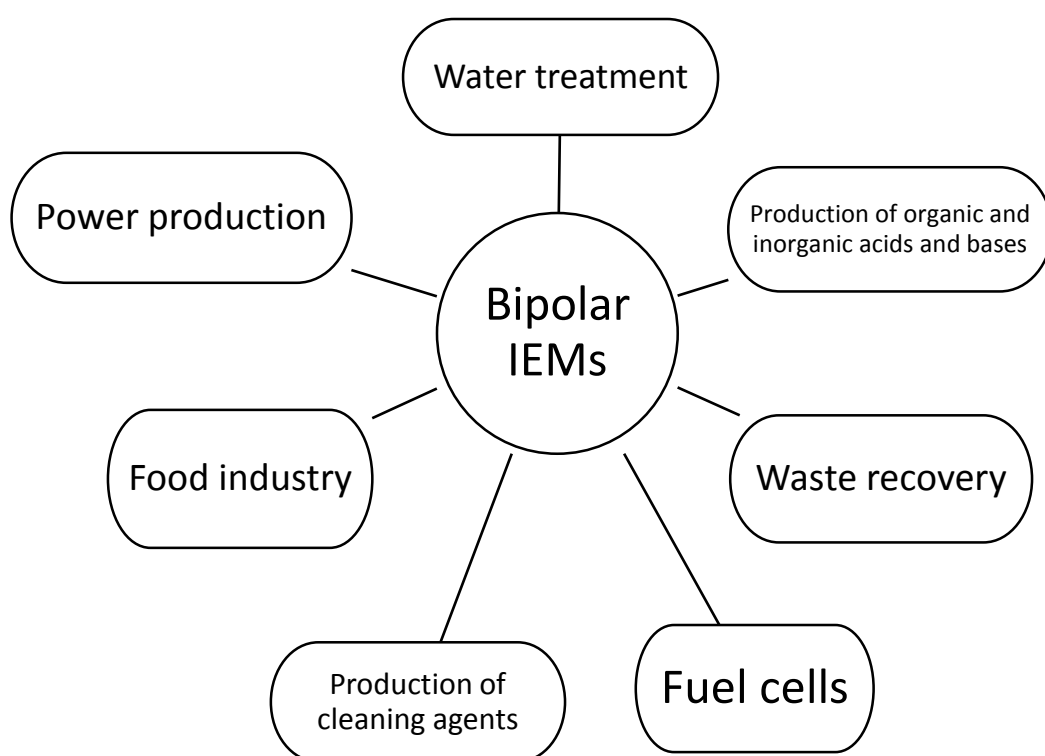
Fig.I.12: Schematic representation of the diversified industrial applications of bipolar IEMs (Bazinet, Lamarche et al. 1998; Girard, Fukumoto et al. 2000; Mafé et al. 2000; Xu 2002; Bazinet 2005; Xu 2005; Nagarale, Gohil et al. 2006; Huang, Xu et al. 2007; Yaroslavtsev and Nikonenko 2009; Bazinet and Castaigne 2011; Fidaleo 2011; Kotsanopoulos and Arvanitoyannis 2013).

I.2.1.4.1   <u>Segmented bipolar membranes</u>

The problem of separation of amino acids inspired Kattan Readi et al. (Kattan Readi, Kuenen et al. 2013) to create a novel concept of bipolar membrane (Fig.I.13). These authors proposed preparing a segmented bipolar membrane by perforating an AEM gluing it onto a CEM. In this case, the CEM is the support membrane and serves as transport membrane for positively charged aminoacids through the perforated areas from the AEM. The non-perforated areas of the AEM glued together to the CEM serve as bipolar areas for enhanced water splitting.
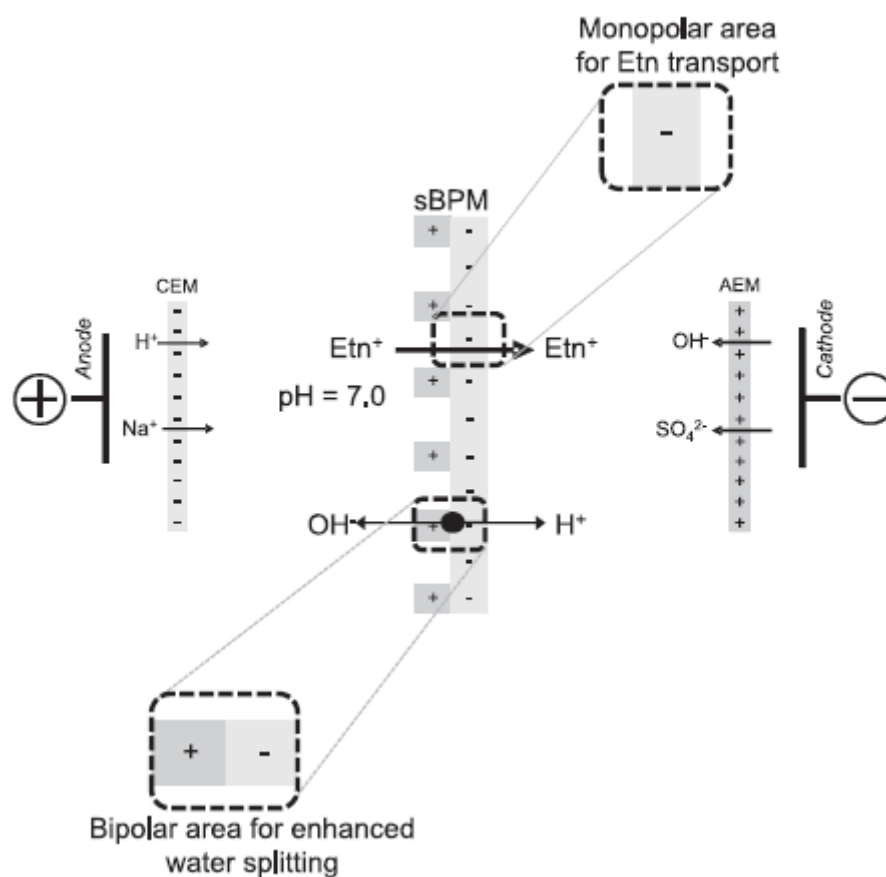
Fig.I.13: Schematic representation of a segmented bipolar membrane for pH control during electrodialysis of ethanolamine (Kattan Readi, Kuenen et al. 2013).

I.2.2 Characterization of IEMs

This section aims to provide information about the most important characteristics of IEMs and methods for their determination. Detailed analysis of membrane characteristics and methods for IEMs characterization was carried out in (Mizutani 1990; Sata 2004; Strathmann 2004; Volodina, Pismenskaya et al. 2005; Berezina, Kononenko et al. 2008).

I.2.2.1 Water uptake

One of the key parameters affecting the IEMs properties is their ability to absorb water (Gebel 2000; Mauritz and Moore 2004; Berezina, Kononenko et al. 2008; Yaroslavtsev and Nikonenko 2009). That is why it is reasonable to start description of IEMs with consideration of water uptake. Why this parameter plays such important role? In the work of Gebel (Gebel 2000) a model of evolution of Nafion membrane structure with different swelling degrees was proposed (Fig.I.14).

This model shows that in the dry state ion-exchange sites do not connect with each other and IEM has a conductivity value around 10^{-5} S/m (Berezina, Kononenko et al. 2008). As soon as the water volume fraction increases, one can see the formation of clusters near to the hydrophilic ion-exchange sites. When the water uptake attains values around 0,25 there is percolation effect leading to an abrupt increase in the membrane conductivity. At the high swelling degrees, it is possible to see the structure inversion and even the dispersion of rod like polymer particles. There are other models providing an additional information about the inside structure of the IEMs during swelling process described in works (Gierke, Munn et al. 1981; Hsu and Gierke 1982; Hsu and Gierke 1983; Berezina, Gnusin et al. 1994; Haubold, Vad et al. 2001; Kreuer 2001; Berezina and Komkova 2003). The IEM swelling depends on nature of the basic polymer, nature of the membrane ion-exchange groups and their structure, degree of cross-linking and the membrane heterogeneity. Moreover, composition of solution with which membrane is in contact plays a very important role on the IEM water content. Thus, water uptake of IEMs having different properties is quite variable (14% - 46%) (Strathmann 2004). For determination of water uptake, membranes should be equilibrated with deionized water for 24 hr. Then their

surface moisture should be mopped with filter papers and the wet membranes should be weighed (W_w). Wet membranes are then dried at a fixed temperature of 80 °C under vacuum during 24 hr and weighed (W_d). Water uptake can be calculated using the following equation (Gohil, Binsu et al. 2006)

$$Water\ uptake\ (\%) = \frac{W_w - W_d}{W_d} \times 100 \qquad \text{I.32}$$
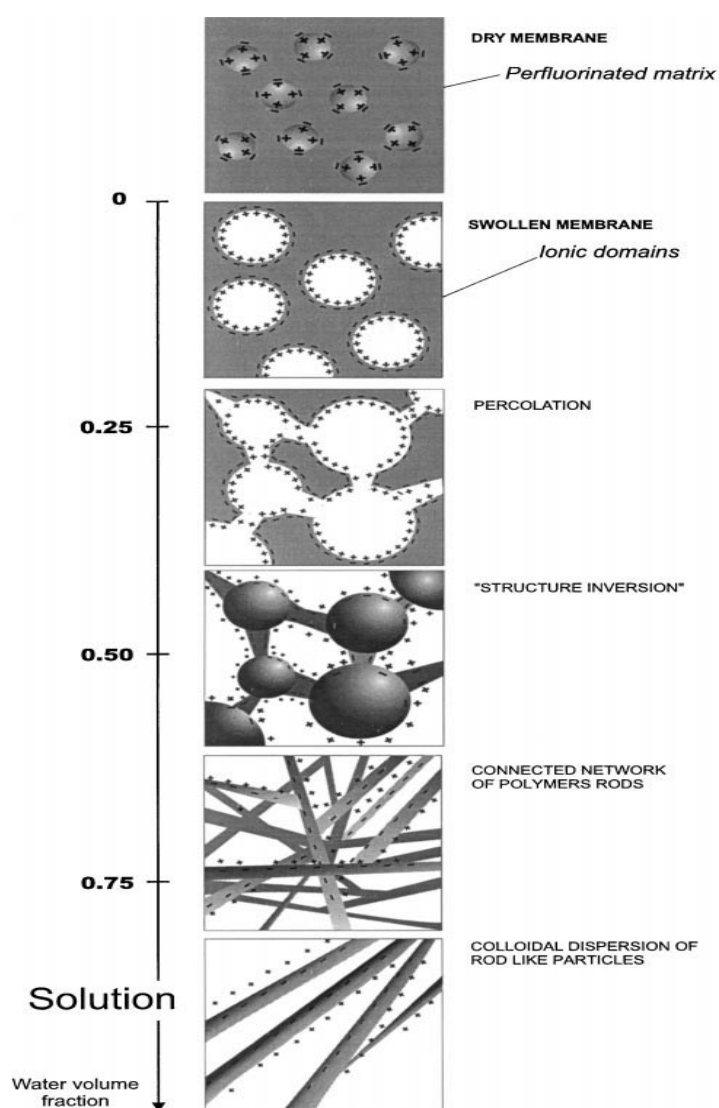
Fig.I.14: Schematic representation of the structural evolution depending on the water content (Gebel 2000).

I.2.2.2 <u>Ion-exchange capacity</u>

Ion-exchange capacity (IEC) is one of the main parameters affecting membrane swelling and consequently other physico-chemical and electrochemical membrane properties. IEC is a measure of the number of fixed charges per unit of dry membrane sample (Strathmann 2004). IEC can be determined on membrane samples in H^+ form balanced with 0,1 N NaOH. Three 25 ml solution samples should be then removed and titrated with 0,1 N HCl. IEC is calculated according to the following equation (Strathmann 2004):

$$IEC = \frac{100-4V}{10m} \qquad\qquad I.33$$

where 100 is the volume of 0,1 N NaOH (in ml), V the total volume of 0,1 N HCl (in ml) used for the titration, and m the mass of the membrane sample (g_{dry} or g_{wet}).

I.2.2.3 <u>Membrane electrical conductivity</u>

Membrane electrical conductivity is a typical parameter for characterization of IEMs. A wide range of methods was developed to measure the membrane electrical conductivity (Zabolotsky and Nikonenko 1996; Berezina and Komkova 2003; Berezina, Kononenko et al. 2008). The widely used method was proposed by Belaid et al. (Belaid, Ngom et al. 1999) and Lteif et al. (Lteif, Dammak et al. 1999). According to their model, membrane electrical conductivity can be obtained via measuring the membrane conductance using the clip-cell containing two platinum electrodes (Fig.I.15). As soon as membrane conductance depends on the temperature, all measurements should be carried out at the same temperature what can be provided by using a thermostat.
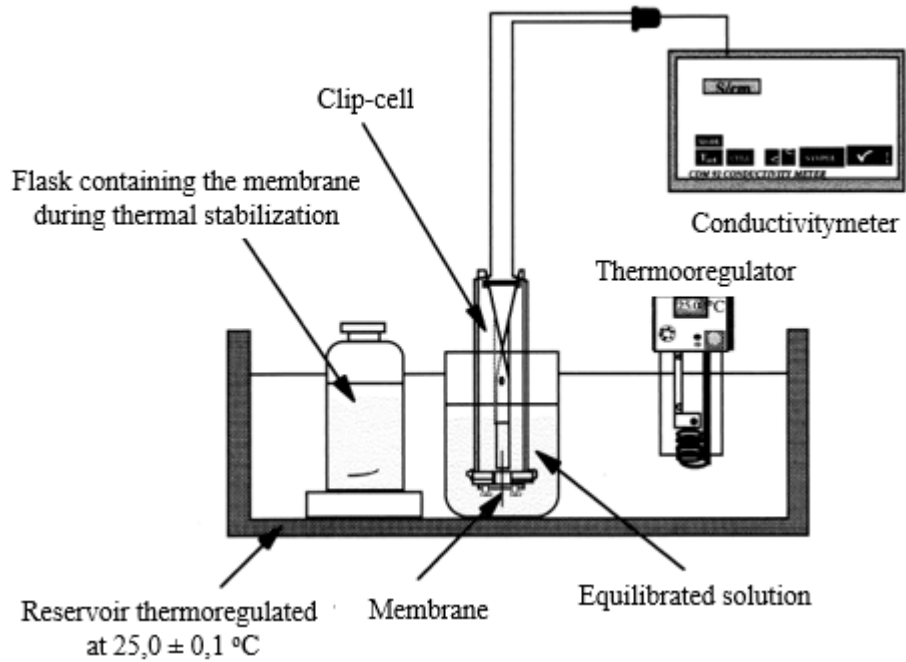
Fig.I.15: Schematic representation of the system for measuring membrane conductance (adapted from (Lteif, Dammak et al. 1999)).

After measuring conductance of the solution and conductance of the solution with membrane it is possible to calculate the electrical resistance of the membrane as

$$R_m = \frac{1}{G_m} = \frac{1}{G_{m+s}} - \frac{1}{G_s} = R_{m+s} - R_s$$

I.34

where R_m is the transverse electric resistance of the membrane (in Ω), R_{m+s} the resistance of the membrane and the reference solution measured together (in Ω), R_s the resistance of the reference solution (in Ω), G_m the conductance of the membrane in Siemens, G_{m+s} the conductance of the membrane and of the reference solution measured together (in S), and G_s the conductance of the reference solution (in S). Finally, the membrane electrical conductivity κ (S/cm) can be calculated as (Lteif, Dammak et al. 1999):

$$\kappa = \frac{L}{R_m A}$$

<div align="right">I.35</div>

where L is the membrane thickness (cm) and A the electrode area (1 cm^2).

I.2.2.4 <u>Voltammetry and chronopotentiometry</u>

To study electrochemical behavior of IEMs in under-limiting, limiting and over-limiting current conditions, voltammetry and chronopotentiometry are privilege methods (Makai 1978; Bobreshova, Kulintsov et al. 1990; Maletzki, Rösler et al. 1992; Krol, Wessling et al. 1999; Krol, Wessling et al. 1999; Choi, Kim et al. 2001; Mishchuk 2010). The dependence of current from potential difference applied to the electrodes on membranes in the ED system is called current-voltage curve (CVC). CVC method provides information about limiting current density (LCD) values and coupled effects of CP.
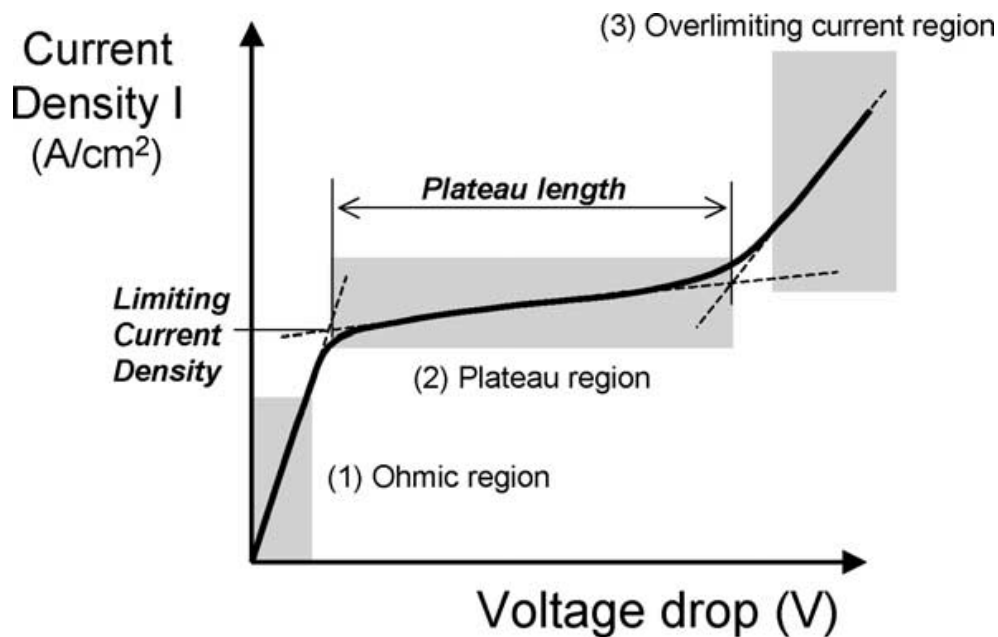
Fig.I.16: Schematic drawing of a typical voltage–current curve of a monopolar IEM (Ibanez, Stamatialis et al. 2004).

Conventional approach considers three regions of CVC (Fig.I.16), however more precise description of CVC curves including interfacial Donnan potential drops and effective resistance of the membrane system at low current densities is given by Belova et al. (Belova

et al. 2006). The first region represents the "ohmic" region where current increases linearly with increasing the voltage according to the Ohms law. Second region starts, when the electrolyte concentration near the diluate side of the membrane surface becomes close to zero (ED system reaches LCD). "Limiting" current region is reflected on the CVC in the form of a plateau. However, on the "plateau" region increase of current still takes place, because of the development of water splitting phenomenon which provides new current carriers (H^+ and OH^-) and the development of gravitational convection and electroconvection (coupled effects of CP), which improve the delivery of current carriers to the membrane surface (Zabolotsky, Nikonenko et al. 1998; Rubinstein and Zaltzman 2000; Nikonenko, Pismenskaya et al. 2010; Nikonenko, Kovalenko et al. 2014). When these coupled effects of CP are strongly developed, ED system passes to the third "overlimiting" current region.
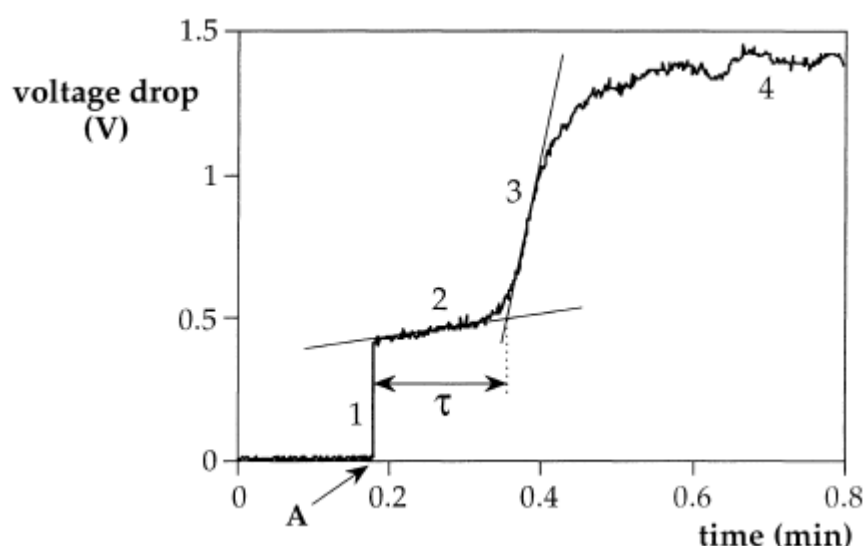
Fig.I.17: Example of chronopotentiometric curve of 0.1 M NaCl at current density 15 mA/cm^2 (Krol, Wessling et al. 1999).

Chronopotentiogram (ChP) represents the dependence of voltage from time under application of fixed current (Fig.I.17). Chronopotentiometry allows the determination of a reduced permeable area of IEMs as well as their electrochemical behavior (Krol, Wessling et al. 1999; Choi, Kim et al. 2001; Pismenskaia, Sistat et al. 2004). Conventional ChP includes the initial vertical region (point 1 on Fig.I.17) corresponding to the "ohmic" drop of potential. Then voltage increases slowly due to the decrease of electrolyte concentration

near the membrane surface (point 2 on Fig.I.17). The next part of the curve corresponds to a drastic increase of potential when the electrolyte concentration becomes zero (point 3 on Fig.I.17). Finally, the system reaches steady state without any substantial changes in voltage (point 4 on Fig.I.17). Duration of the potential drop increasing corresponds to the transition time (τ), which can be calculated according to the Sand eq. (Sand 1901; Krol, Wessling et al. 1999)

$$\tau = \left(\frac{\pi D}{4}\right)\left(\frac{C_i^0 z_i F}{t_i - \bar{t}_i}\right)\frac{1}{i^2} \qquad\qquad \text{I.36}$$

where D is the diffusion coefficient of electrolyte, C_i^0 and z_i the concentration in the bulk and the charge of the counter-ion, respectively, t_i and $\bar{t}_i$ the transport numbers of the counter-ion in the membrane and solution respectively, i the current density, F the Faraday constant. From Eq.I.36 it is possible to see that transition time depends on the transport number. Thereafter, this parameter allows making a conclusion about the membrane permselectivity: transition time is minimal for an ideally permselective membrane with t_i=1 (Pismenskaia, Sistat et al. 2004). Krol et al. (Krol, Wessling et al. 1999) and Choi et al. (Choi, Kim et al. 2001) proposed using the ChP for determination of membrane reduced permeable area. Furthermore, this method is appropriate for investigations of DBL (Sistat and Pourcelly 1997; Kozmai, Nikonenko et al. 2010). There are several approaches for transition time determination from CP. These approaches were discussed by Pismenskaya et al. (Pismenskaia, Sistat et al. 2004). According to the first approach, the transition time corresponds to the intersection point of two tangents to the regions of slow and fast potential growth (regions 2 and 3 on Fig.I.17 respectively). Fig.I.18 (curves 3 and 4) represents the second approach where the transition time is interpreted as the inflection point time. Here A and B are inflection points of heterogeneous MA-41 and homogeneous AMX membranes determined from curves dφ/dt as function of t.
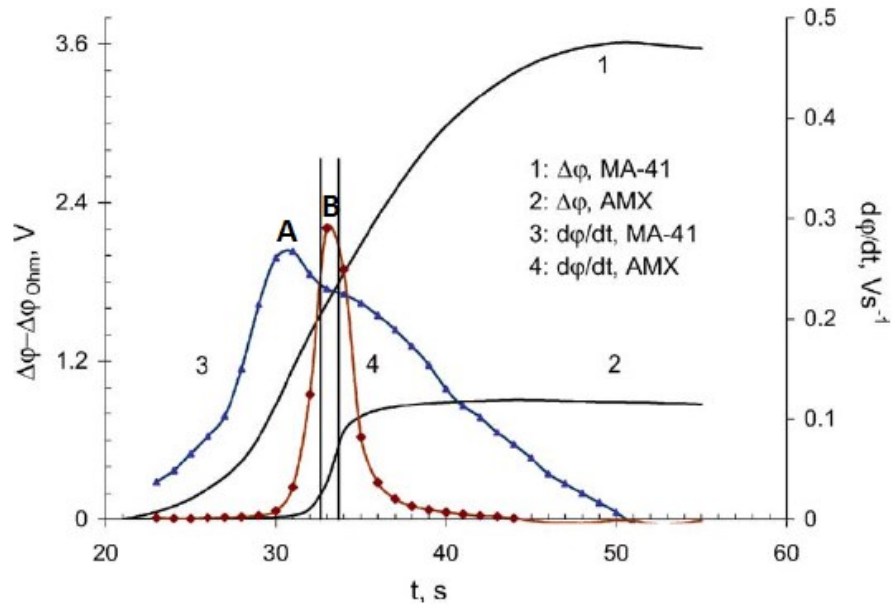
Fig.I.18: Chronopotentiograms and their derivatives of a heterogeneous MA-41 and a homogeneous AMX membranes in 0.1M NaCl. The vertical lines show estimation of the transition time with the Sand equation (interpreted from (Pismenskaia, Sistat et al. 2004).

There are different types of cells allowing measuring CVCs and ChPs (Rubinstein and Shtilman 1979; Bobreshova, Kulintsov et al. 1990; Sistat and Pourcelly 1997; Krol, Wessling et al. 1999; Pismenskaia, Sistat et al. 2004; Berezina, Kononenko et al. 2008; Zabolotskii, Bugakov et al. 2012). One of the most common cell constructions is presented on Figure I.19.
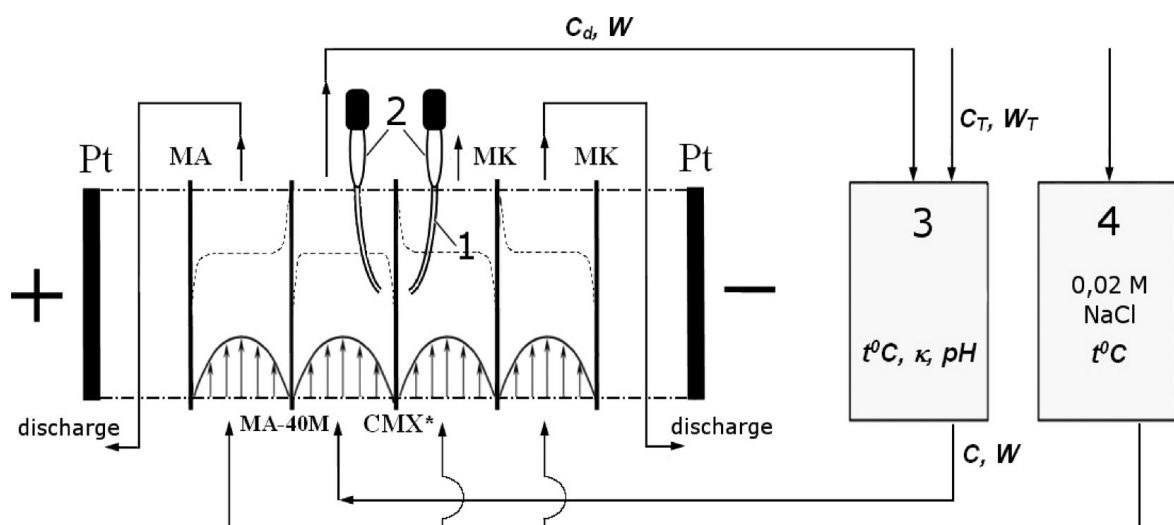
Fig.I.19: General scheme of the membrane cell used for measuring CVC and chronopotentiograms (Pismenskaya, Nikonenko et al. 2007).

The compartments are formed by five membranes each of them inserted between two plastic frames with connecting pipes and comb-shaped input-output devices. The membrane under study (Fig.I.19 CMX membrane) forms a desalination channel together with an anion-exchange MA-40M membrane characterized by a low water splitting in overlimiting current regimes. Auxiliary anion-exchange (AEM) and cation-exchange (CEM) membranes prevent the penetration of electrode reaction products from platinum plane anode and cathode to the central DC. The concentration profiles formed under a direct current are schematically shown in Figure I.19. The tips of the Luggin's capillaries (1) with an external diameter of 0.8 mm are located in CMX membrane compartments near the center of the membrane at a distance of about 1 mm from its surface. The Luggin capillaries are connected with Ag/AgCl electrodes (2) used to measure the potential difference across the CMX membrane and two adjacent solution layers.

I.2.2.5 <u>Contact angles</u>

Contact angles measurements allow to investigate one of the most important parameters affecting development of current induced convection such as surface hydrophobicity (Pismenskaya, Nikonenko et al. 2007; Nikonenko, Pismenskaya et al. 2010; Pismenskaya, Nikonenko et al. 2012). Usually contact angles of different membranes could be measured by goniometer with a measurement range of contact angle 0–180°. The measurement procedure includes the registration of the contact angles between a drop of a liquid (distilled water or organic liquid) and a membrane surface (Hamilton 1972; Ko, Ratner et al. 1981; Arcella, Ghielmi et al. 2003; Curtin, Lousenberg et al. 2004; Gohil, Binsu et al. 2006). A drop of liquid may be applied onto a dry membrane or onto a swollen membrane mopped with a filter paper to remove the excessive water from the surface (Ghassemi, McGrath et al. 2006; Gohil, Binsu et al. 2006; He, Guiver et al. 2013). Furthermore, there are two approaches of contact angles measurements such as in air (Fig.I.20A)) and under the liquid (Fig.I.20B)) (Hamilton 1972; Ko, Ratner et al. 1981; Zhang, Wahlgren et al. 1989; Zhang and Hallström 1990; Rosa and de Pinho 1997).
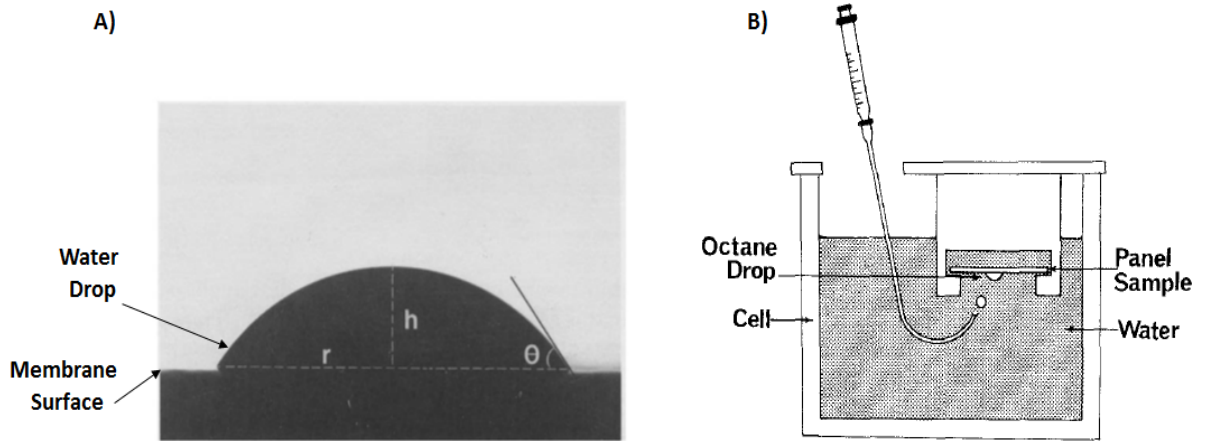
Fig.I.20: Examples of contact angles measurement methods A) in air and B) in liquid (adapted from (Hamilton 1972; Zhang, Wahlgren et al. 1989)).

I.2.2.6 <u>Scanning electron microscopy (SEM)</u>

Visualization of the membrane surface and inside structure allows investigations of its homogeneity/heterogeneity (Fig.I.21 A) and B)), integrity during ED processes at different operation modes (Fig.I.21 C)) and modification procedures (Fig.I.21 D)). This technique was involved in number of investigations providing better understanding of the transport phenomena and the development of coupled effects of CP (Mizutani and Nishimura 1980; Pismenskaia, Sistat et al. 2004; Yaroslavtsev and Nikonenko 2009; Nikonenko, Pismenskaya et al. 2010; Belashova, Melnik et al. 2012; Pismenskaya, Melnik et al. 2012).
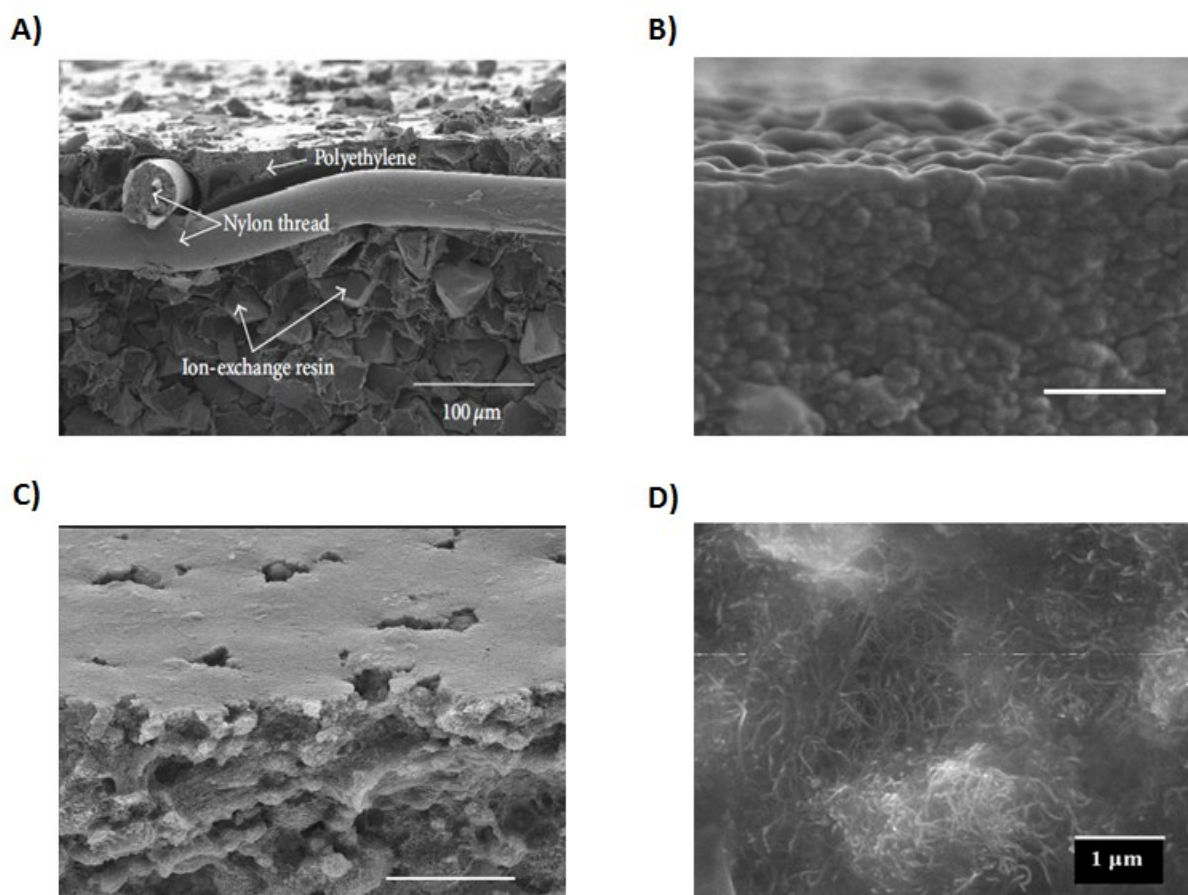
Fig.I.21: Examples of SEM images of IEMs: A) heterogeneous MK-40 (Pismenskaya, Melnik et al. 2012), B) fresh homogeneous CMX and C) homogeneous CMX after its operation in intensive current regimes (Pismenskaya, Nikonenko et al. 2012), D) Nafion modified by Nafion film with carbon nanotubes (Belashova, Melnik et al. 2012).

I.2.2.7 Microfluidic ED platforms and laser interferometry

Visualization in situ of fluid flow and concentration profiles with application of microfluidic platforms and laser interferometry allows detailed direct investigations of CP and current induced convection. Microfluidic platform consists of transparent silicon rubber having microscale channels (Fig.I.22). This platform is installed on an inverted epifluorescence microscope with a thermoelectrically cooled charge-coupled device camera. To visualize fluid flow and salt concentration a fluorescence dye is added in the diluate solution (Kwak, Guan et al. 2013). In addition to direct visualization, it is possible

to simulate the development of concentration profiles and electroconvective vortices (Fig.I.22)

.
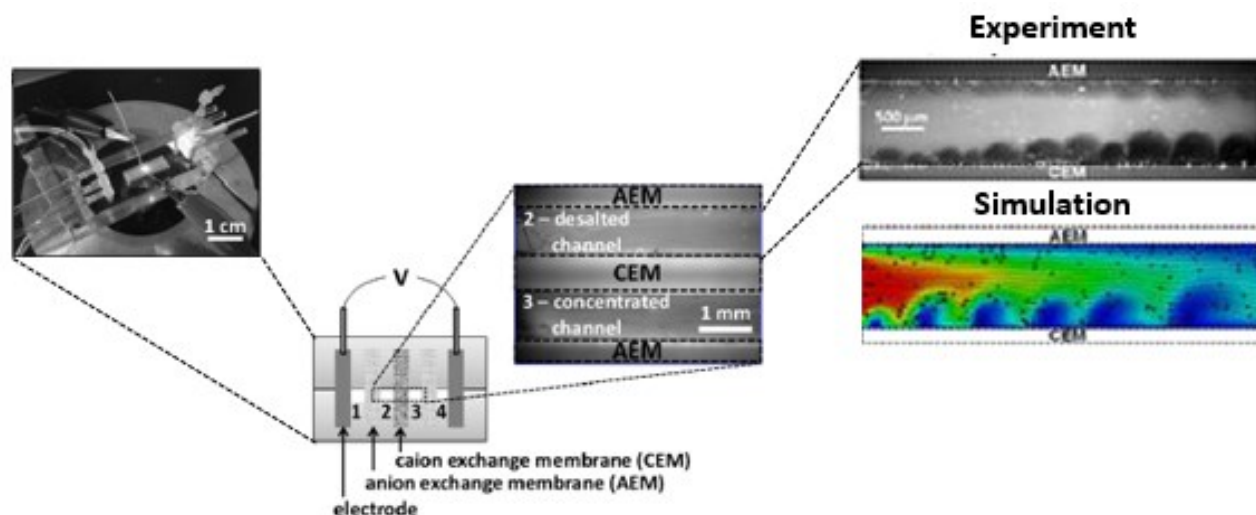
Fig.I.22: Microscale ED system with representation of desalted channel under overlimiting current (experiment and simulation) (adopted from (Kwak, Guan et al. 2013; Nikonenko, Kovalenko et al. 2014)).

Laser interferometry measurements can be performed with a Zender–Mach interferometer (Fig.I.23 A)). A beam from a laser monochromatic light source (1) falls on a semitransparent plate (2), which separates it into two beams. Both beams are then reflected from the mirrors (3). One of the beams passes through an optical electrodialysis cell. The beams formed an interferogram, which is taken with a digital photo camera (Fig.I.23 B)). This allows recording both individual images and video clips. The advantage of a Zender–Mach interferometer is that it allows one to move the beams apart for rather large distances, and the equal-thick fringes can be localized in an arbitrary plane (Shaposhnik, Vasil'eva et al. 2006; Vasil'eva, Shaposhnik et al. 2006; Shaposhnik, Vasil'eva et al. 2008).
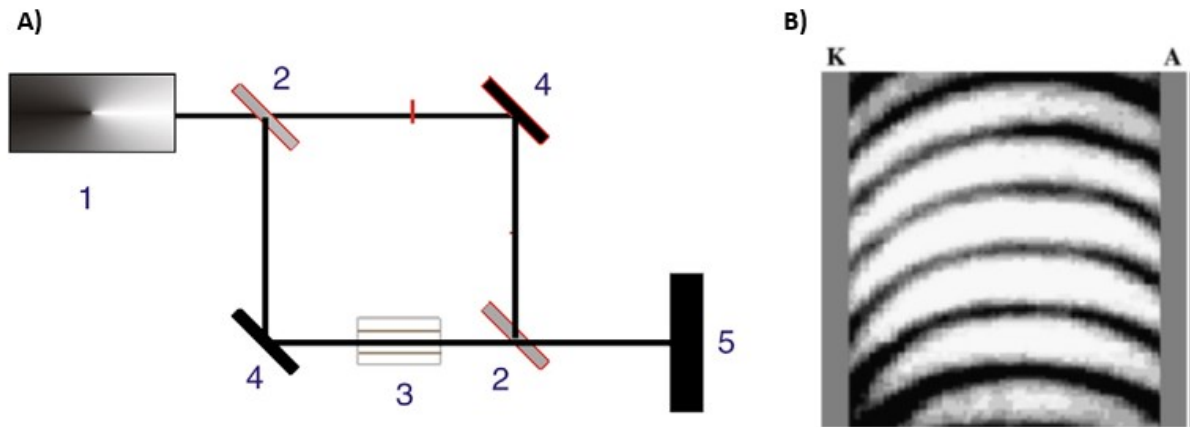
Fig.I.23: Scheme of the Zender–Mach interferometer (A) and interferogram of 0.01 mol/l sodium chloride solution in desalination compartment (B) (adapted from (Shaposhnik, Vasil'eva et al. 2008).

I.3 ED performance indicators

I.3.1 Overall ED stack resistance

Overall ED stack resistance may provide general information about development of phenomena occurring during ED process such as water-splitting, current induced convection, membrane destruction and formation of membrane fouling (Simons 1985; Gyo Lee, Moon et al. 1998; Lee, Oh et al. 2003; Tanaka 2003; Bazinet and Araya-Farias 2005; Casademont, Araya-Farias et al. 2008; Casademont, Sistat et al. 2009; Strathmann 2010; Cifuentes-Araya, Pourcelly et al. 2011). The overall ED stack resistance can be determined using Ohm's Law, from the voltage and the current intensity reading directly from the indicators on power supply.

I.3.2 Solution conductivity and demineralization rate

Solution conductivity is related to the migration fluxes of ions occurring in the solution. Conductivity depends on the solution concentration. With increase in solution concentration conductivity increases due to increase in the number of ions. However, after

a certain concentration, solution conductivity tends to decrease due to the ion-ion interactions and association processes. Moreover, there is an increase in solution viscosity with increase in solution concentration what slows down the migration of ions (Damaskin 2001). Therefore, the dependence of conductivity from solution concentration is usually the curve with maximum (Fig.I.24).
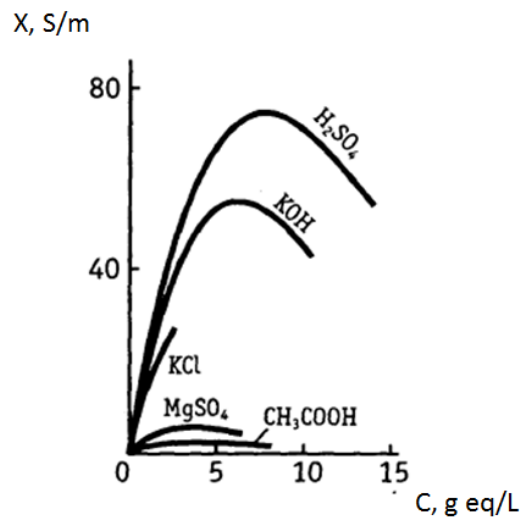
Fig.I.24: Conductivity as a function of electrolyte concentration (adapted from (Damaskin 2001)).

In ED systems, solution conductivity is usually used for determination of demineralization rate (DR), which can be calculated according to the following equation (Ruiz, Sistat et al. 2007):

$$DR = \left(1 - \frac{\text{model salt solution conductivity at time t}}{\text{model salt solution conductivity at time t} = 0} \right) \times 100$$

I.37

I.3.3 Current efficiency and energy consumption

In ED it is assumed that the total current through the membrane is carried by ions only. The theoretical electric current (I_{theor}) required to perform the separation is directly proportional to the number of charges transported across the ion exchange membrane and is given by the following expression (Baker 2012)

$$I_{theor} = z\Delta CFQ \qquad \text{I.38}$$

where Q is the feed flow rate, ΔC the difference in molar concentration between the concentrate and the dilute solutions, z the valence of the salt, and F the Faraday constant. The efficiency of ED treatment depends on the number of cell pairs and can be expressed as (Bazinet and Castaigne 2011)

$$\eta = \frac{z\Delta CFQ}{NI} \qquad \text{I.39}$$

where η is the current efficiency, N the number of cell pairs and I the current. For well-designed laboratory ED stacks the current efficiency is greater than 90%, while for commercial units it may reduce to about 50% (Bazinet and Castaigne 2011; Fidaleo 2011). Estimations of overall energy consumption (EC) in the ED stack may be performed from expression

$$EC = \int_{0}^{\bar{t}} I(t)U(t)dt \qquad \text{I.40}$$

where $\bar{t}$ is the time of the experiment run, I(t) the current as a function of time, U(t) the voltage as a function of time and dt the time variation. Most of the difficulties in ED are due to the CP phenomena which leads to the decrease in current efficiency and to the increase in EC (Strathmann 1981; Ruiz, Sistat et al. 2007; Choi, Chae et al. 2011; Cifuentes-Araya, Pourcelly et al. 2011; Cifuentes-Araya, Pourcelly et al. 2013). However, there are other factors causing loss of current and increase in EC such as

- Nonideal permselectivity causing co-ions leakage;

- Water transport by osmotic effects and ionic hydration shells;
- Partial current flow through the stack manifold;
- Presence of membrane fouling.

I.4   Fouling on IEMs

One of the most serious limitations of ED processes is the formation of membrane fouling. The formation of deposit may occur on the membrane surface and/or inside the membrane causing an increase in electrical resistance, a decrease in membrane permselectivity and membrane alteration (Thompson and Tremblay 1983; Bleha, Tishchenko et al. 1992). Membrane fouling directly affects the ED process economics because cleaning procedures and membrane replacement accounting up to 47% of the overall operating costs of ED treatment (Grebenyuk, Chebotareva et al. 1998).

I.4.1   Classification of IEMs fouling

I.4.1.1 Colloidal fouling

Colloids are non-dissolved suspended solids, which are present in natural and processed waters and many effluent streams in forms of clay minerals, colloidal silica, iron oxide, aluminum oxide, manganese oxide and organic colloids (T. Brunelle 1980; Lee, Park et al. 2003). The size of colloid particles may vary from 10 Å to 2 microns in diameter. For instance, the majority of colloidal particles found in natural waters are small aluminum silicate clays. These clays are in the 0.3 to 1.0 micron diameter size range. The main feature of colloids is an excessive charge on the surface (net charge), which provides adsorption of ions from the surrounding solution. Fig.I.25 represents a general model of the colloid structure which was developed by Gouy (Gouy 1910) and Chapman (Chapman 1913) and later by Stern (Stern 1924). The solid in this model has an excessive positive surface charge, which attracts negatively charged molecules from the solution. The Stern layer is tightly adjusted to the solid due to electrostatic forces compensating most part of excessive positive

charge. The ions from diffusion layer neutralize the rest of excessive charge. The diffusion layer acts as a caution preventing colloids coming in contact with one another and coagulating (T. Brunelle 1980).
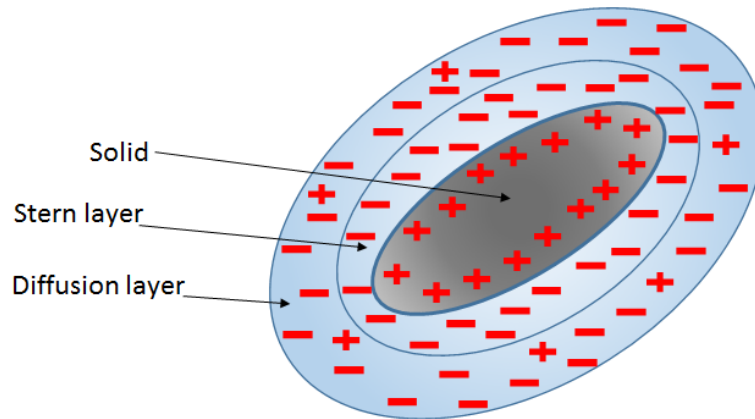
Fig.I.25: Model of colloidal particle.

Thereafter, colloid particles have a net charge, which from the one hand plays important role in terms of colloid stability (according to the theory of Derjaguin, Landau, Verwey and Overbeek (DLVO) (Derjaguin and Landau 1941; Verwey and Overbeek 1948)) and from the other hand may lead to the attachment of colloid to the membrane surface. Number of works is dedicated to the investigation of nature, structure and stability of colloidal fouling as well as to the mechanisms of its formation on the membrane surface. Most of these investigations are related to membrane filtration processes (T. Brunelle 1980; Cohen and Probstein 1986; Vladisavljević, Milonjić et al. 1992; Bacchin, Aimar et al. 1995; Elimelech, Xiaohua et al. 1997; Yiantsios and Karabelas 1998; Schwarz, Lunkwitz et al. 2000; Vrijenhoek, Hong et al. 2001; Yiantsios, Sioutopoulos et al. 2005; Aimar and Bacchin 2010). In ED processes, the attention usually focuses on the AEMs colloidal deposit since most of colloids treated by ED are negatively charged and they interact with positively charged ion-exchange groups of AEMs (Korngold, de Körösy et al. 1970; Korngold 1971; Lee, Park et al. 2003; Lee and Moon 2004; Mondor, Ippersiel et al. 2009). The above works reported factors affecting colloidal fouling such as concentration of foulant particles as well as dissolved salt concentration, pH, temperature, membrane properties, mode of operation and hydrodynamic conditions. Taking into account these factors, one may create unfavorable conditions for the formation of colloidal deposits on the membrane surface.

50

I.4.1.2 <u>Organic fouling</u>

Organic fouling is similar to organic colloidal fouling except for the fact that organic foulants are initially dissolved in the solution treated by ED. Additionally, the colloidal state of organic molecules is maintained by weak, long-range van der Waals forces of attraction and electrostatic forces of repulsion, in contrast to ordinary organic molecules, which predominantly have covalent bonds (Tadors 2013). Organic fouling occurs when treated solution contains organic substances such as oil, carbohydrates, proteins, aromatic substances, humic acid and anti-foaming agents (Audinos 1989; Bleha, Tishchenko et al. 1992; Lindstrand, Sundström et al. 2000; Lee, Oh et al. 2003; Park, Chilcott et al. 2005; Ayala-Bribiesca, Araya-Farias et al. 2006; Lin Teng Shee, Arul et al. 2007; Ruiz, Sistat et al. 2007; Ren, Wang et al. 2008; Banasiak and Schäfer 2009; Banasiak and Schäfer 2010; Banasiak, Van der Bruggen et al. 2011; Ren, Wang et al. 2011; Shi, Cho et al. 2011; Choi, Yu et al. 2013; Husson, Araya-Farias et al. 2013; Vermaas, Kunteng et al. 2013; Guo, Xiao et al. 2014). These organic substances stick to the surface of the membrane and/or lodge themselves inside the membrane. This type of membrane fouling has a real importance due to the large number of treated products with different matrices containing organic matter (Fig.I.26).
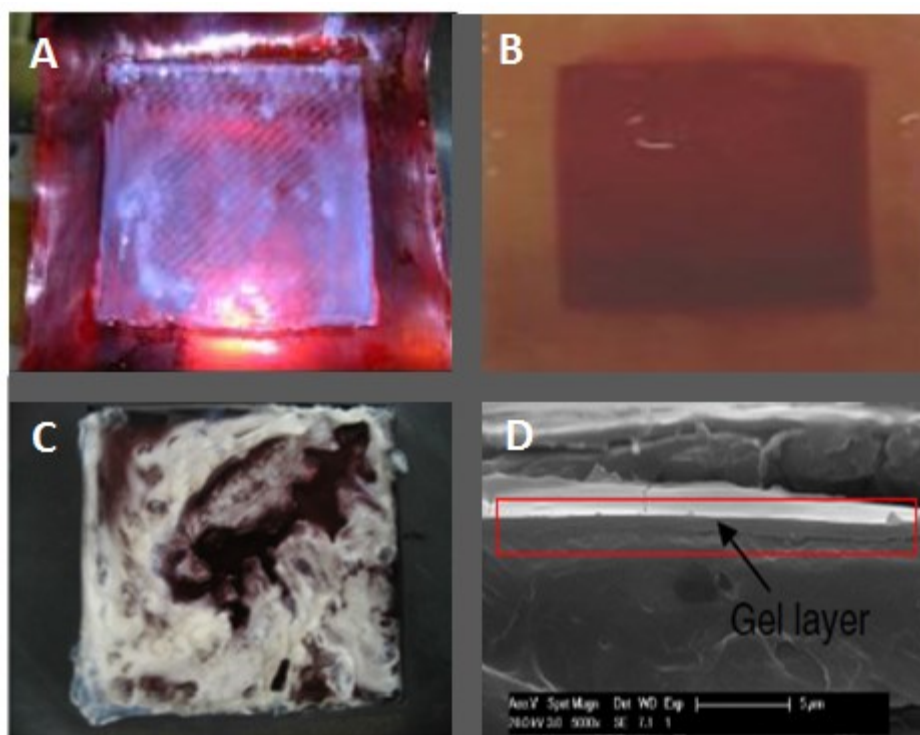
Fig.I.26: Examples of organic fouling: A) Chitosan fouling (Lin Teng Shee, Arul et al. 2007), B) Antocyanin fouling (Husson, Araya-Farias et al. 2013), C) Protein fouling (Ruiz, Sistat et al. 2007), D) Polyacrylamide fouling (Guo, Xiao et al. 2014).

Several investigations have been reported providing information about mechanisms of organic fouling formation (Lindstrand, Sundström et al. 2000; Banasiak and Schäfer 2010; Banasiak, Van der Bruggen et al. 2011; Langevin and Bazinet 2011; Guo, Xiao et al. 2014). Organic fouling on the IEM surface and inside the IEM may be due to electrostatic and hydrophobic interactions which is different from colloidal fouling where the majority of interactions have electrostatic nature only. One can distinguish several parameters affecting organic fouling formation such as concentration, size and structure of organic molecules as well as membrane structure and regimes of ED treatment. Bukhovets et al. (Bukhovets, Eliseeva et al. 2010) reported important role of current regimes applying during ED. It has been found that at current densities close to the limiting values where water splitting takes place, IEM becomes fouled by phenylalanine. Langevin et al. (Langevin and Bazinet 2011) studied effect of acidification and basification of the IEM surface on the fouling by peptides. These conditions are close to those occurring when current reaches limiting value and water splitting takes place. It was found that the crucial role in linking between peptides and IEMs play electrostatic interactions.

I.4.1.3 <u>Scaling</u>

Scaling on IEM occurs when salts present in the water precipitate out and settle on the membrane surface and/or within membrane channels. The major scaling ions present in solutions treated by ED include magnesium, calcium, barium, hydroxyl, bicarbonate and sulfate (Thompson and Tremblay 1983; Bleha, Tishchenko et al. 1992; Bazinet, Lamarche et al. 1999; Bazinet, Montpetit et al. 2001; Ayala-Bribiesca, Pourcelly et al. 2007; Lin Teng Shee, Angers et al. 2008; Chang, Choo et al. 2009; Cifuentes-Araya, Pourcelly et al. 2011; Van Geluwe, Braeken et al. 2011; Wang, Yang et al. 2011; Choi, Yu et al. 2013; Franklin June 2009). The Precipitation occurs when the equilibrium of solution has been changed in a way that decreases the solubility below the concentration of salts causing some to precipitate out of the solution. Conventionally, two main factors affect precipitation in solutions such as concentration of ions and solution temperature (Franklin June 2009). When speaking about the precipitation, it is worth to emphasize the effect of the membrane structure and regimes of ED. Bazinet et al. (Bazinet, Ippersiel et al. 2000) reported that scaling may be reversible or irreversible depending on the membrane permselectivity. Van Geluwe et al. (Van Geluwe, Braeken et al. 2011) compared how different types of scaling may be prevented on homogeneous and heterogeneous membranes. A very important factor affecting scaling formation is pH of treated solution. Basic pH values mean excessive presence of OH$^-$ ions. From the one hand, it leads to the precipitation of hydroxides due to the interaction of OH$^-$ with Ca^{2+} and Mg^{2+} as follow (Gence and Ozbay 2006):

$$Mg^{2+}{}_{(aqueous)} + 2OH^-{}_{(aqueous)} \rightleftarrows Mg(OH)_{2(solid)} \qquad \text{I.41}$$

$$Ca^{2+}{}_{(aqueous)} + 2OH^-{}_{(aqueous)} \rightleftarrows Ca(OH)_{2(solid)} \qquad \text{I.42}$$
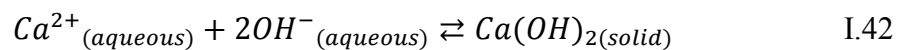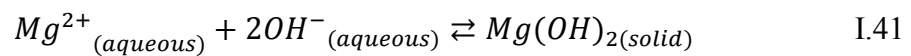
From the other hand, OH$^-$ can shift the balance of weak-acid anions. For instance, in the solution with basic pH the balance between carbonic ions is shifted into carbonate ions (Fig.I.27) what leads to precipitation of carbonates (Eq.I.43, I.44).
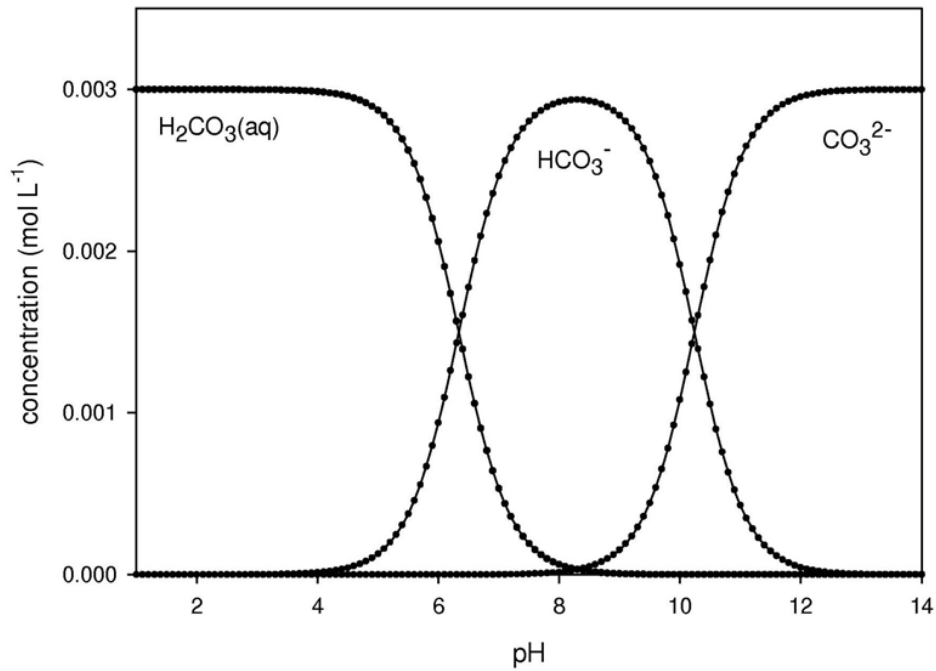
Fig.I.27: Speciation of major carbon species depending on pH (total concentration 0.003 mol/l, T = 20°C, closed system, and ionic strength I = 0) (Nehrke 2007).

$$Mg^{2+}_{(aqueous)} + CO_3^{2-}_{(aqueous)} \rightleftarrows MgCO_{3(solid)} \qquad \text{I.43}$$

$$Ca^{2+}_{(aqueous)} + CO_3^{2-}_{(aqueous)} \rightleftarrows CaCO_{3(solid)} \qquad \text{I.44}$$
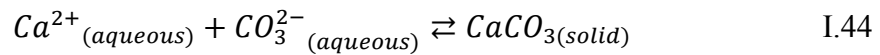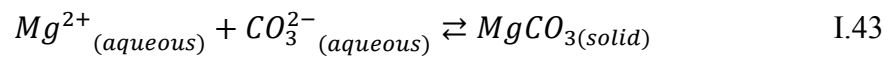
Detailed studies of pH influence on scaling on IEMs was carried out by Casademont et al. (Casademont, Araya-Farias et al. 2008). These authors maintained a certain pH value in the concentrate compartment during ED treatment while pH of the diluate compartment was not kept constant changing from its initial value (6.5). It was reported that the membrane scaling formed by minerals of Ca^{2+} and Mg^{2+} on AEM surface mostly takes place at neutral pH values, however CEM surface was scaled at basic pH (Fig.I.28). Additionally to pH factor, the type of IEM can play an important role in the scaling formation. Furthermore, as for the organic fouling, application of current higher than the limiting current affects scaling quantity and composition. Generation of OH^- ions by CEM provides conditions for the scaling formation, however H^+ ions generated by AEM may create a "proton barrier" preventing precipitation of minerals (Casademont, Araya-Farias et al. 2008; Cifuentes-Araya, Pourcelly et al. 2012; Cifuentes-Araya, Pourcelly et al. 2013).
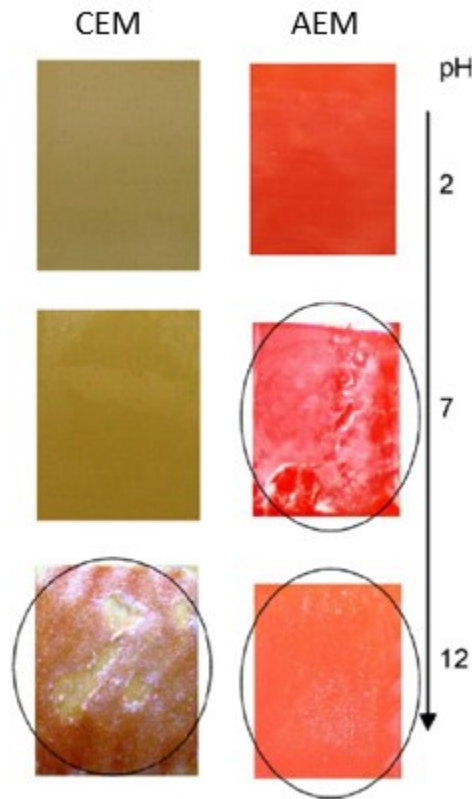
Fig.I.28: Scaling on CEM and AEM depending on pH (adapted from (Casademont, Araya-Farias et al. 2008)).

An additional factor influencing the scaling formation is the ratio of the scaling ions due to the competition during their migration from the diluate compartment towards the concentrate and due to the cross-effects of different scaling ions on nucleation and crystal growth (Zhang and Dawe 2000; Hołysz, Chibowski et al. 2003; Chen, Neville et al. 2006; Casademont, Pourcelly et al. 2007; Firdaous, Malériat et al. 2007; Casademont, Araya-Farias et al. 2008; Casademont, Pourcelly et al. 2008; De Silva, Bucea et al. 2009; Cifuentes-Araya, Pourcelly et al. 2012). Moreover, consecutive ED treatment leads to the formation of scaling multilayers having different composition (Casademont, Pourcelly et al. 2009). Recent studies of Cifuentes-Araya et al. revealed mechanisms of the membrane scaling formation and created graphical models including possible interactions between scaling ions and IEMs (Cifuentes-Araya, Pourcelly et al. 2012; Cifuentes-Araya, Astudillo-Castro et al. 2014).

I.4.1.4 <u>Biofouling</u>

Biofouling seems to be the less studied fouling type occurring in conventional ED processes. Most of the studies are dedicated to the micro-, ultra-, nanofiltration and reverse osmosis (Flemming and Schaule 1988; Flemming 1997; Baker and Dudley 1998; Herzberg and Elimelech 2007; Huertas, Herzberg et al. 2008; Ivnitsky, Minz et al. 2010; Khan, Stewart et al. 2010; Lee, Ahn et al. 2010; Majamaa, Johnson et al. 2012). However, rapid development of biotechnology with application of IEMs makes biofouling an actual problem. For instance, biofouling is a major problem in microbial desalination cells (Fig.I.29). The main feature of these microbial cells is implication of special bacteria on the anode surface. These bacteria may oxidize biodegradable substrates and produce electrons and protons. Electrons move towards the cathode completing the electric loop. Separating anode and cathode by CEM and AEM, one can obtain classical desalting channel (Korngold, Aronov et al. 1998; Sun, Wang et al. 2008; Długołęcki, Dąbrowska et al. 2010; Drews 2010; Choi, Chae et al. 2011; Luo, Xu et al. 2012; Brastad and He 2013; Kim and Logan 2013). There are number of different microbial electrochemical systems aiming production of electricity and chemicals, desalination, waste treatment etc. Most part of these systems was recently been described by Wang et al. (Lee, Hong et al. 2009).
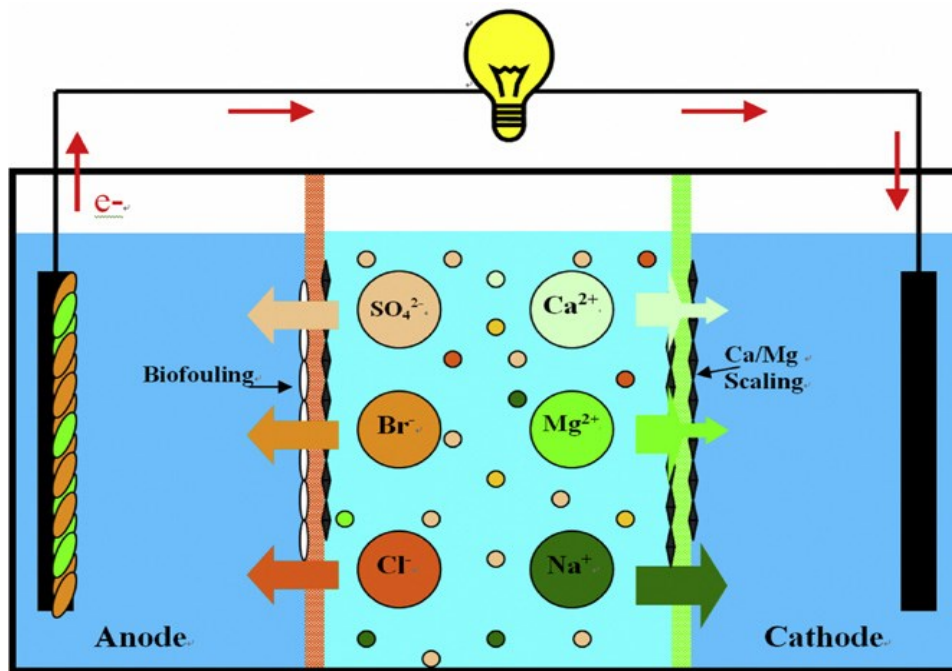
Fig.I.29: Schematic of a three-chamber microbial desalination cell for simultaneous substrate removal (anode), desalination (middle chamber), and energy production (Sun, Wang et al. 2008).

The lifecycle of the biofilm is represented on Fig.I.30 with microphotograph of each stage of biofilm development (Flemming, Wingender et al. 2011). Initial interaction of bacteria with a surface is reversible (1) whereas subsequent adhesion is irreversible (2). After attaching to the membrane surface bacteria start production and excretion of extracellular polymer substances (2), which allow cells to become cemented to the surface. Continuous growth results in the development of microcolonies (3). As the microcolonies continue to increase in size (4), cells in the interior of the microcolonies will experience overcrowding, decreased availability of nutrients, increased concentrations of waste-products, toxins and excreted metabolites including cell-to-cell signaling molecules, along with changes in their physicochemical environment. At last, matrix within a microcolony is digested, cells become free to move by active motility or browning motion (5). Eventually, a breach is made in the matrix at a margin of the microcolony through which the bacteria are able to escape into the surrounding bulk liquid.
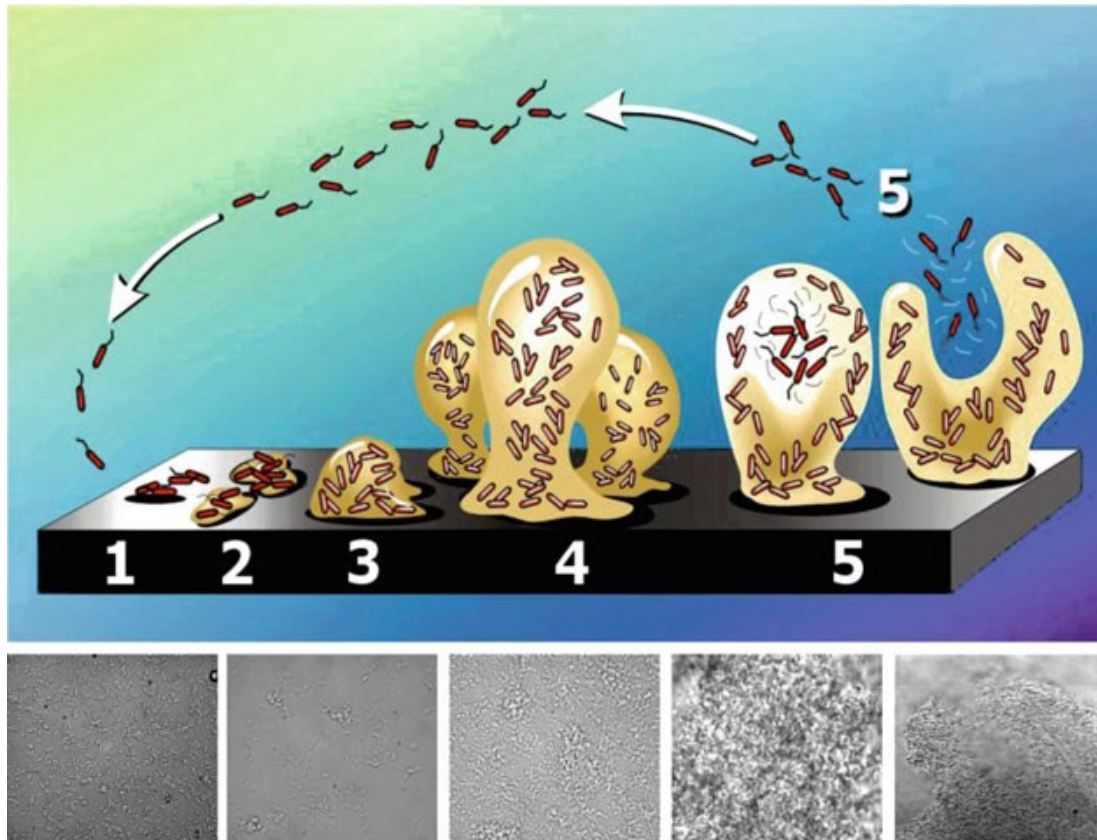
Fig.I.30: Biofilm lifecycle. Stages in the development and dispersion of biofilm are shown proceeding from right to left. Lower panel shows photomicrographs of bacteria at each of the five stages shown in the schematic above (Flemming, Wingender et al. 2011).

Fleming et al. (Flemming and Schaule 1988) distinguished factors affecting formation and development of biofilms on the membrane surfaces (Tab.I.1)

Tab.I.1: Factors affecting biofilm formation on membrane surface

• **Microorganisms factor**	• **Membrane surface factor**	• **Solution factor**
o Species	o Chemical composition	o Temperature
o Composition of mixed population	o Surface charge	o pH
o Cell number	o Surface tension	o substances forming a conditioning film

58

o Growth phase	o Surface hydrophobicity	o dissolved organic/inorganic substances
o Nutrient status	o Roughness	o suspended matter and colloids
o Hydrophobicity	o Porosity	o viscosity
o Surface charge		o surface tension
o Physiological response on adhesion		o flow rate

I.4.2 Characterization of IEMs fouling

I.4.2.1 Visualization of IEMs fouling

Conventional methods allowing visualization of membrane fouling are following (Fig.I.31)

- Photo imaging
- Optical microscopy
- Scanning electron microscopy (SEM)
- Confocal laser scanning microscopy (CLSM)
- Atomic force microscopy (AFM)
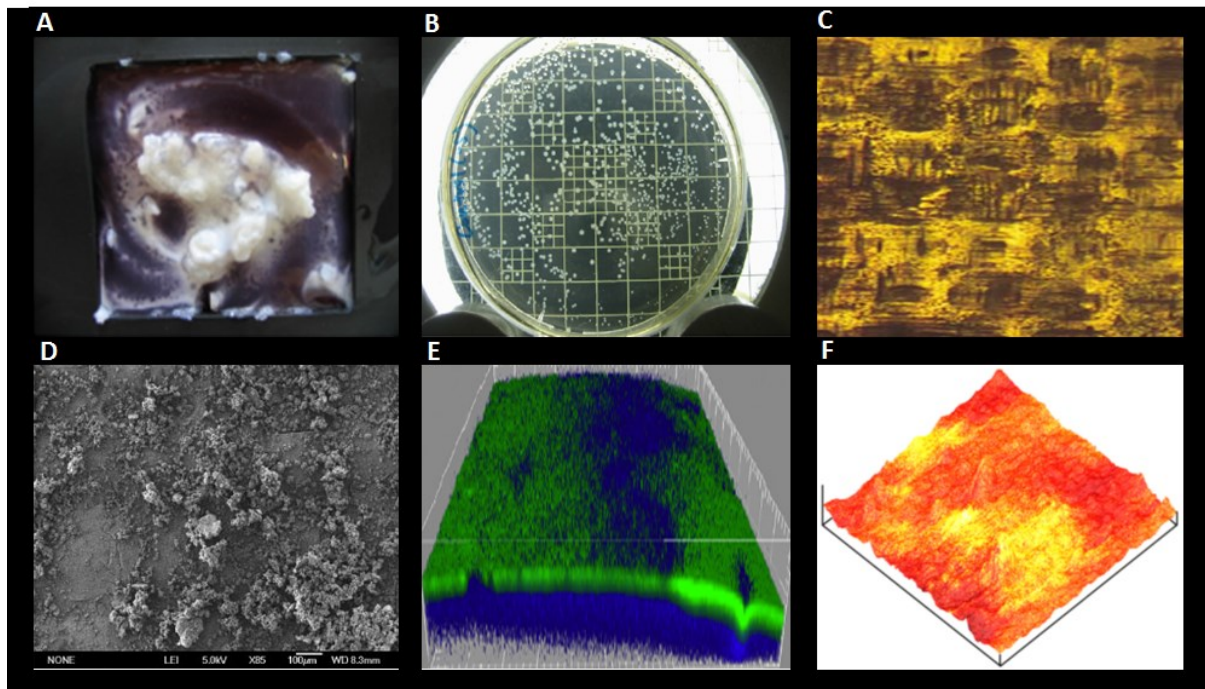
Fig.I.31: Visualization of membrane fouling by photo imaging (A,B) (Ruiz, Sistat et al. 2007; Liu, Zhang et al. 2010), optical microscopy (C) (Ayala-Bribiesca, Pourcelly et al. 2007), SEM (D) (Ren, Wang et al. 2008), CLSM (E) (Sweity, Ying et al. 2011), AFM (F) (Ivnitsky, Katz et al. 2007).

These methods may be applied to identify the presence of membrane fouling, to reveal the fouling structure and distribution along the membrane surface or inside the membrane, to study the effects of different ED conditions on fouling development and effectiveness of cleaning procedures. Thereafter, the fouling type and the goal of research should determine the choice of one or another method. For instance, the majority of membrane fouling investigations are performed with using SEM, however CLSM is used mostly for biofouling investigations.

I.4.2.2 <u>Membrane characteristics</u>

As soon as membrane fouling changes membrane properties by modification of membrane surface and/or incorporation in the inner membrane structure, it is possible to

establish membrane characteristics after ED treatment. Estimation of fouling influence may be performed by the following methods:

- *Membrane electrical conductivity* (described in I.2.2.3): usually fouling phenomena lead to the decrease in membrane conductivity due to the 1) increase in membrane resistance by formation of surface fouling layer or internal membrane fouling and 2) deposition of fouling agents on membrane ion-exchange groups (Lindstrand, Jönsson et al. 2000; Lindstrand, Sundström et al. 2000; Bazinet, Montpetit et al. 2001; Lee and Moon 2005; Araya-Farias and Bazinet 2006; Ruiz, Sistat et al. 2007; Lee, Hong et al. 2009; Mondor, Ippersiel et al. 2009; Bukhovets, Eliseeva et al. 2010; Ping, Cohen et al. 2013);

- *Voltammetry and chronopotentiometry* (described in I.2.2.4): allow monitoring of the phenomena such as CP, water splitting, electroconvection etc. which are affected by the presence of IEM fouling (Korngold, de Körösy et al. 1970; Grossman and Sonin 1972; Grebenyuk, Chebotareva et al. 1998; Park, Choi et al. 2006; Guo, Xiao et al. 2014);

- *Electrical impedance spectroscopy* provides an information about conduction and capacitive properties of membrane systems (Park, Lee et al. 2003). It involves the measurement of the amplitudes of sinusoidal current and voltage stimuli of small magnitude and the phase shift between the stimuli as a function of the sinusoidal frequency. The ratio of the amplitudes of the current and voltage yields the magnitude of the admittance (reciprocal of impedance), which for zero phase-shift yields the conductance (reciprocal of resistance). The measurement of phase shifts in a membrane system indicates a capacity to store electric charge dielectrically, chemically and/or via electromembrane processes (e.g. fouling) and artifacts of the experimental system (e.g. electrode configuration). The dispersions of the conductance and capacitance with frequency provide a means of distinguishing between the varieties of mechanisms for storing electric charge. Electrical impedance spectroscopy offers a means of investigating fouling phenomena in ion-selective membrane systems and characterizing noninvasively those electro-membrane processes leading to fouling. (Park 2006);

- *Transport numbers* measurements allow to indicate the presence of fouling since fouling phenomena hamper the migration of counter-ions through the IEM (Lee, Hong et al. 2009; Choi, Chae et al. 2011; Pontié, Ben Rejeb et al. 2012);

- *Ion-exchange capacity* (described in IV.1.2.4.3) measurements as well as above mentioned methods allow indication of membrane fouling since some fouling agents interact with membrane ion-exchange groups blocking them and decreasing ion-exchange capacity (Lee and Moon 2005; Lee, Hong et al. 2009; Mondor, Ippersiel et al. 2009; Pontié, Ben Rejeb et al. 2012; Guo, Xiao et al. 2014);

- *Water uptake* (described in IV.1.2.4.4) measurements can indicate the presence of fouling phenomena since fouling usually blocks the ion-exchange sites leading to the decrease of the ability of IEM to absorb water (Lee, Hong et al. 2009);

- *Contact angles* (described in IV.1.2.4.5) measurements indicate the modification of IEM surface hydrophobicity due to the formation of a fouling layer (Lee and Moon 2005; Lee, Hong et al. 2009; Bukhovets, Eliseeva et al. 2010; Lee, Ahn et al. 2010; Guo, Xiao et al. 2014);

- *Membrane thickness* characterizes the thickness of fouling layer formed on IEM surfaces after the treatment (Bazinet, Montpetit et al. 2001; Cifuentes-Araya, Pourcelly et al. 2011);

- *Zeta potential* measurements can provide information about magnitude of the electrostatic or charge repulsion/attraction forces of fouling agents and IEMs surfaces allowing control of their possible interactions (Park, Lee et al. 2003; Lee, Ahn et al. 2010);

I.4.2.3 ED performance parameters

Assuredly, membrane fouling affects ED performance. Thereafter, one may estimate negative influence of the membrane fouling formation taking into account following parameters of ED, which were described above in the I.3 section (Banasiak and Schäfer 2009; Casademont, Sistat et al. 2009; Lee, Hong et al. 2009; Bukhovets, Eliseeva et al. 2010; Cifuentes-Araya, Pourcelly et al. 2011; Fidaleo 2011; Mulyati, Takagi et al. 2012; Cifuentes-Araya, Pourcelly et al. 2013)

- Overall ED stack resistance
- Energy consumption
- Demineralization rate/Migration rate
- Current efficiency

I.4.2.4 <u>Fouling composition</u>

For analyzing composition of the membrane fouling one should take into account the fouling type. If membrane deposit contains any organic substances then the following methods may be appropriate for characterization of its composition (Casademont, Sistat et al. 2009; Lee, Hong et al. 2009; Bukhovets, Eliseeva et al. 2010; Langevin and Bazinet 2011; Guo, Xiao et al. 2014)

- ✓ Nitrogen content analysis
- ✓ Ultraviolet (UV) absorbance
- ✓ Attenuated Total Reflectance Fourier Transform Infrared spectroscopy (ATR–FTIR)
- ✓ High Performance Liquid Chromatography with Mass Spectrometry (HPLC-MS)

Characterization of the mineral fouling composition and crystal structure is usually carried out by the following methods (Bazinet, Montpetit et al. 2001; Casademont, Pourcelly et al. 2009; Wang, Yang et al. 2011; Cifuentes-Araya, Pourcelly et al. 2012; Cifuentes-Araya, Astudillo-Castro et al. 2014)

- ❖ Energy dispersive x-ray spectroscopy (EDS)
- ❖ X-ray diffraction analysis (XRD)
- ❖ Inductively Coupled Plasma analysis (ICP)
- ❖ Ash content

Biofouling characterization usually includes various steps of biochemical procedures such as implication of Polymerase Chain Reaction (PCR), Denaturing Gradient Gel Electrophoresis (DGGE), Sequencing procedures, Dubois, Lowry, Bradford assays etc. described in following works (Sun, Wang et al. 2008; Drews 2010; Luo, Xu et al. 2012).

I.4.3   Strategies of prevention and cleaning of IEMs fouling

There are numbers of different strategies allowing fouling control in ED processes. However, one should always take into account the fouling nature because certain strategy can be appropriate for one fouling type and ineffective for another. Thereafter, in the ED systems containing different fouling types a complex procedure comprising application of numbers of prevention and cleaning procedures may be involved. This section will provide a general information about prevention and cleaning of IEMs fouling.

I.4.3.1 Modification of IEMs

Generally, IEM modification aims to change the membrane surface properties such as

- Surface charge
- Hydrophobic/hydrophilic balance
- Roughness

Grebenyuk et al. (Grebenyuk, Chebotareva et al. 1998) demonstrated a success in modification of AEM by high molecular mass surfactants against organic fouling what led consequently to 1.7 times reduction in consumption of electric power. Kusumoto et al. (Kusumoto, Mizumoto et al. 1975) found that the oxidizing treatment of the AEM may generate thin and neutral layer on the membrane surface making AEM resistant to organic fouling. Modification of the AEM surface by sulfonating agents considerably improves antifouling potential (Kusumoto and Mizutani 1975; Mulyati, Takagi et al. 2012). This improvement happens due to the decrease in membrane surface hydrophobicity and increase in its negative surface charge density (Fig.I.32). Moreover, using layer-by-layer modification, simultaneous improvement of antifouling potential and monovalent anion selectivity may be performed (Mulyati, Takagi et al. 2013). Recently, Vaselbehagh et al. (Vaselbehagh, Karkhanechi et al. 2014) also reported IEM modification by polydopamine against fouling. Authors also emphasized that the increase in surface negative charge and the decrease in surface hydrophobicity has a positive influence on antifouling potential, while the increase in surface roughness decreased the antifouling potential.
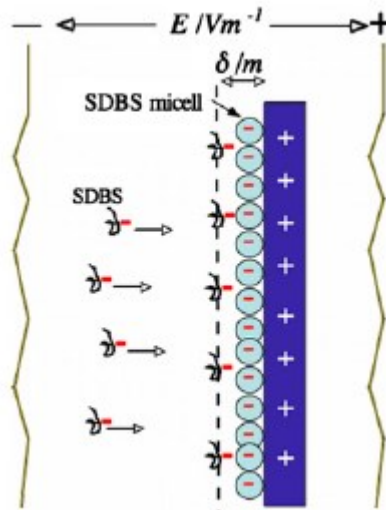
Fig.I.32: Example of fouling prevention by modification of CEM surface (Mulyati, Takagi et al. 2012).

Situation with biofouling seems to be more complex. Surface hydrophobicity and charge density are although important factors (Khan, Stewart et al. 2010) are not effective criteria in membrane modification for biofouling control. The more important role plays the nature of surface charges. Membrane modification in biofouling control aims two goals such as anti-adhesive approach that prevents the initial attachment of bacteria on a membrane and anti-microbial approach that aims to kill bacteria already attached on the membrane. These approaches were demonstrated by membrane surface modification with biocides such as nanosilver particles (Yang, Lin et al. 2009; Liu, Zhang et al. 2010; Zhu, Bai et al. 2010; Pontié, Ben Rejeb et al. 2012).

I.4.3.2 Cleaning agents

Taking into account the fouling nature one can chose cleaning agents to remove the fouling form the surface of IEMs or to prevent fouling formation during ED treatment (Tab.I.2). However, rinsing by chemical addition may have a negative influence on the membrane performance (Korngold, de Körösy et al. 1970). Furthermore, addition of some chemicals may have consecutive negative effect on the quality of ED products what becomes really important when speaking about food industry.

Tab.I.2: Cleaning agents for different types of membrane fouling

Fouling type	Examples	Cleaning agents
Colloidal[a,b,c]	SiO_2, $Fe(OH)_3$, $Al(OH)_3$, etc.	Chlorination, alkali rinsing, anticoagulants and dispersants
Organic[d,e,f]	Polysaccharides, proteins, peptides, fatty acids, humate, surfactans	Alkali rinsing salt solutions, isopropanol
Scaling[d,g,h]	$CaCO_3$, $Ca(OH)_2$, $Mg(OH)_2$, $CaSO_4$, etc.	Citric acid, EDTA, hydrochloric acid, antiscalants
Biofouling[i,j]	Bacteria, biofilms, transparent exopolymer particles, etc.	Enzymes, surface active substances, chaotropic agents, biocides, nitric oxide, etc.

[a](Korngold 1971), [b](Korngold, de Körösy et al. 1970), [c](Ning, Troyer et al. 2005), [d](Lee, Moon et al. 2002), [e](Langevin and Bazinet 2011), [f](Franklin June 2009), [g](Wang, Yang et al. 2011), [h](He, Sirkar et al. 2009), [i](Flemming, Wingender et al. 2011), [j](Kristensen, Meyer et al. 2008).

I.4.3.3 Pretreatment

I.4.3.3.1 Pressure-driven membrane processes

Rejection of particles causing formation of a fouling layer on the ion-exchange membranes or clogging the ED stack is possible by application of pressure-driven membrane processes as a pretreatment technique prior to ED. These filtration techniques use the pressure gradient as a driving force and allow separation of particles according to their size or molecular weight. General classification distinguishes pressure-driven membrane processes according to the pore size and applied pressure (Fig.I.33), and

includes microfiltration (MF), ultrafiltration (UF), nanofiltration (NF) and reverse osmosis (RO).

	Pression (in bar)	Pores (in μm)
MF — Particles, bacteria	<1	10^{-1}-10^{1}
UF — Proteins, pigments	1-10	10^{-2}-10^{-1}
NF — Carbohydrates, polyvalent ions	20-40	10^{-3}-10^{-2}
RO — Monovalent ions	30-60	10^{-4}-10^{-3}
Water		
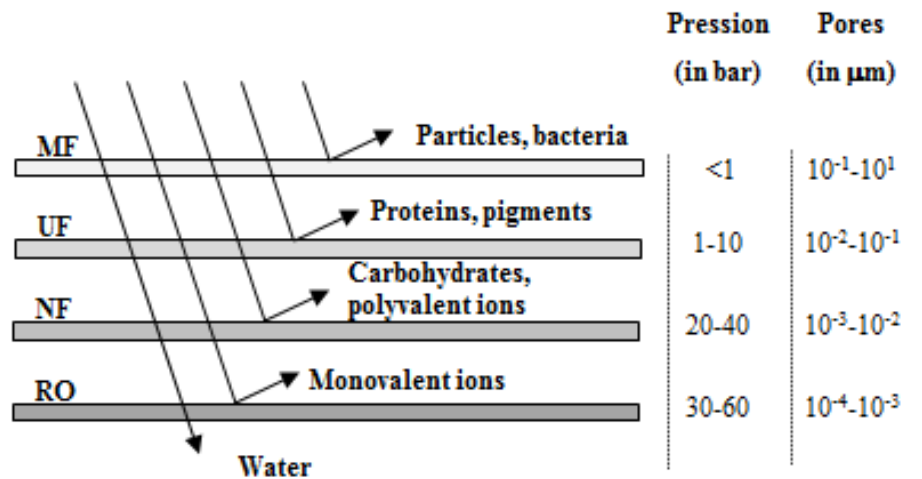
Fig.I.33: Classification of pressure-driven membrane processes (adapted from Bazinet, Firdaous and Pouliot, Chap.17 in (Bazinet and Castaigne 2011)).

Filtration processes can operate in two modes: dead-end and cross-flow (Fig.I.34). In dead-end mode, the stream of the feed solution flows perpendicularly to the membrane surface and only one flow leaves the membrane module. In cross-flow mode, the feed solution flows tangentially to the membrane surface, and there are two streams leaving the membrane module. For the majority of the modern pressure-driven membrane processes dead-end mode is inappropriate due to the severe accumulation of the rejected particles on the membrane surface leading to an abrupt decrease of the permeate flux. The tangential flow can help to shear away the accumulated rejected particles and attain relatively high flux of permeate. Assuredly, pressure-driven membrane processes as electromembrane processes also suffer from the fouling phenomena, however this subject is out of consideration in the present review. The more recent information concerning fouling in pressure-driven membrane processes is described in the following papers (Gao, Liang et al. 2011; Guo, Ngo et al. 2012; Goode, Asteriadou et al. 2013; Shi, Tal et al. 2014; Franklin June 2009).
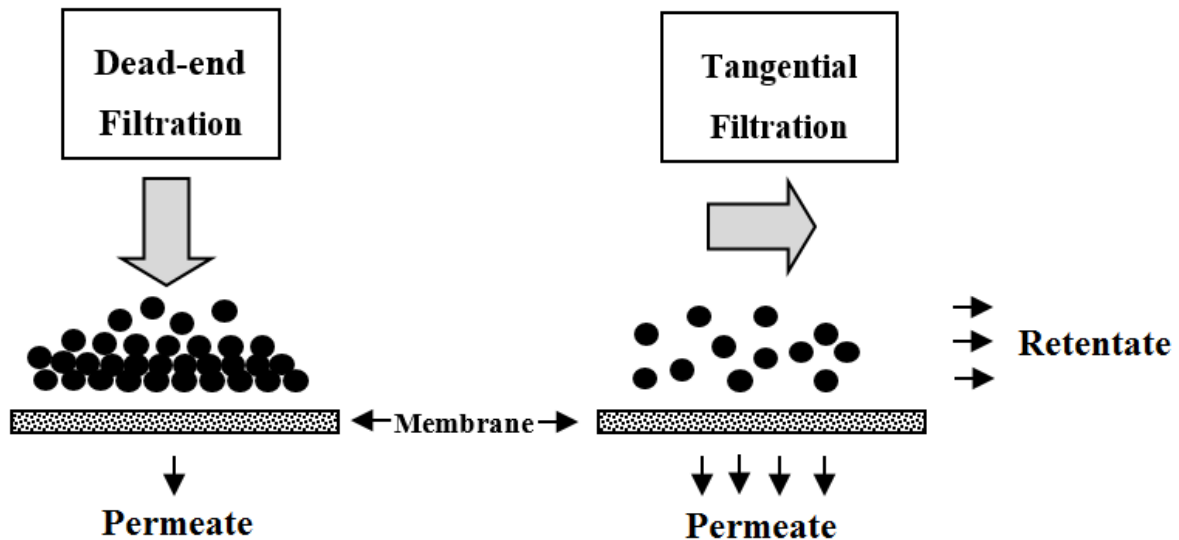
Fig.I.34: Filtration modes in pressure-driven membrane processes (adapted from Bazinet, Firdaous and Pouliot, Chap.17 in (Bazinet and Castaigne 2011)).

Successful applications of pressure-driven membrane processes as a pretreatment step prior ED were performed during production and separation of proteins (Jain 1981; Marquardt, Pederson et al. 1985; Kelly, Kelly et al. 2000; Alibhai, Mondor et al. 2006; Bazinet and Firdaous 2011), production and fermentation of organic acids and its derivatives (Boyaval, Corre et al. 1987; Datta 1989; Danner, Madzingaidzo et al. 2000; Datta and Henry 2006; Huang, Xu et al. 2007; Wang, Li et al. 2013), juice deacidification (Calle, Ruales et al. 2002; Vera, Ruales et al. 2003; Vera, Sandeaux et al. 2007; Bazinet and Firdaous 2011), waste water treatment (Sekoulov, Figueroa et al. 1991; Yang and Yang 2004; Nataraj, Sridhar et al. 2007), green production of polyaluminium salts (Chen, Xue et al. 2014).

I.4.3.3.2   Other pretreatment techniques

Avoiding some types of membrane fouling may be successfully carried out by application of following techniques:

- *Activated carbon* allows removal of dissolved organic matter prior ED. The mechanism of action is based on adsorption of organic particles by the porous

activated carbon with a large surface area (Tsun, Liu et al. 1998; Huang, Xu et al. 2007; Bazinet and Firdaous 2011; Fidaleo 2011);

- *Filtration* is used to reject high molecular weight residues which can cause fouling of IEMs and clogging of ED stack (Datta 1989; Datta and Henry 2006; Huang, Xu et al. 2007; Bazinet and Firdaous 2011; Fidaleo 2011);

- *Centrifugation* can be used to separate suspensions from solutions treated by ED (Jain 1981)

- *Pellet reactor* is a column filled with a garnet sand, which acts as absorber of mineral ions such as Ca^{2+} and Mg^{2+} preventing the formation of scaling on IEMs (Tran, Zhang et al. 2012; Tran, Jullok et al. 2013);

- *UV irradiation* inactivates bacteria and can be used for the control of biofouling (Lakretz, Ron et al. 2009; Flemming, Wingender et al. 2011);

- *Willow field* is a new technique consisted of the removal of organic compounds by willow trees prior to ED (Ghyselbrecht, Van Houtte et al. 2012).

I.4.3.4 <u>Mechanical action</u>

Prevention and destruction of fouling by mechanical procedures such as ultrasound, vibration, air sparge etc. are involved in filtration processes (Ebrahim 1994; Band, Gutman et al. 1997; Lim and Bai 2003; Franklin June 2009). However, in ED processes mechanical cleaning is applied rarely due to the changes in membrane properties and even membrane deterioration (Wang, Ma et al. 2014; Franklin June 2009). Nevertheless, recently Wang et al. (Wang, Yang et al. 2011) reported that ultrasound treatment in combination with acid treatment can be effective against CEM fouling. In addition, Parvizian et al. (Parvizian, Rahimi et al. 2012) showed that impose of ultrasound could successfully improve the membrane potential, transport number and selectivity and decrease its electrical resistance. These investigations of ultrasound application may be attractive in terms of fouling prevention and improving ED performance, however additional studies in this field should be carried out.

I.4.3.5 <u>Changing regimes of ED treatment</u>

I.4.3.5.1   <u>Control of hydrodynamic conditions</u>

In some cases, control of hydrodynamic conditions of ED treatment may be sufficient to avoid fouling formation. Grossman et al. (Grossman and Sonin 1972; Grossman and Sonin 1973) reported, that an increase in flow rate and introduction of spacers promoting turbulence are advantageous in terms of fouling mitigation. The design of the spacers is important in terms of increasing current efficiency and number of works are dedicated to the spacer design (Kim, Kim et al. 1983; Korngold, Aronov et al. 1998; Messalem, Mirsky et al. 1998; Długołęcki, Dąbrowska et al. 2010). The tendency of spacers design moves towards the creation of ion-exchange spacers. From the one hand, ion-exchange spacers have positive effect on ED performance, from the other hand, they tend to be more fouled due to their surface charge in comparison with uncharged spacers. Blaster et al. (Balster, Stamatialis et al. 2009) proposed an approach alternative to spacers such as air sparging. This approach allows increasing solution turbulence which may be also advantageous in the reduction of a membrane deposit.

I.4.3.5.2   <u>Electrodialysis with reversal polarity</u>

Another perspective method proposed for the fouling control is ED with reversal polarity (Katz 1979; Katz 1982; Fubao 1985; Strathmann 2004; Nagarale, Gohil et al. 2006; Chao and Liang 2008; Valero and Arbós 2010; Valero, Barceló et al. 2011). This process consists of inverting the polarities of the electrodes periodically (i.e., at time intervals varying from a few minutes to several hours), as well as the hydraulic flow streams. When the polarity of electrodes is reversed, foulants attaching to the membrane surface (usually charged oppositely to ion-exchange groups) become detached moving in the opposite direction (Fig.I.35). There are evident advantages of ED with reversal polarity such as prevention of membrane fouling, dissolution of scale seeds and absence of chemical additives. However, there is inconvenience related to the time (usually 1-2 minutes) after the reverse of polarity when both diluate and concentrate streams become "off

specification" and diverted automatically to waste or back to feed tank (Katz 1982; Fubao 1985).
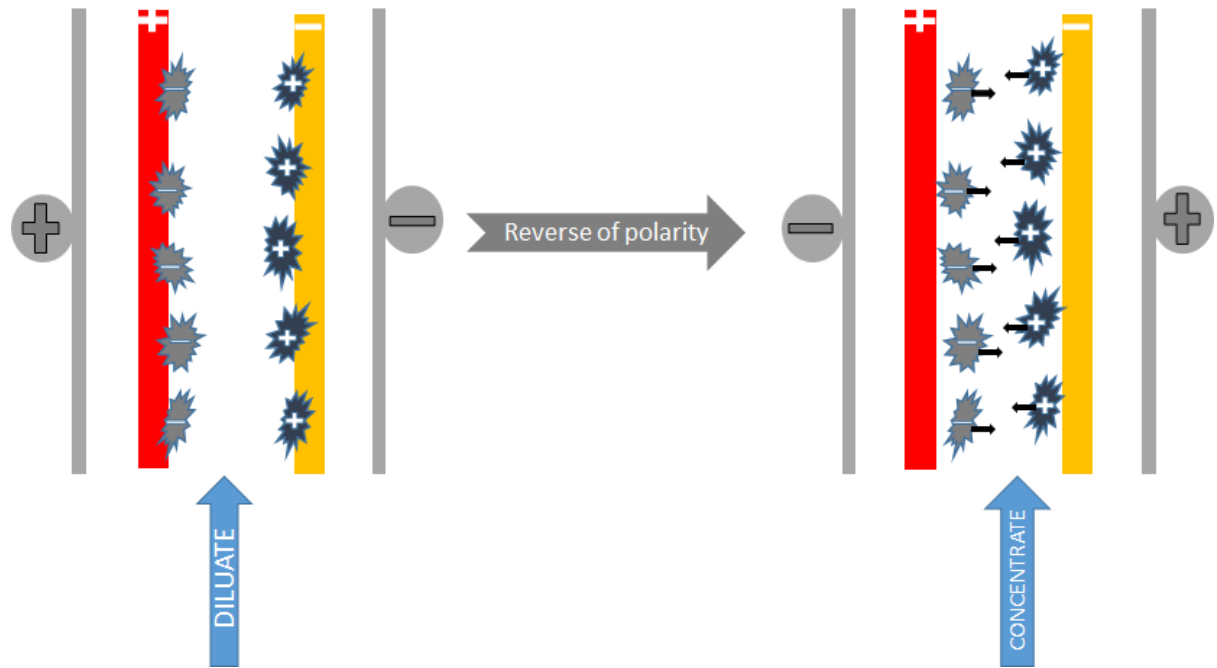
Fig.I.35: Scheme of ED with reversal polarity and presence of foulants.

I.4.3.5.3   Pulsed electric field

The use of pulsed electric field (PEF) demonstrated very good results in terms of fouling prevention. PEF procedure consists in application of consecutive pulse and pause lapses (T_{on}/T_{off}) of certain duration (Fig.I.36).
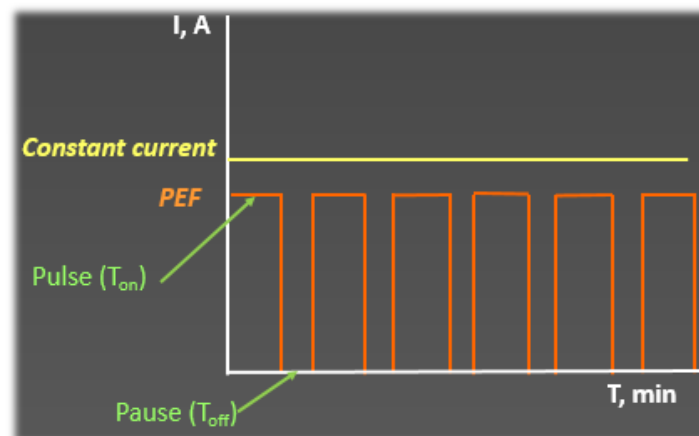
Fig.I.36: Scheme of PEF with constant current.

PEF has number of advantages such as

- ✓ Increase of current efficiency due to the suppression of CP phenomena;
- ✓ Effectiveness against fouling;
- ✓ Simplicity of equipment, which makes integration of such approach into industrial scale really easy and inexpensive.

First of all, the positive influence of PEF was found in terms of decrease of CP phenomena and consequently decrease in water dissociation and increase in ED power efficiency (Mishchuk, Koopal et al. 2001; Nikonenko, Pismenskaya et al. 2010; Sun, Ottosen et al. 2012; Malek, Ortiz et al. 2013). Secondly, Lee et all. (Lee, Moon et al. 2002) and Park et al. (Park, Lee et al. 2003) reported mitigation of fouling containing humates and Ruiz et al. (Ruiz, Sistat et al. 2007) had success in protein deposit mitigation. Success in scaling mitigation was demonstrated in (Casademont, Sistat et al. 2009; Cifuentes-Araya, Pourcelly et al. 2011; Cifuentes-Araya, Pourcelly et al. 2012; Cifuentes-Araya, Pourcelly et al. 2013; Cifuentes-Araya, Pourcelly et al. 2013; Cifuentes-Araya, Astudillo-Castro et al. 2014). Profound investigations has been made in order to reveal the mechanisms of scaling formation under the action of PEF. The results of these works show the importance of pulse/pause duration in terms of scaling inhibition and control of phenomena favoring scaling development such as water splitting and OH^- leakage. Moreover, authors tested relatively long PEF modes (20s – 5s) and created a 3D model of influence of pulse/pause duration on demineralization rate. Further calculations based on this 3D model suggested the use of shorter PEF modes as a following step of the demineralization improvement (Cifuentes-Araya, Pourcelly et al. 2013).

I.4.3.5.4   Overlimiting current regime

Contemporary investigations revealed reasonableness of overlimiting currents for improving ED (Nikonenko, Kovalenko et al. 2014). Electroconvective vortices created by application of overlimiting current may also affect the formation of fouling. Bukhovets et al. (Bukhovets, Eliseeva et al. 2011) proposed the "washing out" effect of electroconvection on the organic fouling. However, the approach of using overlimiting current modes is new and demands more profound investigations to reveal underlying mechanisms.

72

CHAPTER II. PROBLEMATIC, HYPOTHESIS AND OBJECTIVES

II.1 <u>Problematic</u>

It is well known that electrodialysis (ED) attracts high attention of scientists working in desalination, separation, purification and power production. Indeed, ED processes are widely applied in the industry. However, the majority of the ED processes faces fouling and concentration polarization (CP) as the key locks. Many efforts were applied to find the optimal approach allowing control and inhibition of fouling. Conventional approaches involve modification of the membrane structure, improving the membrane module construction and pretreatment procedures. Despite the effectiveness of these approaches, they usually demand substantial investments. Studies of non-stationary electric fields or pulsed electric fields (PEF) revealed the possibility of CP inhibition. Further, successful applications of PEF to control the different fouling types were reported. Among all fouling types, control of mineral fouling designated as scaling was one of the most common goals due to prevalence of scaling in a wide range of ED processes. The most harmful effect of scaling is associated with cation-exchange membranes (CEM) in comparison with anion-exchange membranes (AEM). This fact is due to the positive charge of most part of scaling agents what provokes its strong electrostatic interactions with negatively charged ion-exchange groups of CEM. Recent works were devoted to study scaling phenomena in severe conditions comprising high concentration of scaling agents and alkaline pH under the influence of different PEF modes. It was revealed that water splitting phenomenon and OH^- leakage as well as the pulse/pause duration are the main factors affecting the scaling formation. Water splitting may act positively and negatively at the same time since H^+ generation hamper scaling formation (proton barrier) while OH^- generation enhances scaling formation. OH^- leakage through the CEM, arising due to the decrease of CEM permselectivity, was reported as a very serious problem promoting the scaling formation. Perturbations created by PEF can control scaling formation and water splitting. Relatively long pulse/pause lapses (40s – 5s) were tested in order to find the optimal PEF mode allowing better scaling prevention and CP control as well as to explain the mechanism of PEF action. Despite very profound investigations concerning the studies

of scaling quantities, composition and structure as well as the influence of water splitting and OH⁻ leakage, the optimal PEF modes are still disputable. Moreover, there are no studies concerning the influence of electroconvection (another important phenomenon arising due to the development of CP) and intrinsic membrane properties on scaling formation under the action of PEF.

II.2 **Hypothesis**

The type of electric field (continuous current or pulsed electric field with a certain pulse/pause duration), electroconvection and intrinsic membrane properties have an impact on the quantity, structure and composition of membrane scaling, development of water splitting and OH⁻ leakage, and process performance during electrodialysis of model salt solutions or more complex food solutions containing scaling agents.

II.3 **Specific research questions**

1. Is it possible to eliminate completely the scaling on AEM and substantially decrease the scaling on CEM during electrodialysis of solutions with high concentration of scaling agents by application of relatively short pulse/pause modes (0.5s − 3s) and what is the mechanism of scaling formation and CP development at these pulse/pause lapses?

2. What is the influence of electroconvection and intrinsic properties of cation-exchange membrane on nature, structure and quantity of scaling, and process performance under the action of PEF?

3. Is it possible to apply pulsed electric field mode during bipolar membrane electroacidification of milk (or mineral milk fraction) and what is the impact of pulsed electric field on scaling formation and process performance?

II.4 <u>Objectives</u>

II.4.1 <u>General objective</u>

The main objective of this project will be to understand the influence of short pulse/pause conditions (0.5s – 3s) on scaling formation mechanism, structure and composition as well as on process efficiency during conventional electrodialysis and electrodialysis with bipolar membranes of complex solutions containing high concentration of scaling agents.

II.4.2 <u>Specific objectives</u>

In order to confirm or infer the hypothesis, specific objectives will be carried-out**:**

1) To study the application of short pulse/pause modes (0.5s – 3s) during electrodialysis of model salt solutions containing high concentration of Ca^{2+} and Mg^{2+} scaling ions and to find the optimal pulsed electric field mode;

2) To understand the influence of electroconvection and intrinsic membrane properties on scaling formation:

   a) to evaluate physico-chemical properties of two different lots of cation-exchange membranes,
   b) to evaluate the development of water splitting and electroconvection by means of voltammetry, chronopotentiometry and visualization by microfluidic platform,
   c) to perform electrodialysis under the same conditions as in the first objective applying the optimal pulsed electric field modes;

3) To explore the scaling formation and process performance under the pulsed electric field during isoelectric casein precipitation by means of bipolar membrane electrodialysis of skim milk:

   a) to study the use of an ultrafiltration module prior to electrodialysis module for the prevention of clogging of electrodialysis stack by casein curd,
   b) to study the scaling phenomenon and process performance under pH 4.6 and 5.0,
   c) to compare continuous current and optimal pulsed electric field mode.

CHAPTER III. INTENSIFICATION OF DEMINERALIZATION PROCESS AND DECREASE IN SCALING BY APPLICATION OF PULSED ELECTRIC FIELD WITH SHORT PULSE/PAUSE CONDITIONS

CONTEXTUAL TRANSITION

From the literature review, it is clear that scaling can be controlled by PEF modes. On the one hand, perturbations created by pulse/pause lapses inhibit the scaling formation and growth. On the other hand, PEF modes affect the development of water splitting, which is very important due to the sensitivity of scaling to the pH changes. Indeed, alkaline pH favors scaling formation while acid pH plays a role of scaling inhibitor. Recently, it was established that not only water splitting (generation of H^+ and OH^-) but also OH^- leakage trough the CEM might lead to pH fluctuations. Thus, pH can be shifted by H^+ generated during water splitting which has a positive influence on scaling suppression ("proton barrier") while generated during water splitting and leaked OH^- ions create a favorable environment for the scaling formation and growth.

Thorough investigations of the scaling formation mechanisms showed that the duration of pulse/pause lapses is a relevant parameter affecting the scaling nature and quantity as well as water splitting and OH^- leakage. Therefore, numbers of authors tested different PEF modes in order to find the optimal conditions allowing control of scaling and phenomena affecting pH. Results of these investigations show that the use of relatively long pulse/pause lapses (40s – 5s) allows good scaling inhibition though the optimal mode is still disputable. In this context, the present chapter will focus on the study of different PEF modes with short pulse/pause lapses (0.33s – 3s) in order to evaluate their influence on scaling formation and ED performance as well as to find the optimal PEF mode allowing better scaling control.

This chapter has been the subject of an article entitled:

"**Intensification of demineralization process and decrease in scaling by application of pulsed electric field with short pulse/pause conditions**", was published in "Journal of Membrane Science (2014) Vol. 468, pp. 389-399". The authors are Sergey Mikhaylin (Ph. D. Candidate: planning and realization of the experiments, analysis of the results and writing of the manuscript), Victor Nikonenko (Thesis Co-director: scientific supervision of the student, revision and correction of the manuscript), Gérald Pourcelly (Thesis Co-director: scientific supervision of the student, revision and correction of the manuscript) and Laurent Bazinet (Thesis Director: scientific supervision of the student, revision and correction of the manuscript).

III.1 <u>Intensification of demineralization process and decrease in scaling by application of pulsed electric field with short pulse/pause conditions</u>

<u>Abstract</u>

Pulsed electric field (PEF) can affect positively the membrane scaling mitigation and the intensification of electrodialytic (ED) process. Recent studies considered the use of PEF with relatively long pulse/pause conditions (5s-40s). The present work was focused on the application of specific PEF conditions with short pulse/pause duration as a following perspective step in improving demineralization. Therefore, in this study six conditions were tested (1s/0.33s, 1s/1s, 2s/0.5s, 2s/0.67s, 3s/0.33s, 3s/1s) in order to investigate the influence of short PEF lapses and to find the optimum among all PEF conditions. Results indicate that PEF conditions of 2s/0.5s and 2s/0.67s allowed the highest demineralization rates. A decrease of scaling on the cation-exchange membrane surface in comparison with previous data was observed in all PEF conditions. In addition, the absence of scaling on the anion-exchange membrane was observed for the first time in such extreme conditions of demineralization and solution composition. These results highlighted the successful use of short pulse/pause lapses during electrodialysis.

III.1.1 <u>Introduction</u>

The main lockers for electrodialysis (ED) development are concentration polarization (CP) phenomena and fouling formation at ion-exchange membrane (IEM) interfaces (Strathmann 2004). CP arises due to the ability of IEM to readily transport ionic species. As a result, the salt concentration decreases at one side of the membrane and increases at the other (Nikonenko, Pismenskaya et al. 2010). If a sufficiently high voltage is applied, the electrolyte concentration near the diluate side of the membrane becomes close to zero: the limiting current density (LCD) is then reached. It means that with increasing the voltage the mass transfer of ionic species is no more improved and water splitting phenomenon occurred. Thus CP is influenced by the state of flow in the desalting

cell (Tanaka 2004) and provides generation of H^+ and OH^- ions as current carriers (Nikonenko, Pis'menskaya et al. 2005). Further voltage increase leads to the development of current-induced convection (electroconvection and gravitational convection) which improves ion transport to the membrane surface and hampers water splitting. Concerning membrane fouling, its formation includes the adsorption of foulants at the interfaces of the membrane (diluate or concentrate sides) or inside the membrane. The main difference between the types of fouling (colloidal fouling, organic fouling, scaling and biofouling) is the nature of the particles that cause the fouling (Franklin June 2009). In addition, fouling can be a physical and/or chemical phenomenon (Zhao, Wu et al. 2000).

Among all methods which can help to solve both types of limitations, pulsed electric field (PEF) is considered as one of the most effective (Mishchuk, Koopal et al. 2001; Ruiz, Sistat et al. 2007; Nikonenko, Pismenskaya et al. 2010). PEF perturbations may scale down the CP, because during pause lapse ion transport from the bulk of solution to the membrane layer is continued by means of diffusion and convection; thereby the concentration gradient decreases before application of the pulse lapse (Nikonenko, Pismenskaya et al. 2010). Furthermore, inertial properties of liquid movement can exist after pulse lapse, which can intensify ion transfer (Mishchuk, Koopal et al. 2001). Successful uses of PEF for reducing membrane fouling were reported by Ruiz et al. (Ruiz, Sistat et al. 2007) for a protein deposit, Lee at al. (Lee, Moon et al. 2002) and Park et al. (Park, Lee et al. 2003) for humate deposit, and by Casademont et al. (Casademont, Sistat et al. 2009) and Cifuentes-Araya et al. (Cifuentes-Araya, Pourcelly et al. 2012) for scaling. After the thorough investigations of the mineral deposit structure, the scaling formation mechanism was proposed by Cifuentes-Araya et al. (Cifuentes-Araya, Pourcelly et al. 2012). Two main factors were indicated as the most important for building up the membrane deposit: OH^- generation during the water splitting phenomenon and OH^- leakage. These hydroxyl ions can create the necessary environment for precipitation of two main mineral foulant agents Mg^{2+} and Ca^{2+} ions in the different polymorphic forms of $Mg(OH)_2$ and $CaCO_3$. From the identified mechanisms and polymorphic forms generated during ED in different PEF conditions (Cifuentes-Araya, Pourcelly et al. 2012; Cifuentes-Araya, Pourcelly et al. 2013), it was proposed to use short pulse/pause lapses (less than 5s) instead of long pulse/pause lapses (5s – 40s) (Mishchuk, Koopal et al. 2001; Ruiz, Sistat et al. 2007; Cifuentes-Araya, Pourcelly et al. 2011; Cifuentes-Araya, Pourcelly et al. 2012; Cifuentes-Araya, Pourcelly

80

et al. 2013). In addition, the use of pause lapse values less than pulse lapse values may also have a positive effect on scaling prevention (Cifuentes-Araya, Pourcelly et al. 2013). Furthermore, recent investigations by Malek et al. (Malek, Ortiz et al. 2013) revealed the feasibility of using short PEF regimes for improving the ED performance by suppression of water splitting phenomenon. However, their experiments were performed on an ideal system containing only NaCl and thus provided no information on the possible benefits of this approach to limiting fouling.

Thus, the present work will focus on PEF application combining different short pulse/pause lapses conditions in order to intensify the desalination process and decrease the membrane scaling as well as to find the optimal PEF conditions during ED treatment of more complex solutions containing Mg^{2+} and Ca^{2+} salts.

III.1.2 <u>Experimental methods</u>

III.1.2.1 <u>Material</u>

$CaCl_2.2H_2O$, $MgCl_2.6H_2O$, NaCl and KCl (ACS grade) were obtained from Laboratoire MAT (Quebec, QC, Canada). Na_2CO_3 was obtained from EMD (EMD Chemicals, Gibbstown, NJ), NaOH (1 M) and HCl (1 M) from Fisher Scientific (Nepean, ONT, Canada).

III.1.2.2 <u>Electrodialysis cell</u>

The electrodialysis cell was a Microflow-type cell (Electro-Cell AB, Täby, Sweden) comprising two Neosepta CMX-SB cation-exchange membranes and two Neosepta AMX-SB anion-exchange membranes (Tokuyama Soda Ltd., Tokyo, Japan). The anode was a dimensionally stable electrode (DSA) and the cathode a 316 stainless-steel electrode. This arrangement defines three closed loops (Fig.III.1) containing the diluate model salt solution (330 ml, flow rate of 600 mL/min), a 2 g/L KCl aqueous concentrate solution at constant

pH (330 mL, 600 mL/min) and a 20 g/L NaCl electrolyte solution (500 mL, 900 mL/min). The membranes tested, of 10 cm² membrane effective surface, were in contact with the model salt solution on one side and the pH-controlled KCl solution on the other side (Fig.III.1). Each closed loop was connected to a separated external plastic reservoir, allowing continuous recirculation. The electrodialysis system was not equipped to maintain constant temperature, but this parameter undergo low variations.
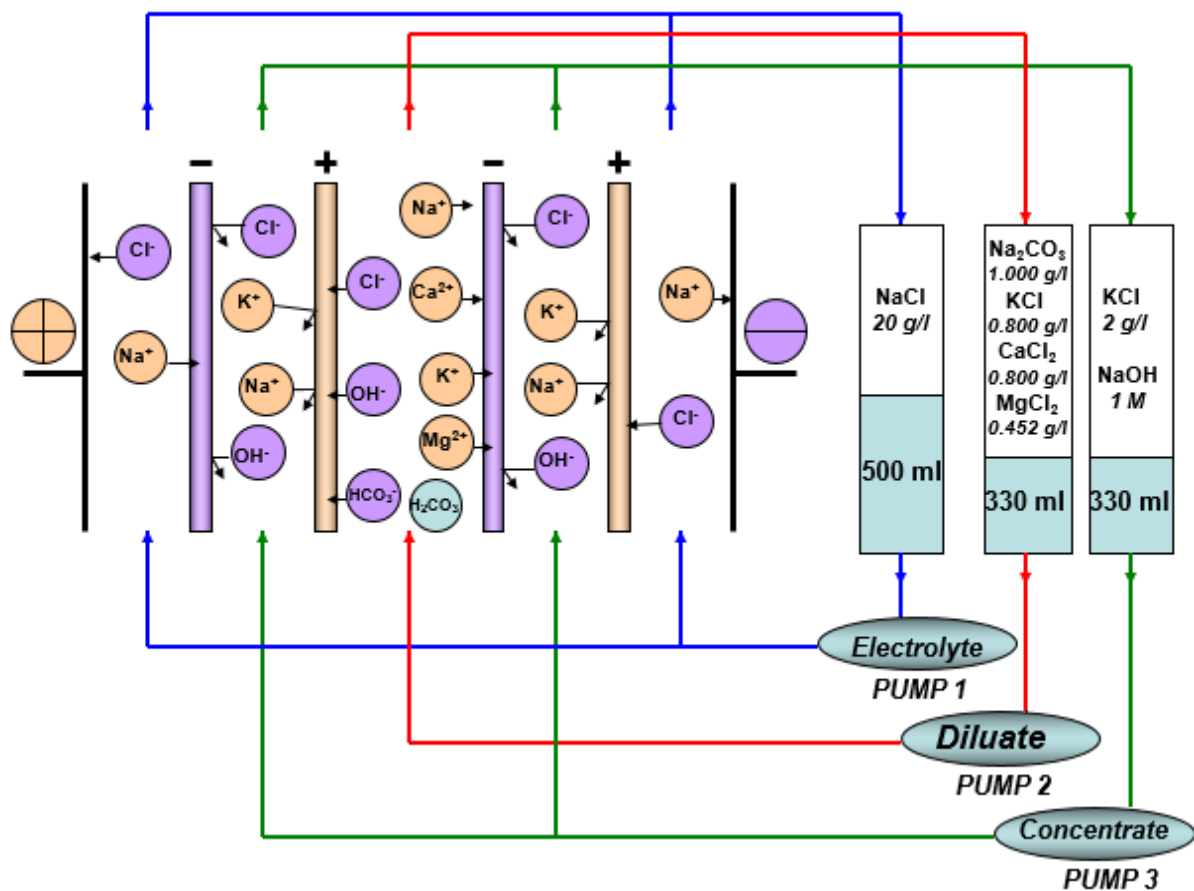
Fig.III.1: Electrodialysis cell configuration.

III.1.2.3 Protocol

Preliminary tests were performed to determine the limiting current density according to the method described by Cowan and Brown (Cowan and Brown 1959). Limiting current density value was 21 mA/cm². ED was carried out in batch process at a

constant current density of 40 mA/cm^2 using a Xantrex power supply (Model HPD 60-5SX; Burnaby, BC, Canada). This current density was chosen in order to explore a possible scaling mitigation when water splitting and current-induced convection occurred and to compare our results with those reported by Cifuentes-Araya et al. (Cifuentes-Araya, Pourcelly et al. 2012; Cifuentes-Araya, Pourcelly et al. 2013). The model salt solution was composed of Na$_2$CO$_3$ (1000 mg/L), KCl (800 mg/L), CaCl$_2$ (800 mg/L) and MgCl$_2$ (452 mg/L) in order to maintain a Mg/Ca ratio of 2/5 (Cifuentes-Araya, Pourcelly et al. 2011): this ratio is double as the one contained in milk (Amiot, Fournier et al. 2002) to ensure membrane scaling formation (Cifuentes-Araya, Pourcelly et al. 2012; Cifuentes-Araya, Pourcelly et al. 2013). The model salt solution was prepared just before the beginning of ED process. The initial pH of the model salt solution was fixed at 6.5 by manual addition of HCl (1 M). The pH of concentrate solution was maintained constant (pH=12) during the whole ED process by manual additions of NaOH (1 M) to ensure the continuous precipitation of minerals (Cifuentes-Araya, Pourcelly et al. 2012; Cifuentes-Araya, Pourcelly et al. 2013). The ED treatments were stopped after the maximum voltage capacity of the power supply was reached (62.5 V). To find the optimal PEF conditions the following regimes were performed: T_{on}/T_{off}=3s/1s (PEF ratio 3), T_{on}/T_{off}=2s/0.67s (PEF ratio 3), T_{on}/T_{off}=1s/0.33s (PEF ratio 3), T_{on}/T_{off}=3s/0.3s (PEF ratio 10), T_{on}/T_{off}=2s/0.5s (PEF ratio 4) and T_{on}/T_{off}=1s/1s (PEF ratio 1). These PEF modes were selected based on the data obtained by Ruiz et al. (Ruiz, Sistat et al. 2007), and Cifuentes-Araya et al. (Cifuentes-Araya, Pourcelly et al. 2013). Four repetitions were carried out for each PEF condition. ED parameters (current intensity, voltage, solution conductivities) were recorded every five minutes all along the treatments. After ED treatment, membrane thickness and scaling content were determined. In certain conditions and according to the membrane type a precipitate formation was observed visually on the wet membrane (before drying). On a 4-cm^2 dried membrane sample, electron microscopy photographs and X-ray elemental analysis were taken on the CEM and AEM surfaces in contact with the concentrate and diluate solutions in order to visualize the presence or not of scaling.

III.1.2.4 <u>Analysis methods</u>

III.1.2.4.1 <u>Membrane thickness</u>

The membrane thickness was measured with a Mitutoyo micrometer (Model 500-133, Kanagawa-Ken, Japan). The Digimatic indicator was equipped with a 10-mm-diameter flat contact point. The membrane thickness values were averaged from six measurements at different locations on the effective surface of each membrane

III.1.2.4.2 <u>Scaling content</u>

For the scaling content (SC) determination, 2.5×3 cm membrane samples were placed in an oven at 80°C for 12 h under vacuum. After drying, the membranes were kept in a desiccator for 30 minutes, the dry weight of membranes was then recorded. The SC (in %) was calculated using the following equation:

$$SC = \frac{W_w - W_c}{W_c} \times 100$$

eq. III.1

where W_w is the dry weight of the working membrane after ED (in g) and W_c is the dry weight of the control membrane (in g).

III.1.2.4.3 <u>Scanning electron microscopy and X-ray elemental analysis</u>

Images were taken with a scanning electron microscope JEOL (Japan Electro Optic Laboratory, model JSM840A, Peabody, Massachusetts, USA) equipped with an energy dispersive spectrometer (EDS) (Princeton Gamma Tech.), Princeton, New Jersey, USA). The EDS conditions were 15 kV accelerating voltage with a 13-mm working distance. The

84

dried samples (drying procedure like in 2.4.2) of initial and ED treated membranes were coated with a thin layer of gold/palladium in order to make them electrically conductive and to improve the quality of the microscopy photographs (Cifuentes-Araya, Pourcelly et al. 2011). For X-ray analysis membrane sample preparation was the same like for SEM. Therefore, membrane scaling is formed during ED treatment. The bonds between salts of Ca^{2+} and Mg^{2+} and groups SO^{3-} are really strong because Ca^{2+} and Mg^{2+} ions have strong affinity to membrane ion-exchange groups. That is why this fouling is irreversible.

III.1.2.4.4 pH

The pH values of diluate and concentrate solutions was measured with a pH-meter Model SP20 (epoxy gel combination pH electrode, VWR Symphony), manufactured by Thermo Orion (West Chester, PA, USA).

III.1.2.4.5 Solution conductivity and demineralization rate

The conductivity of diluate and concentrate solutions was measured with an YSI conductivity instrument (model 3100–115 V, YSI Inc. Yellow Springs, Ohio, USA) equipped with an automatic temperature compensation (ATC) immersion probe (model 3252, k = 1/cm, YSI Inc.). The demineralization rate (DR) was calculated according to the following equation (Ruiz, Sistat et al. 2007):

$$DR = \left(1 - \frac{\text{model salt solution conductivity at time t}}{\text{model salt solution conductivity at time t} = 0}\right) \times 100 \qquad \text{eq. III.2}$$

III.1.2.4.6 Overall ED stack resistance

The overall ED stack resistance was determined using Ohm's Law, from the voltage and the current intensity read directly from the indicators on the power supply.

III.1.2.4.7 Energy consumption (EC)

The energy consumption was calculated according to Ruiz et al. (Ruiz, Sistat et al. 2007)

$$EC = \int_0^{\bar{t}} I(t)U(t)dt$$

eq. III.3

where $\bar{t}$ is the time of the experiment run (in h), U(t) is the voltage (in V) as a function of time; I(t), the intensity (in A) as a function of time; and dt, the time variation (in h). EC was expressed in Wh.

III.1.3 Results

III.1.3.1 Electrodialysis parameters

III.1.3.1.1 Demineralization rate

The demineralization rates (DRs) were calculated from diluate solution conductivity value (Cifuentes-Araya, Pourcelly et al. 2011). On Figure III.2 optimal PEF conditions is clearly visible in term of DR. This diapason existed at T_{on}=2s and there were no significant difference between both treatments at T_{off}=0.67s and T_{off}=0.5s: respective DR of 78.8% and 79.3%. Application of PEF regimes with T_{on}=1s decreased DR of

86

approximately 10 % with no real difference according to the pause lapse duration (T_{off}=1s and T_{off}=0.33s). Increase of PEF modes to 3s/1s and 3s/0.33s led to similar intermediary DRs values around 75 %.

These results are in accordance with previous results concerning the DR values reached. However, Cifuentes-Araya (Cifuentes-Araya, Pourcelly et al. 2013) reported DR variations ranging from 1 to 9 % between conditions with the similar pulse lapse but different pause lapses: this can be explained by longer time intervals (5-20 s) and the fact that authors used ratios in which T_{on}<T_{off}.
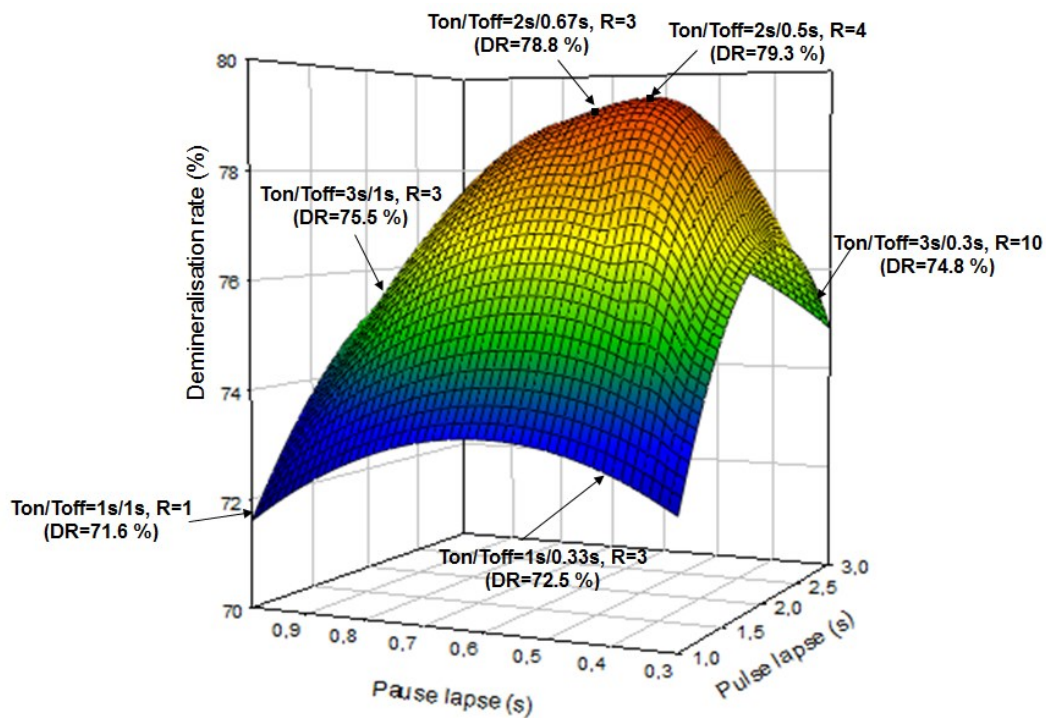
Fig.III.2: Demineralization rate (average values from 4 experiments) in the different PEF conditions (R is pulse/pause ratio).

III.1.3.1.2 Energy consumption and overall ED stack resistance

Energy consumption (EC) was minimal for 1s/0.33s and 1s/1s PEF modes (Fig.III.3). Moreover, the value of EC for T_{off}=1s was significantly better than those obtained for all the other conditions tested in the present study and EC values reported by

Cifuentes-Araya et al. (Cifuentes-Araya, Pourcelly et al. 2011). By comparing figures III.2 and III.3, the trends are quite similar meaning that a high DR value is linked with a high EC value: the more the demineralization, the highest the EC was. Energy consumption per percentage unit of demineralization (ratio EC/DR) was not the same for each condition and did not increase linearly with the increase in demineralization (Fig.III.4).

Comparing our results with what was highlighted by Casademont et al. (Casademont, Sistat et al. 2009) it is possible to see the increase in EC in our case. This increase can be explained by applying different current densities (40 mA/cm^2 versus 15mA/cm^2 for Casademont et al.) and by testing different effective membrane surface (10 cm^2 versus 20 cm^2 for Casademont et al.).
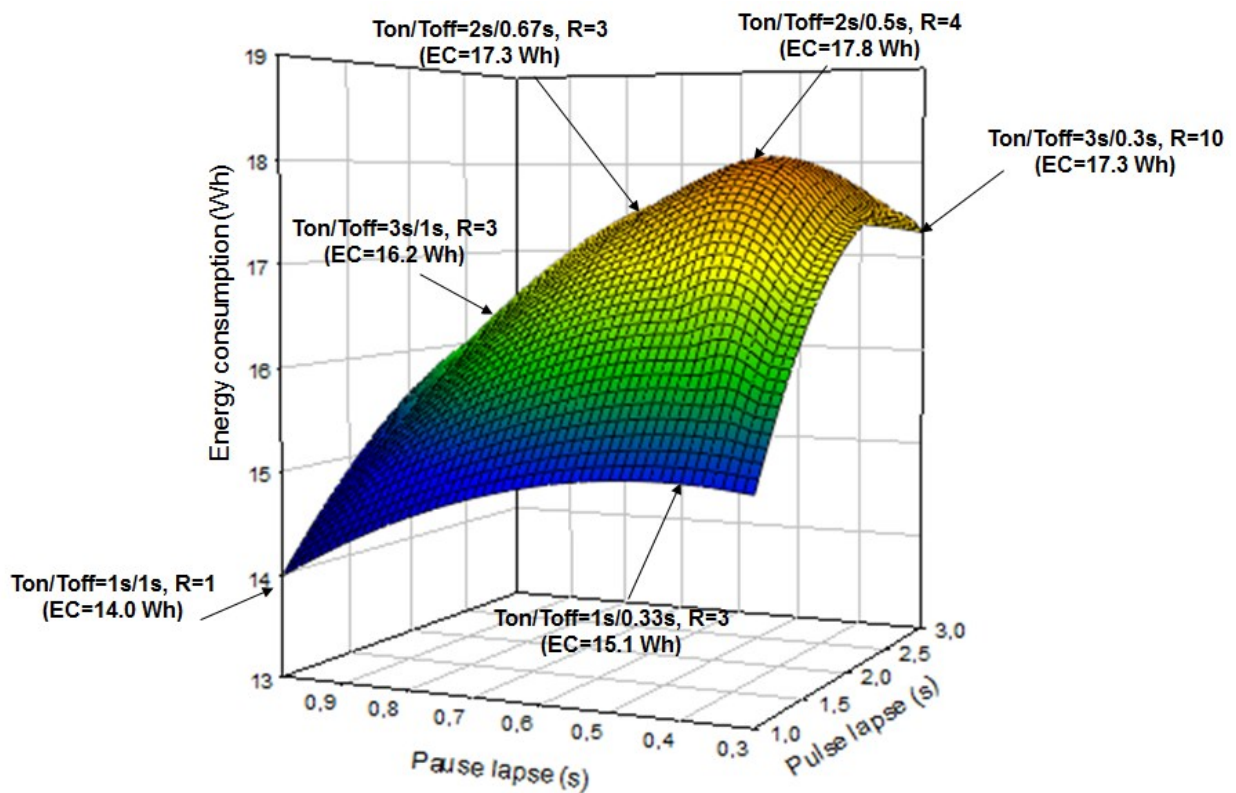
Fig.III.3: Energy consumption (average values from 4 experiments) in the different PEF conditions (R is pulse/ pause ratio).
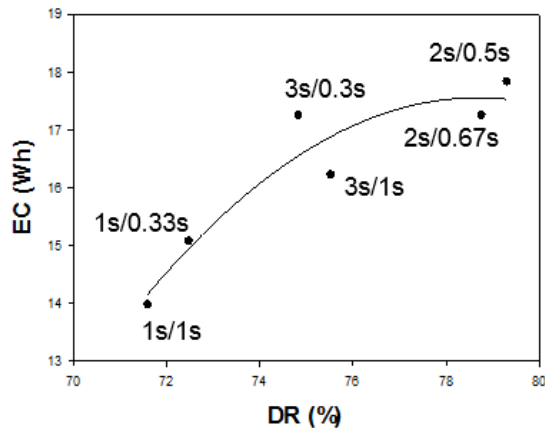
Fig.III.4: Energy consumption as a function of DR percentage in the different PEF conditions.

The overall ED stack resistance was measured as a function of ED time. The curves representing the resistance evolution were close to linear (Fig.III.5), but with different slopes. Hence, for pulse lapse of 3s and 2s whatever the pause lapse, the slopes were the same. However, for the 1s/1s condition, the slopes were very different between 1s off and 0.33 s off which was related with difference between duration of ED treatment.

Different slopes of resistance curves may be attributed 1) to the duration of pulse/pause and 2) to the different development of the coupled effects of CP (such as water splitting and electroconvection) (Pismenskaya, Nikonenko et al. 2007) as well as formation of scaling. If we take a look on fig.III.5 and PEF with pulse lapse 3 the slopes of resistance curves are almost the same as well as the time of ED treatment though pause lapses and ratios are different. Apparently, for 3s/1s, 3s/0.3s and 1s/0.33s coupled effects of CP were less developed in comparison with other PEF conditions, which gave rise to more abrupt increase of overall ED stack resistance. Contrary, for 2s/0.5s and 2s/0.67s slopes of resistance curves were less abrupt. That may indicate the development of electroconvection and intensification of the demineralization, what was confirmed by the highest DR values (79.3% and 78.8% for 2s/0.5s and 2s/0.67s respectively). In the case of 1s/1s it is clearly visible that the slope of resistance curves was the least abrupt among all PEF conditions and it is possible to speculate that there will be a high demineralization. However, DR for this condition was also the least. Because of the long duration of ED treatment (120 min), seemingly, more scaling was formed on the membrane surface, which could lead to the

decrease in mass transfer. Most probably, the small plateau on the curve might be related to the suppression of water splitting by coupled-induced convection, what caused a positive effect on the ion transfer.
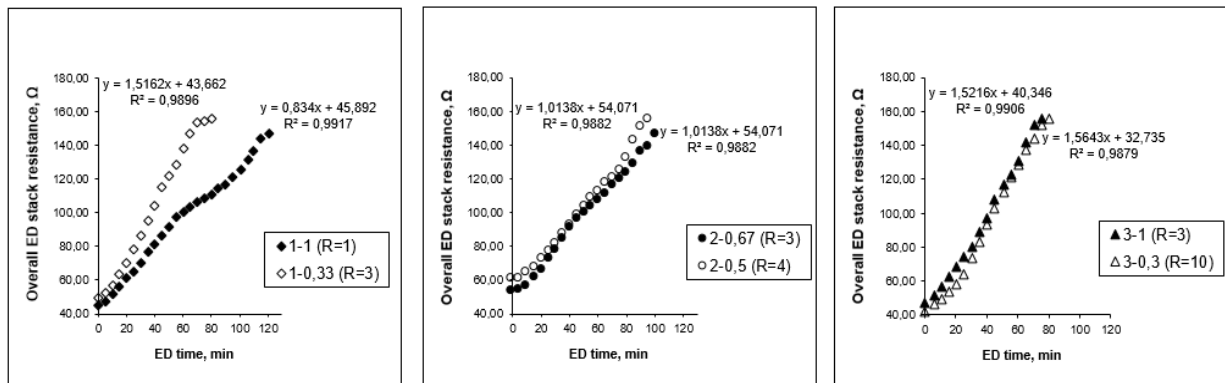
Fig.III.5: Overall ED stack resistance as a function of time in the different PEF conditions (R is pulse/ pause ratio).

III.1.3.1.3 pH evolution in the diluate compartment

Following pH evolutions is of importance in this study since pH is sensitive to two types of phenomena, which may prompt the membrane scaling formation: OH^- leakage through the CEM and water-splitting (Cifuentes-Araya, Pourcelly et al. 2011). According to the pulse lapse, pH curve trends were different: quite linear increase at 1s and 3s, increase and then decrease at 2s (Fig.III.6 a,b,c). In the case of 2s/0.5s condition pH was quite stable up to 70 min of treatment but after reaching 6.9 value this parameter decreased and at the end of the experiment pH reached a value even lower than its respective initial value.

The shape of curves at pulse lapses 3s and 1s was in accordance with what was presented by Cifuentes-Araya (Cifuentes-Araya, Pourcelly et al. 2011) for 10s/10s and 10s/33.3s T_{on}/T_{off} regimes. However, at the pulse lapse 2s some differences were indicated, especially for 2s/0.5s condition, which shape was similar to the shape of the curve for dc-current regime (Cifuentes-Araya, Pourcelly et al. 2011). An interesting angle of view may be obtained from the ΔpH-ED time curves, where ΔpH was the difference between previous and subsequent pH values measured in diluate stream with an interval of time equal to 5

90

min. For 1s/0.33s mode the steep increase in ΔpH began after 30 minutes (Fig.III.6d), which may indicate intensive water splitting on the membrane surface over LCD. After 60 minutes ΔpH grew slowly which may be related with suppressing of CP phenomenon by PEF and/or formation of a scaling. This kind of curves with peak were also observed for 3s/1s and 3s/0.3s PEF conditions (Fig.III.6f). For 1s/1s and 2s/0.67s modes ΔpH increased uniformly, though for the last condition insignificant decreasing after 75 min was observed. Another shape of curves was indicated in 2s/0.5s lapse. In this case no peak was observed. Based on the curves of pH and ΔpH it might be concluded that conditions with pulse lapse 2s are special. Presumably, these PEF conditions suppress CP and/or OH^- leakage in a better way compare to other modes and result in consequently higher DR values and potentially lower scaling.
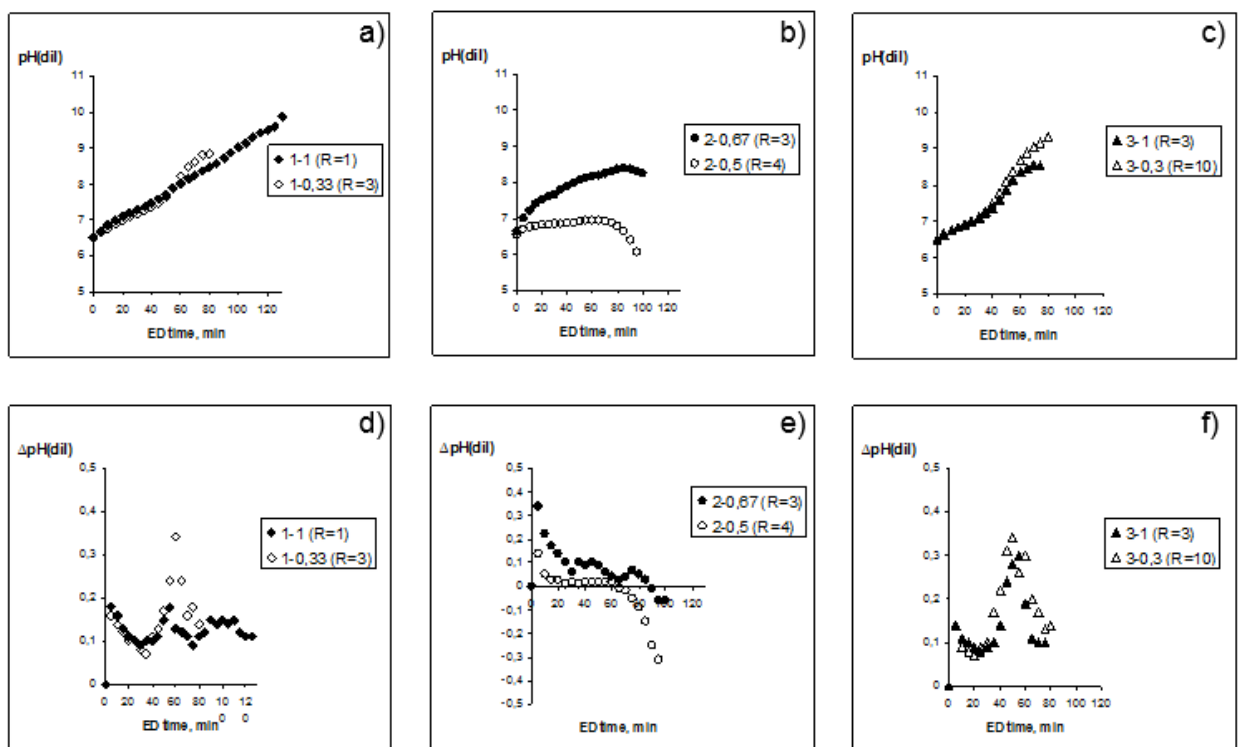
Fig.III.6: pH and ΔpH dependences in the different PEF conditions (R is pulse/ pause ratio).

III.1.3.2 <u>Membrane thickness and scaling content</u>

The thicknesses of CEM and AEM after ED treatment were compared with initial values of control CMX-SB (0.17±0.01 mm) and AMX-SB (0.13±0.01 mm). These control values were comparable to those reported in previous studies for control CEMs (CMX-SB) and (Hołysz, Chibowski et al. 2003; Chen, Neville et al. 2006) AEMs (AMX-SB) (Cifuentes-Araya, Pourcelly et al. 2011).

Concerning the membrane thickness and scaling content (SC) the most efficient PEF modes were 1s/0.33s and 2s/0.5s. The thickness and SC of AMX-SB membranes did not show any significant difference in all PEF conditions and presented an average value of 0.13±0.01 mm and 0 – 1.7 % respectively, which indicates the absence of scaling on the membrane surfaces.

Our results (Tab.III.1) demonstrated that the CEM membrane thickness are lower whatever the PEF modes in comparison with data obtained by Cifuentes-Araya et al. (0,385±0,046 mm for 10s/10s and 0,343±0,024 for 10s/33,3s) (Cifuentes-Araya, Pourcelly et al. 2011). Moreover, Casademont et al. (Casademont, Pourcelly et al. 2007) in their experiments used CMX-S membrane and after conventional ED treatment the membrane thickness was 0.4048±0.0319 mm. With application of CMX-SB and PEF the scaling was significantly diminished.

Tab. III.1: CMX thickness (mm) and SC (%) for the different PEF modes.

	PEF modes (Ton/Toff), Ratio (R)					
	1s/1s R=1	1s/0.33s R=3	2s/0.67s R=3	2s/0.5s R=4	3s/1s R=3	3s/0.3s R=10
Thickness (mm)	0.31±0.02	0.25±0.03	0.29±0.04	0.26±0.01	0.28±0.04	0.30±0.02
SC (%)	40.6±2.2	34.2±3.3	38.7±7.1	31.9±3.2	43.6±1.3	45.6±5.9

III.1.3.3 <u>Scanning electron microscopy</u>

III.1.3.3.1 <u>CEM</u>

III.1.3.3.1.1 <u>Diluate side</u>

Microscopy photographs for the T_{on}/T_{off} condition 1s/1s (Fig.III.7) showed that the entire membrane surface was covered by a thin layer of scaling comprising some crystal particles. With a decrease in pause lapse from 1s to 0.33 s bigger crystal spots were observed. For the 2s/0.67s PEF mode the membrane surface was also covered by aggregates having spot shape, but in contradiction to 1s/0.33s mode, spots were distributed evenly and had smaller size. With increasing the magnitude of microscopic analysis ($\times$ 750) and focusing on the boarder of these spots, it is possible to see round-like crystals presumably of $CaCO_3$. The presence of small spherical particles with some quite big aggregates have been shown for the 3s/1s condition. Association of scalant particles into larger aggregates was observed with the decreasing the pause lapse to 0.3 s for the same pulse lapse of 3s. This tendency was similar for the 1s/1s and 1s/0.33s conditions, which was also confirmed by previous SC analysis. The unconventional shape of $CaCO_3$ crystals indicates the influence of Mg^{2+} ions, which can inhibit nucleation, growth and lead to a change in morphology (Hołysz, Chibowski et al. 2003; Chen, Neville et al. 2006; Casademont, Pourcelly et al. 2007). Also, PEF conditions affect the formation of different crystal structures as observed by Cifuentes-Araya (Cifuentes-Araya, Pourcelly et al. 2011). This was confirmed by our investigation. Diluate side for 2s/0.5s mode was abruptly different from the others, the scaling layer consisted in spherical particles with small patches of mountain-like crystals.

Original
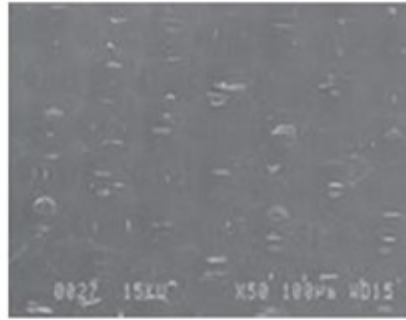
1s/0.33s (R=3)   **2s/0.67s (R=3)**   **3s/1s (R=3)**
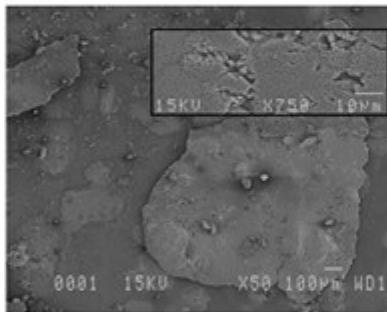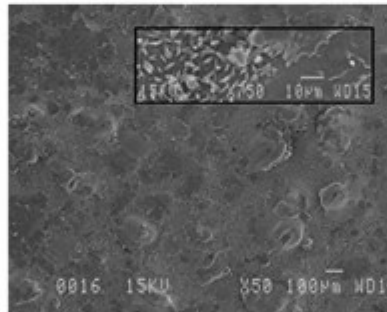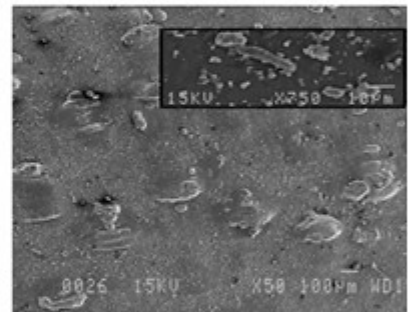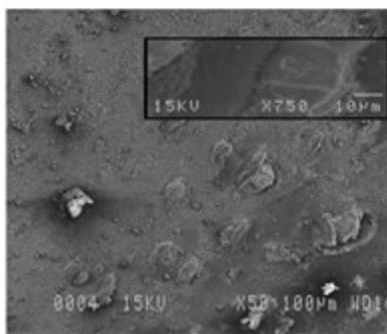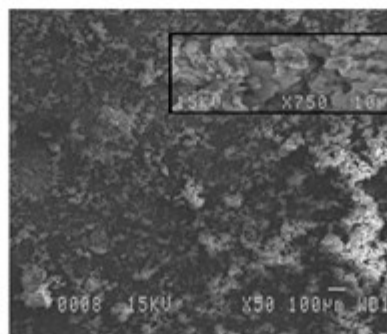
1s/1s (R=1)   **2s/0.5s (R=4)**   **3s/0.3s (R=10)**
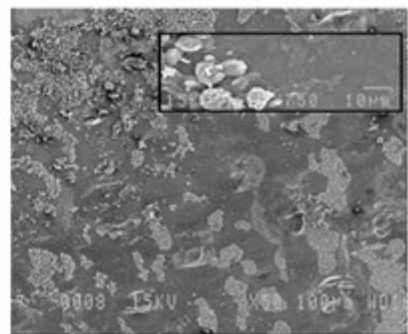
Fig.III.7: Scanning electron microscopy photographs of the original CEM and diluate side of CEMs under the different PEF conditions (R is pulse/ pause ratio).

III.1.3.3.1.2 <u>Concentrate side</u>

For the treatment carried out at PEF 1s/1s, SEM photographs (Fig.III.8) showed that the scaling aggregates were evenly distributed on the whole membrane surface. The same distribution of scaling was noted for PEF condition 2s/0.67s. However, another relevant feature was the needle-like layer under the crystal coat. Accumulation of scaling with decreasing the pause lapse from 0,67s to 0,5s was observed. This tendency was also observed for the 1s/0.33s condition. The shape of crystals was the same as for 1s/1s condition, but with a more compact structure due to the aggregation of small particles. The scaling at 2s/0.67s mode covered the whole membrane surface and had unusual lamellar shape. These lamellar layers were distributed perpendicular to the membrane surface and each thin plate was tightly adjoined to another with formation of homogeneous layer. For 2s/0.5s condition the membrane surface was also completely covered by a deposit, however the structure was different and included spherical particles with small quantities of rocky crystals. The rod-like crystals were horizontally distributed on the lamellar layer at 3s/1s condition. The extension of SC with the decrease of pause lapse to 0.3s was similar to the concentrate side. However, the crystal aggregated, which was distributed also on the lamellar layer, had round-like shape.
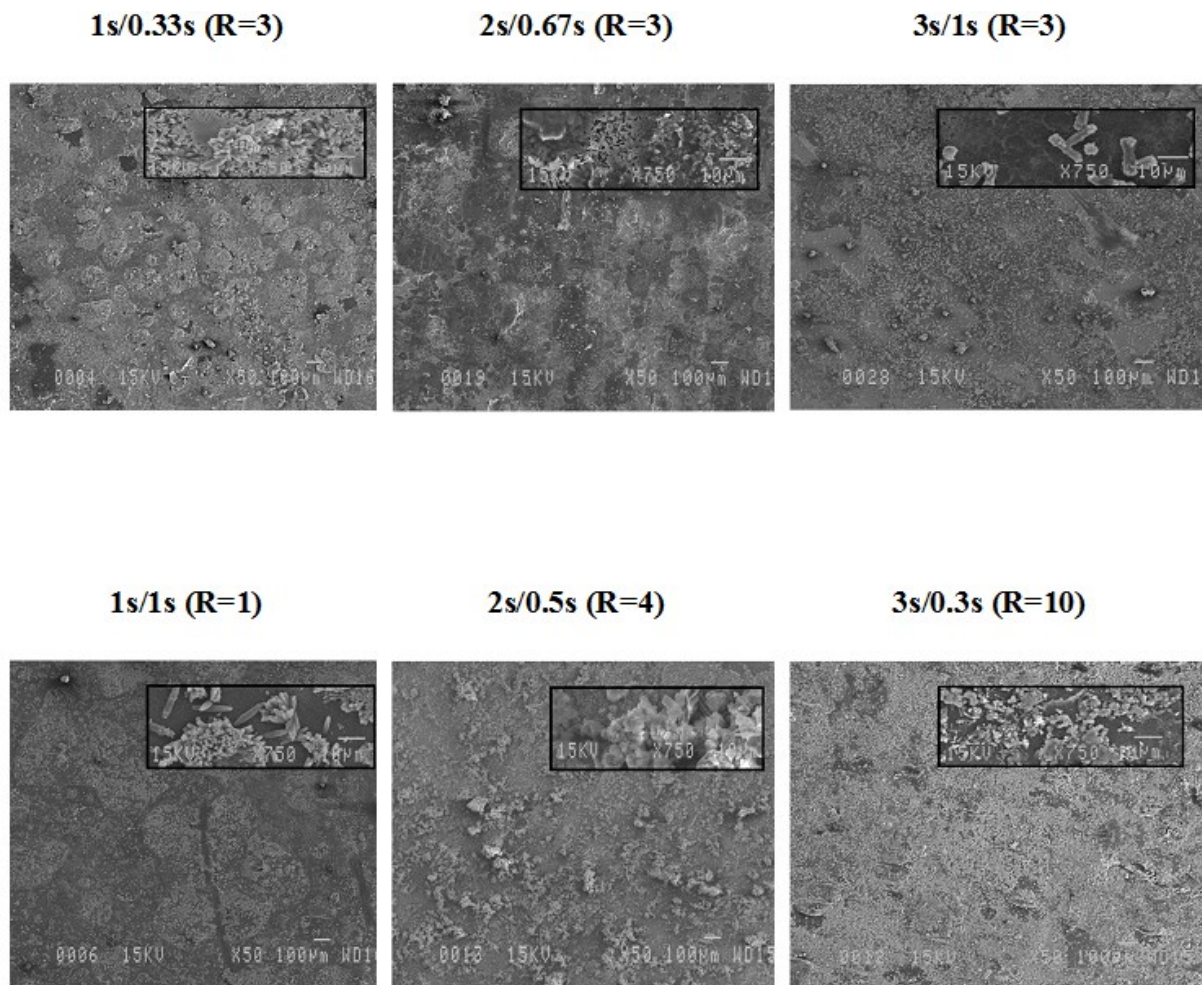
Fig.III.8: Scanning electron microscopy photographs of the concentrate side of CEMs under the different PEF conditions (R is pulse/ pause ratio).

III.1.3.3.2 <u>AEM</u>

III.1.3.3.2.1 <u>Diluate side</u>

The surface of AEM did not contain any scalant agents, except for the 2s/0.5s condition (Fig.III.9), where a really low quantity of scaling was observed. This small scaling was formed of crystals with average diameter around 10 μm representative of calcite in rhombohedral shape (Kitamura 2001).

original

1s/0.33s (R=3)   **2s/0.67s(R=3)**   **3s/1s (R=3)**

1s/1s (R=1)   **2s/0.5s (R=4)**   **3s/0.3s (R=10)**
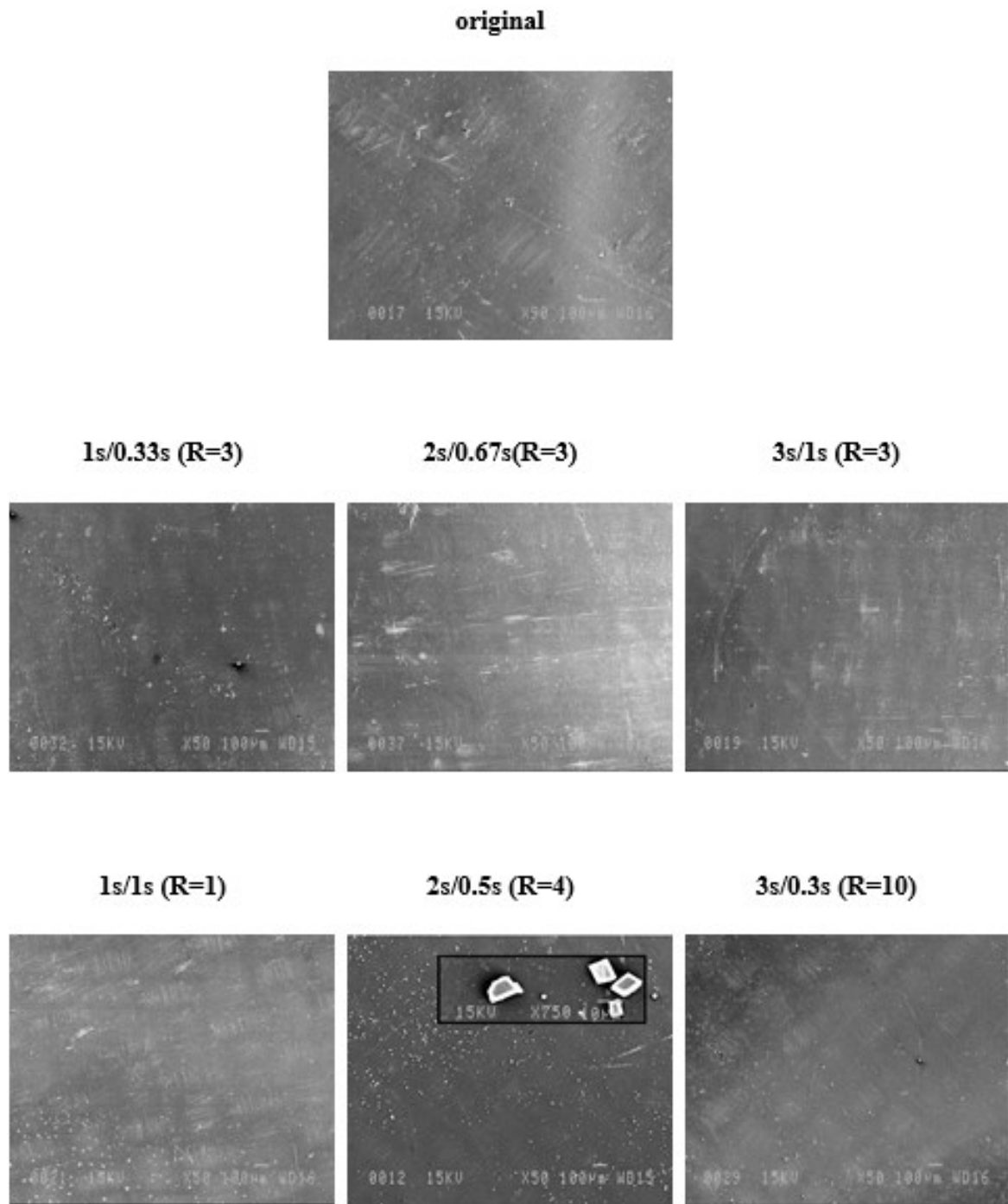
Fig.III.9: Scanning electron microscopy photographs of the original AEM and diluate side of AEMs under the different PEF conditions (R is pulse/ pause ratio).

III.1.3.3.2.2 <u>Concentrate side</u>

Basically, for most PEF conditions no sufficient quantities of deposit were observed (Fig.III.10) and it was concluded that scaling was absent on AEMs. However, two conditions (2s/0.5s and 3s/1s) had a distribution of small particles on the membrane surface. The shape of scaling particles was rhombohedral which indicates the presence of calcite scaling as mentioned above for the diluate side of AEM.

1s/0.33s (R=3)   2s/0.67s (R=3)   3s/1s (R=3)

1s/1s (R=1)   2s/0.5s (R=4)   3s/0.3s (R=10)
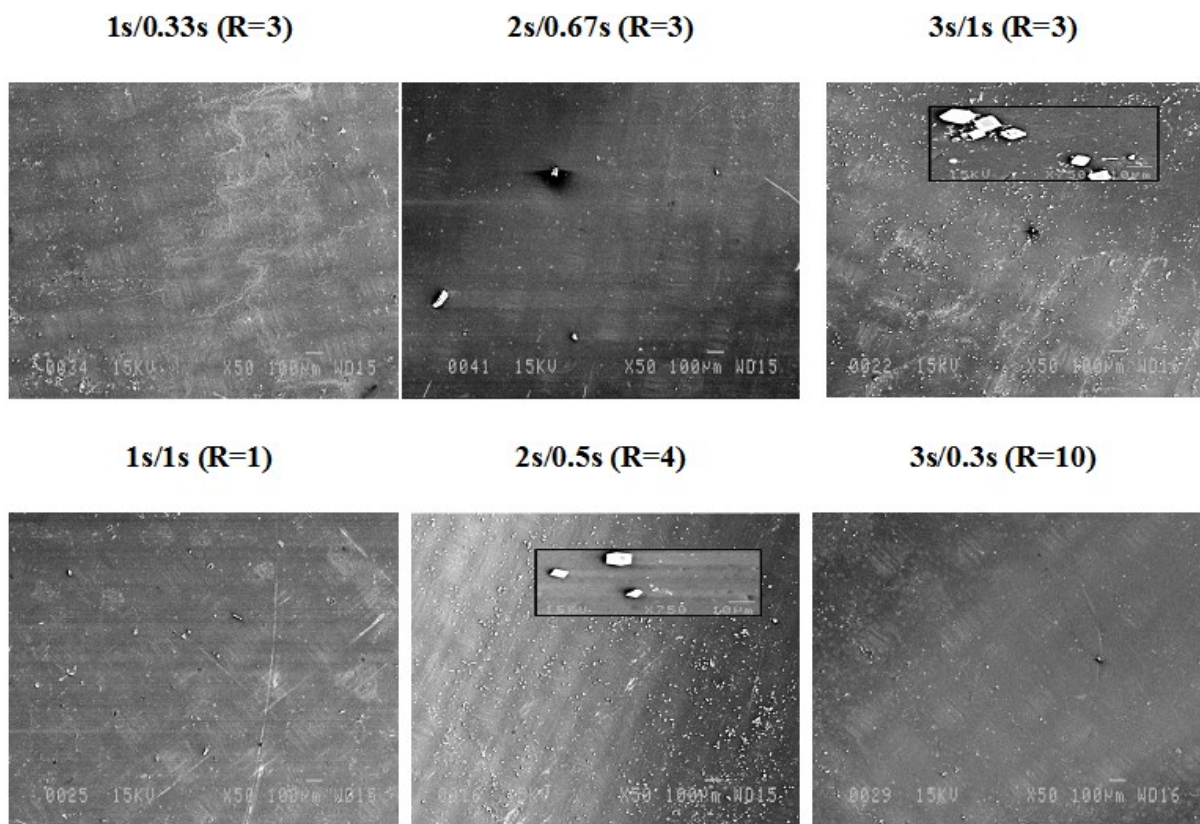
Fig.III.10: Scanning electron microscopy photographs of the concentrate side of AEMs under the different PEF conditions (R is pulse/ pause ratio).

III.1.3.4 <u>X-ray elemental analysis</u>

X-ray elemental analysis was carried out to determine the elemental composition of the membrane scaling under the influence of different PEF regimes. Original CEM

contained two dominant elements Cl and S and in less significant quantities Na, C, O. Au and Pd were reflected on the photographs because they were used to coat the membrane surface and to increase the analysis quality. For AEM the same elemental composition was observed, although the content of S was really low in comparison with the CEM.

III.1.3.4.1 CEM

III.1.3.4.1.1 Diluate side

The presence of two main scalant agents Ca^{2+} and Mg^{2+} was observed for all samples after ED treatments (Fig.III.11). The percentage of these elements varied with change in PEF modes and is in agreement with previous results obtained by Cifuentes-Araya et al.(Cifuentes-Araya, Pourcelly et al. 2012) (Cifuentes-Araya, Pourcelly et al. 2012). However, our results had more significant difference between each other. For the 1s/1s regime X-ray images showed the equal concentrations of Ca and Mg. Knowing Kps = 4.4–8.8 × 10^{-12} $(mol/l)^3$, 1.25 × 10^{-11} $(mol/l)^3$, 1.6 × 10^{-9} $(mol/l)^2$, 3.7 × 10^{-9} $(mol/l)^2$, 4.57×10^{-9} $(mol/l)^2$ and 4.35–8 × 10^{-6} $(mol/l)^3$ (Roques 1990; Gal, Bollinger et al. 1996), for $Mg(OH)_2$ in brucite crystal form, amorphous $Mg(OH)_2$, calcite, aragonite, and portlandite respectively and based on the observations of Cifuentes-Araya et al. it is possible to assume that the membrane surface deposit was composed of $Mg(OH)_2$ and $CaCO_3$. The analysis of quite big agglomerates on the membrane surface revealed the high peak of Ca, which means that it might be one of the forms of calcium carbonate. The increase in Ca concentration for 1s/0.33s mode was due to the presence of large particles of $CaCO_3$. However, the surface analysis under the increasing magnitude showed the high peak of Mg with small peak of Ca. Conditions with pulse lapse 2s were special; for 2s/0.67s condition the presence of high quantities of Ca with small quantities of Mg were observed. With decreasing the pause lapse to 0.5s, an opposite situation was noted with presence of high Mg peak and low peak of Ca. It indicates the diverse influence of PEF conditions on the structural organization of the membrane deposit. For 3s/1s mode approximately equal quantities of Ca and Mg were indicated with the insignificant prevalence of Mg. With decreasing the pause lapse to 0.3s the membrane surface contained more $CaCO_3$ and in this case the concentrations of Mg and Ca were equal. In all above cases the detail analysis of

the membrane surface between CaCO₃ agglomerates also revealed the drastic increase in Mg content.
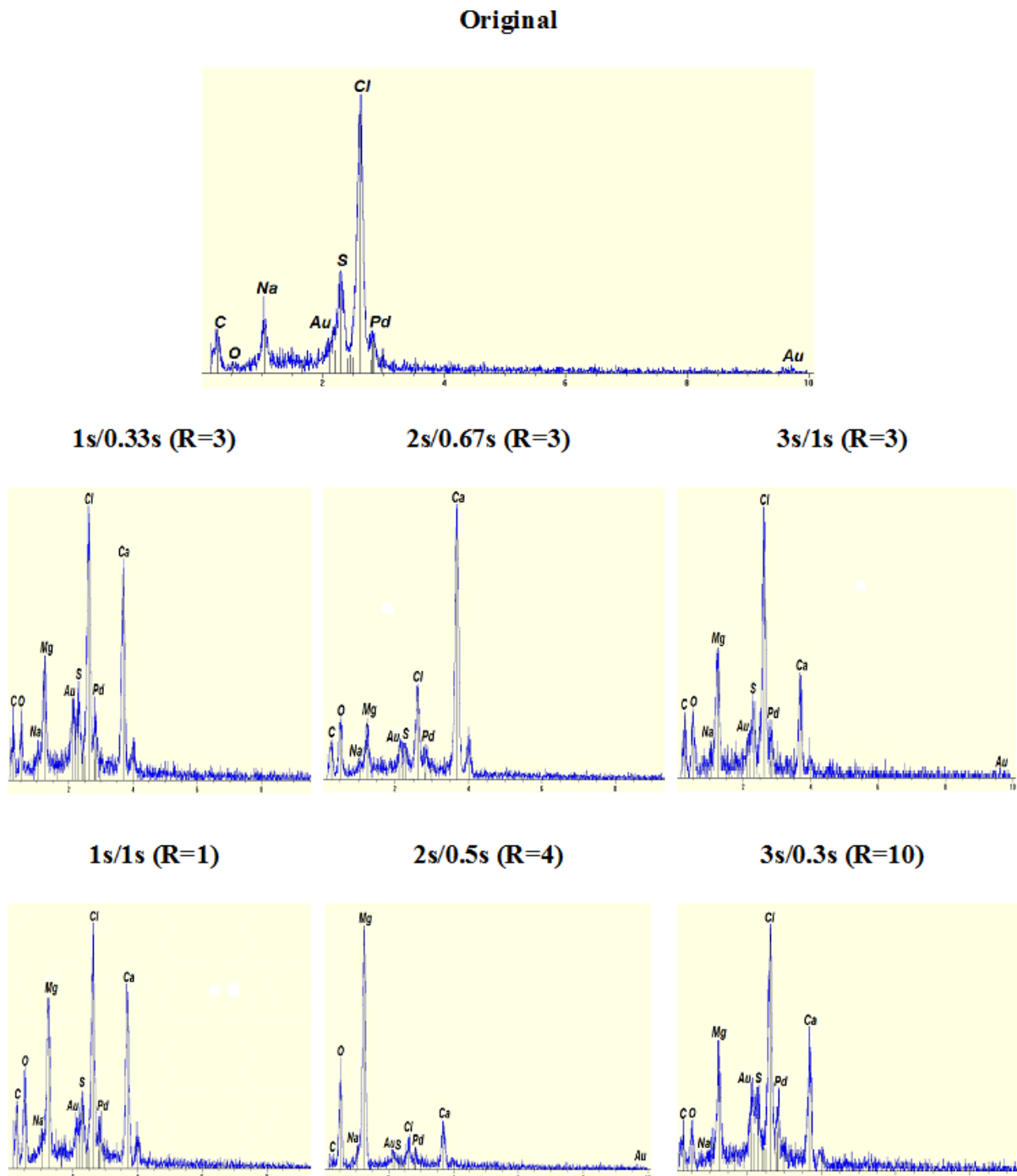
Original

Fig.III.11: X-ray elemental analysis of the original CEM and diluate side of CEMs under the different PEF conditions (R is pulse/ pause ratio).

III.1.3.4.1.2 <u>Concentrate side</u>

Differences in membrane surface deposit composition appeared also on the concentrate side of CEM (Fig.III.12). For all conditions tested and as mentioned previously for diluate side during the detail surface analysis the presence of high Mg peaks was observed. For the 1s/1s condition X-ray images showed two high peaks of Mg and Ca elements with predominance of Ca. With change in regime to 1s/0.33s SEM photographs showed more dense sediment of $CaCO_3$. This mode shifts the balance of elements in favor of calcium. High peaks of Mg and small peaks of Ca were observed at 2s/0.67s and 2s/0.5s modes. These results are different in comparison with diluate side of CEM for the same conditions. Density of scaling at 0.5s pause lapse, which is mostly formed of $Mg(OH)_2$, is higher than the one at 0.67s pause lapse, which resulted in a decrease of the total Ca content. The prevalence of Mg content with high Ca content was observed at 3s/1s condition. The rod-shape crystals on the surface of the membrane in this specific condition was indicative of $CaCO_3$. The increase in scaling with decreasing pause lapse is caused by the growth of the Ca peak. This trend was also confirmed for 3s/0.3s condition.
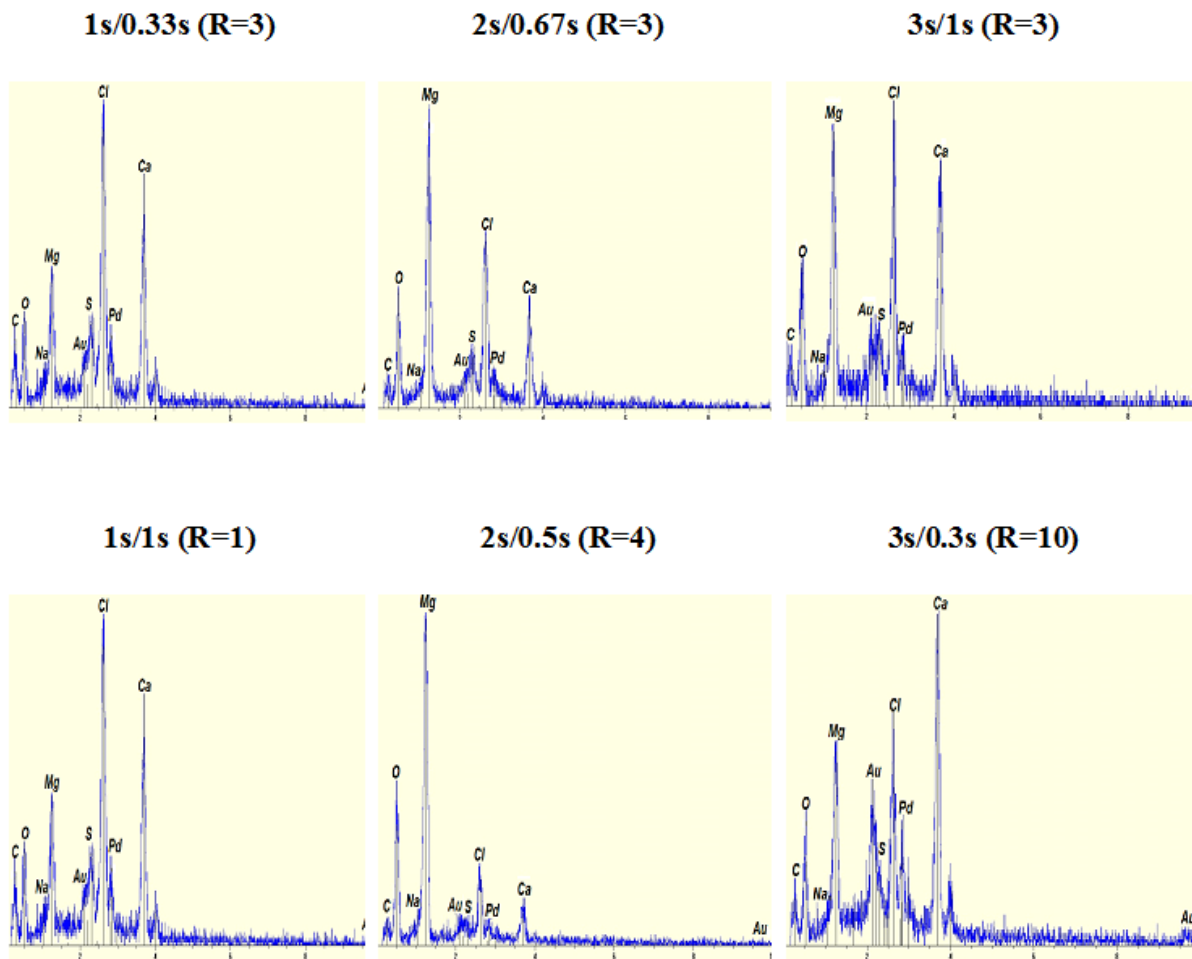
Fig.III.12: X-ray elemental analysis of the concentrate side of CEMs under the different PEF conditions (R is pulse/ pause ratio).

III.1.3.4.2 <u>AEM</u>

The X-ray elemental analysis showed peak of carbon, which was higher than the one in the original sample (Fig. III.13 and III.14). This increase can be explained by the residual content of HCO_3^- ions which migrated through the membrane towards the anode during ED treatment. Trace quantities of Ca and Mg were observed. Considering both sides of the AEMs it was concluded that no scaling was present on the membrane surfaces. This is a significant improvement of ED treatment due to pulse application with short duration, because in previous works using PEF the AEM scaling always took place (Cifuentes-Araya, Pourcelly et al. 2012).
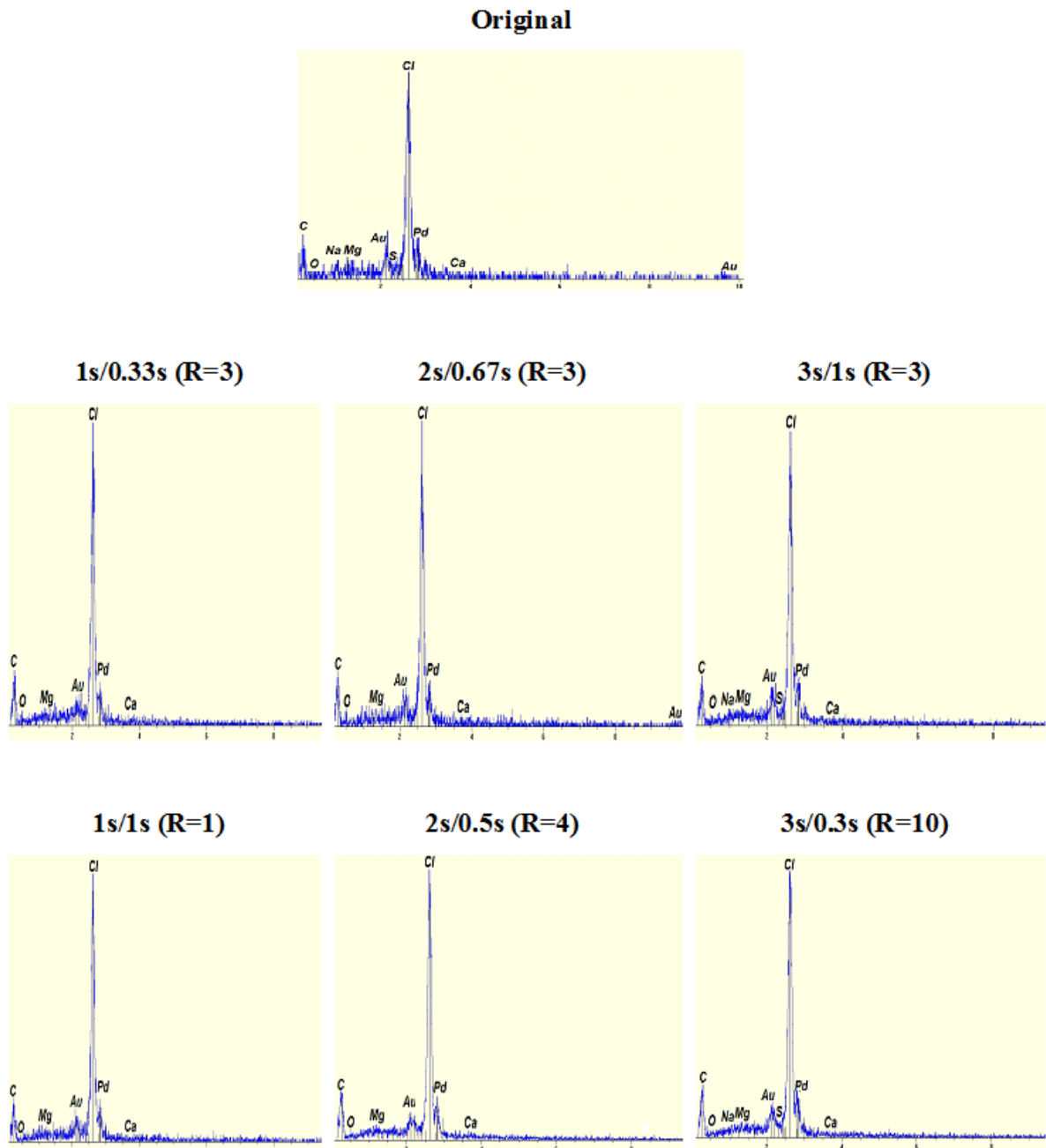
Fig.III.13: X-ray elemental analysis of the original AEM and diluate side of AEMs under the different PEF conditions (R is pulse/ pause ratio).
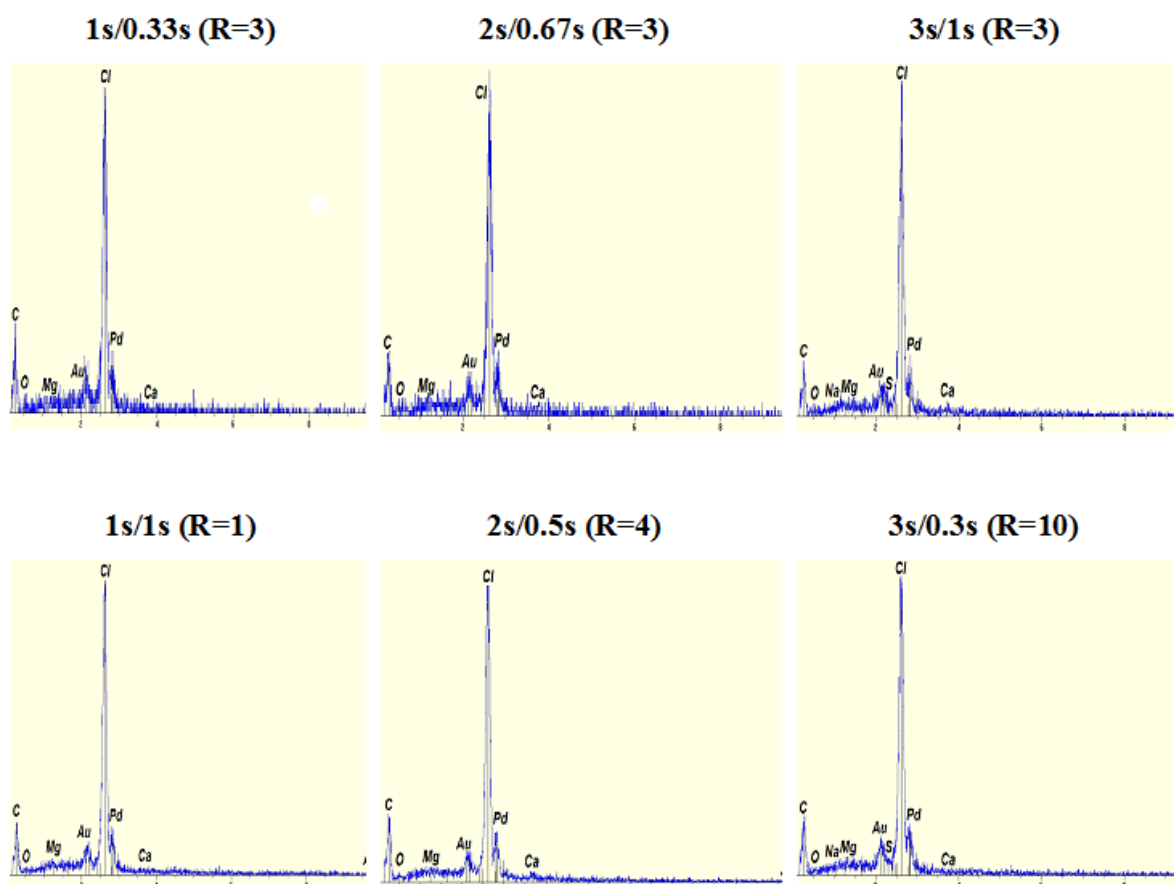
Fig.III.14: X-ray elemental analysis of the concentrate side of AEMs under the different PEF conditions (R is pulse/ pause ratio).

III.1.4 Discussion

From these results it appeared that the best pulse/pause ratios among all the conditions tested are $T_{on}=2s$ with $T_{off}=0.5s$ or $T_{off}=0.67s$. In these conditions, the DR were the highest with values around 80 %. Also, it is interesting to note that for these combinations of pulse/pause the pH had different evolution in comparison with other modes. For $T_{off}=0.67s$ the increase of pH was not so abrupt and the final value did not exceed 8.4. Furthermore, for $T_{off}=0,5s$ pH was quite stable around 7.0. On the other hand, the EC was the highest in comparison with all other conditions. However, as mentioned previously, the EC increased quite linearly with the demineralization rate. This trend is generally quite linear up to a critical level where the EC is then too high in comparison with

the demineralization efficiency. This critical value is reported to be around 85% of demineralization depending on the solution composition (Choi, Han Jeong et al. 2001; Cifuentes-Araya, Pourcelly et al. 2011). In this case, the EC in our best conditions is realistic. Indeed, the demineralization of the diluate compartment leads to an increase in the energy. Concerning scaling, the data of X-ray elemental analysis for both PEF conditions showed that the scaling consists mostly of $Mg(OH)_2$. In addition, the formation of $CaCO_3$ was almost completely suppressed on both sides of CEM for 2s/0.5s mode and only on the concentrate side for 2/0.67s. Moreover, looking on the results of thickness and SC it is evident that 2s/0.5s has the best values (0.26 mm and 31.9 % respectively). It is worth to note that 2s/0.5s PEF condition resulted in the formation of small quantities of $CaCO_3$ on the AEM, but this scaling was substantially less than what was obtained by Cifuentes-Araya et al. (Cifuentes-Araya, Pourcelly et al. 2011) and it can be neglected. In addition, it was the first time that the quite complete non-scaling of the AEM was reported in the literature during demineralization of such a mineral solution.

The fact that a good DR value was reached might be explained by the use of optimal pulse frequency and pulse/pause duration (Mishchuk, Koopal et al. 2001). These optimal conditions would have impacted on 1) hydrodynamic conditions on the surface of the membrane (electroconvection and diffusion), 2) reduction of $CaCO_3$ formation and 3) pH evolution. Indeed, these modes may provide better intensification of the electroconvection (Nikonenko, Pismenskaya et al. 2010) and ion diffusion during the pause lapses (Mishchuk, Koopal et al. 2001), which cause an increase of the electrolyte concentration in the main body of DBL. PEF can affect the hydrodynamic conditions near to the membrane surface (during the pause lapse diffusion layer and consequently concentration gradients between bulk solution and the membrane surface become smaller). It can be hypothesized, that the pulse lapse of 2s can provide the formation of sufficiently big electroosmotic vortices while pause lapse of 0.5s is too short for the complete disappearance of these vortices. As a result, relatively big electroconvective vortices formed during the pulse lapse continues ion transfer improvement accompanying by diffusion during the pause lapse. Additionally, perturbations created by PEF action and electroosmotic vortices reduce the formation of tight crystalline structures of $CaCO_3$ on the surface of CEM. A similar effect was observed by Barret et al. (Barrett and Parsons 1998) and Higashitani et al. (Higashitani, Kage et al.

1993) with application of magnetic field. This field affected the formation of $CaCO_3$ by suppression of nucleation and acceleration in crystal growth. The effect of PEF has also an effect on pH evolution during treatment. Indeed, for PEF 2s/0.5s the increase in pH was really small and the final value was even lower than initial. The same shape of pH curve was observed by Cifuentes-Araya et al. (Cifuentes-Araya, Pourcelly et al. 2011) for ED with dc current. This can be explained by proton barrier: protons generated from AEM diluate side during water splitting phenomenon after the system reaches the LCD. These protons can compensate hydroxyl ions which are formed from the diluate side of CEM (Cifuentes-Araya, Pourcelly et al. 2013). However, for most of our PEF conditions the quantity of generated protons was not enough for compensation of OH^- ions in the diluate compartment except 2s/0.5s mode. It can be hypothesized that for this mode most of these OH^- ions (produced by water splitting and transported by leakage) were spent for building up of the $Mg(OH)_2$ deposit on both CEM surfaces. Our investigations showed that with suppression of CaCO3 formation (when scaling consists of Mg(OH)2) by PEF pH does not tend to increase what hamper the scaling formation and improve demineralization. For understanding the pH development, it is necessary to measure pH value in the vicinity of the membrane surface but we did not have these possibilities. In the case of 2s/0.67s mode Ca^{2+} ions interacted with CO_3^{2-} ions, which could be obtained by the reaction between HCO_3^- and OH^- ions, to form calcite. Presumably, this $CaCO_3$ covering the diluate side of the CEM allowed a more intensive OH^- leakage through this membrane and consequently increasing pH. Indeed, the formation of $CaCO_3$ prevent the formation of $Mg(OH)_2$. To better understand these results it is necessary to note the interesting fact about catalytic properties of Ca^{2+} and Mg^{2+} ions (Oda and Yawataya 1968; Simons 1984). These ions can participate to water splitting by the following equation (Simons 1984):

$$M^{2+} + 2H_2O \rightleftarrows M(OH)_2 + 2H^+, \qquad\qquad eq.III.4$$
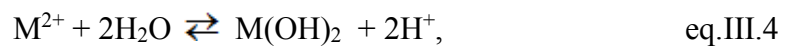
where M^{2+} is Mg^{2+} or Ca^{2+} ion.

However, the role of Ca^{2+} and Mg^{2+} ions in increasing water-splitting phenomenon is not similar. The ability of Ca^{2+} to take part in water splitting is much weaker than that of the Mg^{2+} (Oda and Yawataya 1968). Sheldeshov proposed a more complete model of water

106

dissociation in ED system with presence of ions of heavy metals as shown in eq. III.5-8 (Sheldeshov 2002). In this case, it is possible to see that $MgOH^+$ ions apart from Mg^{2+} can interact with water.

$$Mg^{2+} + OH^- \rightleftarrows MgOH^+ \qquad\qquad eq.III.5$$

$$Mg^{2+} + 2H_2O \rightleftarrows MgOH^+ + H_3O^+ \qquad\qquad eq.III.6$$

$$MgOH^+ + OH^- \rightleftarrows Mg(OH)_2 \qquad\qquad eq.III.7$$

$$MgOH^+ + 2H_2O \rightleftarrows Mg(OH)_2 + H_3O^+ \qquad\qquad eq.III.8$$
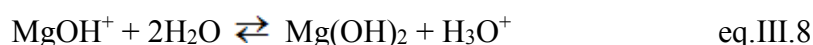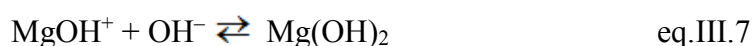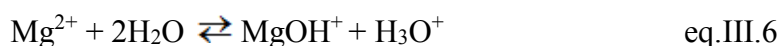
Thus, Mg^{2+} ions, which form insoluble hydroxide on the membrane surface, hastened the water-splitting process. Now, based on equations III.6 and III.8, the decrease of pH in the diluate compartment at 2s/0.5s mode can be explained. The pH decrease was observed at this PEF mode since the formation of significant quantities of $CaCO_3$ have been prevented. OH^- ions from concentrate compartment and from water-splitting reaction were neutralized by interaction with Mg^{2+} and $MgOH^+$ ions. Additionally, the proton barrier created by protons from water splitting on the AEM, becomes more pronounced due to additional protons generated from interactions of water with Mg^{2+} and $MgOH^+$.

Concerning pulse conditions of 1s (T_{off} = 1s (R=1) and 0.33s (R=10)), the lowest DR values among all PEF modes were observed. Values of SC and membrane thickness were variable for both these conditions. This can be explained by the difference in scaling composition on both sides of the membranes. For T_{off}=1s the concentration of Ca was lower than for T_{off}=0.33 s and duration of ED treatment was longer for the first mode. This larger duration would have affected the polymorphic transformations with formation of different crystal and amorphous compounds, whose densities were different (Duffy, Ahrens et al. 1991; Desgranges, Calvarin et al. 1996; Nehrke 2007). Moreover, thorough exploration of the surface allows presuming the presence of a multilayer scaling. First of all, magnesium hydroxide built up on both sides and after the formation of calcium carbonate on the basis

of the magnesium layer took place. The assumptions were favored by the constant solubility values of 4.4 to 8.8×10^{-12} (mol/l)^3 and 3.7×10^{-9} (mol/l)^2 for $Mg(OH)_2$ and $CaCO_3$ respectively (Cifuentes-Araya, Pourcelly et al. 2012), and stronger interactions of Mg^{2+} ions versus Ca^{2+} ions with sulphonic groups of CEM (Bribes, El Boukari et al. 1991). This difference in solubility constant coupled with a different pH evolution can explain the different scaling structure observed between both PEF modes. Indeed, although the pH evolution was similar to that reported by Cifuentes-Araya et al. (Cifuentes-Araya, Pourcelly et al. 2011), for 1s/1s mode the change of the curve slope began approximately after 30 minutes.

Comparing 3s pulse PEF conditions (T_{off} =1s (R=3) and 0.3s (R=1)) with previous results it may be concluded that they have middle position in terms of membrane deposit and intensification of ED treatment. The composition of the membrane scaling was similar to the 1s/1s and 1s/0.33s modes, although the SC values were higher. With the decrease of pause lapse the diluate and concentrate sides of the membrane surface were covered by more tight deposit. From the data of X-ray elemental analysis the increase in Ca concentration was observed which means that these changes in the regimes allowed the formation of $CaCO_3$. Looking at ΔpH-time curves the presence of a peak was observed. Apparently, it could be caused by the new type of deposit or by polymorphous transformations of the already formed deposit. Additionally, this peak might be caused by attaining the LCD value and generation of OH$^-$ ions and more significant leakage of these ions through CEM from concentrate compartment (Cifuentes-Araya, Pourcelly et al. 2012). The same peak and shape of pH curve for 1s/0.33s was indicated. Furthermore, the overall ED stack resistance curves had also similar shape for these three modes. This could be due to the same effect from perturbations of PEF on the processes in the DBL (especially at the LCD) and creation of resembling scaling layers.

III.1.5 <u>Conclusion</u>

These results demonstrated successfully the intensification of the demineralization process by the application of a non-stationary electric field. The use of short pulse/pause lapses during ED treatment for systems with possibilities of scaling formation was carried out for the first time. It has been found that duration of pulse and pause lapses plays important role in terms of scaling composition and quantity, pH evolution and most probably development of electroconvective vortices. The advantages of using short PEF lapses are the absence of scaling on AEM, the decrease in CEM scaling and the fact that high DRs were reached without too large increase in EC. All parameters put together, the best condition among the six conditions tested was $T_{on}/T_{off}=2s/0.5s$ with the highest DR, lowest SC and membrane thickness.

Experiments concerning the effect of electroconvective vortices on membrane scaling are currently under way. For a next step in research, consecutive ED treatments in the best PEF mode should be carried out to investigate the effectiveness of using these specific conditions for persistent process. Besides, study of the membrane scaling evolution and electrical properties of the CEM will help to understand deeply the influence of PEF.

Acknowledgments

CHAPTER IV. HOW INTRINSIC PROPERTIES OF CATION-EXCHANGE MEMBRANE AFFECT MEMBRANE SCALING AND ELECTROCONVECTIVE VORTICES: INFLUENCE ON PERFORMANCE OF ELECTRODIALYSIS WITH PULSED ELECTRIC FIELD.

CONTEXTUAL TRANSITION

The results of the first objective revealed the complexity of scaling formation mechanisms during ED with PEF. The main factors affecting scaling formation are pulse/pause duration, water splitting and OH^- leakage. Moreover, it was hypothesized that electroconvection may have an additional influence on scaling formation and growth. Besides the influence of each mentioned factor on scaling phenomenon, there are cross-influences, for instance, electroconvection has an influence on development of water splitting. Furthermore, scaling, water splitting, OH^- leakage and electroconvection assuredly affect the performance of ED treatment. Additionally, it is well known that intrinsic membrane properties have an important role on development of electroconvection. However, the influence of intrinsic membrane properties on scaling structure and composition is unstudied yet. In the light of above, this chapter will aim to study the influence of intrinsic physico-chemical membrane properties and electroconvection on structure, composition and quantity of scaling and ED performance. In this study, two lots of CEM with different intrinsic properties will be considered. Firstly, physico-chemical characteristics of both CEMs lots will be determined in order to understand their structural features. The second step will be dedicated to the CEMs characterization by voltammetry, chronopotentiometry and by using microfluidic ED platform in order to evaluate the development of electroconvection. Further, both CEMs will be treated by ED with two PEF modes (2s/0.5s and 2s/0.67s) considering ED parameters used in the previous chapter. This third step will allow revealing: 1) the significance of electroconvection in building-up the scaling under the action of PEF, and 2) the influence of CEM physico-chemical properties on scaling composition and structure.

This chapter has been the subject of an article entitled:

"**How nanostructure and surface properties of cation-exchange membrane affect membrane scaling and electroconvective vortices: influence on performance of electrodialysis with pulsed electric field**", submitted in "Journal of Membrane Science". The authors are Sergey Mikhaylin (Ph. D. Candidate: planning and realization of the experiments, analysis of the results and writing of the manuscript), Victor Nikonenko (Thesis Co-director: scientific supervision of the student, revision and correction of the manuscript), Natalia Pismenskaya (supervised the experimental part performed in French-Russian International Associated Laboratory "Ion-exchange membranes and related processes" (Kuban State University, Krasnodar, Russia) and was responsible for the discussion of the results obtained), Gérald Pourcelly (Thesis Co-director: scientific supervision of the student, revision and correction of the manuscript), Siwon Choi and Hyukjin Jean Kwon (fabricated the microfluidic devices and built-up the measurement system in "Research Laboratory of Electronics at MIT" (Massachusetts Institute of Technology, Cambridge, USA)), Jongyoon Han (supervised the microfluidic visualization experiments in "Research Laboratory of Electronics at MIT" (Massachusetts Institute of Technology, Cambridge, USA)) and Laurent Bazinet (Thesis Director: scientific supervision of the student, revision and correction of the manuscript).

IV.1 <u>**How nanostructure and surface properties of cation-exchange membrane affect membrane scaling and electroconvective vortices: influence on performance of electrodialysis with pulsed electric field.**</u>

<u>Abstract</u>

Two different lots of cation-exchange membranes (CMX-SB-1 and -2) were compared in terms of physico-chemical properties. Additionally, for both lots, electrochemical characterization was performed by voltammetry and chronopotentiometry and electroconvective vortices were visualized with a microfluidic platform. Further, electrodialysis (ED) treatments with samples of both membrane lots were carried out in two pulsed electric field (PEF) conditions (T_{on}/T_{off} 2s/0.5s and 2s/0.67s) on model salt solution containing Ca^{2+} and Mg^{2+} ions. It was found that CMX-SB-1 was more scaled with prevalence of Ca compounds on both membrane sides. CMX-SB-2 contained less scaling with prevalence of Ca compounds on the diluate side and mostly Mg compounds with traces of Ca compounds on the concentrate side. The different behavior of membranes was due to the difference in their properties. The structure of an ion-exchange membrane may be presented as a network of hydrophilic nanoscale channels with charged walls confined within a hydrophobic matrix. The CMX-SB-2 membrane has higher concentration of fixed charges and higher water content that causes larger size of nanochannels and easier transport of highly hydrated Mg^{2+} ions; narrower nanochannels of CMX-SB-1 hamper Mg^{2+} ions transfer that explains the low quantity of these ions on the CMX-SB-1 concentrate side. Additionally, the surface hydrophobicity and heterogeneity of CMX-SB-2 is higher than that of CMX-SB-1. This property allows water slip on the membrane surface that facilitates electroconvection. Higher electroconvection enhances ion transfer from the solution bulk to the membrane surface and mitigates scaling formation. The latter fact is confirmed by demineralization rates. More scaled CMX-SB-1 membrane with less developed electroconvection yielded lower values of demineralization (59.0% and 57.2% for 2s/0.5s and 2s/0.67s conditions respectively) than the less scaled CMX-SB-2 with better developed electroconvection (77.3% and 75.2% respectively).

IV.1.1 <u>Introduction</u>

Electrodialytic (ED) processes are more and more involved in the modern agri-food industrial market (Strathmann 2010; Kotsanopoulos and Arvanitoyannis 2013; Ramchandran and Vasiljevic 2013). However, scientists have to solve the problems of concentration polarization phenomena (CP) and fouling formation to make ED more attractive and to increase its applications on complex systems such as food. The application of non-stationary electric current regimes such as pulsed electric field (PEF) was successful in diminishing CP phenomena (Mishchuk, Koopal et al. 2001). Moreover, recent studies revealed reasonableness of using PEF to prevent the formation of scaling (Cifuentes-Araya, Pourcelly et al. 2011), organic (Lee, Moon et al. 2002) and protein fouling (Ruiz, Sistat et al. 2007) on membrane surface. More recently, Mikhaylin et al. (Mikhaylin et al. 2014) demonstrated that the application of short pulse/pause lapses limits the amount of scaling formed on the cation-exchange membrane (CEM) and completely suppresses scaling on the anion-exchange membrane (AEM). In systems containing mineral salts, main agents contaminating the membrane surface are usually salts of Ca^{2+} and Mg^{2+} (Lin Teng Shee, Angers et al. 2008; Franklin June 2009). The precipitation of certain type of Ca^{2+} and Mg^{2+} based compounds depends on the Mg/Ca ratio (Zhang and Dawe 2000; Chen, Neville et al. 2006; Casademont, Pourcelly et al. 2007) and the pulse/pause lapses ratio of applied PEF (Cifuentes-Araya, Pourcelly et al. 2011). Concerning ED performances, better demineralization rates were obtained when Ca^{2+} compounds were almost suppressed and scaling was composed mostly of Mg^{2+} compounds (Mikhaylin et al. 2014). Additionally to PEF modes and Mg/Ca ratio, water splitting and OH^- leakage were reported as main phenomena affecting membrane scaling formation during ED (Cifuentes-Araya, Pourcelly et al. 2011). Despite of thorough investigations of scaling formation mechanisms, there are two factors, which have not been considered yet in studies: 1) the influence of intrinsic properties of ion-exchange membranes (IEMs) and 2) the influence of electroconvection. Firstly, it is known that intrinsic physico-chemical properties of IEMs determine the organization of membrane nanochannels playing the role of transport arteries for the ions. Hence, the dimension of membrane nanochannels is a relevant parameter in competitive migration of scaling ions, which can affect, ipso facto, the scaling properties. Secondly, surface properties of IEM affect the development of electroconvection arising during the development of CP and affecting positively the mass transfer (Nikonenko, Pismenskaya et

al. 2010). In recent studies of Mikhaylin et al. (Mikhaylin, Nikonenko et al. 2014) it was hypothesized that electroconvection may as well affect scaling formation.

In this context, the first part of the present work will focus on the determination of the physicochemical characteristics of two different lots of CMX-SB membrane in order to understand the structural and surface features of each membrane lot. Further, electrochemical behavior of two CMX-SB membranes will be characterized by means of current-voltage curves (CVC), chronopotentiograms (ChP) and visualization of electroconvective vortices by microfluidic ED platform. These experiments aiming membrane characterization will allow investigating the development of phenomena affecting the mass transfer and scaling formation (Krol, Wessling et al. 1999; Krol, Wessling et al. 1999; Rubinstein and Zaltzman 2000; Nikonenko, Pismenskaya et al. 2010; Pismenskaya, Nikonenko et al. 2012). In the second part, ED treatments, in two different PEF conditions, of model salt solutions containing Ca^{2+} and Mg^{2+} will be carried out to study the influence of the membrane nanostructure and surface properties on scaling formation and ED performances (demineralization rate and energy consumption).

IV.1.2 <u>Experimental methods</u>

IV.1.2.1 <u>Material</u>

CaCl$_2$.2H$_2$O, MgCl$_2$.6H$_2$O, NaCl and KCl (ACS grade) were obtained from Laboratoire MAT (Quebec, QC, Canada). Na$_2$CO$_3$ was obtained from EMD (EMD Chemicals, Gibbstown, NJ), NaOH (1 M) and HCl (1 M) from Fisher Scientific (Nepean, ONT, Canada).

IV.1.2.2 <u>Electrodialysis cell</u>

The electrodialysis cell was a Microflow-type cell (Electro-Cell AB, Täby, Sweden) comprising two Neosepta CMX-SB cation-exchange membranes and two Neosepta AMX-SB anion-exchange membranes (Tokuyama Soda Ltd., Tokyo, Japan). The anode was a

dimensionally stable electrode (DSA) and the cathode a 316 stainless-steel electrode. This arrangement defines three closed loops (Fig.IV.1) containing the diluate model salt solution (330 ml, flow rate of 600 mL/min), a 2 g/L KCl aqueous concentrate solution at constant pH (330 mL, 600 mL/min) and a 20 g/L NaCl electrolyte solution (500 mL, 900 mL/min). The membranes tested, of 10 cm^2 membrane effective surface, were in contact with the model salt solution on one side and the pH-controlled KCl solution on the other side (Fig. IV.1). Each closed loop was connected to a separated external plastic reservoir, allowing continuous recirculation. The electrodialysis system was not equipped to maintain constant temperature, but this parameter undergo low variations.
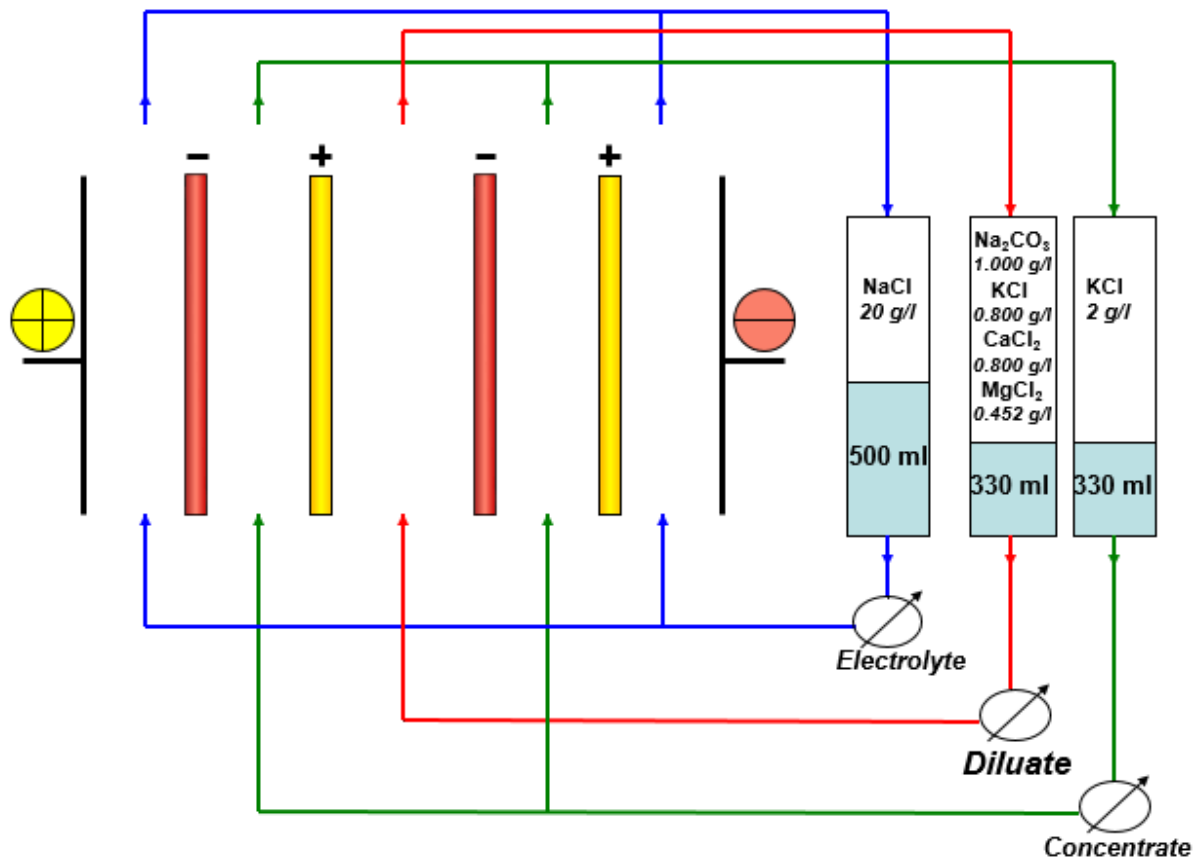
Fig.IV.1: Electrodialysis cell configuration.

IV.1.2.3 Protocol

ED was carried out in batch process using a constant current density of 40 mA/cm^2 generated by a Xantrex power supply (Model HPD 60-5SX; Burnaby, BC, Canada). This current density is higher than the limiting current density (Mikhaylin et al. 2014) and was

116

chosen in order to explore a possible scaling mitigation when water splitting and current-induced convection occurred and to compare our results with those reported by Cifuentes-Araya et al. (Cifuentes-Araya, Pourcelly et al. 2011; Cifuentes-Araya, Pourcelly et al. 2013). The model salt solution was composed from Na_2CO_3 (1000 mg/L), KCl (800 mg/L), $CaCl_2$ (800 mg/L) and $MgCl_2$ (452 mg/L) in order to maintain a Mg/Ca ratio of 2/5 (Casademont, Pourcelly et al. 2007): this ratio is twice as much compared to that in milk (Amiot, Fournier et al. 2002) to ensure membrane scaling formation (Casademont, Pourcelly et al. 2007; Cifuentes-Araya, Pourcelly et al. 2011; Cifuentes-Araya, Pourcelly et al. 2013). The model salt solution was prepared immediately before the beginning of ED process. The initial pH of model salt solution was fixed at 6.5 by manual addition of HCl (1M). The pH of concentrate solution was maintained constant (pH=12) during all ED process by manual addition of NaOH (1 M). The ED treatments were stopped after the maximum voltage capacity of the power supply was reached (62.5 V) (Cifuentes-Araya, Pourcelly et al. 2011). To evaluate the influence of the CEM physico-chemical characteristics, two different lots of CMX-SB membranes were tested (CMX-SB-1 and -2). Thickness, membrane electrical conductivity, ion-exchange capacity, water uptake, contact angles, current-voltage curves and chronopotentiograms were measured and electroconvective vortices were visualized on both CMX-SB lots. After determination of their intrinsic physico-chemical characteristics, these membranes were used for ED treatments. In order to decrease the scaling on the CEM two PEF regimes (2s/0.5s and 2s/0.67s) were applied. These PEF modes were selected based on the data obtained very recently by Mikhaylin et al. (Mikhaylin 2014). Four repetitions were carried out for each PEF condition and for each membrane lot. On a 4-cm^2 dried membrane sample, electron microscopy photographs, X-ray elemental analysis, X-ray diffraction were taken on the CEM surface in contact with the concentrate and diluate solutions in order to visualize the structure and composition of scaling. ED parameters were recorded every five minutes all along the treatments.

IV.1.2.4 <u>Analyses</u>

IV.1.2.4.1 <u>Membrane thickness</u>

The membrane thickness was measured with a Mitutoyo micrometer (Model 500-133, Kanagawa-Ken, Japan). The Digimatic indicator was equipped with a 10-mm-diameter flat contact point. The membrane thickness values were averaged from six measurements at different locations on the effective surface of each membrane

IV.1.2.4.2 <u>Membrane electrical conductivity</u>

The membrane electrical conductance (G) was measured with a specially designed cell (Laboratoire des Materiaux Echangeurs d'Ions, Créteil, France) coupled to a YSI conductivity meter (Model 35; Yellow Springs Instrument Co., Yellow Springs, OH, USA) as described by Cifuentes-Araya (Cifuentes-Araya, Pourcelly et al. 2011). A 0.1 M NaCl reference solution was used. According to the model developed by Lteif et al. (Lteif, Dammak et al. 1999) and Lebrun et al. (Lebrun, Da Silva et al. 2003), the membrane electrical resistance was calculated according to:

$$R_m = R_{m+s} - R_s$$

eq. IV.1

where R_m is the transverse electric resistance of the membrane (in Ω), R_{m+s} is the resistance of the membrane and of the reference solution measured together (in Ω), R_s is the resistance of the reference solution (in Ω). Finally, the membrane electrical conductivity κ (S/cm) was calculated as (Lteif, Dammak et al. 1999):

$$\kappa = \frac{L}{R_m A}$$

eq. IV.2

where L is the membrane thickness (cm) and A the electrode area (1 cm^2).

IV.1.2.4.3 <u>Ion-exchange capacity</u>

118

Ion-exchange capacity (IEC) was determined on 2 g of membrane samples in H^+ form balanced with 0,1 M NaOH. Three 25 ml solution samples were then removed and titrated with 0,1 M HCl. IEC was calculated according to the following equation (1972):

$$IEC = \frac{100 - 4V}{10m}$$ eq. IV.3

 where 100 is the volume of 0,1 N NaOH (in ml), V the total volume of 0,1 N HCl (in ml) used for the titration, and m the mass of the membrane sample (g_{dry} or g_{wet}).

IV.1.2.4.4 Water uptake

For the determination of water uptake, membranes were equilibrated with deionized water for 24 hr. Then their surface moisture was mopped with filter papers and the wet membranes weighed (W_w). Wet membranes were then dried at a fixed temperature of 80 ºC under the vacuum during 24 hr and weighed (W_d). Water uptake was calculated using the following equation (Gohil, Binsu et al. 2006):

$$Water\ uptake\ (\%) = \frac{W_w - W_d}{W_d} \times 100$$ eq. IV.4

IV.1.2.4.5 Contact angle measurements

Contact angles of different wet membranes were measured by goniometer FTA200 (First Ten Angstroms, Inc, Portsmouth, VA, USA) with a measurement range of contact angle 0–180º. The measurement procedure included the registration of the contact angles between a drop of a distilled water applied onto a swollen membrane mopped with a filter paper to remove the excessive water from the surface (Ghassemi, McGrath et al. 2006; He, Guiver et al. 2013). Data were treated using software Build 340 (Version 2.1).

IV.1.2.4.6 <u>Current-Voltage curves and Chronopotentiograms</u>

Current-Voltage Curves and Chronopotentiograms were measured in a direct-flow six-compartment cell without spacer between the membranes (Fig. IV.2) previously described

by Pismenskaya et al. (Pismenskaya, Nikonenko et al. 2012).
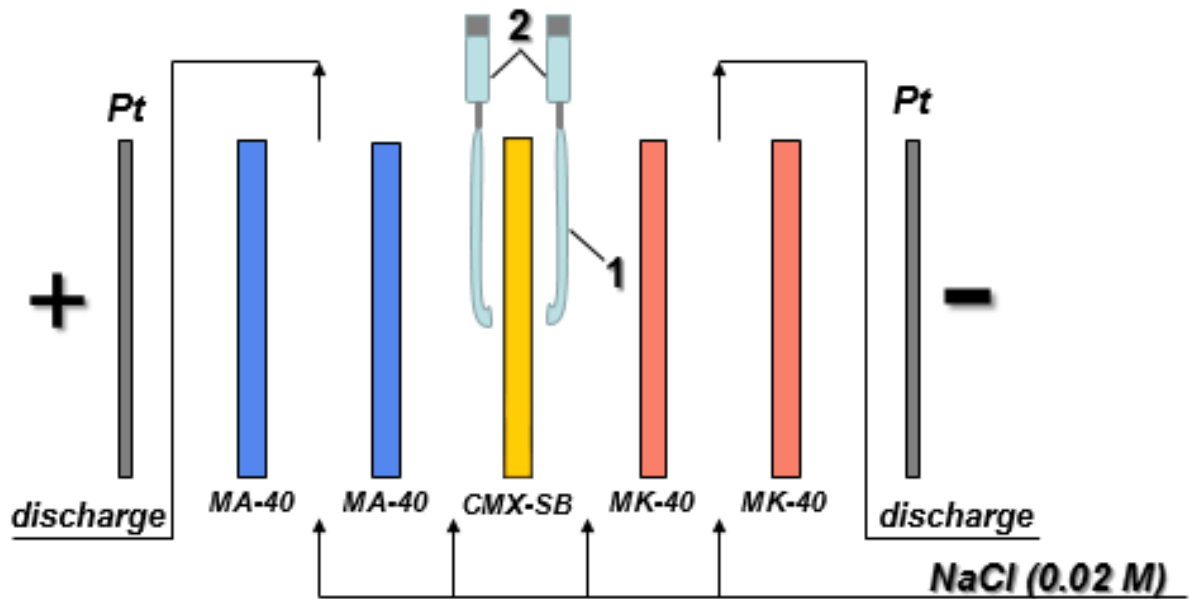
Fig.IV.2: General scheme of the membrane cell used for measuring CVC and chronopotentiometric characteristic. The tips of Luggin's capillaries (1) on each side of the membrane under study are about 1mm; they are connected with Ag/AgCl measurement electrodes (2).

The compartments are formed by five membranes each of them inserted between two plastic frames with connecting pipes and comb-shaped input-output devices. The thickness of the frame is 5.0 mm, which together with the thickness of two sealing gaskets makes the spacing between two neighboring membranes, h = 6.3 mm. The square aperture (S) of the frame available for electric current flowing is 2×2 cm^2. The average flow velocity (V) between two neighboring membranes used in all experiments was 0.36 cm s^{-1}. The CMX-SB membrane under study forms a desalination channel (DC) together with an anion-exchange MA-40M membrane characterized by a low water splitting in overlimiting current regimes. Auxiliary anion-exchange (AEM) and cation-exchange

(CEM) membranes prevent the penetration of electrode reaction products from platinum plane anode and cathode to the central DC. The tips of the Luggin's capillaries (1) with an external diameter of 0.8 mm are located in CMX membrane compartments near the center of the membrane at a distance of about 1 mm from its surface. The Luggin capillaries are connected with Ag/AgCl electrodes (2) used to measure the potential difference across the CMX membrane and two adjacent solution layers.

IV.1.2.4.7 <u>Visualization of electroconvective vortices by microfluidic ED platform</u>

Figure IV.3 shows a micro ED platform described in detail by Kwak et al. (Kwak, Guan et al. 2013). This micro ED platform consists of a single unit cell with two IEMs that separate the desalting channel (central channel) and two electrode channels (Fig.IV.3a). To visualize ion and fluid transport within the cell, a microchannel is formed between the two IEMs. Polydimethylsiloxane (PDMS) is selected as a material for device fabrication because of its optical transparency and flexibility. A flexible PDMS device can make conformal contact with the surface of membranes and electrodes, preventing fluid leakages. Two PDMS blocks have four slots for two ion exchange membranes (IEM) and two electrodes. The micro ED process is observed under a microscope. Real time microscopic images of the ED cell can be obtained using an inverted epifluorescence microscope (Olympus, IX-71), with a thermoelectrically cooledcharge-coupled device camera (Hamamatsu Co., Japan). Sequences of images were analyzed by ImageJ (NIH, Bethesda, MD, USA). The hydrodynamic pressure is generated by a syringe pump (Harvard apparatus, PHD 2200). To visualize fluid flow and salt concentration, 1 µM Alexa Fluor ® 488 dye (Molecular Probes) is added in 20 mM NaCl solution.
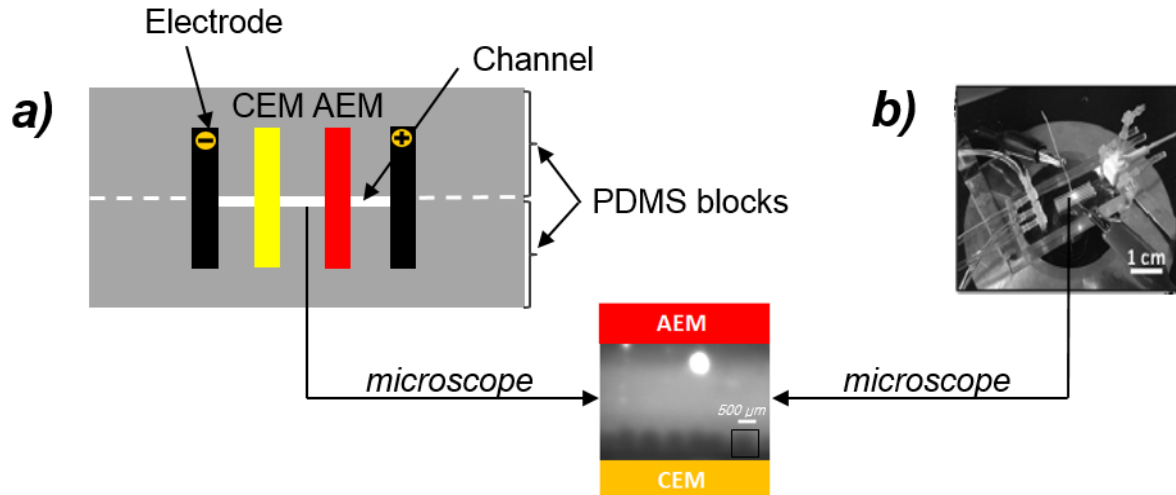
Fig.IV.3: Schematic diagram of microscale electrodialysis system (a) and image of microscale device (b). The ED model system consists of two PDMS blocks (separated on figure 3a) by the white dashed lines), one anion exchange membrane (AEM), one cation exchange membrane (CEM) and two electrodes. Inset figure shows the microscopic fluorescence image of the desalted channel with depletion zone by vortices near the CEM. The geometry of the channels is 200 μm in height, 1.4 mm in width and 15 mm in length.

IV.1.2.4.8 Solution conductivity and demineralization rate

The conductivity of diluate and concentrate solutions was measured with an YSI conductivity instrument (model 3100–115 V, YSI Inc. Yellow Springs, Ohio, USA) equipped with an automatic temperature compensation (ATC) immersion probe (model 3252, k = 1/cm, YSI Inc.). The demineralization rate (DR) was calculated according to the following equation (Cifuentes-Araya, Pourcelly et al. 2011):

$$DR = \left(1 - \frac{\text{model salt solution conductivity at time t}}{\text{model salt solution conductivity at time t} = 0} \right) \times 100$$

eq. IV.5

IV.1.2.4.9 Energy consumption (EC)

The energy consumption was calculated according to Cifuentes-Araya et al. (Cifuentes-Araya, Pourcelly et al. 2011):

$$EC = \int_0^{\bar{t}} I(t)U(t)dt \qquad \text{eq. IV.6}$$

where $\bar{t}$ is the duration of the experiment (in h), U(t) is the voltage (in V) as a function of time; I(t), the intensity (in A) as a function of time; and dt, the time variation (in h). EC was expressed in Wh.

IV.1.2.4.10 <u>Scanning electron microscopy and Energy dispersive x-ray spectroscopy (EDS)</u>

Images of the dry CEMs (drying procedure like in 2.4.4) were taken with a scanning electron microscope JEOL (Japan Electro Optic Laboratory, model JSM840A, Peabody, Massachusetts, USA) equipped with an energy dispersive spectrometer (EDS) (Princeton Gamma Tech.), Princeton, New Jersey, USA). The EDS conditions were 15 kV accelerating voltage with a 13-mm working distance. The samples were coated with a thin layer of gold/palladium in order to make them electrically conductive and to improve the quality of the microscopy photographs (Cifuentes-Araya, Pourcelly et al. 2011).

IV.1.2.4.11 <u>X-ray diffraction (XRD)</u>

The analyses of the dry CEMs (drying procedure like in 2.4.4) were performed by X-ray powder diffraction using a D5000 Siemens diffractometer equipped with a curved graphite crystal monochromator and a goniometer theta–theta (in reflection) with a rotating sample holder. The radiation source (Cu K_α) was a copper lamp with a wavelength of λ = 1.5406 Å. The K_α radiation of copper was generated at 30 mA and 40 kV. The scan rate of 0.02º (2θ) was applied to record patterns for 2θ ranging between 20º and 70º, with a counting time of 1.2 s per step.

IV.1.2.4.12 <u>Statistical analyses</u>

The data of DR, EC and membrane thickness were subjected to an analysis of variance using SAS software (SAS version 9.3, 2011). LCD and Waller-Duncan post-hoc tests were used.

IV.1.3 <u>Results</u>

IV.1.3.1 <u>Physico-chemical characteristics of CEMs</u>

The two lots of CMX-SB membranes showed different thickness values: 0.173±0.010 mm vs 0.183±0.010 mm for CMX-SB-1 and CMX-SB-2 respectively. However, according to the manufacturer, the CMX's thickness may be variable at a value of 0.180±0.010 mm . Concerning membrane conductivities, CMX-SB-1 has lower values (1.95±0.09 mS/cm) in comparison with CMX-SB-2 (3.97±0.03 mS/cm). This was confirmed by IEC measurements since CMX-SB-1 presented values of 1.26±0.05 mmol/g_{wet} or 1.47±0.06 mmol/g_{dry} in comparison with values for CMX-SB-2 of 1.41±0.04 mmol/g_{wet} or 1.75±0.03 mmol/g_{dry}: 19.5 % difference. Consequently, water uptake of both membrane lots was different; 31.4 % and 37.2 % for CMX-SB-1 and CMX-SB-2 respectively indicating that CMX-SB-2 is more hydrophilic. The membrane swelling characterized by the water uptake is the key factor of the ion transfer (Berezina, Kononenko et al. 2008). In the dry state, IEMs are dielectrics. In contact with aqueous solution, there is formation of the labyrinth of ion and water transport nanochannels under the interaction of water molecules with fixed ion-exchange groups (Hsu and Gierke 1983; Mizutani 1990; Zabolotsky and Nikonenko 1996; Berezina, Kononenko et al. 2008). With increasing water content, there is an abrupt increase in the membrane conductivity. Higher water content leads to larger conducting channels/pores and greater ion mobility through channels. Hence, one can expect that the mobility of cations is higher in the more swelled CMX-SB-2. This can explain why the ratio of CMX-SB-2 to CMX-SB-1 conductivity is higher than the ratio of IECs for these membranes. Interesting remark could be made from the data of contact angles. Figure IV.4 represents changes in the water contact angles as a function of time: the more hydrophilic CMX-SB-2 lot has more hydrophobic surface (θ=32.17º) in comparison with CMX-SB-1 lot (θ=24.76º). This fact can be explained by a non-uniform distribution of the ion-exchange polymer in the inner structure and at the surface of the membrane. There is more ion-exchange material (which has strong affinity to the water) on the surface of CMX-SB-1 which leads to its higher surface hydrophilicity in comparison with CMX-SB-2.
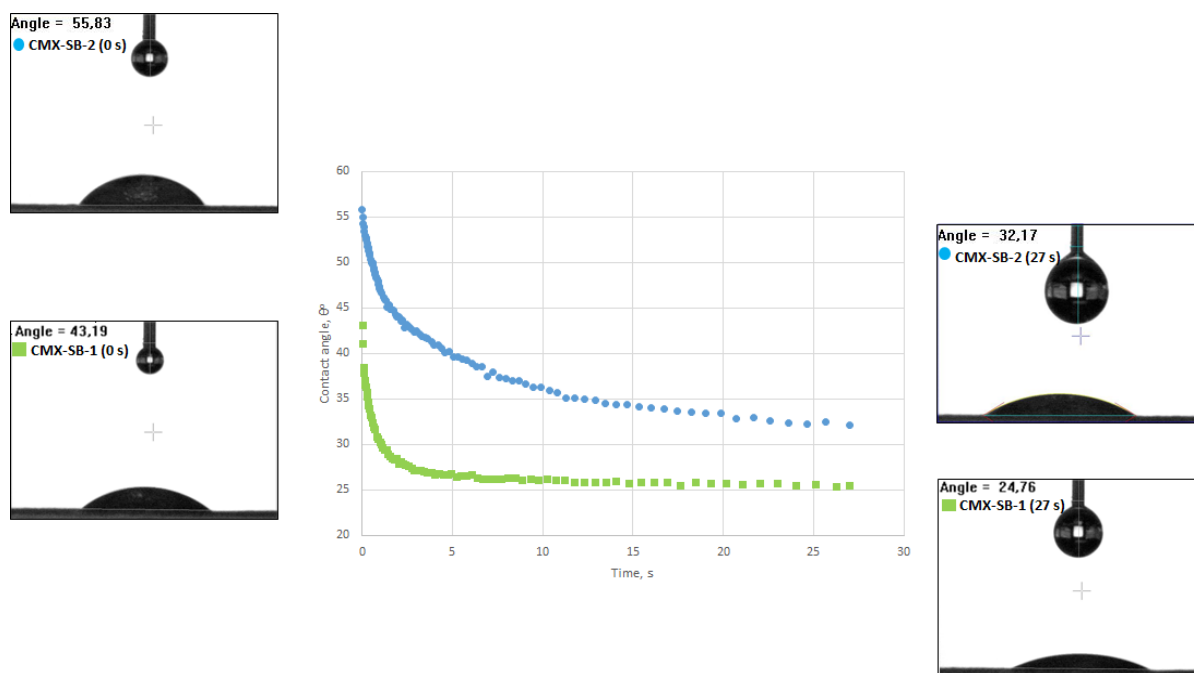
Fig.IV.4: Water contact angles of CMX-SB-1 and SMX-SB-2.

Although both CMX-SB membrane lots were from the same membrane type, the different physico-chemical properties may be explained by variations in the membrane composition (content of styrene-divinylbenzene and polyvinylchloride) (Lue, Wang et al. 2004) and differences arising during manufacturing by the paste method (Krol, Wessling et al. 1999).

IV.1.3.2 Electrochemical characteristics of CEMs

Current-voltage curves (CVC) measurements were performed in order to estimate the behavior of the two CMX-SB lots when current is applied. The first region of CVC (Fig.IV.5a) represents the "ohmic" part where current increases linearly with increasing voltage according to the Ohms law. The second region ("limiting") is characterized by the development of concentration polarization (CP), when the electrolyte concentration near the diluate side of the membrane surface becomes close to zero, meaning the difficulties in current transfer due to insufficient quantities of current carriers at the membrane depleted surface. The "limiting" current region is reflected on the CVC in the form of a plateau. However, in this "plateau" region, increase of current still takes place due to the development of coupled effects of CP such as water splitting phenomenon which provides new current carriers (H^+ and OH^-) and gravitational convection and electroconvection

which improve the delivery of current carriers to the membrane surface. In relatively diluted solutions, such as natural waters and the most of food solutions, the predominant influence is due to electroconvection. When electroconvection is strongly developed, the system passes to the third "overlimiting" current region. Hence, Figure IV.5b represents current-voltage dependences of both cation-exchange membranes where the dashed line corresponds to the theoretical limiting current density (LCD) (i_{lim}^{theor}) 2.1 mA/cm^2 and i_{lim}^{exp} relates to the LCD value obtained from the experimental data. The "ohmic" regions have different lengths and slopes for CMX-SB-2 and CMX-SB-1 with different values of LCD (2.3 mA/cm^2 and 1.7 mA/cm^2 respectively). CVC of CMX-SB-2 has a plateau length of approximately 0.8 V while the plateau length of CMX-SB-1 was longer (approximately 1.8 V). These data indicate that electroconvection is developed differently for both membrane lots. According to Urtenov et al. (Urtenov, Uzdenova et al. 2013), in conditions of forced flow, there are two types of vortices (Fig.IV.5a): stable (at $i<i_{lim}$ and at $i>i_{lim}$ related to the smooth sloping plateau of CVC) and instable (related to the "overlimiting" region of CVC characterized by oscillations of current/potential) ones. When looking at figure IV.5b, it can be noted, that in the case of CMX-SB-2 the development of instable vortices started much earlier than for CMX-SB-1. Instable vortices have bigger size in comparison with stable vortices and lead to a better delivery of ions, all contributing to a better mass transfer.
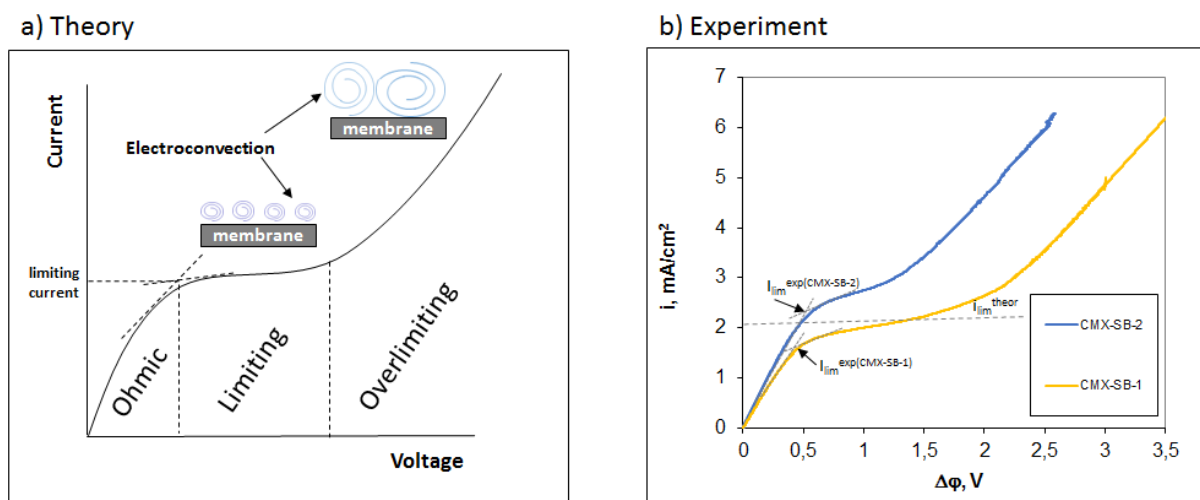
Fig.IV.5: Current-Voltage curves: a) sketch of theoretical curve with representation of electroconvection, b) experimental curves of CMX-SB-1 and CMX-SB-2 membranes.

The IEM surface heterogeneity was characterized via chronopotentiometry. Chronopotentiometry allows the measurement of potential difference as a function of time under a certain current. The transition region of chronopotentiogram (Fig. IV.6a and b) contains a zone with a relatively low increase of the potential drop, which is followed by a fast potential increase corresponding to a salt concentration close to zero at the membrane depleted surface and finally the potential drop reaches its stationary state. As one can see (Fig. IV.6b), the rate of initial potential increase is higher in the case of CMX-SB-2, while the stationary value of the potential drop is lower for this membrane. This behavior can be explained by its higher surface heterogeneity (Choi, Kim et al. 2001).
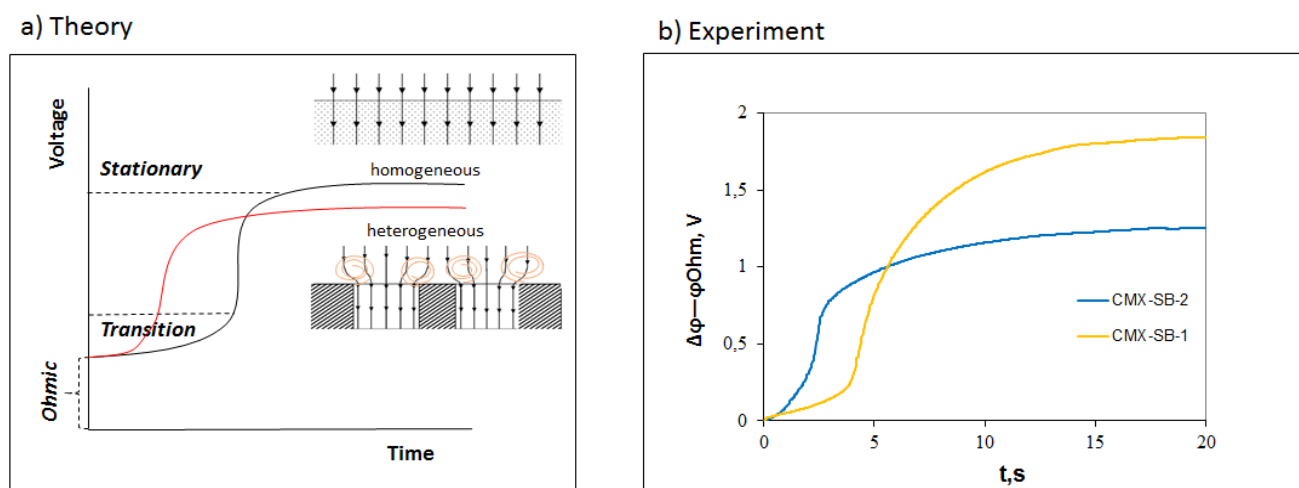
Fig.IV.6: Chronopotentiograms: a) sketch of theoretical curves (— heterogeneous membrane, — homogeneous membrane) with demonstration of current lines adapted from (Balster, Yildirim et al. 2007), b) experimental curves of CMX-SB-1 and CMX-SB-2 with subtracted ohmic part (i=5.00 mA/cm^2).

According to Rubinstein et al. (Rubinstein, Staude et al. 1988; Rubinstein, Zaltzman et al. 2002), electric heterogeneity of the membrane surface leads to funneling effect (Fig. IV.6a): concentration of electric current streamlines within the conducting region where the local current density is high and results in higher concentration polarization hence, higher potential drop. Electroosmosis in the form of electroconvective vortices at the CMX-SB-2 is favored by its higher surface hydrophobicity and apparently by its electric heterogeneity what confirms CVC measurements. The possibility of higher electroconvection near heterogeneous surface was theoretically predicted by Rubinstein et al. (Rubinstein, Staude et al. 1988) and by Dukhin and Mishchuk (Dukhin and Mishchuk 1989) due to the action

127

of tangential electric field, which occurs near a heterogeneous surface and more easily brings in motion charged solution volume. However, it should be noted that the electrical heterogeneity of the membrane surface leads to two effects (Nikonenko, Pismenskaya et al. 2010). On the one hand, it favors electroconvection via the occurrence of tangential electric field. On the other hand, the presence of poorly conducting or non-conducting regions on the surface results in increasing current density through the conducting regions, hence, ceteris paribus, in higher CP and in higher voltage. For example, a homogeneous CMX and heterogeneous MK-40 membranes compared in (Pismenskaya, Nikonenko et al. 2012) had close contact angles but at certain voltages the current density across the CMX was higher. Thus, one can see that the degree of the surface heterogeneity is a subject of optimization (Balster, Yildirim et al. 2007).

IV.1.3.3 <u>Visualization of electroconvective vortices by microfluidic ED platform</u>

Visualization by microfluidic platform demonstrates the evolution of depletion zones by electroconvective vortices near the CEMs with time after applying the current (Fig. IV.7). The development of electroconvective vortices is not the same for both membrane lots as was predicted above by voltammetry and chronopotentiometry. Vortices on the CMX-SB-2 are more developed whatever the time as observed in terms of height by dashed lines on Fig. IV.7. Comparative analysis of microfluidic visualization with contact angles and shapes of chronopotentiometric curves allows to conclude that the membrane surface properties play an important role on vortices formation, particularly its surface heterogeneity and hydrophobicity: heterogeneous and highly hydrophobic membrane surface favors the development of electroconvection (Choi, Kim et al. 2001; Balster, Yildirim et al. 2007).

128
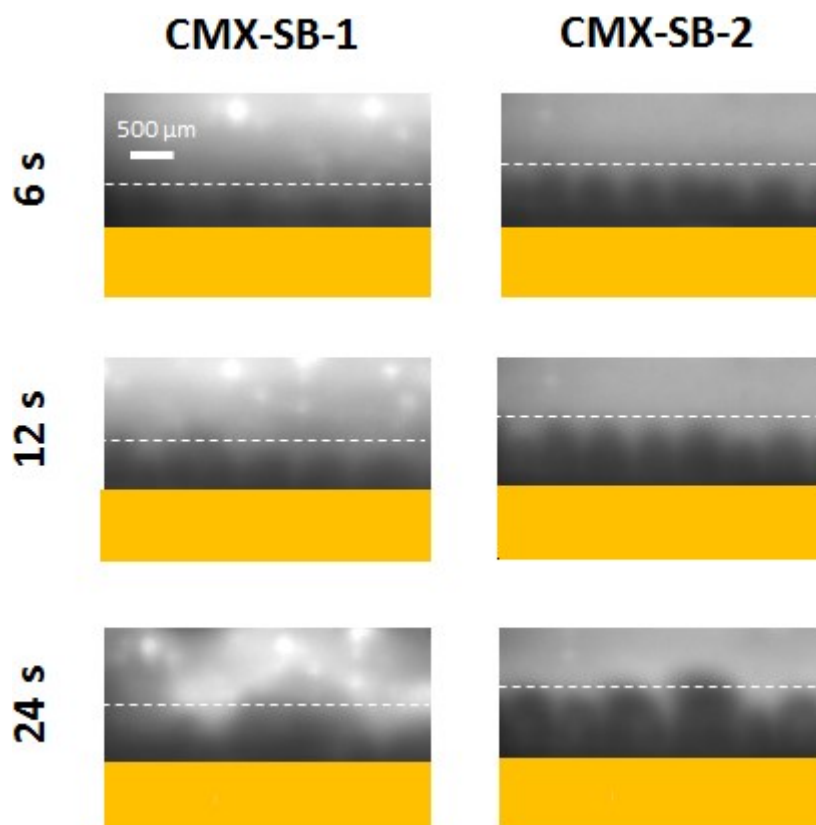
Fig.IV.7: Evolution of electroconvective vortices as a function of time in a 20 mM NaCl solution, with zero flow velocity and a current density of 6.0 mA/cm². Dashed lines indicate the average heights of vortices

IV.1.3.4 Electrodialysis parameters

In this second part, since both membrane lots have different electrochemical behavior due to the different physico-chemical properties, the impact of such differences will be evaluated on demineralization performances as well as on scaling formation on the membrane surface during ED treatment.

A small difference in demineralization rate (DR) values (Tab.IV.1) was observed between 2s/0.5s and 2s/0.67s PEF conditions for the same CMX-SB sample (around 2 units of DR %) and a high one between both CMX-SB lots for similar PEF condition (around 18 units of DR %). To explain the high difference in DR between the CMX-SB samples it is necessary to take into account two groups of membrane properties: 1) initial physico-chemical and electrochemical membrane properties and 2) membrane properties that are

changed during ED treatment under influence of PEF and scaling formation. Firstly, it appears from membrane characterization that CMX-SB-2 has a more hydrophobic surface than CMX-SB-1. It is directly linked with the development of coupled effects of CP (gravitational convection and electroconvection) in the "overlimiting" current region. The gravitational convection seems to have insignificant contribution to mass transfer due to low salt concentration, high flow velocity and small intermembrane space (Nikonenko, Kovalenko et al. 2014). That is why the electroconvection as the main contributor in mass transfer will be considered. In the case of CMX-SB-2 instable electroconvective vortices were more developed and provided easier ion transport through the membrane and consequently allow better demineralization (DR$_{average}$=76.3 %) in comparison with CMX-SB-1 (DR$_{average}$=58.1 %) where smaller stable vortices dominated. Secondly, it was established earlier (Mishchuk, Koopal et al. 2001; Mikhaylin 2014) that PEF may have an influence on the development of electroconvection as well as on the formation of the membrane scaling in the systems with mineral salts. Solution DR assuredly depends on both phenomena. However, no statistical difference in DR values between two close PEF conditions was observed, since pause lapses used were very close. This is in agreement with the previous results of Mikhaylin et al. (Mikhaylin et al. 2014) who also observed no difference between DR values with the same PEF conditions.

Concerning energy consumption (EC), the lowest values were obtained for ED treatments using CMX-SB-1 and that, for both PEF conditions (Tab.IV.1). EC is proportional to the electrical energy needed to transfer ionic species through the IEM: more ions is transferred (higher DR value) more energy is required. The same tendency was also observed by Mikhaylin et al. (Mikhaylin et al. 2014). It is worth to note that the difference in the average DR between two CMX-SB lots is 23.9 %, however difference between EC is just 17.5%. The fact that growth of EC does not follow to the same trend as DR growth could be explained by taking into account development of two processes: water splitting and scaling formation (Cifuentes-Araya, Pourcelly et al. 2011; Malek, Ortiz et al. 2013). Indeed, according to the CVC, water splitting on CMX-SB-2 is hampered by early-developed instable electroconvective vortices and it is possible to anticipate that these big instable vortices can also hamper the scaling formation which consequently slows down the growth in EC for CMX-SB-2 lot. Evident advantage of CMX-SB-2 lot in terms of EC may be observed comparing EC values at one specific DR value: indeed, less EC is required for attaining 50% of demineralization for ED treatment with CMX-SB-2 and that is for both PEF conditions (Tab.IV.1).

130

Tab.IV.1: Demineralization rate (%) and Energy consumption (Wh) for CMX-SB-1 and CMX-SB-2 under different PEF conditions.

Pulse/Pause	Demineralization rate, in %		Energy consumption, in Wh		Energy consumption at DR=50%, in Wh	
	2s/0.5s	2s/0.67s	2s/0.5s	2s/0.67s	2s/0.5s	2s/0.67s
CMX-SB-1	59,0±2,9[b*]	57,2±2,0[b]	11,8±0,4[b]	12,8±0,7[b]	8,7±0,7[b]	10,4±0,4[b]
CMX-SB-2	77,3±0,9[a]	75,2±1,7[a]	15,5±1,0[a]	14,7±1,5[a]	7,7±0,5[a]	7,3±0,4[a]

* Mean values followed by different letters are significantly different ($p < 0.05$).

IV.1.3.5 <u>Membrane thickness</u>

The values of membrane thickness measured after ED treatment show that the quantity of scaling varied according to the membrane lots and PEF conditions (Tab.IV.2). CMX-SB-1 presented the highest thickness values with respective percentage of scaling thicknesses of 54.9 % and 91.9 % for 2s/0.5s and 2s/0.67s PEF conditions respectively : for this sample it can be concluded that scaling was formed intensively in comparison with CMX-SB-2 which presented respective percentage of scaling thicknesses of 19.7% and 48.6%. Concerning PEF modes, it appeared that for both membrane lots, the lowest quantity of scaling was obtained for the 2s/0.5s mode. This result confirmed the fact that the application of shorter pause lapse limits the amount of scaling formed (Cifuentes-Araya, Pourcelly et al. 2011; Mikhaylin 2014). Additionally, between both PEF ratios for the same membrane sample it is clear that an increase in thickness also decreases the DR. The high quantity of scaling on CMX-SB-1 can be connected with low DR values. This confirmed the negative effect of scaling on the performance of ED treatment.

Tab.IV.2: Membrane thickness (mm) and ΔThickness (difference between thickness after ED and initial value) (mm) for CMX-SB-1 and CMX-SB-2 under different PEF conditions.

Pulse/Pause	Thickness, in mm		ΔThickness, in mm	
	2s/0.5s	2s/0.67s	2s/0.5s	2s/0.67s
CMX-SB-1	0,268±0,004[b*]	0,332±0,011[a]	0,095	0,159
CMX-SB-2	0,219±0,011[c]	0,272±0,021[b]	0,036	0,089

* Mean values followed by different letters are significantly different (p<0.05).

The low quantity of scaling on CMX-SB-2 is apparently due to the higher development of electroconvection near this membrane. Fluid flow produced by electroconvection not only enhances the ion transport from the bulk to the surface, but also washes out the nuclei of salt deposit on the surface. Moreover, lower CP caused by electroconvection mitigates water splitting, hence, contributes to decreasing OH^- ions concentration in the depleted boundary solution. This reduces the rate of poorly soluble compounds formation in the alkaline media and at the membrane surface.

IV.1.3.6 <u>Scanning electron microscopy (SEM)</u>

Concerning diluate side of the CMX-SB-1 membrane, in the 2s/0.5s PEF condition, scaling is distributed on the whole surface in the form of particles (Fig.IV.8a). However, the shape of these particles does not correspond to the shape of the crystal structure of Ca and/or Mg compounds, which may indicate the influence of Mg^{2+} on the formation of Ca compounds and, inversely, influence of Ca^{2+} on the formation of Mg compounds (Zhang and Dawe 2000; Chen, Neville et al. 2006). Moreover, for 2s/0.67s there is almost no particles and scaling distributed on the membrane surface as a uniform layer, and that may indicate the amorphous character of this scaling. Diluate side of the CMX-SB-2 membrane surface at both PEF conditions contains scaling with almost the same morphology (Fig.IV.8b). This scaling mostly consists of cauliflower-shape crystals, but does not correspond to a specific nature of crystals. However, in comparison with CMX-SB-1 these crystal structures are larger due to the processes of agglomeration. Last fact may indicate that for the CMX-SB-2 the scaling formation is more orientated to crystal growth instead of initiation of new crystal particles, and that was opposite for CMX-SB-1.
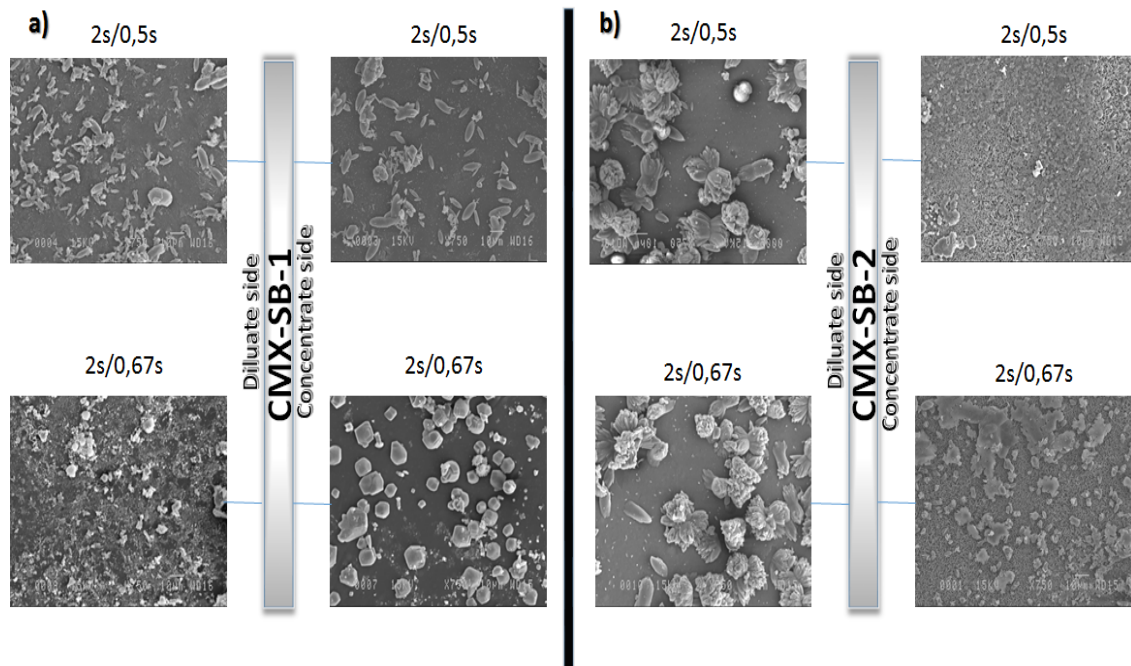
Fig.IV.8: Scanning electron microscopy photographs of the concentrate and diluate sides of CMX-SB-1 (a) and CMX-SB-2 (b) at the different PEF conditions.

The concentrate side of CMX-SB-1 (Fig.IV.8a) contains crystals at both PEF conditions. At 2s/0.5s in comparison with the diluate side these crystals have larger size due to the agglomeration of smaller crystals. The scaling structure of 2s/0.67s is also different from the diluate side and presents a crystalline form. However, the crystal shapes on the concentrate side of the membrane between two PEF conditions are not similar: long crystals in 2s/0.5s condition and mostly hexagonal crystals with rhombohedral or pyramidal terminations in 2s/0.67s condition. For CMX-SB-2, its concentrate side surfaces are not covered similarly in comparison with diluate side (Fig.IV.8b). Needle-like crystals with presence of small islands of agglomerated crystals are shown in 2s/0.5s condition. Apparently, at 2s/0.67s scaling was developed similarly as in 2s/0.5s condition, but for 2s/0.67s crystal agglomerates above the layer of needle crystals are larger and are distributed on the whole membrane surface. Small variations of the scaling structure for CMX-SB-2 may indicate that the influence of both PEF conditions on the scaling structure is almost identical. However, regarding the membrane thickness, it is shown that at 2s/0.67s there is more scaling, which can be connected with the more developed character of scaling agglomerates on the concentrate side of CMX-SB-2.

The differences in the scaling structure between both PEF conditions evidently indicate the direct influence of PEF on the formation and development of certain types of crystal structures (Cifuentes-Araya, Pourcelly et al. 2013; Mikhaylin 2014). Comparing the scaling structures of CMX-SB-1 and CMX-SB-2 with previous structures observed by Mikhaylin et al. (Mikhaylin 2014) for a CMX-SB membrane in the same PEF conditions, it may be noted that scaling structures were different in all cases. Additionally, the PEF influence for each membrane lot was not the same. For CMX-SB-1 effect of different pulse/pause lapses showed real differences in the scaling structure, though for CMX-SB-2 this effect was not as pronounced. This fact may also confirm the influence of the physico-chemical membrane properties on the development of the membrane scaling.

IV.1.3.7 Energy dispersive X-ray spectroscopy (EDS)

According to figure IV.9a, it appears that the diluate side of CMX-SB-1 at both PEF modes was covered by compounds of Mg and Ca. The same scaling composition was on the concentrate side of CMX-SB-1. Moreover, whatever the membrane side, the peaks of Ca were higher in 2s/0.5s condition in comparison with 2s/0.67s. Diluate side of CMX-SB-2 contains the same ratio of both scaling agents also with predominance of Ca (Fig.IV.9b). However, mostly the Mg compounds covered the concentrate side.

Influence of the Mg and Ca on the properties of the membrane surface is not similar (Tanaka 2007; Mikhaylin et al. 2014). It is well known that Mg^{2+} ions have an effect on the formation of crystals of Ca compounds by adsorption on its surface and incorporation in the crystal structure (Zhang and Dawe 2000; Chen, Neville et al. 2006). In addition, Mg^{2+} ions can catalyze the reactions of water splitting much better than Ca^{2+} ions. During interactions of Mg^{2+} ions with water molecules, protons are generated (Mikhaylin et al. 2014). These protons decrease pH and lead to shift the balance between CO_3^{2-} and HCO_3^- ions to the prevalence of HCO_3^- which impedes the formation of $CaCO_3$. The prevention of $CaCO_3$ formation affects positively the DR value (Mikhaylin 2014). Indeed, comparing DR values reached for both membrane samples it is clear that in the case of CMX-SB-2 with high Mg content on the concentrate side DR was much higher (Tab.IV.1) than for CMX-SB-1.

134
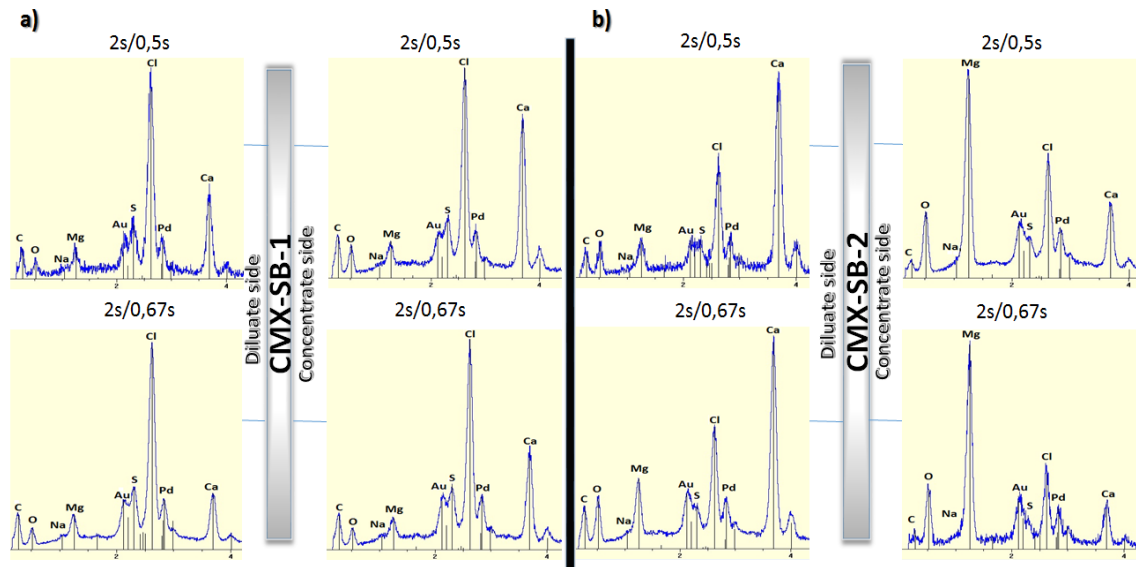
Fig.IV.9: Energy dispersive x-ray spectroscopy of the concentrate and diluate sides of CMX-SB-1 (a) and CMX-SB-2 (b) at the different PEF conditions.

IV.1.3.8 X-ray diffraction (XRD)

Mineral compounds of CMX-SB-1 scaling (Fig.IV.10a) are present in brucite and calcite forms on the diluate side and in portlandite with small presence of brucite and calcite on the concentrate side. These results are in accordance with EDS analysis. However, EDS analysis shows quite high peak of Ca whereas there is just small peak of calcite on the diffractogram. This could be explained by the fact that Ca was presented in amorphous calcite or portlandite forms, which cannot be detected by XRD (Casademont, Pourcelly et al. 2007). For CMX-SB-2 scaling (Fig.IV.10b) a prevalence of calcite is revealed on the diluate side for both PEF modes. On the CMX-SB-2 concentrate side, prevalence of brucite at 2s/0.5s and almost equal concentration of calcite and brucite at 2s/0.67s were observed. Results of XRD for CMX-SB-2 are also in agreement with EDS analysis, except for 2s/0.67s diluate side. At this condition, peak of Mg on the diffractogram was significantly lower than on the EDS graph. Once again it could be explained by the presence of $Mg(OH)_2$ in amorphous form.

According to XRD results, it appears that the membrane deposits on each membrane lot were developed differently. Furthermore, the formation of scaling in portlandite form

on the diluate side of CMX-SB-1 (Fig.IV.10a) was unexpected. According to the portlandite K_s=4.35 to $8{\times}10^{-6}$ (mol/l)^3 (Brečević and Nielsen 1989; Roques 1990) it is supposed to precipitate at least in comparison with $Mg(OH)_2$ in brucite crystal form (K_s= 4.4 to $8.8{\times}10^{-12}$ (mol/l)^3), $Mg(OH)_2$ in amorphous form (K_s=$1.25{\times}10^{-11}$ (mol/l)^3 to $1.6{\times}10^{-9}$ (mol/l)^3), $CaCO_3$ in calcite form (K_s=$3.7{\times}10^{-9}$ (mol/l)^2) and $CaCO_3$ in amorphous form (K_s=$4.0{\times}10^{-7}$ (mol/l)^2). Casademont et al. (Casademont, Pourcelly et al. 2007) observed the same effect of portlandite precipitation on the concentrate side of CEM. However, the authors used a CMX-S membrane with an electrical conductivity value of 1.120 ± 0.010 mS/cm. The conductivity value of CMX-SB-1 is quite close to the one for CMX-S. That fact allows to speculate that both CMX-SB-1 and CMX-S samples have some similarities in terms of membrane structure (Berezina, Kononenko et al. 2008) and this membrane microstructure could be preferable for portlandite formation. Additionally, it is necessary to notice that on the diluate side of CMX-SB-2 the formation of brucite was almost suppressed. Mikhaylin et al. (Mikhaylin et al. 2014) reported the presence of $Mg(OH)_2$ on the diluate side at 2s/0.5s with higher DR (79.3%) in comparison with DR of the present work (77.3%). This comparison also demonstrates an influence of different physico-chemical properties between CMX-SB samples on the scaling structure and consequently on DR.
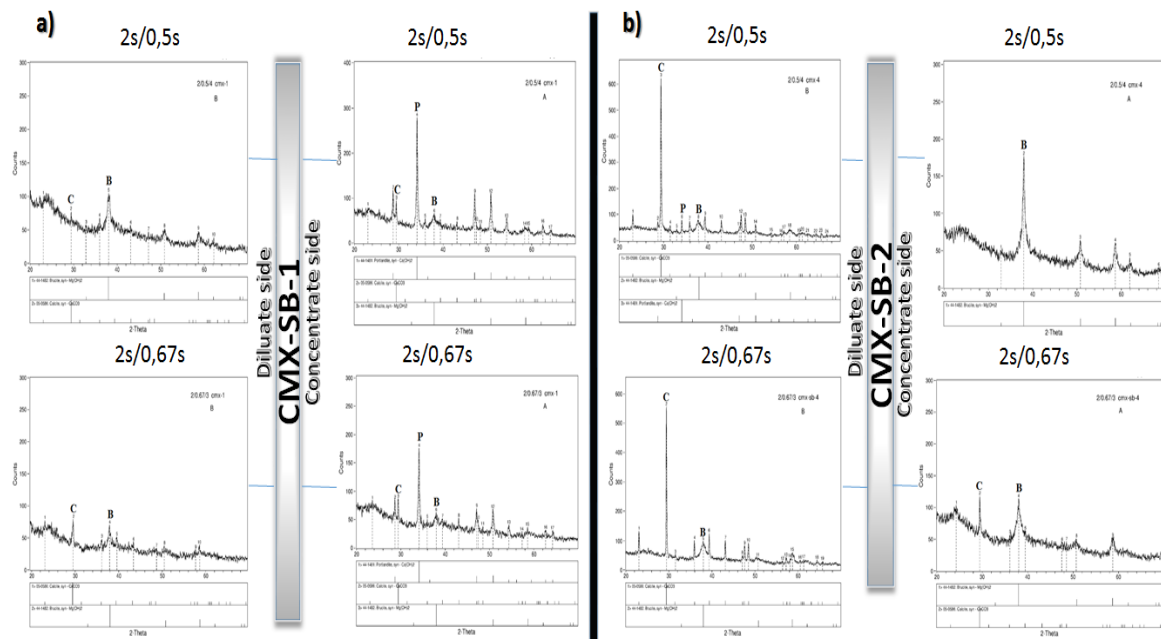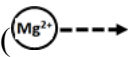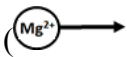
Fig.IV.10: X-ray diffraction of the concentrate and diluate sides of CMX-SB-1 (a) and CMX-SB-2 (b) at the different PEF conditions (C is calcite ($CaCO_3$), B is brucite ($Mg(OH)_2$) and P is portlandite ($Ca(OH)_2$)).

IV.1.4 <u>Discussion</u>

From previous results, it appears that different lots of the same membrane type may have different physico-chemical properties thus different dimensions of nanochannels and different surface properties. This fact leads to different electrochemical behavior of membranes, which is possible to observe on CVCs, ChPs and via images obtained with a microfluidic ED platform. The development of electroconvective vortices, one of the major factors affecting positively ion transport in the "overlimiting" current region, was not the same for both CMX-SB lots. Images from the microfluidic ED platform show better development of electroconvective vortices for the CMX-SB-2. In addition, the "overlimiting" current region on the CVC for CMX-SB-2 starts under the potential difference 1.3 V, while for CMX-SB-1 it starts just under 2.3 V. This indicates that bigger instable electroosmotic vortices, which are the most effective in improving ion transfer, are developed earlier for CMX-SB-2 (Fig.IV.12a CMX-SB-2) in comparison with CMX-SB-1, where smaller stable vortices dominate until 2.3 V (Fig.IV.12a CMX-SB-1). Furthermore, bigger instable vortices lead to suppression of negative water splitting

137

phenomenon in comparison with stable vortices where water splitting is more pronounced. Thus, better ED performance might be expected with usage of CMX-SB-2. Indeed, results of ED treatment confirm this expectation. For CMX-SB-2 final demineralization was higher whatever PEF regime ($DR_{average}$=76.3%) in comparison with CMX-SB-1 ($DR_{average}$=58.1%). In addition to above, electroconvective vortices can prevent the formation and growth of scaling. Indeed, CMX-SB-1 with instable vortices was 2.8 times (for 2s/0.5s) and 1.9 times (for 2s/0.67s) more fouled in comparison with CMX-SB-2 with stable vortices. Concerning the scaling composition, it can be proposed that the membrane hydrophobicity and consequently the size of membrane nanopores and nanochannels played important role in the competitive migration of Na^+, Ca^{2+} and Mg^{2+} (Sata, Sata et al. 2002; Firdaous, Malériat et al. 2007). It appears that CMX-SB-1 with less water uptake value is more hydrophobic what may indicate that their microstructure would contain more narrow nanopores and nanochannels than the microstructure of CMX-SB-2 (Berezina, Kononenko et al. 2008). In addition, it is known, that migration of Mg^{2+} through CEM is the slowest in comparison with Na^+ and Ca^{2+} due to: 1) larger hydration radius and hydration energy of Mg^{2+} (Bucher and Porter 1986; Marcus 1991) what plays the role of obstacle for the entrance in CEM; 2) higher affinity of Mg^{2+} to the SO_3^- groups (Firdaous, Malériat et al. 2007) (Fig.IV.12b), which prevents it from jumping from site to site inside the CEM. Thereby, more narrow nanopores and nanochannels of CMX-SB-1 hampered Mg^{2+} migration ( ) what consequently leads to the formation of portlandite on the concentrate side of this lot (Fig.IV.12b CMX-SB-1). Casademont et al. (Casademont, Pourcelly et al. 2007) observed the same effect of portlandite formation on the concentrate side of CEM when the concentration of Mg^{2+} was low. Contrary, relatively large nanopores and nanochannels of CMX-SB-2 allow better migration of Mg^{2+} ions ( ) which causes an increase of Mg^{2+} concentration on the concentrate side of CEM (Fig.IV.12b CMX-SB-2). Mathematical model based on Nernst-Planck and Poisson equations and developed by Urtenov et al. (Urtenov, Kirillova et al. 2007) allows estimation of concentration profiles in the depleted diffusion layer of CEM (Fig.IV.11) which might be helpful for the deeper understanding of scaling phenomena in the ED systems.
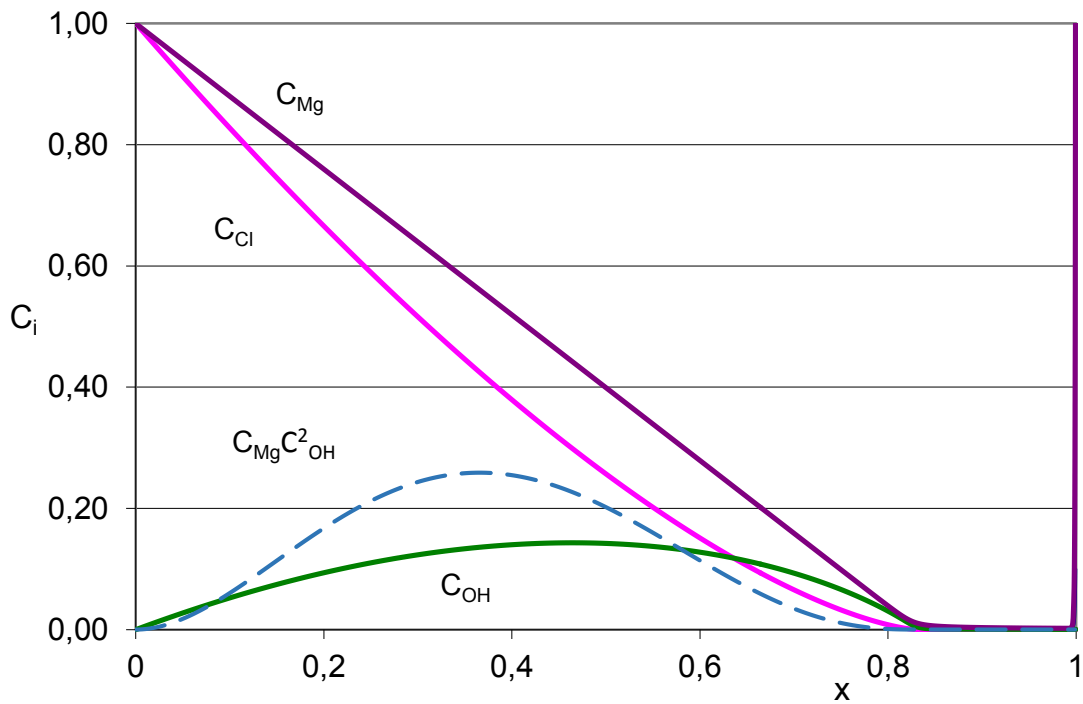
Fig.IV.11: Concentration profiles obtained by using the mathematical model developed by Urtenov et al. (Urtenov, Kirillova et al. 2007); the solid lines show the equivalent fractions of ions (C_i), the dashed line shows the product ($C_{Mg} C^2_{OH} \times 50$).

In this model, the diffusion layer is divided in two regions: the electroneutral region from the bulk solution side, and the space charge region (SCR) at the membrane surface. The ion concentrations within the SCR are small, of the order of $c_0 (L_D / \delta)$, where c_0 is the electrolyte concentration in the solution bulk, δ is the diffusion layer thickness, and L_D is the Debye length. When taking $L_D = 2$ nm and $\delta = 50$ μm, for the bulk concentration of Mg^{2+} (about 0.02 mol/L), one can find that in the SCR the concentration of Mg^{2+} should be about 8×10^{-7} mol/L. Assuming that the concentration of OH^- ions is of the same order, the product of $c_{Mg^{2+}} (c_{OH^-})^2$ is about 5×10^{-19} (mol/l)^3. This value is much lower than the solubility product constant, K_s, of $Mg(OH)_2$ (the minimum value related to the brucite crystal form is about 5×10^{-12} (mol/l)^3). However, with increasing distance from the membrane, the concentration of both Mg^{2+} and OH^- first increases, as well as the product $c_{Mg^{2+}} (c_{OH^-})^2$. Under the conditions of calculation (Fig. IV.11), $c_{OH^-} / c_{Mg^{2+}}$ becomes as high as about 0.5 in the center of the diffusion layer (a rather high degree of concentration

139

polarization and water splitting rate were used in the calculations), then c_{OH^-} decreases to reach the value 10^{-7}, which is imposed by the bulk (feed) solution. The evaluation of the product $c_{Mg^{2+}}\left(c_{OH^-}\right)^2$ in the center of the diffusion layer for the above conditions gives 5×10^{-8} (mol/l)^3 that is higher than the maximum solubility product constant of Mg(OH)$_2$ relating to the amorphous form, 1.6×10^{-9} (mol/l)^3. Thus, within the suggested conditions one can expect that the formation of precipitation will mainly occur at a certain distance from the CEM depleted interface. However, in the conditions of present ED treatments when the OH$^-$ leakage from the alkaline concentrate compartment to the diluate compartment takes place (Fig.IV.12b) ←(OH)), precipitation may occur closer to the depleted CEM surface.

Similar reasoning concerns with Ca^{2+}. However, the value of K$_s$ for Ca(OH)$_2$, portlandite, is rather high, 4.35 to 8×10^{-6} (mol/l)^3 (Brečević and Nielsen 1989; Roques 1990), hence, one can expect its precipitation only if the concentration of OH$^-$ ions is high, and that of Mg^{2+} is low. The precipitation of portlandite is more expected on the concentration side of CEM where a highly alkaline solution is presented, if the transfer of Mg^{2+} ions across the membrane is hampered what was described above for the case of CMX-SB-1. Another possibility is the precipitation of CaCO$_3$, whose value of K_s in calcite form is Ks=3.7×10^{-9} (mol/l)^2. Though the K_s value for calcite is essentially higher than that for brucite, the probability of precipitation of both compounds in the conditions of present experiments should be rather close. The reason is that in the case of calcite the product of the second degree $c_{Ca^{2+}}c_{CO_3^{2-}}$ and not the third as in the case of brucite must be compared with K_s. For example, considering the center of the diffusion layer and assuming $c_{Ca^{2+}} = 10^{-2}$ mol/l (the half of the bulk concentration), and $c_{CO_3^{2-}} = 10^{-3}$ mol/l (assuming a part of HCO$_3^-$ is transformed in CO$_3^{2-}$) their product is 10^{-5} (mol/l)^2 . The latter is approximately in the same relation with the calcite K_s as the concentration product $c_{Mg^{2+}}\left(c_{OH^-}\right)^2$ in the case of brucite with its K_s. These relations may be easily shifted in the "profit" of calcite or brucite, if some parameters of the electromembrane separation are changed (Mikhaylin, Nikonenko et al. 2014).
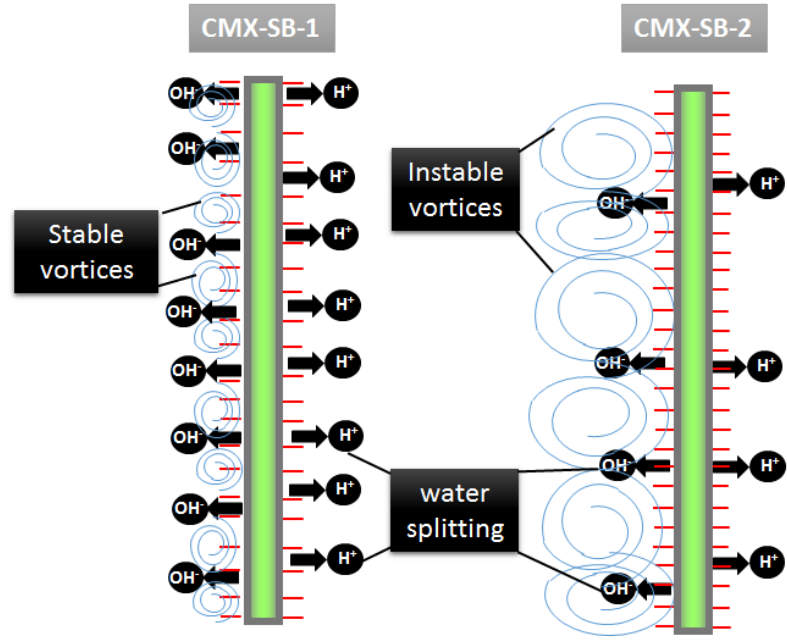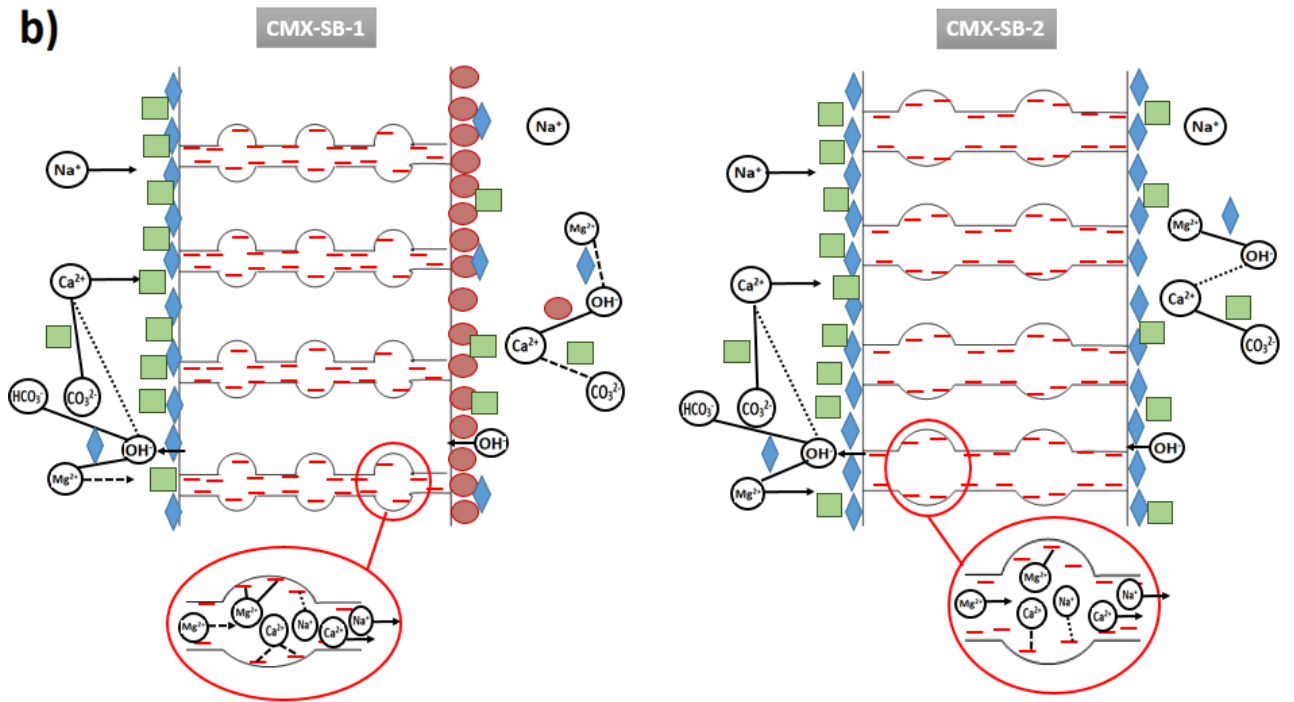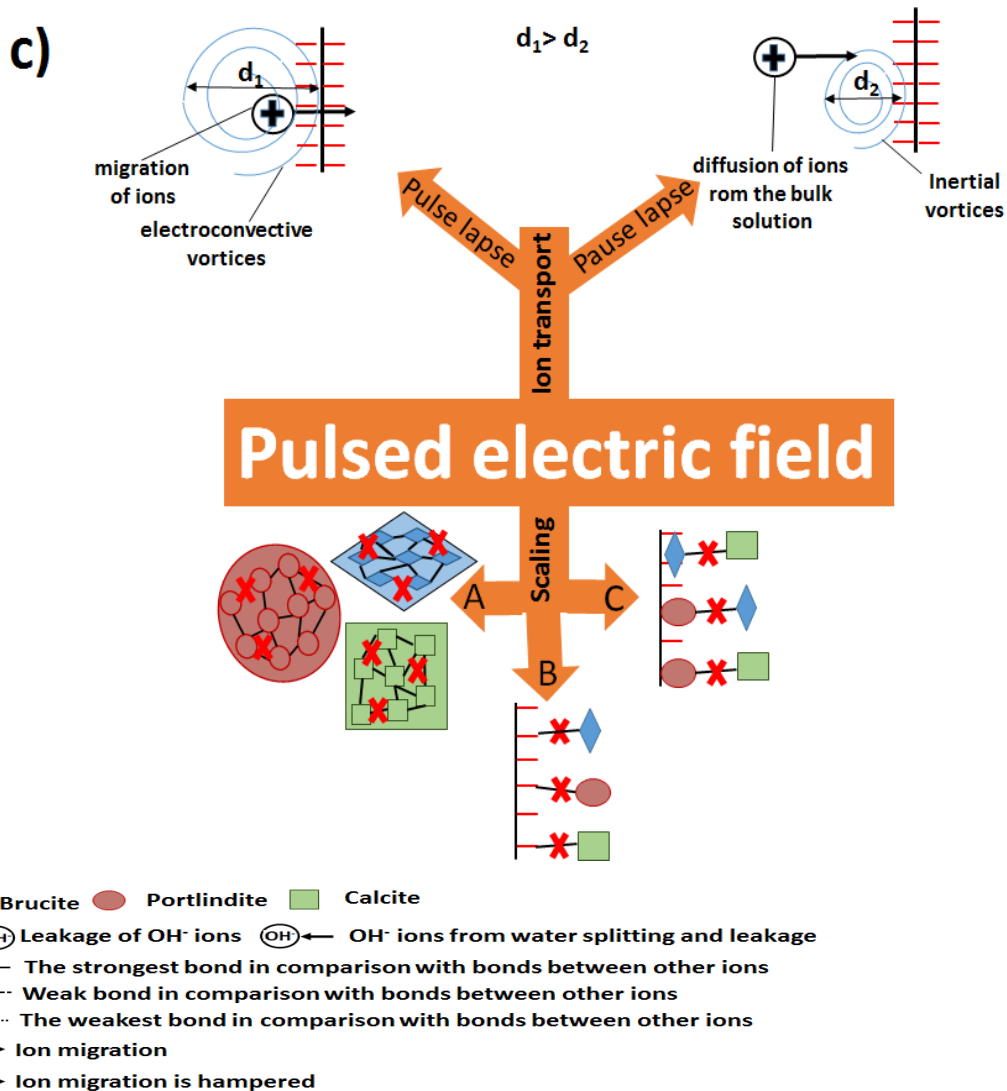
Fig.IV.12: Model of effects on the CEM during ED treatment with application of PEF.

Apart from the influence of the physico-chemical membrane properties, there is also the influence of PEF, which could be divided in two groups: 1) influence on the ion transport and 2) influence on the scaling formation (Fig.IV.12c). Two states of the ED system during application of PEF can be proposed. The first state (pulse lapse) when the current is turned on has already been characterized and the main effect improving the ion transport is electroconvective vortices. Consequently, there is the second state (pause lapse) when the current is turned off. In this case, the transfer of ions from the bulk solution to the membrane surface is provided by diffusion and inertial vortices, which continue their rotation, though they become smaller with increasing pause lapse duration. Simulation of occurrence of electroconvective vortices during the pause lapse was recently made by Uzdenova et al. (Uzdenova, Kovalenko et al. 2015). The authors found that inertial forces

after the current turn-off are effective only for the first 0.01 s, and then the vortices are fed by the chemical energy of non-uniform concentration field. Mikhaylin et al. (Mikhaylin 2014) showed that pulse/pause duration can affect the ion transport and the changes of each lapse type even on 1s can drastically change DR. That fact is most probably related with the size of electroosmotic and inertial vortices. Electroosmotic vortices can be insufficiently developed if the pulse lapse is too small and inertial vortices can disappear if the pause lapse is too long. Concerning the influence of PEF on the scaling formation (fig.IV.12c), three possible cases of influence can be hypothesized: 1) suppression of the nucleation and growth of each scaling type (arrow A), 2) suppression of interaction between scaling and ion-exchange groups of CEM (arrow B) and 3) suppression of multilayer scaling formation (arrow C). It is not easy to emphasize the main effect among these three because they exist at the same time and are accompanied by additional suppressive effect from electroosmotic vortices. However, based on results of the present work (CMX-SB-2) and previous investigations of Mikhaylin et al. (Mikhaylin et al. 2014) it appears that less scaling and better demineralization are attained when there is suppression of multilayer scaling formation.

IV.1.5 <u>Conclusion</u>

The present work may be considered as a bridge between the properties, nanostructure and behavior during ED treatment of cation-exchange membranes (CMX-SB) in a complex system containing scalant agents. It was established that there is a triangle of the main influences on the ED performances in the "overlimiting" current regimes such as electroconvective vortices, PEF and scaling formation. There is a clear pattern: in the case of CMX-SB-2 with development of big instable electroconvective vortices, there was less scaling, higher demineralization and gain in energy consumption in comparison with CMX-SB-1 with smaller stable electroconvective vortices. Additionally, the passage from the 2s/0.5s mode to the 2s/0.67s mode leads to increasing the amount of total precipitate. Moreover, the organization of the membrane nanochannels and nanopores plays important role in competitive migration of certain ions affecting, ipso facto, the composition of the membrane scaling. All above factors assuredly have an influence on each other during the

ED treatment and experiments are currently under way to investigate deeper the influence of each factor separately.

Acknowledgements

CHAPTER V. HYBRID BIPOLAR MEMBRANE ELECTRODIALYSIS/ ULTRAFILTRATION TECHNOLOGY FOR CASEIN PRODUCTION: EFFECT OF PULSED ELECTRIC FIELD ON MEMBRANE SCALING AND PROCESS PERFORMANCE

CONTEXTUAL TRANSITION

Previous chapters allowed to find the optimal PEF conditions improving ED treatment by membrane scaling inhibition. The present chapter aims to apply gained knowledge about positive influence of PEF to solve scaling problem during a real food process. Acidification of skim milk by bipolar membrane electrodialysis (EDBM) for production of caseins (major milk proteins) was chosen since scaling is reported as one of the major locks of this technology. Furthermore, from the author's knowledge, there is no information about application of PEF to EDBM process what makes interesting to investigate the viability of such an approach.

In this context, the present chapter will focus on the application of optimal PEF mode (2s/0.5s) to solve the CEM scaling during EDBM of skim milk. However, prior to performing the PEF approach it is necessary to solve another problem arising during EDBM of skim milk such as stack clogging by precipitated proteins. Indeed, during electroacidification, when pH reaches the isoelectric point of caseins, their intensive precipitation occurs in milk reservoir as well as inside EDBM stack. Stack clogging increases the system resistance and hinders the membrane surfaces, both phenomena contribute to a decrease of the whole process efficiency. Thus, an ultrafiltration module allowing retention of protein fraction will be applied prior to the EDBM module to avoid EDBM stack clogging by caseins.

The influence of pH of electroacidification on CEM scaling will be one of the objectives of this chapter since from the literature it is known that in milk part of Ca^{2+} and Mg^{2+} scaling agents is present bonded with casein micelles and do not migrate until they become free after disruption of micelles by lowering pH. Moreover, free Ca^{2+} and Mg^{2+} ions migrate insignificantly until pH 5.0 due to predominant electromigration of K^+ ions.

Thereby, two pH values (conventional 4.6 and 5.0) will be tested to estimate differences in scaling formation.

This chapter has been the subject of an article entitled:

"**Hybrid bipolar membrane electrodialysis/ultrafiltration technology assisted by pulsed electric field for casein production**", will be submitted in "Green Chemistry". The authors are Sergey Mikhaylin (Ph. D. Candidate: planning and realization of the experiments, analysis of the results and writing of the manuscript), Victor Nikonenko (Thesis Co-director: scientific supervision of the student, revision and correction of the manuscript), Gérald Pourcelly (Thesis Co-director: scientific supervision of the student, revision and correction of the manuscript) and Laurent Bazinet (Thesis Director: scientific supervision of the student, revision and correction of the manuscript).

V.1 Hybrid bipolar membrane electrodialysis/ultrafiltration technology assisted by pulsed electric field for casein production

Abstract

Electrodialysis with bipolar membranes (EDBM) is an ecofriendly technology providing a wide spectrum of solutions for the modern industries. The main advantage of EDBM is the absence of chemicals during the treatment which makes it very attractive especially in the food and pharmaceutical sectors. The production of casein, the major milk proteins, by means of EDBM is a very interesting approach in a sustainable development context due to the high product purity, no waste generation and absence of hazardous reagents. Casein is widely used as a food additive in order to improve food nutritional value as well as to create the desirable functional properties. Moreover, casein is a source of bioactive peptides having beneficial effects on human health. However, the major lock hampering the industrial application of EDBM for production of casein with improved quality is precipitation of casein inside EDBM stack and membrane scaling. Here we propose a hybrid technology comprising EDBM module coupled with an ultrafiltration module (UF). Our results show that the use of UF module prior EDBM allows complete prevention of casein precipitation inside the EDBM stack what plays a crucial role in the improvement of EDBM efficiency. In addition, we have found that electroacidification may be performed until pH 5.0 instead of the conventional value of 4.6 with more than 90 % of casein recovery what allows a substantial decrease in membrane scaling. Finally, application of pulsed electric field mode allows inhibition of scaling formation and hampering of OH^- leakage, which hastens the EDBM process and increases the membrane lifetime.

V.1.2 <u>Introduction</u>

Proteins play an important role in the maintenance of the normal body composition and function throughout the life cycle. In addition, proteins are a source of bioactive peptides having beneficial effects on cardiovascular, nervous, gastrointestinal and immune systems preventing hypertension, diabetes, cancer and other diseases (Korhonen and Pihlanto 2006). Furthermore, modern trends are directed away from the high carbohydrate towards the high protein diet (Astrup and Geiker 2014; Clifton, Condo et al. 2014; von Bibra, Wulf et al. 2014) in order to prevent obesity and risks of cardiovascular diseases (Phillips 2014). To satisfy demands in increased protein level, modern industry proposes the use of protein ingredients. Caseins, the major proteins of milk, are widely used as food ingredients in order to increase the nutritional value of food as well as to provide functional benefits such as structure formation, foaming, heat stability, water binding and emulsification (Singh 2011). There are two main casein types, such as rennet casein and acid casein, which are usually produced by industries. Rennet-induced casein coagulation comprises two stages: 1) application of special enzyme for hydrolysis of κ-casein with production of para-κ-casein and casein macropeptides and 2) coagulation of para-κ-casein by Ca^{2+}. Acid-induced precipitation are based on pH decrease until the isoelectric point of caseins by addition of acid, by fermentation or by application of cation-exchange resins (Mulvihill and Ennis 2003). In addition to the conventional methods, several alternative methods are reported, such as use of ethanol, ultrafiltration with following cryo-destabilization, use of anionic polysaccharide, high-pressure CO_2 precipitation, electrodialysis coupled with mineral acid addition etc. (Bazinet, Lamarche et al. 1999; Mulvihill and Ennis 2003). Bazinet et al. (Bazinet, Lamarche et al. 1999) reported the successful application of an ecofriendly membrane technology for casein production. The proposed approach is a variant of isoelectric casein precipitation without any chemicals use by means of electrodialysis with bipolar membranes (EDBM). EDBM technology allows modification of pH via water dissociation at a bipolar membrane (BM) under the effect of an applied electric field resulting in the production of H^+ and OH^-. In the case of milk, electroacidification until pH=4.6 results in precipitation of casein with small ash content due to the additional milk demineralization during EDBM. In spite of the attractiveness of EDBM, precipitation of casein inside the stack and scaling on cation-exchange membrane

148

affect the process performance hampering industrial application of this technique (Bazinet, Lamarche et al. 1999). To answer this problematic, Balster et al. (Balster, Pünt et al. 2007) proposed a complex approach avoiding clogging of the EDBM stack by caseins. This approach consists of a classical chemical acidification (for the first batch) of milk in a precipitator followed by separation of casein from whey. The whey flux is further directs to the EDBM stack for demineralization and neutralization. The acid generated in the acidification compartment of EDBM is then used in the precipitator for further milk acidifications. Mier et al. (Mier, Ibañez et al. 2008) placed an on-line basket centrifuge allowing separation of whey from casein behind the EDBM cell and in front of the milk reservoir. In spite of promising results of above studies, the presence of scaling, organic fouling by whey proteins or by casein curd was reported.

In this work, we propose an alternative approach comprising an ultrafiltration module (UF) prior to the EDBM module, electroacidification at a higher pH value (5.0) and application of pulsed electric field (PEF). First of all, UF module would allow prevention of casein curd formation inside the EDBM stack due to the UF membrane cut-off. In fact, UF permeate containing no protein instead of milk is electroacidified in the EDBM stack and follows to the milk reservoir where isoelectric precipitation of caseins occurred (Fig.V.1). Secondly, electroacidification until pH 5.0 instead of 4.6 would allow decrease in scaling since part of Ca^{2+} (Mg^{2+}) scaling ions remain bonded with casein micelles (Walstra 1990) and free Ca^{2+} (Mg^{2+}) migrate substantially at pH lower than 5.0 due to the predominant migration of K^+ ions at higher pH values (Bazinet, Ippersiel et al. 2000). Thus, most part of scaling ions remains in the diluate compartment with acid medium which is unfavorable for scaling formation. Thirdly, the application of PEF to EDBM module would hamper the fouling and scaling formation. Indeed, recent studies reported the prevention of scaling (over 85 %) and protein fouling (up to 100 %) by application of PEF (Ruiz, Sistat et al. 2007; Cifuentes-Araya, Pourcelly et al. 2011; Mikhaylin, Nikonenko et al. 2014). Additional benefit of PEF is prevention of concentration polarization phenomena on ion-exchange membranes which leads to a better efficiency of ED treatment (Mishchuk, Koopal et al. 2001).

V.1.3 Experimental methods

V.1.3.1 Material

The raw material used in this study was a commercial fresh pasteurized and homogenized skim milk (Quebon, Naturel, Longueuil, Canada). NaCl and KCl (ACS grade) were obtained from Laboratoire MAT (Quebec, Canada).

V.1.3.2 Configuration of electrodialysis with bipolar membrane (EDBM) and ultrafiltration (UF) modules

The EDBM (Fig.V.1) module used was an MP type cell (100 cm^2 of effective surface) from ElectroCell Systems AB Company (Täby, Sweden). The cell consists of five compartments separated by two Neosepta AMX-SB anion-exchange membranes, one Neosepta CMX-SB cation-exchange membrane and one Neosepta BP-1 bipolar membrane: all membranes manufactured by (Tokuyama Soda Ltd., Tokyo, Japan). The three electrolytes: skim milk (EDBM) (2.5 L, 150 ml/min) or ultrafiltrated milk fraction (MUF) (EDBM-UF), 2 g/l KCl (500 ml, 150 ml/min) and 20 g/l NaCl (500 ml, 500 ml/min) were circulated using three centrifuge pumps. The anode, a dimensionally-stable electrode (DSA) and the cathode, a 316 stainless steel electrode, were supplied with the MP cell. The UF module (Fig.V.1) was equipped with a spiral wound membrane with a molecular weight cut-off of 10 kDa and a surface of 4200 cm^2 (GE Water and Process technologies, model PW1812T, Vista, USA). The UF system was run at a room temperature (22±1°C) under a pressure of 25 psi.
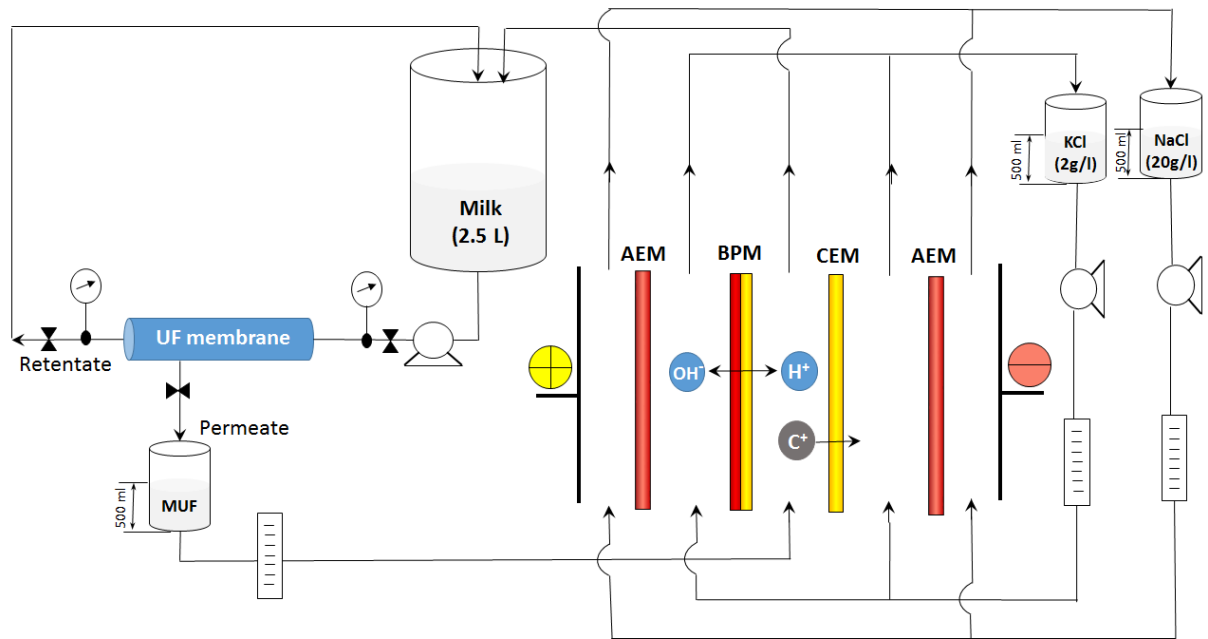
Fig.V.1: Configuration of EDBM-UF system coupling an electrodialysis with bipolar membrane (EDBM) module and an ultrafiltration (UF) module. C^+ are migrating cations.

V.1.3.3 Protocol

A scheme of different modes of EDBM tested and research questions to be answered are shown on Figure V.2. EDBM was carried out in batch process using a constant current density of 20 mA/cm^2 generated by a Xantrex power supply (Model HPD 60-5SX; Burnaby, Canada). The electroacidification was stopped after the pH reached 5.4 due to the high global system resistance. For EDBM-UF, the permeate from the UF module (MUF) passed directly to the EDBM cell and electroacidification was stopped when pH in the UF reservoir reached 4.6 or 5.0. These two pH values were chosen in order to evaluate the influence of pH of electroacidification on CMX-SB scaling. Additionally to continuous current mode of EDBM treatment, pulsed electric field (PEF) mode with pulse/pause lapses 2s/0.5s was tested to hamper the scaling formation. This pulse/pause duration was reported to be the optimal PEF mode allowing the best scaling inhibition among all PEF modes tested (Mikhaylin, Nikonenko et al. 2014). Three replicates of each mode were performed. During each treatment, 1.5 mL-samples of the acidified milk solution were taken at every 0.4 pH unit decrease. The time required to reach the final pH value, the anode/cathode voltage difference and the temperature were recorded as the treatment progressed. The

151

concentration of soluble protein was determined on the supernatants of freshly acidified 1.5 mL samples. After electroacidification, photographs of dismantled EDBM cell and CMX-SB membranes were taken. Membrane thickness, ash content, inductive coupled plasma analysis, scanning electron microscopy analysis, energy dispersive X-ray spectroscopy were carried out on CMX-SB in order to evaluate the quantity, structure and composition of membrane scaling.
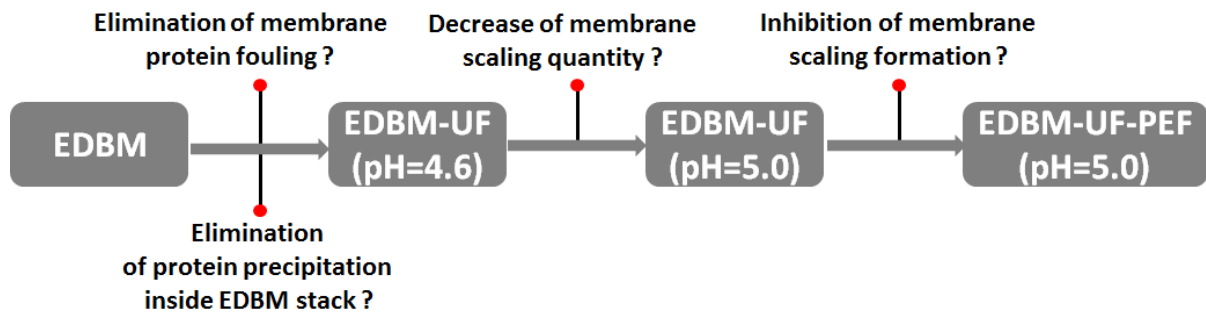
Fig.V.2: Scheme of different EDBM configurations tested and research questions to be answered.

V.1.3.4 <u>Analyses</u>

V.1.3.4.1 <u>Scanning electron microscopy (SEM) and Energy dispersive X-Ray spectroscopy (EDS)</u>

Images of the CEMs (dried under vacuum at 80 °C during 16 h) were taken with a scanning electron microscope JEOL (Japan Electro Optic Laboratory, model JSM840A, Peabody, Massachusetts, USA) equipped with an energy dispersive spectrometer (EDS) (Princeton Gamma Tech., Princeton, New Jersey, USA). The EDS conditions were 15 kV accelerating voltage with a 13-mm working distance. The samples were coated with a thin layer of gold/palladium in order to make them electrically conductive and to improve the quality of the microscopy photographs (Cifuentes-Araya, Pourcelly et al. 2011).

V.1.3.4.2 <u>Ash content</u>

The ash content of CMX-SB membranes was determined according to the AOAC method no. 945-46. Approximately 1.5 g of dried CMX-SB sample was added to the cooled crucibles, and the mass recorded. The sample was then ashed at 550 °C for 16 hours and weighed again when they reached room temperature.

V.1.3.4.3 <u>Cation concentration determination</u>

Magnesium, calcium, sodium and potassium concentrations were determined by Inductively Coupled Plasma (ICP-OES, Optima 4300, Dual view, Perkin-Elmer, Shelton, CT, USA). The wavelengths used for these elements were: 285.219, 317.933, 589.592 and 766.490 nm, respectively (Bazinet, Ippersiel et al. 2000). The cation analyses were carried out in radial view.

V.1.3.4.4 <u>Soluble protein determination</u>

The protein concentration determination was done using an FP-428 LECO apparatus (LECO Corporation, Saint Joseph, MI). The instrument was calibrated each time with ethylenediaminetetraacetic acid (EDTA) as a nitrogen standard (Bazinet, Lamarche et al. 1999).

V.1.3.4.5 <u>Statistical analyses</u>

The data of soluble protein content, ash content and ICP analyses were subjected to an analysis of variance using SAS software (SAS version 9.3, 2011). LCD and Waller-Duncan post-hoc tests were used.

V.4 <u>Results and discussion</u>

V.1.4.1 <u>Characterization of fouling</u>

V.4.1.1 <u>Casein fouling</u>

As expected during conventional EDBM of milk, casein precipitation inside the acidification compartment occurred (Fig.V.3a). This is in agreement with the work of Bazinet et al. (Bazinet, Lamarche et al. 1999) who reported the same precipitation effect. However, these authors used higher flow rates and modified spacers which allowed to continue the EDBM treatments until pH 4.0. In the present work, the relatively slow flow rate was applied in order to compare conventional EDBM and EDBM-UF where the maximum flow rate of the UF permeate was 150 ml/min. At this flow rate, EDBM treatment was stopped after pH in milk reservoir reached 5.4 due to complete clogging of acidification compartment (Fig.V.3a). Casein curd blocks spacers between membranes and hinders surface of CEM and BM making impossible to continue following acidification. Coupling of EDBM cell with ultrafiltration module seems to be a very promising solution. Indeed, Fig.V3 b. shows the absence of casein curd inside the EDBM stack at the end of electroacidification. In fact, the major protein fractions of milk including caseins and whey proteins were rejected by ultrafiltration membrane with cut-off of 10 kDa. Therefore, this coupling approach allows prevention of organic fouling caused either by caseins or by whey proteins.
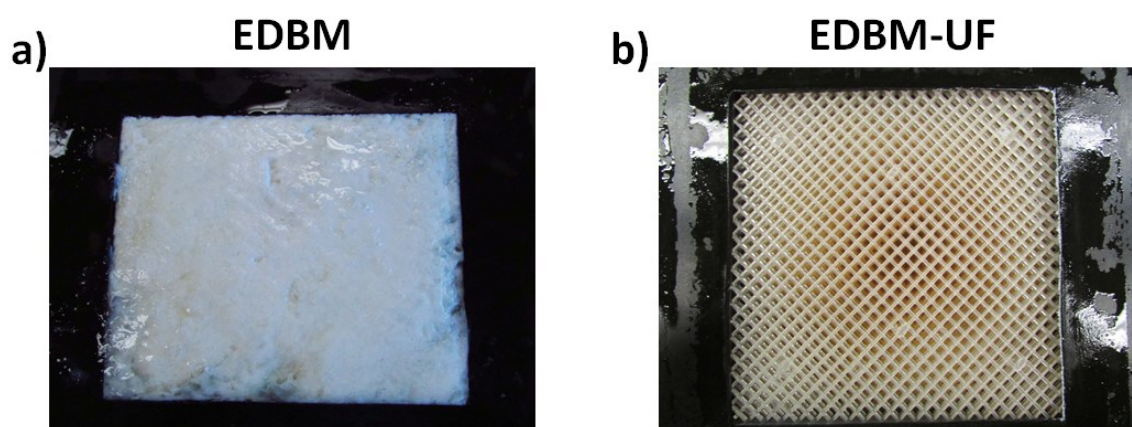
Fig.V.3: Photographs of spacers in the acidification compartment of EDBM: a) conventional EDBM, b) EDBM-UF.

V.4.1.2 <u>Scaling</u>

V.4.1.2.1 <u>Ash content and ICP analysis</u>

The lowest mineral content was observed for the CMX-SB treated by the conventional EDBM procedure (Fig.V.4a). However, in this condition electroacidification was performed just until pH=5.4 and it is well known, that at this pH part of Ca^{2+} ions still remains bonded with casein micelles (Walstra 1990). Moreover, until pH 5.0 K^+ ions migrate predominantly towards the alkaline compartment and most part of free Ca^{2+} and Mg^{2+} ions remains in the diluate compartment with acid medium, which is unfavorable for scaling formation (Bazinet, Ippersiel et al. 2000). Thereby, less scaling on CMX-SB is well expected and corroborates with data of ICP analysis presenting smaller concentration of Ca^{2+} and Mg^{2+} scaling ions for EDBM (pH=5.4) in comparison with other EDBM treatments (Fig.V.4b). Further, looking at ash and mineral contents after EDBM-UF at pH=4.6 when all Ca^{2+} and Mg^{2+} ions are completely liberated from the casein micelles, one can see a drastic increase of scaling quantity (Fig.V.4a and b). If EDBM-UF treatment is carried out until pH=5.0, there is a substantial decrease in membrane scaling which becomes even more pronounced with application of PEF. In the case of EDBM-UF-PEF at pH=5.0 the final ash content is close to the EDBM mode at pH=5.4. Additionally, the differences in scaling between EDBM-UF (pH=5.0) and EDBM-UF-PEF (pH=5.0) are mainly due to the lower content of Ca^{2+} ions under the PEF treatment with 2s/0.5s lapses (Fig.V.4b). This is in agreement with the study of Mikhaylin et al. (Mikhaylin et al. 2014) who reported the inhibition of scaling by Ca compounds at this specific PEF mode.

a)
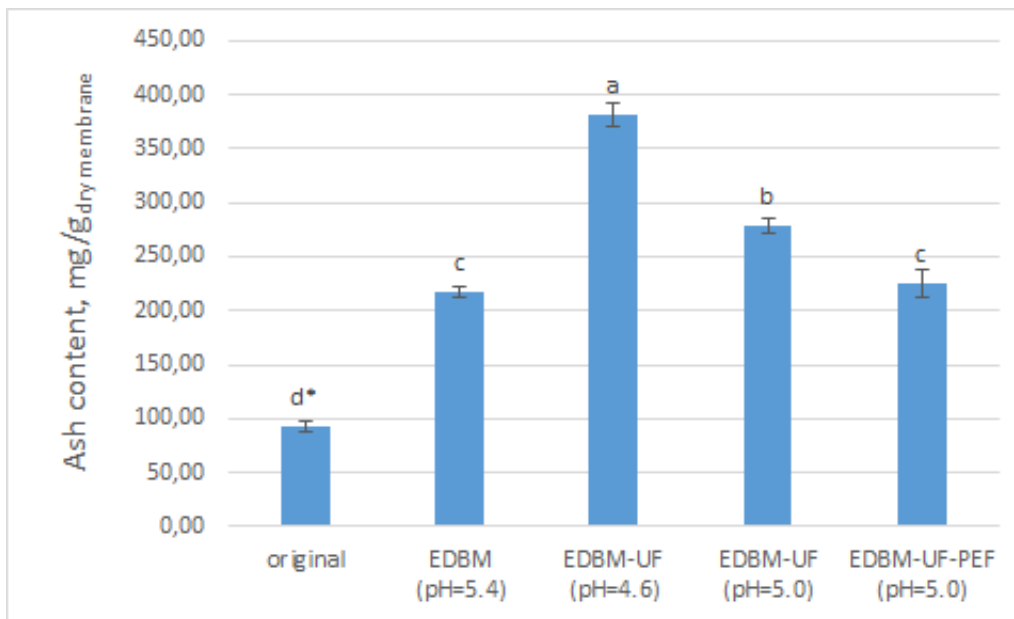
*- Bars followed by different letters are significantly different (p<0.05)

b)
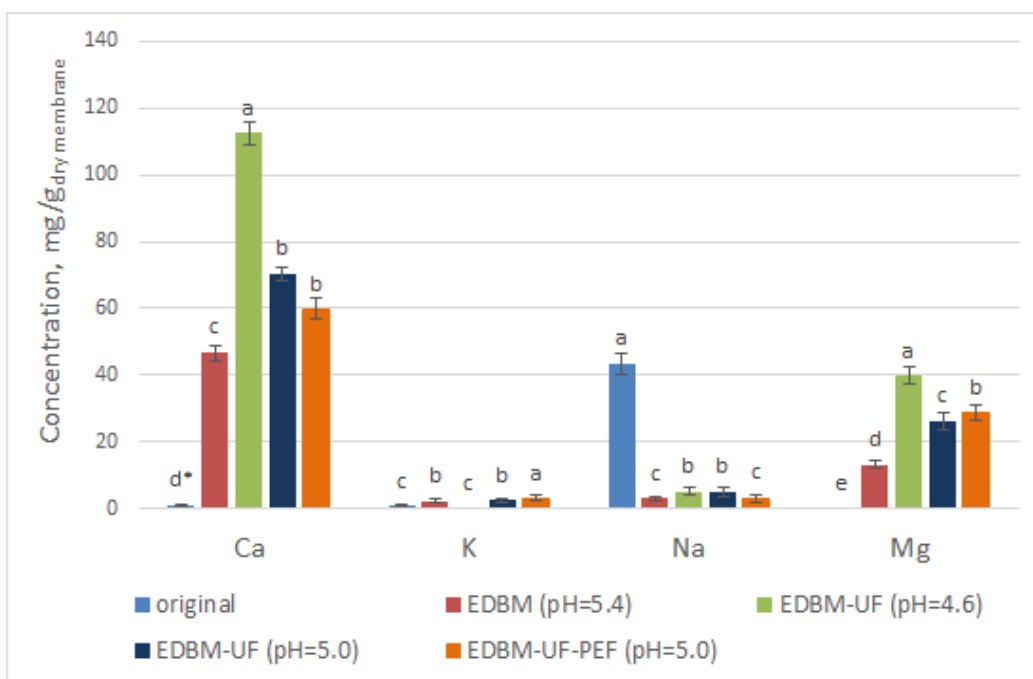
*- For each element, bars followed by different letters are significantly different (p<0.05)

Fig.V.4: a) ash content and b) ICP elemental analysis of original CMX-SB and CMX-SB after different EDBM treatments.

V.4.1.2.2 <u>Scanning electron microscopy (SEM) and Energy dispersive x-ray spectroscopy</u>
<u>(EDS)</u>

SEM and EDS images of nontreated CMX-SB (Fig.V.5) showed the plane membrane surface, which does not contain any scalant ions. However, after all EDBM modes CMX-SB surface was covered by Ca^{2+} and Mg^{2+} compounds (Fig.V.5 and V.6). This is in accordance with data of ICP analysis and works of Bazinet et al. (Bazinet, Montpetit et al. 2001) who reported that three types of CEM scaling after EDBM of skim milk are possible such as calcium carbonate and calcium and magnesium hydroxides. The concentrate side of CMX-SB after EDBM and EDBM-UF (pH=4.6) had a similar scaling structure comprising the scaling layer consisting of mixture of Ca^{2+} and Mg^{2+} compounds and big agglomerates consisting of Ca^{2+} compounds (Fig.V.5). The scaling layer and agglomerates do not correspond to the specific and well-known crystalline structure due to the influence of Mg^{2+} ions on the formation of Ca^{2+} crystals (Berner 1975; Zhang and Dawe 2000; Loste, Wilson et al. 2003; Chen, Neville et al. 2006). Mg^{2+} ions can incorporate into the amorphous phase of calcium compounds significantly retarding its transformation into crystalline phase or Mg^{2+} ions can be adsorbed onto the surface of calcite or portlandite crystals inhibiting their growth. When EDBM-UF treatment was stopped at pH 5.0, less Ca^{2+} ions were present in the MUF fraction in comparison with pH 4.6. This fact directly affects the scaling composition and structure. One can see the smaller peak of Ca on the EDS image and no big spherical agglomerates. Scaling for EDBM-UF (pH=5.0) mostly consists of relatively small crystals being presumably of portlandite nature (Rodriguez-Navarro, Hansen et al. 1998). Application of PEF leads to the decrease in Ca peak on the EDS. This is in accordance with above discussed ICP analyses and work of Mikhaylin et al. (Mikhaylin et al. 2014) who reported the inhibition of Ca^{2+} formation and growth at pulse/pause lapse 2s/0.5s. Additionally, on SEM image scaling is present in the form of amorphous layer without big agglomerates and crystalline structures, which confirms a positive effect of PEF on inhibition of scaling development.
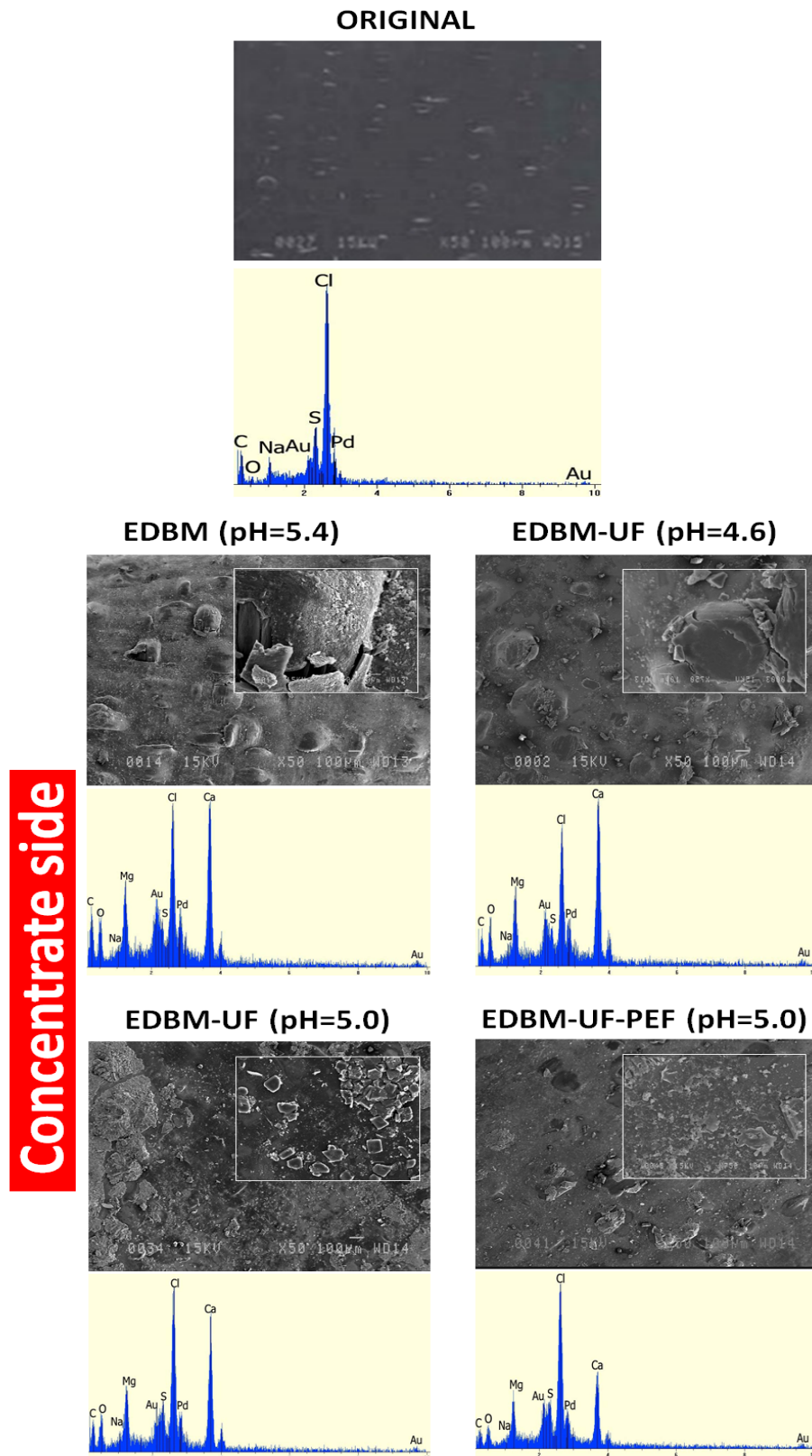
Fig.V.5: Scanning electron microscopy photographs and energy dispersive x-ray spectrograms of original non-treated CMX-SB membrane and the concentrate side of CMX-SB membrane after the different EDBM treatments.

Concerning diluate side directed to the acid stream, much less scaling was observed with predominance of Ca^{2+} compounds (Fig.V.6). Indeed, acid pH is unfavorable to the formation of Ca^{2+} and Mg^{2+} hydroxides due to a lack of OH^- ions and to calcium carbonate due to a shift of the balance from carbonate ions towards hydrocarbonate ions and then towards the carbonic acid (Nehrke 2007). However, with EDBM, EDBM-UF (pH=5.0) and EDBM-PEF modes, the CMX-SB diluate side was covered with crystals being of calcite nature and at EDBM-UF (pH=4.6) scaling consisted of calcium carbonate crystals with presence of amorphous calcium carbonate and/or hydroxide. The formation of calcium carbonate is induced by leakage of OH^- ions from the base compartment and possible water splitting phenomenon (Cifuentes-Araya, Pourcelly et al. 2012). Hydroxyl ions from base compartment or generated by water splitting deprotonate carbonic acid resulting in the production of carbonate ions, which are able to interact with Ca^{2+}. For EDBM-UF (pH=4.6) OH^- leakage seems to be severe, leading to a higher scaling content on diluate side among all EDBM modes. Severe OH^- leakage is due to the high scaling content on concentrate side, which blocked the positively charged ion-exchange sites decreasing membrane permselectivity (Bleha, Tishchenko et al. 1992). Oppositely, EDBM-UF-PUF mode shows just traces of scaling. This fact is due to the less scaling content observed on concentrate side with this mode in comparison to EDBM (pH=4.6) and to the effect of PEF, which inhibits scaling formation and decreases concentration polarization which means decrease of water splitting (Mikhaylin, Nikonenko et al. 2014).
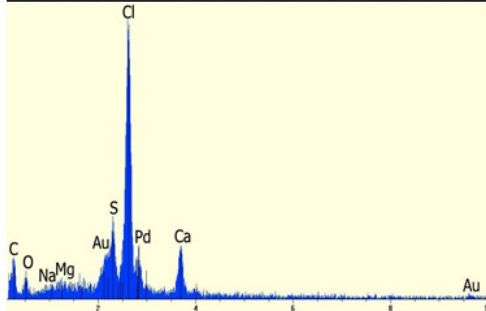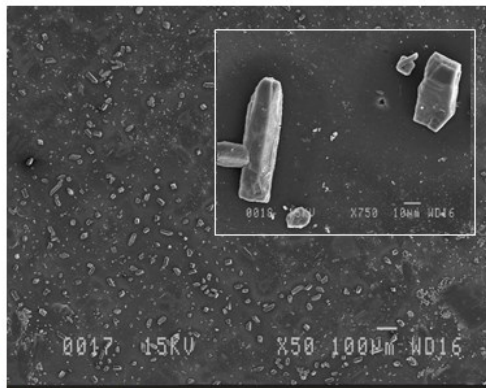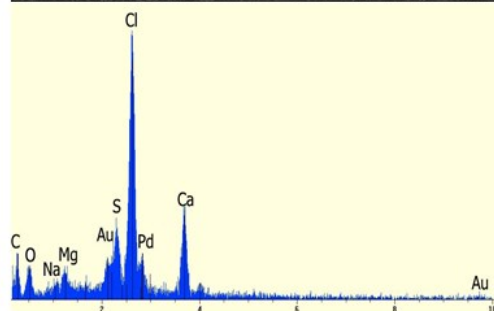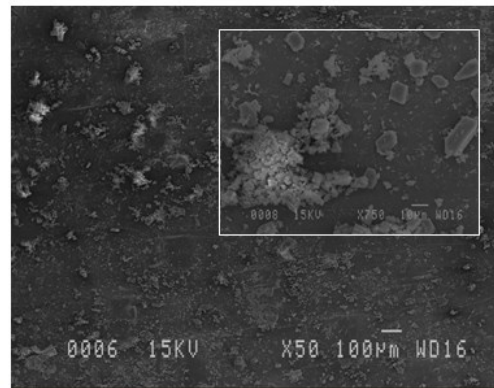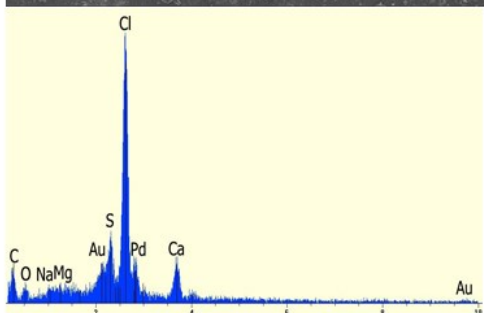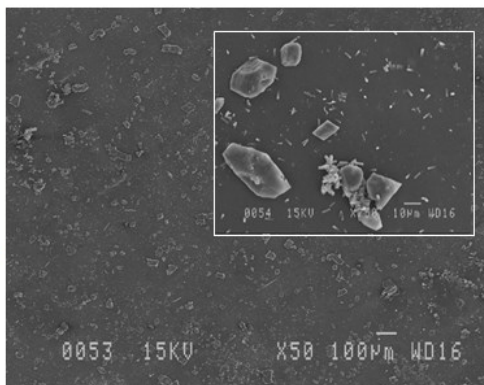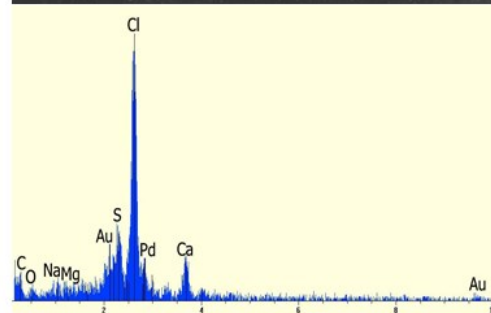
Fig.V.6: Scanning electron microscopy photographs and energy dispersive x-ray spectrograms of the diluate side of CMX-SB membrane after the different EDBM treatments.

V.1.4.2 Evolution of pH and global system resistance

The evolution of pH during EDBM treatment is different from all EDBM-UF treatments (Fig.V.7). When milk directly passes to the EDBM stack (conventional EDBM), it is possible to see the plateau region followed by a linear decrease of pH. However, when permeate from UF module (MUF) passes to the EDBM stack (EDBM-UF), there is no such a plateau. The delay in acidification during conventional EDBM treatment is related to the relatively low flow rate of skim milk and consequently relatively low circulation of H^+ produced at the bipolar membrane. Bazinet et al. (Bazinet, Lamarche et al. 1999) observed the same delay phenomenon. However, these authors report the disappearance in delay of acidification at increased flow rate due to the better mixing of H^+ and skim milk in the bulk reservoir. In the present work, application of UF module apparently allows better mixing of acidified recirculated permeate (MUF) and retentate. Hence, pH of milk during EDBM-UF decreases right after the beginning of electroacidification and no plateau was observed. It is worth to note, that the buffer capacity of skim milk retentate seems to be close to those in initial skim milk due to the low volumetric concentration factor (1.25:1) (Srilaorkul, Ozimek et al. 1989). Therefore, changes in buffer capacity, which may affect pH evolution of milk, may be neglected.

Comparing EDBM-UF treatments, the same trends in pH evolution were observed. However, application of PEF mode seems to be advantageous in comparison with continuous current mode. Indeed, after reaching 6.5, pH decreases more readily for EDBM-UF-PUF treatment and there is less amount of charge transported needed to reach the final pH value. This fact can be explained by two influences of PEF: 1) influence on BM performance and 2) influence on CEM performance. Firstly, the influence of PEF on BM performance seems to be rather minimal because H^+ generation depends on applied current and at the same number of charge transported the same amount of H^+ should be generated. However, additional investigations are needed for better comprehension of H^+/OH^- generation on BM under PEF. Secondly, the influence of PEF on CEM performance seems to be predominant because it is known that PEF decreases the concentration polarization (Mishchuk, Koopal et al. 2001; Nikonenko, Pismenskaya et al. 2010) and hampers membrane scaling (Cifuentes-Araya, Pourcelly et al. 2011; Mikhaylin, Nikonenko et al. 2014). Both above mentioned PEF effects prevent the migration of OH^- ions into the acid compartment. A decrease in concentration polarization by PEF means a decrease of OH^-

generated by water-splitting on the CEM surface directed to the acid stream. Consequently, inhibition of scaling by PEF helps to maintain the high value of CEM permselectivity and to decrease the OH$^-$ leakage from the base compartment (Cifuentes-Araya, Pourcelly et al. 2011). Thus, PEF mode, preventing OH$^-$ migration into the acid compartment, which leads to the neutralization of generated H$^+$, hastens the electroacidification of MUF in comparison with continuous current mode.
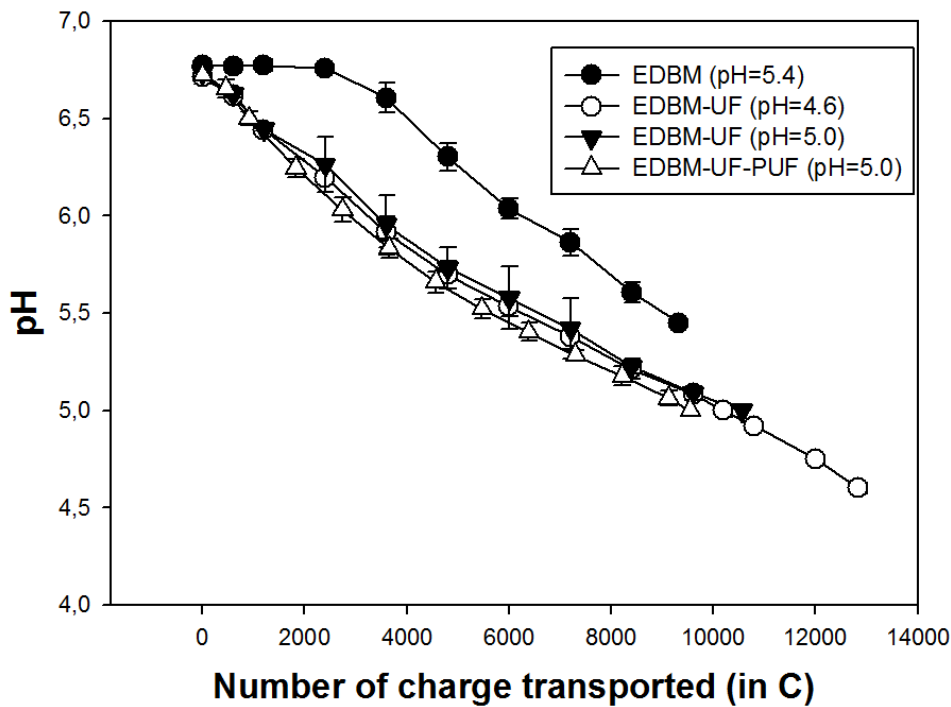
Fig.V.7: pH evolution during electroacidification at different EDBM modes.

The evolution of global system resistance has a similar trend at the beginning of all EDBM treatments. The decrease of system resistance during electroacidification was previously explained by Bazinet et al. (Bazinet, Lamarche et al. 1999). Generation of highly conductive H$^+$ ions and migration of cations across the CEM towards the compartment where OH$^-$ ions are produced at the BM induced the overall decrease in system resistance. The following increase of system resistance is due to the presence of fouling and/or scaling (Bazinet, Lamarche et al. 1999; Mier, Ibañez et al. 2008). In the case of conventional EDBM, the sharp increase in system resistance after a certain number of charges was transported is due to the casein precipitation inside the spacers of the EDBM stack (Fig.V.3). Comparing EDBM-UF treatments, one can see the higher system resistance when PEF is applied. This can be connected with a better demineralization of MUF under

162

PEF. Better demineralization means the loss of K^+, which are predominant ions electromigrating from the acid compartment at the beginning of electroacidification until certain pH. When the concentration of K^+ ions becomes too low, there is migration of others cations, which is not sufficient to counterbalance generated H^+ ions which leads to the electromigration of H^+ and decrease of the current efficiency of EDBM (Bazinet, Ippersiel et al. 2000) .
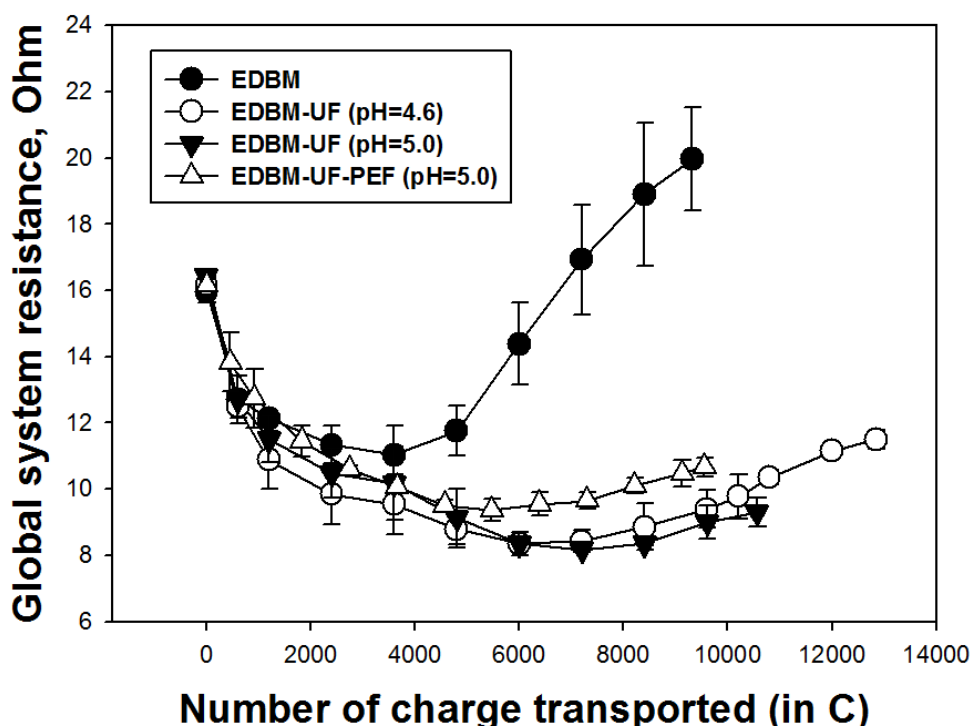
Fig.V.8: Global system resistance evolution during electroacidification in different EDBM modes.

V.1.4.3 Soluble protein content

Analysis of supernatants of electroacidified milk samples (Tab.V.1) shows that at pH 4.6 22.4 % of protein remain soluble. According to the literature, this protein fraction corresponds to the whey proteins, which represent around 20 % of total proteins (Bazinet, Lamarche et al. 1999; O'Mahony and Fox 2013). Thereby, the precipitated fraction, which is clearly visible (Fig.V.9), represents caseins. These results demonstrate the viability of EDBM-UF as a method for casein precipitation by electroacidification until pH 4.6. Furthermore, figure V.9 shows protein precipitation even at pH 5.0, which is confirmed by

LECO nitrogen analysis indicating just around 30 % of soluble proteins (Tab.V.1). Precipitation of more than 90 % of caseins at pH 5.0 can be explained by demineralization of milk in EDBM stack. The migration of salts leads to the decrease in ionic strength of milk solution, which affects the stability of casein micelles. Generally, casein micelles are considered as fluffy particles with a κ-casein on its surface (De Kruif and Holt 2003). This surface κ-casein is present in a form of salted polyelectrolyte brush stabilizing casein micelle. A change in ionic strength may lead to the collapse of polyelectrolyte brush and destabilization of casein micelle. Thereby, demineralization during EDBM decreases the ionic strength of milk solution leading to the easier destabilization of casein micelles and consequently to the shift of the isoelectric point of caseins via more alkaline pH. This is in agreement with results obtained by Bazinet et al. (Bazinet, Ippersiel et al. 2001) who observed the opposite salting-in effect when isoelectric point of caseins was shifted towards acid pH values by increase of milk ionic strength by salt addition.

Tab.V.1: Soluble protein content under different EDBM modes (%).

Mode/pH	6.8	6.2	5.8	5.4	5.0	4.6
EDBM	99.8±0.2[a]*	93.8±1.3[b]	88.1±1.6[c]	72.7±2.6[d]	-	-
EDBM-UF	99.8±0.3[a]	92.8±0.4[b]	90.3±5.0[b]	78.3±1.9[c]	31.0±0.1[d]	22.4±0.9[e]
EDBM-UF	99.8±0.2[a]	92.1±1.6[ba]	90.9±8.2[ba]	85.3±7.3[b]	33.9±3.6[c]	-
EDBM-UF-PEF	99.8±0.2[a]	92.0±7.6[ba]	90.1±9.2[b]	81.6±2.8[c]	29.4±2.5[d]	-

*- Mean values at the same line followed by different letters are significantly different (p<0.05).
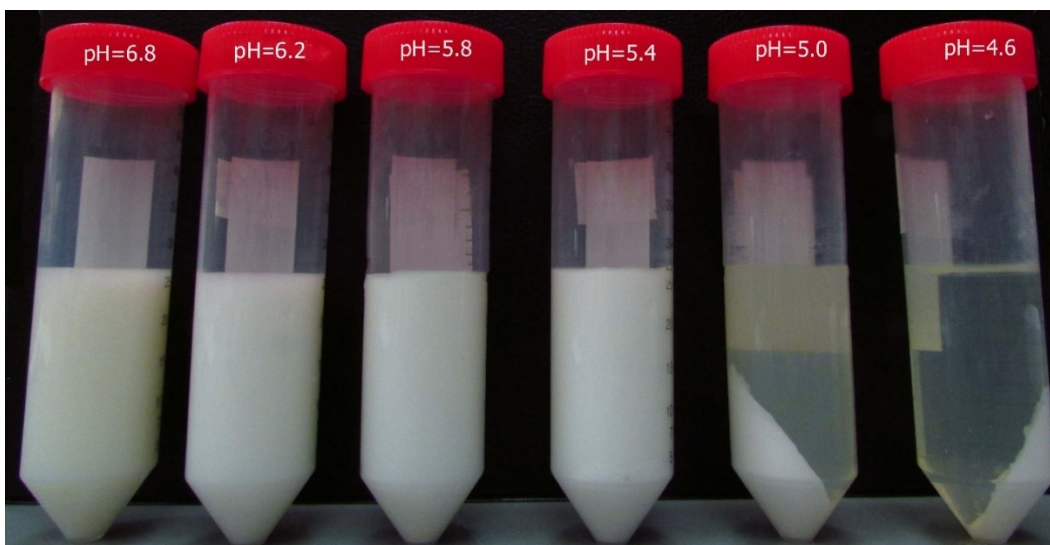
Fig.V.9: Skim milk after EDBM-UF treatment at different pH values.

164

V.5 <u>Conclusion</u>

Results obtained in this study demonstrate for the first time the effectiveness of a new approach for precipitation of caseins from bovine skim milk. This approach comprises application of electrodialysis with bipolar membranes coupling with ultrafiltration module (EDBM-UF). EDBM-UF allows casein production without use of chemicals and waste generation.

- ✓ The main advantage of the proposed approach is the complete inhibition of protein precipitation in the EDBM stack and at the surfaces of CEM and BM.

- ✓ Furthermore, it was found that more than 90 % of caseins are precipitated at pH 5.0, which is interesting in terms of scaling hampering. Indeed, at pH 5.0: 1) a part of calcium and magnesium is still present in a colloidal form binding with casein micelles which means less free Ca^{2+} (Mg^{2+}) ions migrating via the base compartment and less CEM scaling, 2) a substantial part of Ca^{2+} (Mg^{2+}) ions remain in the diluate solution due to the predominant migration of K^+ ions. This was confirmed by results of ash content and ICP analysis.

- ✓ Final step in the improvement of EDBM technique is the application of PEF (EDBM-UF-PEF). From the author's knowledge, the present work demonstrates for the first time application of PEF to EDBM. Indeed, PEF hampers the formation of scaling and prevents the leakage of OH^- ions from the base stream which leads to the better performance of EDBM treatment and to the longer membrane lifetime.

Further research will focus on the improvement of the UF module in order to obtain higher flow rate of permeate allowing a better performance of EDBM treatment. Moreover, the addition of KCl during treatment seems to perspective step allowing inhibition of Ca^{2+} (Mg^{2+}) migration and consecutively scaling inhibition.

Acknowledgements

CHAPTER VI. GENERAL CONCLUSION

VI.1 <u>Return to the objectives</u>

VI.1.1 <u>Short PEF modes: effectiveness against AEM and CEM scaling, influence on ED performance, mechanisms of action</u>

The first objective of the present work was to evaluate the suitability of short PEF modes (0.5s – 3s) in terms of scaling prevention, influences on development of CP and ED performance. Results of this objective demonstrate that short PEF modes allow avoiding AEM scaling and decreasing CEM scaling in comparison with longer PEF and continuous current modes. The optimal mode was 2s/0.5s among all modes tested and reported in literature. This mode showed less CEM scaling and better demineralization. Additionally, the feature of this PEF condition was a specific pH evolution. Indeed, at 2s/0.5s pH remained constant almost all duration of ED treatment while at other PEF modes pH increased during ED. There are two phenomena affecting pH evolution such as water splitting and OH^- leakage and at 2s/0.5s lapses both phenomena were hampered. Water splitting was hampered due to the presence of well-developed electroconvective vortices (during pulse lapse) and inertial vortices (during pause lapse). Electroconvective and inertial vortices facilitate the ionic transfer to the membrane surface shrinking the CP layer and inhibiting water splitting. Secondly, the prevention of OH^- leakage was due to the suppression of scaling by Ca^{2+} compounds at 2s/0.5s mode. Indeed, at this special mode scaling was composed of Mg^{2+} only while at all other PEF modes scaling was presented as a mixture of Ca^{2+} and Mg^{2+}. From literature it is known, that Mg^{2+} ions form preferably $Mg(OH)_2$ while Ca^{2+} ions form $CaCO_3$. $Mg(OH)_2$ can be formed by interaction of Mg^{2+} ions with OH^- and Mg^{2+} ions with H_2O with generation of H^+. Thus, Mg^{2+} and H^+ ions neutralize OH^- ions preventing leakage.

VI.1.2 Intrinsic properties of CEM: influence on scaling (composition, structure and quantity), development of electroconvection and ED performance

The aim of the second objective was to study the influence of intrinsic membrane properties and electroconvection on scaling phenomenon and ED performance. It is known that physico-chemical membrane properties and electroconvection affect development of CP however, there is no information about the influence on scaling formation. Thereby, this study subjected two parts: 1) characterization of physico-chemical membrane properties and following characterization of electrochemical properties (particularly the development of electroconvection) and 2) ED treatment at two PEF modes (2s/0.5s and 2s/0.67s) with solution containing scaling agents.

This study focused only on CEM since at short PEF AEM does not contain scaling. Thus, two CEM lots with different physico-chemical properties were chosen. Concerning scaling quantity and ED performance, results showed that the CEM lot with well-developed electroconvective vortices and suppressed water splitting was substantially less scaled in comparison with CEM with poorly-developed electroconvective vortices and quite developed water splitting. Thereby, less scaled sample showed higher demineralization rate (around 80 %) and less energy consumption (7.5 Wh) than the more scaled one with smaller demineralization rate (around 60 %) and higher energy consumption (9.5 Wh). The development of electroconvection was different due to the differences in surface properties: one membrane lot had a higher degree of surface hydrophobicity and heterogeneity in comparison with the other one. Hydrophobic and heterogeneous surface more easily brings in motion charged solution facilitating formation of electroconvective vortices. Thus, well-developed electroconvection seems to be advantageous due to the facilitation of ionic transfer (i.e. suppression of water splitting and increasing current efficiency) and due to the suppression of scaling formation contributing to the better ED performance.

The next aspect of this study is the influence of PEF. The mechanism of PEF action was present and included two aspects:

- PEF influence on scaling,
- PEF influence on vortices.

Firstly, it was hypothesized that PEF might hamper: 1) formation of bounds between membrane ion-exchange groups and scaling ions, 2) scaling growth and 3) formation of multilayer scaling. Secondly, pulse/pause duration affects the development of electroconvective vortices (existing during the pulse lapse) and inertial vortices (remaining during the pause lapse). Results demonstrate that at 2s/0.5s there were less scaling and better ED performance in comparison with 2s/0.67s. That may indicate that at pause lapse of 0.5s inertial vortices act quite well while pause lapse of 0.67 is quite long for the action of inertial vortices i.e. they are really small or even dissipated. The very recent studies of Uzdenova et al. (Uzdenova, Kovalenko et al. 2015) showed that the lifetime of inertial vortices after turning-off the current is several tenth of seconds which corroborates with our investigations. However, it is worth to note that authors used a simple solution consisting of 0.01M and in the case of complex solution, as used in the present study, the lifetime of inertial vortices may be quite different.

Finally, it was established that physico-chemical properties of IEMs affect scaling composition. Indeed, different scaling composition on concentrate sides of two CEM lots was observed. The concentrate side of one lot was composed of $Ca(OH)_2$ while the concentrate side of another one was composed of $Mg(OH)_2$. This fact is due to the influence of inner membrane structure on competitive migration of Mg^{2+} and Ca^{2+} ions. Membrane can be represented as a net of hydrophilic nanochannels confined in the hydrophobic matrix. It is known, that ion-exchange capacity and water uptake are one of the major parameters determining the dimension of nanochannels, i.e. less ion-exchange capacity and water uptake mean narrower nanochannels. In the case of the present study, K^+ and Na^+ migrate relatively easy via nanochannels in comparison with Ca^{2+} and Mg^{2+}. Indeed, Ca^{2+} and Mg^{2+} ions move relatively slow through the CEM in comparison with monovalent ions due to the larger hydration shell and strong affinity to ion-exchange groups and Mg^{2+} moves slower among all four ions. Thus, narrow nanochannels can play the role of obstacle hampering migration of Mg^{2+}. That is why, the concentrate side of CEM lot with relatively narrow nanochannels and inhibited migration of Mg^{2+} consisted of $Ca(OH)_2$ while concentrate side of CEM lot with larger nanochannels and relatively easy migrating Mg^{2+} consisted of $Mg(OH)_2$.

VI.1.3 Application of PEF during isoelectric casein precipitation by means of EDBM of skim milk: studies of membrane scaling and process performance

The aim of this objective was to apply the knowledge of positive action of PEF gained during accomplishment of the previous objectives to a real food process. The EDBM of skim milk for production of caseins (major milk proteins) was chosen due to the similar problem of CEM scaling, which was discussed in a previous research. In spite of the similarity in scaling problematic, there are differences between the EDBM system from the ED system studied before and the major ones are presence of bipolar membrane and complexity of milk solution. Firstly, from author's knowledge, the application of PEF to the system with bipolar membrane was never studied before and this work aimed to evaluate the viability of such application. Secondly, milk is a complex solution containing number of constituents, which interact with scaling ions, which can definitely affect the scaling formation. Furthermore, another lock of EDBM of skim milk, apart from CEM scaling, is EDBM stack clogging by caseins during electroacidification. Thus, before testing the influence of PEF it is necessary to avoid the EDBM stack clogging by caseins, which was done by application of an ultrafiltration module prior to the EDBM module.

Ultrafiltration, one of the pressure-driven membrane processes, is known to be a good pretreatment technique prior to ED. The mechanism of UF action is based on separation of molecules according to their size (molecular mass), i.e. molecules having size larger than the membrane pores are retained while molecules, which are smaller than the membrane pores, pass through. Results of the present work showed the effectiveness of EDBM-UF approach to prevent EDBM stack clogging. Indeed, EDBM-UF approach showed no casein precipitates inside the stack spacers and near the membranes due to the casein retention by UF membrane with cut-off of 10kDa.

Further, prior to testing the application of PEF, the influence of pH of electroacidification (4.6 vs 5.0) on CEM scaling was evaluated. Results demonstrated the substantial decrease in CEM scaling when EDBM treatment was stopped at pH 5.0 in comparison with conventional isoelectric acidification until pH 4.6. This fact is related to two phenomena. First of all, at pH 5.0 part of the scaling agents (Ca^{2+} and Mg^{2+}) is still bonded with casein micelles thus do not participate in the scaling build-up process. Secondly, it is known from literature, that there is competitive migration of cations during

milk electroacidification and until pH 5.0, the K^+ ions migrate predominantly. Thereby, most part of free Ca^{2+} and Mg^{2+} ions remains on the diluate side of CEM, which is unfavorable for scaling formation due to the acid pH. The accomplishment of ED treatment until pH 5.0 is possible since more than 90 % of caseins are already precipitated at this pH.

Finally, PEF mode was compared with continuous current mode during EDBM of skim milk until pH 5.0. Two positive influences of PEF were revealed. Firstly, as was expected, PEF hampered the formation of CEM scaling. Indeed, there was less scaling on concentrate side of CEM and traces of scaling on diluate side of CEM. Secondly, electroacidification of skim milk occurred more readily under the action of PEF in comparison with dc current. This might be due to the influence of PEF treatment on H^+/OH^- generation by BM or on water splitting and OH^- leakage occurring on CEM. The influence of PEF on performance of BM seems to be rather small since H^+/OH^- generation depends on the quantity of applied current, i.e. the same amount of H^+/OH^- ions should be generated at the same number of charge transported. However, additional studies should be provided to verify the influence of PEF on H^+/OH^- generation by BM. The influence of PEF field on water splitting and OH^- leakage occurring on CEM is now well studied. Indeed, results from previous objectives and literature corroborate the fact that PEF hampers water splitting and OH^- leakage. Thereby, if two above-mentioned phenomena are inhibited, there is less OH^- ions pass towards the acid compartment neutralizing H^+ generated by BM. Hence, more readily milk acidification should be well expected.

VI.2 <u>Conclusion</u>

From results of the present work, it is possible to conclude that application of short pulse/pause modes is an effective solution against membrane scaling during ED of model salt solutions containing high concentration of Ca^{2+} and Mg^{2+} ions and during EDBM of bovine skim milk. Indeed, short PEF modes completely eliminate scaling on AEM and substantially inhibit scaling on CEM. Thus, the use of PEF modes with short pulse/pause lapses instead of PEF modes with long pulse/pause lapses and continuous current mode leads to better ED performance and longer lifetime of IEMs all contributing to better economics of the ED process. The optimal PEF mode among all those tested in this work and those reported in literature was 2s/0.5s with less scaling and better demineralization.

171

Several mechanisms of PEF action were discussed in this study and two main directions of PEF influence were emphasized: 1) influence on CP phenomenon (particularly development of water splitting and electroconvection); 2) influence on scaling structure, composition and quantity. Moreover, it was established that differences in intrinsic properties of IEMs might lead to substantial differences in scaling nature and quantity as well as in development of CP phenomenon. Furthermore, the new EDBM-UF-PEF approach proposed was demonstrated to be effective in prevention of two types of fouling such as fouling by caseins and scaling. Moreover, application of PEF to EDBM, which was carried out for the first time, allowed more readily electroacidification of skim milk in comparison with continuous current.

Finally, author anticipates that the results of this project would encourage scientists to deepen the insight of the ED process under the action of PEF and companies to apply PEF modes to ED modules for the intensification of ED treatment.

VI.3 **Perspectives**

This project revealed the feasibility of using short PEF modes to solve the scaling problem and to improve the ED performance. 2s/0.5s reported as an optimal PEF condition with no AEM scaling and low CEM scaling. Further investigations should be accomplished to verify the reasonability of using the short PEF modes for prevention of other fouling types such as organic fouling, colloidal fouling and biofouling since usually solutions treated by ED are the mixtures from different fouling agents.

Number of mechanisms acting under PEF were discussed and the importance of electroconvection in scaling prevention and improvement of ED performance was emphasized. However, further investigation in this direction should be accomplished to deepen the gained insight about the action of electroconvective vortices in solutions containing scaling agents.

The influence of intrinsic membrane properties on scaling structure, composition and quantity as well as on the development of CP phenomena (water splitting and electroconvection) was demonstrated. Further investigations comparing different membrane structures (e.g. homogeneous vs heterogeneous IEMs) should be performed to

evaluate the scaling phenomenon under the action of PEF since a wide spectrum of different IEMs is currently used in modern industries.

A new EDBM-UF-PEF technique was proposed to produce caseins from skim milk. Application of UF model prior EDBM stack allows complete elimination of EDBM stack clogging. Further, use of PEF mode allows the decrease of CEM scaling and more readily electroacidification in comparison with dc current mode. However, the permeate flow rate from UF module was relatively small and with higher flow rate of permeate, better efficiency of EDBM treatment is expected. Thus, UF membrane with larger membrane surface membrane may be used to obtain higher permeate flow.

Studies of the competitive migration of different ionic species revealed the predominant migration of K^+ in comparison with Ca^{2+} and Mg^{2+}. This fact leads to the lower scaling on the concentrate side of CEM during EDBM-UF. Thus, it might be interesting to evaluate if addition of KCl may better hamper the scaling formation.

REFERENCES

NEOSEPTA Ion-Exchange Membranes (catalog). Tokyo, Tokuyama Soda Co. Ltd. (1972).

GOST-17552-72. Ion-exchange membranes. Techniques to meter the total and equilibrium exchange capacity., Izdatelstvo standartov

Aimar, P. and P. Bacchin (2010). "Slow colloidal aggregation and membrane fouling." Journal of Membrane Science **360**(1–2): 70-76.

Alibhai, Z., M. Mondor, et al. (2006). "Production of soy protein concentrates/isolates: traditional and membrane technologies." Desalination **191**(1–3): 351-358.

Amiot, J., F. Fournier, et al. (2002). Composition, propriétés physicochimiques, valeur nutritive, qualité technologique et technique d'analyse du lait. Montréal, Presses internationales Polytechnique.

Araya-Farias, M. and L. Bazinet (2006). "Electrodialysis of calcium and carbonate high-concentration solutions and impact on membrane fouling." Desalination **200**(1–3): 624.

Arcella, V., A. Ghielmi, et al. (2003). "High Performance Perfluoropolymer Films and Membranes." Annals of the New York Academy of Sciences **984**(1): 226-244.

Astrup, A. and N. R. W. Geiker (2014). "Efficacy of higher protein diets for long-term weight control. How to assess quality of randomized controlled trials?" Nutrition, Metabolism and Cardiovascular Diseases **24**(3): 220-223.

Audinos, R. (1989). "Fouling of ion-selective membranes during electrodialysis of grape must." Journal of Membrane Science **41**(0): 115-126.

Ayala-Bribiesca, E., M. Araya-Farias, et al. (2006). "Effect of concentrate solution pH and mineral composition of a whey protein diluate solution on membrane fouling formation during conventional electrodialysis." Journal of Membrane Science **280**(1–2): 790-801.

Ayala-Bribiesca, E., G. Pourcelly, et al. (2007). "Nature identification and morphology characterization of anion-exchange membrane fouling during conventional electrodialysis." Journal of Colloid and Interface Science **308**(1): 182-190.

Bacchin, P., P. Aimar, et al. (1995). "Model for colloidal fouling of membranes." AIChE Journal **41**(2): 368-376.

Baker, J. S. and L. Y. Dudley (1998). "Biofouling in membrane systems — A review." Desalination **118**(1–3): 81-89.

Baker, R. W. (2012). Ion Exchange Membrane Processes – Electrodialysis. Membrane Technology and Applications, John Wiley & Sons, Ltd**:** 417-451.

Balster, J., I. Pünt, et al. (2007). "Electrochemical acidification of milk by whey desalination." Journal of Membrane Science **303**(1–2): 213-220.

Balster, J., D. F. Stamatialis, et al. (2009). "Towards spacer free electrodialysis." Journal of Membrane Science **341**(1–2): 131-138.

Balster, J., M. H. Yildirim, et al. (2007). "Morphology and Microtopology of Cation-Exchange Polymers and the Origin of the Overlimiting Current." The Journal of Physical Chemistry B **111**(9): 2152-2165.

Banasiak, L. J. and A. I. Schäfer (2009). "Removal of boron, fluoride and nitrate by electrodialysis in the presence of organic matter." Journal of Membrane Science **334**(1–2): 101-109.

Banasiak, L. J. and A. I. Schäfer (2010). "Sorption of steroidal hormones by electrodialysis membranes." Journal of Membrane Science **365**(1–2): 198-205.

Banasiak, L. J., B. Van der Bruggen, et al. (2011). "Sorption of pesticide endosulfan by electrodialysis membranes." Chemical Engineering Journal **166**(1): 233-239.

Band, M., M. Gutman, et al. (1997). "Influence of specially modulated ultrasound on the water desalination process with ion-exchange hollow fibers." Desalination **109**(3): 303-313.

Barrett, R. A. and S. A. Parsons (1998). "The influence of magnetic fields on calcium carbonate precipitation." Water Research **32**(3): 609-612.

Bauer, B., F. J. Gerner, et al. (1988). "Development of bipolar membranes." Desalination **68**(2–3): 279-292.

Bazinet, L. (2005). "Electrodialytic Phenomena and Their Applications in the Dairy Industry: A Review." Critical Reviews in Food Science and Nutrition **44**(7-8): 525-544.

Bazinet, L. and M. Araya-Farias (2005). "Electrodialysis of calcium and carbonate high concentration solutions and impact on composition in cations of membrane fouling." Journal of Colloid and Interface Science **286**(2): 639-646.

Bazinet, L. and F. Castaigne (2011). Concepts de génie alimentaire : procédés associés et applications à la conservation des aliments. Paris, Tec et Doc.

Bazinet, L. and L. Firdaous (2011). "Recent Patented Applications of Ion-Exchange Membranes in the Agrifood Sector." Recent Patents on Chemical Engineering **4**(2): 207-216.

Bazinet, L., D. Ippersiel, et al. (2000). "Cationic balance in skim milk during bipolar membrane electroacidification." Journal of Membrane Science **173**(2): 201-209.

Bazinet, L., D. Ippersiel, et al. (2001). "Effect of added salt and increase in ionic strength on skim milk electroacidification performances." Journal of Dairy Research **68**(02): 237-250.

Bazinet, L., D. Ippersiel, et al. (2000). "Effect of membrane permselectivity on the fouling of cationic membranes during skim milk electroacidification." Journal of Membrane Science **174**(1): 97-110.

Bazinet, L., F. Lamarche, et al. (1998). "Bipolar-membrane electrodialysis: Applications of electrodialysis in the food industry." Trends in Food Science & Technology **9**(3): 107-113.

Bazinet, L., F. Lamarche, et al. (1999). "Bipolar Membrane Electroacidification To Produce Bovine Milk Casein Isolate." Journal of Agricultural and Food Chemistry **47**(12): 5291-5296.

Bazinet, L., D. Montpetit, et al. (2001). "Identification of Skim Milk Electroacidification Fouling: A Microscopic Approach." Journal of Colloid and Interface Science **237**(1): 62-69.

Belaid, N. N., B. Ngom, et al. (1999). "Conductivité membranaire: interprétation et exploitation selon le modèle à solution interstitielle hétérogène." European Polymer Journal **35**(5): 879-897.

Belashova, E. D., N. A. Melnik, et al. (2012). "Overlimiting mass transfer through cation-exchange membranes modified by Nafion film and carbon nanotubes." Electrochimica Acta **59**(0): 412-423.

Belova, E. I., G. Y. Lopatkova, et al. (2006). "Effect of Anion-exchange Membrane Surface Properties on Mechanisms of Overlimiting Mass Transfer." The Journal of Physical Chemistry B **110**(27): 13458-13469.

Berezina, N., N. Gnusin, et al. (1994). "Water electrotransport in membrane systems. Experiment and model description." Journal of Membrane Science **86**(3): 207-229.

Berezina, N. P. and E. N. Komkova (2003). "A Comparative Study of the Electric Transport of Ions and Water in Sulfonated Cation-Exchange Polymeric Membranes of the New Generation." Colloid Journal **65**(1): 1-10.

Berezina, N. P., N. A. Kononenko, et al. (2008). "Characterization of ion-exchange membrane materials: Properties vs structure." Advances in Colloid and Interface Science **139**(1–2): 3-28.

Berner, R. A. (1975). "The role of magnesium in the crystal growth of calcite and aragonite from sea water." Geochimica et Cosmochimica Acta **39**(4): 489-504.

Blavadze, E. M. B., O.V. Kulintsov, P.I. (1988). "Concentration Polarisation in the Electrodialysis Process and the Polarisation Characteristics of Ion-selective Membranes." Russian Chemical Reviews **57**(6): 585-591.

Bleha, M., G. Tishchenko, et al. (1992). "Characteristic of the critical state of membranes in ED-desalination of milk whey." Desalination **86**(2): 173-186.

Bobreshova, O. V., P. J. Kulintsov, et al. (1990). "Non-equilibrium processes in the concentration-polarization layers at the membrane/solution interface." Journal of Membrane Science **48**(2–3): 221-230.

Bobreshova, O. V. L., T.E. Shatalov, A.Y. (1980). "Sediment formation on the surface of the membrane MA-40 during electrodialysis of solutions containing ions of Ca^{2+}, CO_3^{2-} and SO_4^{2-}." Russian Journal of Applied Chemistry **53**(3): 665-667.

Boyaval, P., C. Corre, et al. (1987). "Continuous lactic acid fermentation with concentrated product recovery by ultrafiltration and electrodialysis." Biotechnology Letters **9**(3): 207-212.

Brastad, K. S. and Z. He (2013). "Water softening using microbial desalination cell technology." Desalination **309**: 32-37.

Brečević, L. and A. E. Nielsen (1989). "Solubility of amorphous calcium carbonate." Journal of Crystal Growth **98**(3): 504-510.

Bribes, J. L., M. El Boukari, et al. (1991). "Application of Raman spectroscopy to industrial membranes. Part 2–Perfluorosulphonic membrane." Journal of Raman Spectroscopy **22**(5): 275-279.

Bruinsma, R. and S. Alexander (1990). "Theory of electrohydrodynamic instabilities in electrolytic cells." The Journal of Chemical Physics **92**(5): 3074-3085.

Bucher, M. and T. L. Porter (1986). "Analysis of the Born model for hydration of ions." The Journal of Physical Chemistry **90**(15): 3406-3411.

Bukhovets, A., T. Eliseeva, et al. (2011). "The influence of current density on the electrochemical properties of anion-exchange membranes in electrodialysis of phenylalanine solution." Electrochimica Acta **56**(27): 10283-10287.

Bukhovets, A., T. Eliseeva, et al. (2010). "Fouling of anion-exchange membranes in electrodialysis of aromatic amino acid solution." Journal of Membrane Science **364**(1–2): 339-343.

Calle, E. V., J. Ruales, et al. (2002). "Deacidification of the clarified passion fruit juice (P. edulis f. flavicarpa)." Desalination **149**(1–3): 357-361.

Casademont, C., M. Araya-Farias, et al. (2008). "Impact of electrodialytic parameters on cation migration kinetics and fouling nature of ion-exchange membranes during treatment of solutions with different magnesium/calcium ratios." Journal of Membrane Science **325**(2): 570-579.

Casademont, C., G. Pourcelly, et al. (2007). "Effect of magnesium/calcium ratio in solutions subjected to electrodialysis: Characterization of cation-exchange membrane fouling." Journal of Colloid and Interface Science **315**(2): 544-554.

Casademont, C., G. Pourcelly, et al. (2008). "Effect of magnesium/calcium ratios in solutions treated by electrodialysis: Morphological characterization and identification of anion-exchange membrane fouling." Journal of Colloid and Interface Science **322**(1): 215-223.

Casademont, C., G. r. Pourcelly, et al. (2009). "Bilayered Self-Oriented Membrane Fouling and Impact of Magnesium on CaCO3 Formation during Consecutive Electrodialysis Treatments." Langmuir **26**(2): 854-859.

Casademont, C., P. Sistat, et al. (2009). "Electrodialysis of model salt solution containing whey proteins: Enhancement by pulsed electric field and modified cell configuration." Journal of Membrane Science **328**(1–2): 238-245.

Chang, D. I., K. H. Choo, et al. (2009). "Foulant identification and fouling control with iron oxide adsorption in electrodialysis for the desalination of secondary effluent." Desalination **236**(1–3): 152-159.

Chao, Y.-M. and T. M. Liang (2008). "A feasibility study of industrial wastewater recovery using electrodialysis reversal." Desalination **221**(1–3): 433-439.

Chapman, D. L. (1913). "Contribution to the theory of electrocapillarity." Philosophical Magazine Series 6 **25**(148): 475-481.

Chen, Q., C. Xue, et al. (2014). "Green Production of Ultrahigh-Basicity Polyaluminum Salts with Maximum Atomic Economy by Ultrafiltration and Electrodialysis with Bipolar Membranes." Industrial & Engineering Chemistry Research **53**(34): 13467-13474.

Chen, T., A. Neville, et al. (2006). "Influence of on formation—bulk precipitation and surface deposition." Chemical Engineering Science **61**(16): 5318-5327.

Choi, J.-H., S.-H. Kim, et al. (2001). "Heterogeneity of Ion-Exchange Membranes: The Effects of Membrane Heterogeneity on Transport Properties." Journal of Colloid and Interface Science **241**(1): 120-126.

Choi, M.-J., K.-J. Chae, et al. (2011). "Effects of biofouling on ion transport through cation exchange membranes and microbial fuel cell performance." Bioresource Technology **102**(1): 298-303.

Choi, S.-H., Y. Han Jeong, et al. (2001). "Desalination by electrodialysis with the ion-exchange membrane prepared by radiation-induced graft polymerization." Radiation Physics and Chemistry **60**(4–5): 503-511.

Choi, S. Y., J. W. Yu, et al. (2013). "Electrodialysis for desalination of brackish groundwater in coastal areas of Korea." Desalination and Water Treatment **51**(31-33): 6230-6237.

Cifuentes-Araya, N., C. Astudillo-Castro, et al. (2014). "Mechanisms of mineral membrane fouling growth modulated by pulsed modes of current during electrodialysis: Evidences of water splitting implications in the appearance of the amorphous phases of magnesium hydroxide and calcium carbonate." Journal of Colloid and Interface Science **426**(0): 221-234.

Cifuentes-Araya, N., G. Pourcelly, et al. (2011). "Impact of pulsed electric field on electrodialysis process performance and membrane fouling during consecutive demineralization of a model salt solution containing a high magnesium/calcium ratio." Journal of Colloid and Interface Science **361**(1): 79-89.

Cifuentes-Araya, N., G. Pourcelly, et al. (2012). "Multistep mineral fouling growth on a cation-exchange membrane ruled by gradual sieving effects of magnesium and carbonate ions and its delay by pulsed modes of electrodialysis." Journal of Colloid and Interface Science **372**(1): 217-230.

Cifuentes-Araya, N., G. Pourcelly, et al. (2013). "How pulse modes affect proton-barriers and anion-exchange membrane mineral fouling during consecutive electrodialysis treatments." Journal of Colloid and Interface Science **392**(0): 396-406.

Cifuentes-Araya, N., G. Pourcelly, et al. (2013). "Water splitting proton-barriers for mineral membrane fouling control and their optimization by accurate pulsed modes of electrodialysis." Journal of Membrane Science **447**(0): 433-441.

Clifton, P. M., D. Condo, et al. (2014). "Long term weight maintenance after advice to consume low carbohydrate, higher protein diets – A systematic review and meta analysis." Nutrition, Metabolism and Cardiovascular Diseases **24**(3): 224-235.

Cohen, R. D. and R. F. Probstein (1986). "Colloidal fouling of reverse osmosis membranes." Journal of Colloid and Interface Science **114**(1): 194-207.

Cooke, B. A. (1961). "Concentration polarization in electrodialysis—I. The electrometric measurement of interfacial concentration." Electrochimica Acta **3**(4): 307-317.

Cowan, D. A. and J. H. Brown (1959). "Effect of Turbulence on Limiting Current in Electrodialysis Cells." Ind. Eng. Chem. **51**(2): 1445 - 1449.

Curtin, D. E., R. D. Lousenberg, et al. (2004). "Advanced materials for improved PEMFC performance and life." Journal of Power Sources **131**(1–2): 41-48.

Damaskin, B. B. P., O.A. Zyrlina, G.A. (2001). Electrokhimiya. Moscow, Khimiya.

Danner, H., L. Madzingaidzo, et al. (2000). "Extraction and purification of lactic acid from silages." Bioresource Technology **75**(3): 181-187.

Datta, R. (1989). Recovery and purification of lactate salts from whole fermentation broth by electrodialysis. United states, Google Patents. **US4885247 A**.

Datta, R. and M. Henry (2006). "Lactic acid: recent advances in products, processes and technologies — a review." Journal of Chemical Technology & Biotechnology **81**(7): 1119-1129.

De Kruif, C. G. and C. Holt (2003). Casein Micelle Structure, Functions and Interactions. Advanced Dairy Chemistry—1 Proteins. P. F. Fox and P. L. H. McSweeney, Springer US**:** 233-276.

De Silva, P., L. Bucea, et al. (2009). "Chemical, microstructural and strength development of calcium and magnesium carbonate binders." Cement and Concrete Research **39**(5): 460-465.

Derjaguin, B. and L. Landau (1941). "Theory of the stability of strongly charged lyophobic sols and the adhesion of strongly charged particles in solutions of electrolytes." Acta Physico Chemica URSS **14**: 633.

Desgranges, L., G. Calvarin, et al. (1996). "Interlayer interactions in M(OH)2: a neutron diffraction study of Mg(OH)2." Acta Crystallographica Section B **52**(1): 82-86.

Długołęcki, P., J. Dąbrowska, et al. (2010). "Ion conductive spacers for increased power generation in reverse electrodialysis." Journal of Membrane Science **347**(1–2): 101-107.

Drews, A. (2010). "Membrane fouling in membrane bioreactors—Characterisation, contradictions, cause and cures." Journal of Membrane Science **363**(1–2): 1-28.

Duffy, T. S., T. J. Ahrens, et al. (1991). "The shock wave equation of state of brucite Mg(OH)2." Journal of Geophysical Research: Solid Earth **96**(B9): 14319-14330.

Dukhin, S. S. and N. A. Mishchuk (1989). "Disappearance of a phenomenon of limit current in case of an ionite granule." Kolloidnyi Zhurnal **51**(4): 659 - 671.

Ebrahim, S. (1994). "Cleaning and regeneration of membranes in desalination and wastewater applications: State-of-the-art." Desalination **96**(1–3): 225-238.

Eikerling, M., A. A. Kornyshev, et al. (1997). "Electrophysical Properties of Polymer Electrolyte Membranes: A Random Network Model." The Journal of Physical Chemistry B **101**(50): 10807-10820.

Elattar, A., A. Elmidaoui, et al. (1998). "Comparison of transport properties of monovalent anions through anion-exchange membranes." Journal of Membrane Science **143**(1–2): 249-261.

Elimelech, M., Z. Xiaohua, et al. (1997). "Role of membrane surface morphology in colloidal fouling of cellulose acetate and composite aromatic polyamide reverse osmosis membranes." Journal of Membrane Science **127**(1): 101-109.

Fang, Y., Q. Li, et al. (1982). "Noise spectra of sodium and hydrogen ion transport at a cation membrane—solution interface." Journal of Colloid and Interface Science **88**(1): 214-220.

Fang, Y., Q. Li, et al. (1982). "Noise spectra of transport at an anion membrane-solution interface." Journal of Colloid and Interface Science **86**(1): 185-190.

Fidaleo, M. M., M. (2011). Advances in Food and Nutrition Research, Elsevier Science.

Firdaous, L., J. P. Malériat, et al. (2007). "Transfer of Monovalent and Divalent Cations in Salt Solutions by Electrodialysis." Separation Science and Technology **42**(5): 931-948.

Flemming, H.-C. (1997). "Reverse osmosis membrane biofouling." Experimental Thermal and Fluid Science **14**(4): 382-391.

Flemming, H.-C. and G. Schaule (1988). "Biofouling on membranes - A microbiological approach." Desalination **70**(1–3): 95-119.

Flemming, H.-C., J. Wingender, et al. (2011). Biofilm highlights, Springer.

Forgacs, C., J. Leibovitz, et al. (1975). "Interferometric study of concentration profiles in solutions near membrane surfaces." Electrochimica Acta **20**(8): 555-563.

Franklin, A. C. M. (June 2009). Prevention and Control of Membrane Fouling: Practical Implications and Examining Recent Innovations, Membraan Applicatie Centrum Twente b.v.

Frilette, V. J. (1956). "Preparation and Characterization of Bipolar Ion Exchange Membranes." The Journal of Physical Chemistry **60**(4): 435-439.

Fubao, Y. (1985). "Study on electrodialysis reversal (EDR) process." Desalination **56**(0): 315-324.

Gal, J.-Y., J.-C. Bollinger, et al. (1996). "Calcium carbonate solubility: a reappraisal of scale formation and inhibition." Talanta **43**(9): 1497-1509.

Gao, W., H. Liang, et al. (2011). "Membrane fouling control in ultrafiltration technology for drinking water production: A review." Desalination **272**(1–3): 1-8.

Gärtner, R. S., F. G. Wilhelm, et al. (2005). "Regeneration of mixed solvent by electrodialysis: selective removal of chloride and sulfate." Journal of Membrane Science **250**(1–2): 113-133.

Gavish, B. and S. Lifson (1979). "Membrane polarisation at high current densities." Journal of the Chemical Society, Faraday Transactions 1: Physical Chemistry in Condensed Phases **75**(0): 463-472.

Gebel, G. (2000). "Structural evolution of water swollen perfluorosulfonated ionomers from dry membrane to solution." Polymer **41**(15): 5829-5838.

Gence, N. and N. Ozbay (2006). "pH dependence of electrokinetic behavior of dolomite and magnesite in aqueous electrolyte solutions." Applied Surface Science **252**(23): 8057-8061.

Ghassemi, H., J. E. McGrath, et al. (2006). "Multiblock sulfonated–fluorinated poly(arylene ether)s for a proton exchange membrane fuel cell." Polymer **47**(11): 4132-4139.

Ghyselbrecht, K., E. Van Houtte, et al. (2012). "Treatment of RO concentrate by means of a combination of a willow field and electrodialysis." Resources, Conservation and Recycling **65**(0): 116-123.

Gierke, T. D., G. E. Munn, et al. (1981). "The morphology in nafion perfluorinated membrane products, as determined by wide- and small-angle x-ray studies." Journal of Polymer Science: Polymer Physics Edition **19**(11): 1687-1704.

Girard, B., L. R. Fukumoto, et al. (2000). "Membrane Processing of Fruit Juices and Beverages: A Review." <u>Critical Reviews in Biotechnology</u> **20**(2): 109-175.

Gnusin, N. P. G., V.D. Pevnitskaya, M.V. (1972). <u>The Electrochemistry of Ion-exchangers</u>. Novosibirsk, Nauka.

Gohil, G. S., V. V. Binsu, et al. (2006). "Preparation and characterization of mono-valent ion selective polypyrrole composite ion-exchange membranes." <u>Journal of Membrane Science</u> **280**(1–2): 210-218.

Gohil, G. S., V. K. Shahi, et al. (2004). "Comparative studies on electrochemical characterization of homogeneous and heterogeneous type of ion-exchange membranes." <u>Journal of Membrane Science</u> **240**(1–2): 211-219.

Goode, K. R., K. Asteriadou, et al. (2013). "Fouling and cleaning studies in the food and beverage industry classified by cleaning type." <u>Comprehensive Reviews in Food Science and Food Safety</u> **12**(2): 121-143.

Gouy, M. (1910). "Sur la constitution de la charge electrique a la surface d'un electrolyte." <u>Journal of Theoretical and Applied Physics</u> **9**(1): 457-468.

Grebenyuk, V. D., R. D. Chebotareva, et al. (1998). "Surface modification of anion-exchange electrodialysis membranes to enhance anti-fouling characteristics." <u>Desalination</u> **115**(3): 313-329.

Grigin, A. P. (1986). "Distribution of volume charge induced by constant electric current in the cell with plane-parallel electrodes and close-meshed dissipative structures in the binary electrolyte." <u>Soviet Electrochemistry</u> **22**(11): 1458-1462.

Grossman, G. and A. A. Sonin (1972). "Experimental study of the effects of hydrodynamics and membrane fouling in electrodialysis." <u>Desalination</u> **10**(2): 157-180.

Grossman, G. and A. A. Sonin (1973). "Membrane fouling in electrodialysis: a model and experiments." <u>Desalination</u> **12**(1): 107-125.

Guo, H., L. Xiao, et al. (2014). "Analysis of anion exchange membrane fouling mechanism caused by anion polyacrylamide in electrodialysis." <u>Desalination</u> **346**(0): 46-53.

Guo, W., H.-H. Ngo, et al. (2012). "A mini-review on membrane fouling." <u>Bioresource Technology</u> **122**(0): 27-34.

Gyo Lee, E., S.-H. Moon, et al. (1998). "Lactic acid recovery using two-stage electrodialysis and its modelling." <u>Journal of Membrane Science</u> **145**(1): 53-66.

Hamilton, W. C. (1972). "A technique for the characterization of hydrophilic solid surfaces." <u>Journal of Colloid and Interface Science</u> **40**(2): 219-222.

Haubold, H. G., T. Vad, et al. (2001). "Nano structure of NAFION: a SAXS study." Electrochimica Acta **46**(10–11): 1559-1563.

He, C., M. D. Guiver, et al. (2013). "Surface orientation of hydrophilic groups in sulfonated poly(ether ether ketone) membranes." Journal of Colloid and Interface Science **409**(0): 193-203.

He, F., K. K. Sirkar, et al. (2009). "Effects of antiscalants to mitigate membrane scaling by direct contact membrane distillation." Journal of Membrane Science **345**(1–2): 53-58.

Heitner-Wirguin, C. (1996). "Recent advances in perfluorinated ionomer membranes: structure, properties and applications." Journal of Membrane Science **120**(1): 1-33.

Herzberg, M. and M. Elimelech (2007). "Biofouling of reverse osmosis membranes: Role of biofilm-enhanced osmotic pressure." Journal of Membrane Science **295**(1–2): 11-20.

Higashitani, K., A. Kage, et al. (1993). "Effects of a Magnetic Field on the Formation of CaCO3 Particles." Journal of Colloid and Interface Science **156**(1): 90-95.

Hoek, E., M. Guiver, et al. (2013). "Membrane Terminology." Encyclopedia of Membrane Science and Technology **3**: 2219-2228.

Hołysz, L., E. Chibowski, et al. (2003). "Influence of impurity ions and magnetic field on the properties of freshly precipitated calcium carbonate." Water Research **37**(14): 3351-3360.

Hsu, W. Y. and T. D. Gierke (1982). "Elastic theory for ionic clustering in perfluorinated ionomers." Macromolecules **15**(1): 101-105.

Hsu, W. Y. and T. D. Gierke (1983). "Ion transport and clustering in nafion perfluorinated membranes." Journal of Membrane Science **13**(3): 307-326.

Huang, C., T. Xu, et al. (2007). "Application of electrodialysis to the production of organic acids: State-of-the-art and recent developments." Journal of Membrane Science **288**(1–2): 1-12.

Huertas, E., M. Herzberg, et al. (2008). "Influence of biofouling on boron removal by nanofiltration and reverse osmosis membranes." Journal of Membrane Science **318**(1–2): 264-270.

Husson, E., M. Araya-Farias, et al. (2013). "Selective anthocyanins enrichment of cranberry juice by electrodialysis with ultrafiltration membranes stacked." Innovative Food Science & Emerging Technologies **17**(0): 153-162.

Ibanez, R., D. F. Stamatialis, et al. (2004). "Role of membrane surface in concentration polarization at cation exchange membranes." Journal of Membrane Science **239**(1): 119-128.

Ivnitsky, H., I. Katz, et al. (2007). "Bacterial community composition and structure of biofilms developing on nanofiltration membranes applied to wastewater treatment." Water Research **41**(17): 3924-3935.

Ivnitsky, H., D. Minz, et al. (2010). "Biofouling formation and modeling in nanofiltration membranes applied to wastewater treatment." Journal of Membrane Science **360**(1–2): 165-173.

Jain, S. M. (1981). Ion exchanging, desalting. United States, Google Patents. **US 4276140 A**.

Kariduraganavar, M. Y., R. K. Nagarale, et al. (2006). "Ion-exchange membranes: preparative methods for electrodialysis and fuel cell applications." Desalination **197**(1–3): 225-246.

Kattan Readi, O. M., H. J. Kuenen, et al. (2013). "Novel membrane concept for internal pH control in electrodialysis of amino acids using a segmented bipolar membrane (sBPM)." Journal of Membrane Science **443**(0): 219-226.

Katz, W. E. (1979). "The electrodialysis reversal (EDR) process." Desalination **28**(1): 31-40.

Katz, W. E. (1982). "Desalination by ED and EDR—state-of-the-art in 1981." Desalination **42**(2): 129-139.

Kelly, P. M., J. Kelly, et al. (2000). "Implementation of integrated membrane processes for pilot scale development of fractionated milk components." Lait **80**(1): 139-153.

Khan, M. M. T., P. S. Stewart, et al. (2010). "Assessing biofouling on polyamide reverse osmosis (RO) membrane surfaces in a laboratory system." Journal of Membrane Science **349**(1–2): 429-437.

Kharkats, Y. I. (1985). "About the mechanism of appearing the limiting currents in the boundary ion-exchange membrane/electrolyte." Russian Electrochemistry **21**(7): 974-977.

Kharkats, Y. I. (1988). "The role of migration current and complex formation in acceleration of ion transport in elecrochemical systems." Russian Electrochemistry **24**(2): 178-183.

Kim, D. H., I. H. Kim, et al. (1983). "Experimental study of mass transfer around a turbulence promoter by the limiting current method." International Journal of Heat and Mass Transfer **26**(7): 1007-1016.

Kim, S. J., S. H. Ko, et al. (2010). "Direct seawater desalination by ion concentration polarization." Nature Nanotechnology **5**(4): 297-301.

Kim, S. J., Y.-C. Wang, et al. (2007). "Concentration Polarization and Nonlinear Electrokinetic Flow near a Nanofluidic Channel." Physical Review Letters **99**(4): 044501.

Kim, Y. and B. E. Logan (2013). "Microbial desalination cells for energy production and desalination." Desalination **308**(0): 122-130.

Kitamura, M. (2001). "Crystallization and Transformation Mechanism of Calcium Carbonate Polymorphs and the Effect of Magnesium Ion." Journal of Colloid and Interface Science **236**(2): 318-327.

Ko, Y. C., B. D. Ratner, et al. (1981). "Characterization of hydrophilic—hydrophobic polymeric surfaces by contact angle measurements." Journal of Colloid and Interface Science **82**(1): 25-37.

Kononov, Y. A. V., B.M. (1971). "Role of Water Dissociation Products in Electric Current Transfer trough Ionite Membranes." Zhurnal Prikladnoi Khimii **44**: 929-932.

Korhonen, H. and A. Pihlanto (2006). "Bioactive peptides: Production and functionality." International Dairy Journal **16**(9): 945-960.

Korngold, E. (1971). "Prevention of colloidal-fouling in electrodialysis by chlorination." Desalination **9**(3): 213-216.

Korngold, E., L. Aronov, et al. (1998). "Novel ion-exchange spacer for improving electrodialysis I. Reacted spacer." Journal of Membrane Science **138**(2): 165-170.

Korngold, E., F. de Körösy, et al. (1970). "Fouling of anionselective membranes in electrodialysis." Desalination **8**(2): 195-220.

Kotsanopoulos, K. V. and I. S. Arvanitoyannis (2013). "Membrane processing technology in food industry: Food processing, wastewater treatment and effects on physical, microbiological, organoleptic and nutritional properties of foods." Critical Reviews in Food Science and Nutrition.

Kozmai, A. E., V. V. Nikonenko, et al. (2010). "Diffusion layer thickness in a membrane system as determined from voltammetric and chronopotentiometric data." Russian Journal of Electrochemistry **46**(12): 1383-1389.

Kressman, T. R. E. and F. L. Tye (1956). "The effect of current density on the transport of ions through ion-selective membranes." Discussions of the Faraday Society **21**(0): 185-192.

Kressman, T. R. E. and F. L. Tye (1969). "pH Changes at Anion Selective Membranes under Realistic Flow Conditions." Journal of the Electrochemical Society **116**(1): 25-31.

Kressman, T. R. E. a. T., F.L. (1969). "Closure to "Discussion of 'pH Changes at Anion Selectve Membranes Under Realistic Flow Conditions"." Journal of the Electrochemical Society **116**(12): 1714-1715.

Kreuer, K.-D., A. Rabenau, et al. (1982). "Vehicle Mechanism, A New Model for the Interpretation of the Conductivity of Fast Proton Conductors." Angewandte Chemie International Edition in English **21**(3): 208-209.

Kreuer, K. D. (2001). "On the development of proton conducting polymer membranes for hydrogen and methanol fuel cells." Journal of Membrane Science **185**(1): 29-39.

Kreuer, K. D. (2010). Hydrocarbon membranes. Handbook of Fuel Cells, John Wiley & Sons, Ltd.

Kreuer, K. D. (2012). Fuel Cells: Selected Entries from the Encyclopedia of Sustainability Science and Technology, Springer.

Kristensen, J. B., R. L. Meyer, et al. (2008). "Antifouling enzymes and the biochemistry of marine settlement." Biotechnology Advances **26**(5): 471-481.

Krol, J. J., M. Wessling, et al. (1999). "Chronopotentiometry and overlimiting ion transport through monopolar ion exchange membranes." Journal of Membrane Science **162**(1–2): 155-164.

Krol, J. J., M. Wessling, et al. (1999). "Concentration polarization with monopolar ion exchange membranes: current–voltage curves and water dissociation." Journal of Membrane Science **162**(1–2): 145-154.

Kuroda, O., S. Takahashi, et al. (1983). "Characteristics of flow and mass transfer rate in an electrodialyzer compartment including spacer." Desalination **46**(1–3): 225-232.

Kusumoto, K., Y. Mizumoto, et al. (1975). "Modification of anion exchange membranes by oxidation of selected chemical sites for the purpose of preventing fouling during dialysis." Desalination **17**(3): 303-311.

Kusumoto, K. and Y. Mizutani (1975). "New anion-exchange membrane resistant to organic fouling." Desalination **17**(1): 121-130.

188

Kwak, R., G. Guan, et al. (2013). "Microscale electrodialysis: Concentration profiling and vortex visualization." Desalination **308**(0): 138-146.

Kwak, R., V. S. Pham, et al. (2013). "Shear Flow of an Electrically Charged Fluid by Ion Concentration Polarization: Scaling Laws for Electroconvective Vortices." Physical Review Letters **110**(11): 114501.

Lakretz, A., E. Z. Ron, et al. (2009). "Biofouling control in water by various UVC wavelengths and doses." Biofouling **26**(3): 257-267.

Langevin, M.-E. and L. Bazinet (2011). "Ion-exchange membrane fouling by peptides: A phenomenon governed by electrostatic interactions." Journal of Membrane Science **369**(1–2): 359-366.

Lebrun, L., E. Da Silva, et al. (2003). "Elaboration and characterisation of ion-exchange films used in the fabrication of bipolar membranes." Journal of Membrane Science **227**(1–2): 95-111.

Lee, H.-J., M.-K. Hong, et al. (2009). "Fouling of an anion exchange membrane in the electrodialysis desalination process in the presence of organic foulants." Desalination **238**(1): 60-69.

Lee, H.-J. and S.-H. Moon (2004). "Influences of colloidal stability and electrokinetic property on electrodialysis performance in the presence of silica sol." Journal of Colloid and Interface Science **270**(2): 406-412.

Lee, H.-J. and S.-H. Moon (2005). "Enhancement of electrodialysis performances using pulsing electric fields during extended period operation." Journal of Colloid and Interface Science **287**(2): 597-603.

Lee, H.-J., S.-H. Moon, et al. (2002). "Effects of pulsed electric fields on membrane fouling in electrodialysis of NaCl solution containing humate." Separation and Purification Technology **27**(2): 89-95.

Lee, H.-J., S.-J. Oh, et al. (2003). "Recovery of ammonium sulfate from fermentation waste by electrodialysis." Water Research **37**(5): 1091-1099.

Lee, H.-J., J.-S. Park, et al. (2003). "Effects of silica sol on ion exchange membranes: Electrochemical characterization of anion exchange membranes in electrodialysis of silica sol containing-solutions." Korean Journal of Chemical Engineering **20**(5): 889-895.

Lee, W., C. H. Ahn, et al. (2010). "Evaluation of surface properties of reverse osmosis membranes on the initial biofouling stages under no filtration condition." Journal of Membrane Science **351**(1–2): 112-122.

Lim, A. L. and R. Bai (2003). "Membrane fouling and cleaning in microfiltration of activated sludge wastewater." Journal of Membrane Science **216**(1–2): 279-290.

Lin Teng Shee, F., P. Angers, et al. (2008). "Microscopic approach for the identification of cationic membrane fouling during cheddar cheese whey electroacidification." Journal of Colloid and Interface Science **322**(2): 551-557.

Lin Teng Shee, F., J. Arul, et al. (2007). "Chitosan solubilization by bipolar membrane electroacidification: Reduction of membrane fouling." Journal of Membrane Science **290**(1–2): 29-35.

Lindstrand, V., A.-S. Jönsson, et al. (2000). "Organic fouling of electrodialysis membranes with and without applied voltage." Desalination **130**(1): 73-84.

Lindstrand, V., G. Sundström, et al. (2000). "Fouling of electrodialysis membranes by organic substances." Desalination **128**(1): 91-102.

Liu, C. X., D. R. Zhang, et al. (2010). "Modification of membrane surface for anti-biofouling performance: Effect of anti-adhesion and anti-bacteria approaches." Journal of Membrane Science **346**(1): 121-130.

Loste, E., R. M. Wilson, et al. (2003). "The role of magnesium in stabilising amorphous calcium carbonate and controlling calcite morphologies." Journal of Crystal Growth **254**(1–2): 206-218.

Lteif, R., L. Dammak, et al. (1999). "Conductivité électrique membranaire: étude de l'effet de la concentration, de la nature de l'électrolyte et de la structure membranaire." European Polymer Journal **35**(7): 1187-1195.

Lue, S. J., F. J. Wang, et al. (2004). "Pervaporation of benzene/cyclohexane mixtures using ion-exchange membrane containing copper ions." Journal of Membrane Science **240**(1–2): 149-158.

Luo, H., P. Xu, et al. (2012). "Microbial desalination cells for improved performance in wastewater treatment, electricity production, and desalination." Bioresource Technology **105**(0): 60-66.

Mafé, S. R., P. Alcaraz, A. and Aguilella V. (2000). Handbook on bipolar membrane technology: prepared within the framework of the "Thematic Network on Electro-Membrane Processes", Twente University Press.

Majamaa, K., J. E. Johnson, et al. (2012). "Three steps to control biofouling in reverse osmosis systems." Desalination and Water Treatment **42**(1-3): 107-116.

Makai, A. J. T. R. J. C. (1978). "Polarisation in electrodialysis. Rotating-disc studies." Journal of the Chemical Society, Faraday Transactions **74**(1): 2850 - 2857.

Malek, P., J. M. Ortiz, et al. (2013). "Electrodialytic removal of NaCl from water: Impacts of using pulsed electric potential on ion transport and water dissociation phenomena." Journal of Membrane Science **435**(0): 99-109.

Maletzki, F., H. W. Rösler, et al. (1992). "Ion transfer across electrodialysis membranes in the overlimiting current range: stationary voltage current characteristics and current noise power spectra under different conditions of free convection." Journal of Membrane Science **71**(1–2): 105-116.

Manzanares, J. A. K., K. Mafé, S. Aguilella, V.M. Pellicer, J. (1991). "Polarization Effects at the Cation-Exchange Membrane - Solution Interface." Acta Chemica Scandinavica **45**: 115-121.

Marcus, Y. (1991). "Thermodynamics of solvation of ions. Part 5.-Gibbs free energy of hydration at 298.15 K." Journal of the Chemical Society, Faraday Transactions **87**(18): 2995-2999.

Marquardt, R. F., H. T. Pederson, et al. (1985). Modified whey product and process including ultrafiltration and demineralization. United States, Google Patents. **US4497836 A**.

Mauritz, K. A. and R. B. Moore (2004). "State of Understanding of Nafion." Chemical Reviews **104**(10): 4535-4586.

Messalem, R., Y. Mirsky, et al. (1998). "Novel ion-exchange spacer for improving electrodialysis II. Coated spacer." Journal of Membrane Science **138**(2): 171-180.

Mier, M. P., R. Ibañez, et al. (2008). "Influence of process variables on the production of bovine milk casein by electrodialysis with bipolar membranes." Biochemical Engineering Journal **40**(2): 304-311.

Mikhaylin, S., V. Nikonenko, et al. (2014). "Intensification of demineralization process and decrease in scaling by application of pulsed electric field with short pulse/pause conditions." Journal of Membrane Science **468**(0): 389-399.

Mishchuk, N., C. Gonzalez, et al. (2001). "Electroosmosis of the second kind and current through curved interface." Colloids and Surfaces A: Physicochemical and Engineering Aspects **181**(1–3): 131-144.

Mishchuk, N. A. (2010). "Concentration polarization of interface and non-linear electrokinetic phenomena." Advances in Colloid and Interface Science **160**(1–2): 16-39.

Mishchuk, N. A., L. K. Koopal, et al. (2001). "Intensification of electrodialysis by applying a non-stationary electric field." Colloids and Surfaces A: Physicochemical and Engineering Aspects **176**(2–3): 195-212.

Mizutani, Y. (1990). "Structure of ion exchange membranes." Journal of Membrane Science **49**(2): 121-144.

Mizutani, Y. and M. Nishimura (1980). "Microstructure of cation exchange membranes prepared by the paste method." Journal of Applied Polymer Science **25**(12): 2925-2934.

Mondor, M., D. Ippersiel, et al. (2009). "Fouling characterization of electrodialysis membranes used for the recovery and concentration of ammonia from swine manure." Bioresource Technology **100**(2): 566-571.

Mulvihill, D. M. and M. P. Ennis (2003). Functional Milk Proteins: Production and Utilization. Advanced Dairy Chemistry—1 Proteins. P. F. Fox and P. L. H. McSweeney, Springer US**:** 1175-1228.

Mulyati, S., R. Takagi, et al. (2012). "Improvement of the antifouling potential of an anion exchange membrane by surface modification with a polyelectrolyte for an electrodialysis process." Journal of Membrane Science **417–418**(0): 137-143.

Mulyati, S., R. Takagi, et al. (2013). "Simultaneous improvement of the monovalent anion selectivity and antifouling properties of an anion exchange membrane in an electrodialysis process, using polyelectrolyte multilayer deposition." Journal of Membrane Science **431**(0): 113-120.

Nagarale, R. K., G. S. Gohil, et al. (2006). "Recent developments on ion-exchange membranes and electro-membrane processes." Advances in Colloid and Interface Science **119**(2–3): 97-130.

Nataraj, S. K., S. Sridhar, et al. (2007). "Membrane-based microfiltration/electrodialysis hybrid process for the treatment of paper industry wastewater." Separation and Purification Technology **57**(1): 185-192.

Nehrke, G. (2007). Calcite precipitation from aqueous solution: transformation from vaterite and role of solution stoichiometry, Universität Utrecht, Niederlande.

Nicholson, W., A. Carliebe, et al. (1800). "Experiments in galvanic electricity." Philosophical Magazine **7**: 337-347.

192

Nikonenko, V., V. Zabolotsky, et al. (2002). "Mathematical description of ion transport in membrane systems." Desalination **147**(1–3): 369-374.

Nikonenko, V. V., A. V. Kovalenko, et al. (2014). "Desalination at overlimiting currents: State-of-the-art and perspectives." Desalination **342**(0): 85-106.

Nikonenko, V. V., N. D. Pis'menskaya, et al. (2005). "Rate of Generation of Ions H+ and OH− at the Ion-Exchange Membrane/Dilute Solution Interface as a Function of the Current Density." Russian Journal of Electrochemistry **41**(11): 1205-1210.

Nikonenko, V. V., N. D. Pismenskaya, et al. (2010). "Intensive current transfer in membrane systems: Modelling, mechanisms and application in electrodialysis." Advances in Colloid and Interface Science **160**(1–2): 101-123.

Ning, R. Y., T. L. Troyer, et al. (2005). "Chemical control of colloidal fouling of reverse osmosis systems." Desalination **172**(1): 1-6.

Nishimura, M. and Y. Mizutani (1981). "Correlation between structure and properties of cation-exchange membranes prepared by the paste method." Journal of Applied Electrochemistry **11**(2): 165-171.

Nollet, J. A. A. (1752). Recherches sur les causes du bouillonnement des liquides. Histoire de l'Academie Royale des Sciences. Paris**:** 57-104.

O'Mahony, J. A. and P. F. Fox (2013). Milk Proteins: Introduction and Historical Aspects. Advanced Dairy Chemistry. P. L. H. McSweeney and P. F. Fox, Springer US**:** 43-85.

Oda, Y. and T. Yawataya (1968). "Neutrality-disturbance phenomenon of membrane-solution systems." Desalination **5**(2): 129-138.

Ottosen, L. M., H. K. Hansen, et al. (2000). "Water splitting at ion-exchange membranes and potential differences in soil during electrodialytic soil remediation." Journal of Applied Electrochemistry **30**(11): 1199-1207.

Park, J.-S., J.-H. Choi, et al. (2006). "An approach to fouling characterization of an ion-exchange membrane using current–voltage relation and electrical impedance spectroscopy." Journal of Colloid and Interface Science **294**(1): 129-138.

Park, J.-S., H.-J. Lee, et al. (2003). "Determination of an optimum frequency of square wave power for fouling mitigation in desalting electrodialysis in the presence of humate." Separation and Purification Technology **30**(2): 101-112.

Park, J. S., T. C. Chilcott, et al. (2005). "Characterization of BSA-fouling of ion-exchange membrane systems using a subtraction technique for lumped data." Journal of Membrane Science **246**(2): 137-144.

Parvizian, F., M. Rahimi, et al. (2012). "The effect of high frequency ultrasound on diffusion boundary layer resistance in ion-exchange membrane transport." Desalination **286**(0): 155-165.

Peers, A. M. (1956). "Membrane phenomena." Discussions of the Faraday Society **21**: 124-125.

Peers, A. M. (1958). "Electrodialysis Using Ion-Exchange Membranes II. "Demineralization of Solutions Containing Amino-acids"." Journal of Applied Chemistry **8**: 59 - 67.

Phillips, D. L. (2014). "The effects of a high-protein diet on obesity and other risk factors associated with cardiovascular disease." University of Tennessee Honors Thesis Projects.

Ping, Q., B. Cohen, et al. (2013). "Long-term investigation of fouling of cation and anion exchange membranes in microbial desalination cells." Desalination **325**(0): 48-55.

Pis'menskaya, N. D., V. V. Nikonenko, et al. (2012). "Effect of the ion-exchange-membrane/solution interfacial characteristics on the mass transfer at severe current regimes." Russian Journal of Electrochemistry **48**(6): 610-628.

Pismenskaia, N., P. Sistat, et al. (2004). "Chronopotentiometry applied to the study of ion transfer through anion exchange membranes." Journal of Membrane Science **228**(1): 65-76.

Pismenskaya, N., N. Melnik, et al. (2012). "Enhancing Ion Transfer in Overlimiting Electrodialysis of Dilute Solutions by Modifying the Surface of Heterogeneous Ion-Exchange Membranes." International Journal of Chemical Engineering **2012**: 11.

Pismenskaya, N. D., V. V. Nikonenko, et al. (2007). "Coupled convection of solution near the surface of ion-exchange membranes in intensive current regimes." Russian Journal of Electrochemistry **43**(3): 307-327.

Pismenskaya, N. D., V. V. Nikonenko, et al. (2012). "Evolution with Time of Hydrophobicity and Microrelief of a Cation-Exchange Membrane Surface and Its Impact on Overlimiting Mass Transfer." The Journal of Physical Chemistry B **116**(7): 2145-2161.

Pontié, M., S. Ben Rejeb, et al. (2012). "Anti-microbial approach onto cationic-exchange membranes." Separation and Purification Technology **101**(0): 91-97.

194

Ramchandran, I. and I. Vasiljevic (2013). <u>Membrane processing: Dairy and Beverage Applications</u> Blackwell Publishing Ltd.

Ren, H., Q. Wang, et al. (2011). "Characterization of cation-exchange membrane fouling during bipolar membrane electrodialysis of monosodium glutamate isoelectric supernatant." <u>Journal of Chemical Technology & Biotechnology</u> **86**(12): 1469-1474.

Ren, H., Q. Wang, et al. (2008). "Membrane fouling caused by amino acid and calcium during bipolar membrane electrodialysis." <u>Journal of Chemical Technology & Biotechnology</u> **83**(11): 1551-1557.

Rodriguez-Navarro, C., E. Hansen, et al. (1998). "Calcium Hydroxide Crystal Evolution upon Aging of Lime Putty." <u>Journal of the American Ceramic Society</u> **81**(11): 3032-3034.

Roques, H. (1990). Fondement Théorique du Traitement des Eaux. Technique et Documentation Lavoisier, Paris**:** 41-43.

Rosa, M. J. and M. N. de Pinho (1997). "Membrane surface characterisation by contact angle measurements using the immersed method." <u>Journal of Membrane Science</u> **131**(1–2): 167-180.

Rubinstein, I. and L. Shtilman (1979). "Voltage against current curves of cation exchange membranes." <u>Journal of the Chemical Society, Faraday Transactions 2: Molecular and Chemical Physics</u> **75**(0): 231-246.

Rubinstein, I., E. Staude, et al. (1988). "Role of the membrane surface in concentration polarization at ion-exchange membrane." <u>Desalination</u> **69**(2): 101-114.

Rubinstein, I., A. Warshawsky, et al. (1984). "Elimination of acid-base generation ('water-splitting') in electrodialysis." <u>Desalination</u> **51**(1): 55-60.

Rubinstein, I. and B. Zaltzman (2000). "Electro-osmotically induced convection at a permselective membrane." <u>Physical Review E</u> **62**(2): 2238-2251.

Rubinstein, I. and B. Zaltzman (2010). "Extended space charge in concentration polarization." <u>Advances in Colloid and Interface Science</u> **159**(2): 117-129.

Rubinstein, I., B. Zaltzman, et al. (2002). "Ion-exchange funneling in thin-film coating modification of heterogeneous electrodialysis membranes." <u>Physical Review E</u> **65**(4): 041507.

Ruiz, B., P. Sistat, et al. (2007). "Application of relaxation periods during electrodialysis of a casein solution: Impact on anion-exchange membrane fouling." Journal of Membrane Science **287**(1): 41-50.

S. Mikhaylin, V. N., G. Pourcelly, L. Bazinet (2014). "Intensification of demineralization process and decrease in scaling by application of pulsed electric field with short pulse/pause conditions." Journal of Membrane Science **468**: 389-399.

Sakashita, M., S. Fujita, et al. (1983). "Current-voltage characteristics and oxide formation of bipolar PbSO4 precipitate membranes." Journal of Electroanalytical Chemistry and Interfacial Electrochemistry **154**(1–2): 273-280.

Sand, H. J. S. (1901). "On the concentration at the electrodes in a solution, with special reference to the liberation of hydrogen by electrolysis of a mixture of copper sulphate and sulphuric acid." Philosophical Magazine Series 6 **1**(1): 45-79.

Sata, T. (2004). Ion Exchange Membranes: Preparation, Characterization, Modification and Application, Royal Society of Chemistry.

Sata, T., T. Sata, et al. (2002). "Studies on cation-exchange membranes having permselectivity between cations in electrodialysis." Journal of Membrane Science **206**(1–2): 31-60.

Sata, T. Y., R. Mizutani, Y. (1969). "Concentration Polarization Phenomena in Ion-Exchange Membrane Electrodialysis. I. Studies of the Diffusion Boundary Layer be Means of Six Different Measurements." Bulletin of the Chemical Society of Japan **42**: 279-284.

Schwarz, S., K. Lunkwitz, et al. (2000). "Adsorption and stability of colloidal silica." Colloids and Surfaces A: Physicochemical and Engineering Aspects **163**(1): 17-27.

Sekoulov, I., A. Figueroa, et al. (1991). "Investigation on wastewater reuse on passenger aircraft." Water Science & Technology **23**(10-12): 2199-2208.

Shaposhnik, V., V. Vasil'eva, et al. (2006). "Thermoconvective instability during electrodialysis." Russian Journal of Electrochemistry **42**(5): 531-537.

Shaposhnik, V. A. and K. Kesore (1997). "An early history of electrodialysis with permselective membranes." Journal of Membrane Science **136**(1–2): 35-39.

Shaposhnik, V. A., V. I. Vasil'eva, et al. (2008). "The interferometric investigations of electromembrane processes." Advances in Colloid and Interface Science **139**(1–2): 74-82.

Shaposhnik, V. A., V. I. Vasil'eva, et al. (2002). "Optical method for measuring of transport numbers in membranes." Sorption and chromatographic processes **2**(1): 40-47.

196

Sheldeshov, N. V. Doctoral thesis, Kuban State University, Russia (2002).

Shi, S., S.-H. Cho, et al. (2011). "Desalination of fish meat extract by electrodialysis and characterization of membrane fouling." Korean Journal of Chemical Engineering **28**(2): 575-582.

Shi, X., G. Tal, et al. (2014). "Fouling and cleaning of ultrafiltration membranes: A review." Journal of Water Process Engineering **1**(0): 121-138.

Simons, R. (1979). "The origin and elimination of water splitting in ion exchange membranes during water demineralisation by electrodialysis." Desalination **28**(1): 41-42.

Simons, R. (1979). "Strong electric field effects on proton transfer between membrane-bound amines and water." Nature **280**(5725): 824-826.

Simons, R. (1984). "Electric field effects on proton transfer between ionizable groups and water in ion exchange membranes." Electrochimica Acta **29**(2): 151-158.

Simons, R. (1985). "Water splitting in ion exchange membranes." Electrochimica Acta **30**(3): 275-282.

Simons, R. (1986). "A novel method for preparing bipolar membranes." Electrochimica Acta **31**(9): 1175-1177.

Simons, R. (1993). "Preparation of a high performance bipolar membrane." Journal of Membrane Science **78**(1–2): 13-23.

Singh, H. (2011). "Functional properties of milk proteins." Encyclopedia of Dairy Sciences: 887-893.

Sistat, P. and G. Pourcelly (1997). "Chronopotentiometric response of an ion-exchange membrane in the underlimiting current-range. Transport phenomena within the diffusion layers." Journal of Membrane Science **123**(1): 121-131.

Spiegler, K. S. (1971). "Polarization at ion exchange membrane-solution interfaces." Desalination **9**(4): 367-385.

Srilaorkul, S., L. Ozimek, et al. (1989). "The Effect of Ultrafiltration on Physicochemical Properties of Retentate." Canadian Institute of Food Science and Technology Journal **22**(1): 56-62.

Stern, O. (1924). "Zur theorie der elektrolytischen doppelschicht." Zeitschrift für Elektrochemie und angewandte physikalische Chemie **30**(21-22): 508-516.

Strathmann, H. (1981). "Membrane separation processes." Journal of Membrane Science **9**(1–2): 121-189.

Strathmann, H. (2004). Ion-exchange membrane separation processes. Amsterdam, Elsevier.

Strathmann, H. (2010). "Electrodialysis, a mature technology with a multitude of new applications." Desalination **264**(3): 268-288.

Strathmann, H., A. Grabowski, et al. (2013). "Ion-Exchange Membranes in the Chemical Process Industry." Industrial & Engineering Chemistry Research **52**(31): 10364-10379.

Strathmann, H., J. J. Krol, et al. (1997). "Limiting current density and water dissociation in bipolar membranes." Journal of Membrane Science **125**(1): 123-142.

Strathmann, H., H. J. Rapp, et al. (1993). "Theoretical and practical aspects of preparing bipolar membranes." Desalination **90**(1–3): 303-323.

Sun, F.-Y., X.-M. Wang, et al. (2008). "Visualisation and characterisation of biopolymer clusters in a submerged membrane bioreactor." Journal of Membrane Science **325**(2): 691-697.

Sun, T. R., L. M. Ottosen, et al. (2012). "Pulse current enhanced electrodialytic soil remediation—Comparison of different pulse frequencies." Journal of Hazardous Materials **237–238**(0): 299-306.

Sweity, A., W. Ying, et al. (2011). "Relation between EPS adherence, viscoelastic properties, and MBR operation: Biofouling study with QCM-D." Water Research **45**(19): 6430-6440.

T. Brunelle, M. (1980). "Colloidal fouling of reverse osmosis membranes." Desalination **32**(0): 127-135.

Tadors, T. e. (2013). Encyclopedia of Colloid and Interface Science. T. Tadors, Springer Berlin Heidelberg.

Taky, M., G. Pourcelly, et al. (1992). "Polarization phenomena at the interfaces between an electrolyte solution and an ion exchange membrane: Part II. Ion transfer with an anion exchange membrane." Journal of Electroanalytical Chemistry **336**(1–2): 195-212.

Taky, M., G. Pourcelly, et al. (1992). "Polarization phenomena at the interfaces between an electrolyte solution and an ion exchange membrane: Part I. Ion transfer with a cation exchange membrane." Journal of Electroanalytical Chemistry **336**(1–2): 171-194.

Tanaka, Y. (2003). "Mass transport and energy consumption in ion-exchange membrane electrodialysis of seawater." Journal of Membrane Science **215**(1–2): 265-279.

198

Tanaka, Y. (2004). "Concentration polarization in ion-exchange membrane electrodialysis: The events arising in an unforced flowing solution in a desalting cell." Journal of Membrane Science **244**(1–2): 1-16.

Tanaka, Y. (2007). "Acceleration of water dissociation generated in an ion exchange membrane." Journal of Membrane Science **303**(1–2): 234-243.

Tanaka, Y., M. Iwahashi, et al. (1994). "Distribution of electrodialytic condition in an electrodialyzer and limiting current density." Journal of Membrane Science **92**(3): 217-228.

Thompson, D. W. and A. Y. Tremblay (1983). "Fouling in steady and unsteady state electrodialysis." Desalination **47**(1–3): 181-188.

Tran, A. T. K., N. Jullok, et al. (2013). "Pellet reactor pretreatment: A feasible method to reduce scaling in bipolar membrane electrodialysis." Journal of Colloid and Interface Science **401**(0): 107-115.

Tran, A. T. K., Y. Zhang, et al. (2012). "RO concentrate treatment by a hybrid system consisting of a pellet reactor and electrodialysis." Chemical Engineering Science **79**(0): 228-238.

Tsun, H.-Y., C.-M. Liu, et al. (1998). "Recovery and purification of thuringiensin from the fermentation broth of Bacillus thuringiensis." Bioseparation **7**(6): 309-316.

Urtenov, M. A. K., E. V. Kirillova, et al. (2007). "Decoupling of the Nernst−Planck and Poisson Equations. Application to a Membrane System at Overlimiting Currents." The Journal of Physical Chemistry B **111**(51): 14208-14222.

Urtenov, M. K., A. M. Uzdenova, et al. (2013). "Basic mathematical model of overlimiting transfer enhanced by electroconvection in flow-through electrodialysis membrane cells." Journal of Membrane Science **447**(0): 190-202.

Uzdenova, A. M., A. V. Kovalenko, et al. (2015). "Effect of electroconvection during pulsed electric field electrodialysis. Numerical experiments." Electrochemistry Communications **51**(0): 1-5.

Valero, F. and R. Arbós (2010). "Desalination of brackish river water using Electrodialysis Reversal (EDR): Control of the THMs formation in the Barcelona (NE Spain) area." Desalination **253**(1–3): 170-174.

Valero, F., A. Barceló, et al. (2011). "Electrodialysis technology: theory and applications." Desalination, trends and technologies, InTech: 3-20.

Van Geluwe, S., L. Braeken, et al. (2011). "Evaluation of electrodialysis for scaling prevention of nanofiltration membranes at high water recoveries." Resources, Conservation and Recycling **56**(1): 34-42.

Vaselbehagh, M., H. Karkhanechi, et al. (2014). "Improved antifouling of anion-exchange membrane by polydopamine coating in electrodialysis process." Desalination **332**(1): 126-133.

Vasil'eva, V. I., V. A. Shaposhnik, et al. (2006). "The membrane–solution interface under high-performance current regimes of electrodialysis by means of laser interferometry." Desalination **192**(1–3): 408-414.

Vera, E., J. Ruales, et al. (2003). "Deacidification of clarified passion fruit juice using different configurations of electrodialysis." Journal of Chemical Technology & Biotechnology **78**(8): 918-925.

Vera, E., J. Sandeaux, et al. (2007). "Deacidification of clarified tropical fruit juices by electrodialysis. Part I. Influence of operating conditions on the process performances." Journal of Food Engineering **78**(4): 1427-1438.

Vermaas, D. A., D. Kunteng, et al. (2013). "Fouling in reverse electrodialysis under natural conditions." Water Research **47**(3): 1289-1298.

Verwey, E. and J. Overbeek (1948). Theory of the stability of lyophobic colloids. Amsterdam.

Vessler, G. R. K., V.S. Shwarz, P. Linde, H. (1986). "Optical and electrochemical study of dissipative structures in electrolyte solutions." Soviet Electrochemistry **22**(5): 623-628.

Vladisavljević, G. T., S. K. Milonjić, et al. (1992). "Influence of temperature on the ultrafiltration of silica sol in a stirred cell." Journal of Membrane Science **66**(1): 9-17.

Volkov, V. V., B. V. McHedlishvili, et al. (2008). "Membranes and nanotechnologies." Nanotechnologies in Russia **3**(11-12): 656-687.

Volodina, E., N. Pismenskaya, et al. (2005). "Ion transfer across ion-exchange membranes with homogeneous and heterogeneous surfaces." Journal of Colloid and Interface Science **285**(1): 247-258.

von Bibra, H., G. Wulf, et al. (2014). "Low-carbohydrate/high-protein diet improves diastolic cardiac function and the metabolic syndrome in overweight-obese patients with type 2 diabetes." International Journal of Cardiology, Metabolic & Endocrine **2**(0): 11-18.

Vrijenhoek, E. M., S. Hong, et al. (2001). "Influence of membrane surface properties on initial rate of colloidal fouling of reverse osmosis and nanofiltration membranes." Journal of Membrane Science **188**(1): 115-128.

Vyas, P. V., B. G. Shah, et al. (2000). "Studies on heterogeneous cation-exchange membranes." Reactive and Functional Polymers **44**(2): 101-110.

Vyas, P. V., B. G. Shah, et al. (2001). "Characterization of heterogeneous anion-exchange membrane." Journal of Membrane Science **187**(1–2): 39-46.

Walstra, P. (1990). "On the Stability of Casein Micelles." Journal of Dairy Science **73**(8): 1965-1979.

Wang, K., W. Li, et al. (2013). "Integrated Membrane Process for the Purification of Lactic Acid from a Fermentation Broth Neutralized with Sodium Hydroxide." Industrial & Engineering Chemistry Research **52**(6): 2412-2417.

Wang, Q., P. Yang, et al. (2011). "Cation-exchange membrane fouling and cleaning in bipolar membrane electrodialysis of industrial glutamate production wastewater." Separation and Purification Technology **79**(1): 103-113.

Wang, Z., J. Ma, et al. (2014). "Membrane cleaning in membrane bioreactors: A review." Journal of Membrane Science **468**(0): 276-307.

Wilhelm, F. G., I. Pünt, et al. (2001). "Optimisation strategies for the preparation of bipolar membranes with reduced salt ion leakage in acid–base electrodialysis." Journal of Membrane Science **182**(1–2): 13-28.

Xu, T. (2002). "Electrodialysis processes with bipolar membranes (EDBM) in environmental protection—a review." Resources, Conservation and Recycling **37**(1): 1-22.

Xu, T. (2005). "Ion exchange membranes: State of their development and perspective." Journal of Membrane Science **263**(1–2): 1-29.

Yang, G. C. C. and T.-Y. Yang (2004). "Reclamation of high quality water from treating CMP wastewater by a novel crossflow electrofiltration/electrodialysis process." Journal of Membrane Science **233**(1–2): 151-159.

Yang, H.-L., J. C.-T. Lin, et al. (2009). "Application of nanosilver surface modification to RO membrane and spacer for mitigating biofouling in seawater desalination." Water Research **43**(15): 3777-3786.

Yaroslavtsev, A. B. (2013). "Perfluorinated ion-exchange membranes." Polymer Science Series A **55**(11): 674-698.

Yaroslavtsev, A. B. and V. V. Nikonenko (2009). "Ion-exchange membrane materials: Properties, modification, and practical application." Nanotechnologies in Russia **4**(3-4): 137-159.

Yaroslavtsev, A. B., V. V. Nikonenko, et al. (2003). "Ion transfer in ion-exchange and membrane materials." Russian Chemical Reviews **72**(5): 393-421.

Yiantsios, S. G. and A. J. Karabelas (1998). "The effect of colloid stability on membrane fouling." Desalination **118**(1–3): 143-152.

Yiantsios, S. G., D. Sioutopoulos, et al. (2005). "Colloidal fouling of RO membranes: an overview of key issues and efforts to develop improved prediction techniques." Desalination **183**(1–3): 257-272.

Zabolotskii, V. I., V. V. Bugakov, et al. (2012). "Transfer of electrolyte ions and water dissociation in anion-exchange membranes under intense current conditions." Russian Journal of Electrochemistry **48**(6): 650-659.

Zabolotskii, V. I., J. A. Manzanares, et al. (2002). "Steady-state Ion Transport through a Three-Layered Membrane System: A Mathematical Model Allowing for Violation of the Electroneutrality Condition." Russian Journal of Electrochemistry **38**(8): 819-827.

Zabolotskii, V. I., M. V. Sharafan, et al. (2008). "Influence of the nature of membrane ionogenic groups on water dissociation and electrolyte ion transport: A rotating membrane disk study." Russian Journal of Electrochemistry **44**(10): 1127-1134.

Zabolotskii, V. I., N. V. Shel'deshov, et al. (2006). "Electric mass transfer of sodium chloride through cation-exchange membrane MK-40: A rotating membrane disk study." Russian Journal of Electrochemistry **42**(12): 1345-1351.

Zabolotsky, V. I., J. A. Manzanares, et al. (2002). "Space charge effect on competitive ion transport through ion-exchange membranes." Desalination **147**(1–3): 387-392.

Zabolotsky, V. I. and V. V. Nikonenko (1996). Transport of ions in membranes, Nauka.

Zabolotsky, V. I., V. V. Nikonenko, et al. (1996). "On the role of gravitational convection in the transfer enhancement of salt ions in the course of dilute solution electrodialysis." Journal of Membrane Science **119**(2): 171-181.

Zabolotsky, V. I., V. V. Nikonenko, et al. (1998). "Coupled transport phenomena in overlimiting current electrodialysis." Separation and Purification Technology **14**(1–3): 255-267.

Zhang, W. and B. Hallström (1990). "Membrane characterization using the contact angle technique I. methodology of the captive bubble technique." Desalination **79**(1): 1-12.

Zhang, W., M. Wahlgren, et al. (1989). "Membrane Characterization by the Contact Angle Technique: II. Characterization of UF-Membranes and Comparison between the Captive Bubble and Sessile Drop as Methods to obtain Water Contact Angles." Desalination **72**(3): 263-273.

Zhang, Y. and R. A. Dawe (2000). "Influence of Mg2+ on the kinetics of calcite precipitation and calcite crystal morphology." Chemical Geology **163**(1–4): 129-138.

Zhao, Y.-j., K.-f. Wu, et al. (2000). "Fouling and cleaning of membrane-a literature review." ournal of Environmental Sceinces-Beiging **12**(2): 241-251.

Zhu, X., R. Bai, et al. (2010). "Membrane surfaces immobilized with ionic or reduced silver and their anti-biofouling performances." Journal of Membrane Science **363**(1–2): 278-286.